An Antifouling, Structurally Small Carbon Electrode for Detection of the Neurotransmitter Dopamine

by

Rita Roshni

Master of Science, The University of the South Pacific, Fiji

A thesis submitted in fulfilment of the requirements for the degree of

Doctor of Philosophy

Department of Molecular Science

Macquarie University

Sydney, Australia

8 September 2019

Abstract

A long-term goal of the present work is to apply structurally small, antifouling carbon electrodes to acquire meaningful results during *in vivo* detection of the neurotransmitter dopamine. Dopamine is a neurotransmitter in the mammalian brain that plays a crucial role in the central nervous, cardiovascular, renal, and endocrine systems. Under physiological pH (p*Ka* 8.87), dopamine exists as a cation that can be easily oxidised at an electrode. Therefore, electroanalytical techniques have been widely applied to the investigation of neurochemical systems, leading to a better understanding of neurotransmission. Very often, the concentration of dopamine in extracellular fluid is used as a marker for the diagnosis of several neurodegenerative diseases including Parkinson's, Alzheimer's, schizophrenia, and depression. However, a major challenge during *in vivo* measurement of dopamine is electrode fouling, which is caused by the non-specific adsorption of amphiphilic proteins, peptides and lipids present in the extracellular fluid on a hydrophilic carbon surface. This has often yielded compromising results in time dependent *in vivo* dopamine detection experiments. Notably, application of a carbon electrode with a hydrophobic surface is one of the ways of minimising non-specific adsorption of non-targeted species, which can be easily achieved by hydrogenating the electrode surface using a silane reduction. This hydrogenation mechanism involves the reduction of polycarboxylic acids, ketones, aldehydes, and alcohols to alkanes without any effect on the double bonds and ether. A novelty of this work lies in the application of triethylsilane and phenylsilane hydrogenation to yield a low-oxide surface with sp^3 hybridised carbon, leading to a hydrophobic carbon surface. More specifically, this work is aimed at:

1. fabricating and characterising structurally small carbon electrodes hydrogenated by triethylsilane and phenylsilane;
2. evaluating the antifouling characteristics of the hydrogenated carbon electrodes in a laboratory synthetic fouling solution;
3. examining the analytical performance of the hydrogenated carbon electrodes in two real-life biological samples namely the neuroblastoma SH-SY5Y cell line and mouse brain slices.

Chapter 1 begins with a general introduction of the topic including literature review on recent research conducted using electrochemical sensors in detecting dopamine *in vivo* and in real-life biological systems. This Chapter also describes the research conducted to minimise non-specific adsorption by modifying the sensing surfaces modified using a variety of substances including graphene, carbon nanotubes, conducting polymers such as poly(3,4-ethylenedioxythiophene), Nafion, and polyethylene glycol.

All the reagents and experimental procedures used in this study to acquire data are described in Chapter 2. Specifically, it includes the detailed description of the fabrication of structurally small carbon electrodes, the protocols and instrumentation used in their microscopic, spectroscopic and electrochemical characterisation experiments.

Chapter 3 commences with the fabrication of structurally small carbon electrodes by pyrolysing acetylene in and on pulled quartz capillaries with tip diameters of ~2 μm. Initially, all fabricated carbon electrodes were electrochemically characterised using $[Ru(NH_3)_6]^{3+}$ to identify functioning electrodes. These functioning electrodes were then subjected to hydrogenation using either triethylsilane or phenylsilane in the

presence of anhydrous dichloromethane and a catalyst, tris(pentafluorophenyl) borane, under ambient conditions. Following hydrogenation, scanning electron microscopy, X-ray photoelectron spectroscopy and Raman spectroscopy were used to determine the elemental composition and the sp^3 carbon / sp^2 carbon ratio of the electrodes. This Chapter further describes the electrochemical characterisation of hydrogenated electrodes using different redox markers including $[Fe(CN)_6]^{3-}$, dopamine, dihydroxyphenyl acetic acid, 4-methylcatechol and anthraquinone 2,4 disulfonate to determine their responses towards surface sensitive redox analytes. All the results were compared to those of non-hydrogenated carbon electrodes in evaluating the electrochemical behaviour of the hydrogenated carbon surface.

In Chapter 4, we initially describe the surface characteristic of hydrogenated carbon electrodes using two-dimensional atomic force microscopy. Next, electroanalytical detection performance of dopamine at the hydrogenated carbon electrodes was assessed. The sensitivity and limit of detection of the triethylsilane and phenylsilane hydrogenated electrodes were then estimated from the analytical detection of dopamine in a pH 7.4 citrate/phosphate buffer to be 23.15 pA μM^{-1} and 42.89 pA μM^{-1} (compared to 3.24 pA μM^{-1} at non-hydrogenated carbon electrodes) and 0.84 µM (compared to 2.31 µM at their non-hydrogenated counterpart), respectively. The selectivity towards dopamine in the presence of ascorbic acid and uric acid is also evaluated at hydrogenated carbon electrodes. Finally, the Chapter concludes with the performance comparison between non-hydrogenated and the hydrogenated carbon electrodes in a laboratory synthetic fouling solution containing 2.0% (w/v) bovine serum albumin (a protein), 0.01% (w/v) cytochrome *c* (a protein), 0.001% (w/v) human fibrinopeptide (a peptide) and 1.0% (v/v) caproic acid (a lipid). A 30-min incubation of non-

hydrogenated carbon electrodes in the fouling solution resulted in a 53% decline in the dopamine oxidation limiting current, while a corresponding loss of 23% and 18% was obtained at triethylsilane and phenylsilane hydrogenated carbon electrodes. This shows the robustness and stability of the hydrogenated carbon electrodes in the presence of proteins, peptides and lipids.

As previously discussed in Chapters 3 and 4, one significant challenge during dopamine detection both *in vivo* and *in vitro* is electrode fouling, often caused by adsorption of amphiphilic proteins, peptides and lipids present in the biological fluid on hydrophilic carbon electrode surfaces. Chapter 5 examines the performance of triethylsilane and phenylsilane hydrogenated carbon electrodes in the detection of dopamine in two real-life biological samples, the neuroblastoma cell line SHSY-5Y and brain slices. To evaluate fouling in SH-SY5Y cells, a hydrogenated carbon electrode was positioned close (~1 μm) to the cells with the help of an inverted microscope and a micromanipulator. Using amperometry, a constant potential of +0.5 V (estimated from the cyclic voltammogram of dopamine in a pH 7.4 citrate/phosphate buffer) was applied to the carbon working electrode to promote the oxidation of dopamine released from cells that were continuously depolarised using 0.1 M KCl for 1 h. The transient changes in peak height was compared to determine the degree of electrode fouling. To evaluate fouling in a brain slice, a hydrogenated carbon working electrode was positioned in the brain tissue, while fast scan cyclic voltammetry between -0.4 V and +1.2 V (versus a Ag|AgCl reference electrode) at a potential scan rate of 400 V s^{-1}, and a repetition rate of 10 Hz, was applied to oxidatively detect dopamine for 1 h. The degree of electrode fouling was evaluated by comparing the dopamine oxidation peak before and after the electrodes were applied to brain tissues. The results show that the non-hydrogenated electrodes are easily fouled by proteins, peptides and lipids, while the hydrogenated

carbon electrode electrodes showed resistance towards these biomolecules. We attribute the improved performance of the hydrogenated carbon electrodes to the presence of a hydrophobic surface with low oxygen-containing functional groups that led to weak interaction between the biomolecules and the hydrogenated electrode surface.

Chapter 6 concludes with the outcomes of this study including a summary of the performance of the electrodes fabricated in this study. This study demonstrated the antifouling property of the silane hydrogenated carbon electrodes, which was potentially due to low oxygen-containing functional groups with a hydrophobic surface. In addition, one of the features of silane hydrogenation was the formation of siloxane dendrimers on the sensing surface. The use of a bulky siloxane dendrimers has aided in hindering the adsorption of large biomolecules on the electrode surface. Some suggestions for future work are also presented in this Chapter.

Acknowledgements

I direct all my praise to my Lord Jesus Christ, for to Him belongs all honor and glory. Without His eternal grace, bountiful providence, and unfathomable guidance, this thesis and the findings presented in it would not have been entirely possible. Undertaking a PhD has truly been a life-changing experience for me, and I am utterly humbled by the support and guidance I received from a multitude of people throughout this intriguing and unforgettable journey.

Firstly, I would like to thank my PhD supervisor, Dr. Danny Wong, not only for his continuous academic support, but also for introducing me to so many wonderful opportunities and most importantly for believing in me. I sincerely could not have imagined having a better advisor and mentor for my PhD study and I will always reminisce upon our many deliberations and conversations.

My profound gratitude goes to Dr. Christopher McRae and Dr. Shajahan Siraj for their guidance in the hydrogenation procedures and experimental setup used in this research. I also wish to acknowledge Professor Mark Connor from the Department of Biomedical Sciences for accommodating me in his laboratory to carry out work involving neuroblastoma cells.

I would also like to thank Professor Jill Venton for availing her time during the collaborative visit to the Department of Chemistry, University of Virginia. I also wish to thank and offer my appreciation to Jill's PhD student's Max, Mimi and Yuanyu who helped me in conducting experiments involving brain slices. The collaborative trip would not have been possible without a Macquarie University Postgraduate Research Fund for which I am immensely grateful.

This research would not have been possible without the award of an International Macquarie University Research Scholarship and research grants provided by the Department of Molecular Sciences.

I also wish to extend my thanks to all the friends I met during my three-year candidature at Macquarie University including Nathan, Kavita, Mark, Tom, Preeti, Marina and anyone I may have unintentionally missed.

A special thank you to my family. Words cannot describe how grateful I am to my mum, my mother-in-law, my siblings Shyron, Anesh, Reshma and Vinay for fulfilling my responsibilities and obligations in my absence, and my husband Ronal for all the sacrifices you have made on my behalf.

In remembrance of my late dad, the most selfless person I have ever come across, this thesis is dedicated to you.

Declaration

I hereby declare that this thesis represents my own work and efforts in its entirety and has not been submitted for a higher degree or otherwise at any other university, or institution except where due reference is made in the thesis itself.

R.Roshni

Rita Roshni

8 September 2019

Date

Table of Contents

CHAPTER 1: INTRODUCTION

1.1 Brain Chemistry

Neurotransmitters are chemical messengers secreted by neurons and relay messages to target cells in a brain to regulate human behavior and brain functions. These are usually small molecules stored in discrete intracellular packages known as vesicles. The brain uses neurons to carry information throughout the body using a train of electrical signals[1]. Neurons are the specialised cells that perform the fundamental tasks of information integration and communicate at special appositions *via* synapses or synaptic gaps[2]. These consist of a cell body with two specialised extensions for communicating called dendrites and axons. A synaptic gap (~3 nm) is located between the axons of a neuron and the dendrites of an adjacent neuron[3].

Exocytosis is the main process of chemical communication between cells including neurons[4]. Neurotransmission within a mammalian brain is enabled by synaptic vesicles which are small spherical organelles responsible for storing neurotransmitters and stimulate neurotransmitter release between neurons[5]. Figure 1.1 schematically shows the signalling process of neurotransmitters, in which an electrical impulse called an action potential generated in the axon hillock propagates along the axon. The release of the neurotransmitter is initiated by this action potential and each neuron has a resting membrane potential caused by the ionic concentration gradients. When an appropriate neurotransmitter binds to the receptors on the dendrites, the ion channels open, allowing an influx of Na^+ that changes the membrane potential and initiates firing. This firing causes the voltage-gated Ca^{2+} channels to open in the terminal and the resultant Ca^{2+} influx triggers the vesicles to fuse with the cell membrane and release their contents[6-7].

In this way, neurotransmitter molecules are released into the synaptic cleft. Through diffusive or convective mass transport, neurotransmitter molecules reach and bind to their specific synaptic receptors embedded in the postsynaptic membrane and modulate the electrical state of the postsynaptic neuron[8], or sometimes the neurotransmitters are transported a long distance away causing cascades of reactions through which the signal is propagated[9]. A new action potential is then generated at the axon terminal of the next neuron, followed by a similar release of neurotransmitters so that information is communicated to an adjacent neuron[10]. The chemical signaling molecules modulate postsynaptic cell activity in various ways depending on the identity of the neurotransmitter and the receptors that are involved[11]. Once neurotransmitters are released, uptake and recycling events are necessary for continuous neurotransmission cycles. To terminate neurotransmission these molecules are removed from the synapse by transporters, which are selective membrane-bound proteins that reuptake neurotransmitters with high affinity, and by enzymes that catalytically inactivate the neurotransmitters both in and out of the cell[12].

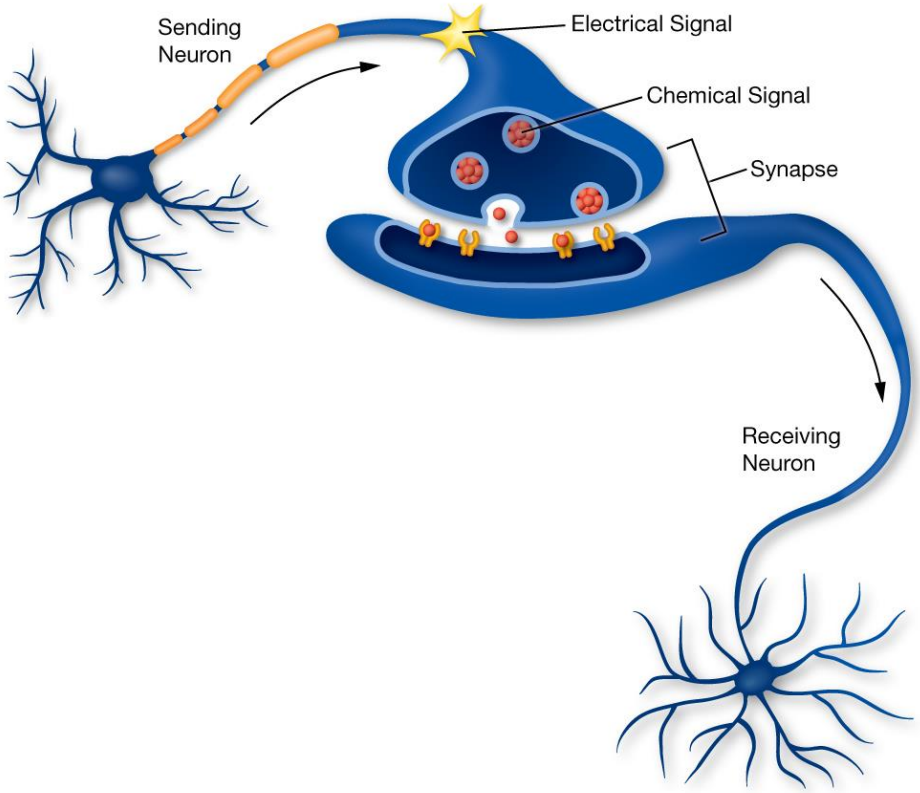

Figure 1.1. Neurotransmission between two cells. Adapted from Reference[13].

Growing experimental evidence has demonstrated that exocytosis does not occur as a simple all-or-nothing process but is adjustable and can occur through different modes including (i) full release, (ii) open-and closed or (iii) kiss-and-run exocytosis. All-or-nothing process involves a fusion event between the secretary vesicle and the plasma membrane during which all the chemical contents are released (full release) and the membrane becomes fully distended to become part of the cell membrane. While work with chemical methods have shown that in contrast to the full release of neurochemical contents, the fusion pore often closes before all the content is released (open and closed release). This type of exocytosis is where a vesicle opens to allow a large portion of the contents to be released before it closes again to end the exocytosis event. This has been reported to be the dominant mechanism in terms of frequency of these events[14]. The "kiss and run" type of exocytosis involves an initial fusion of pores of a vesicle

with the cell membrane followed by a rapid closure again with only a tiny fraction of the contents being released[4, 9]. However, currently not much is known of how this regulation occurs or which factors influence the mode of exocytosis, probably for the lack of technical approaches to determine the extent of the fraction released upon each fusion event[4].

1.2 Classification of Neurotransmitters

Neurotransmitters can be classified into several distinct groups according to 1) their molecular structure; 2) their mode of direct action or as a neuromodulator; and 3) their excitatory or inhibitory physiological functions[15]. We have categorised neurotransmitters based on their chemical structures to amino acids, biogenic amines, acetylcholine and soluble gases with their associated diseases as summarised in Table 1.1. However, in this study we will only emphasise on biogenic amines, also known as monoamine neurotransmitters.

1.2.1 Monoamine Neurotransmitters

Monoamine neurotransmitters are generally small nonpeptide molecules that are not encoded by genes but rather (mostly enzymatically) synthesised from precursors taken up with nutrition[16]. For example, the derivatives of amino acids, whereby, 5-hydroxy tryptamine (serotonin) is produced from tryptophan through the enzymes tryptophane hydroxylase and aromatic L-amino-acid decarboxylase. The catecholamines dopamine, noradrenaline, and adrenaline are synthesised from each other starting from the amino acid tyrosine, which is converted to 3,4-dihydroxyphenylalanine (DOPA) through tyrosine hydroxylase. DOPA is then metabolised to dopamine through aromatic L-amino-acid decarboxylase (DOPA-decarboxylase) and is then taken up into

presynaptic vesicles *via* the vesicular monoamine transporter 2. In noradrenergic cells or chromaffin cells of the adrenal medulla, these vesicles possess membrane-bound dopamine-β-hydroxylase that produces noradrenalin. In adrenergic and chromaffin cells (body's main source of uptaking and circulating catecholamines), noradrenaline is released back into the cytoplasm *via* the vesicular monoamine transporter 1 and here it is converted into adrenalin through phenylethanolamine-N-methyltransferase[16]. A comprehensive metabolism pathway of neurotransmitters is presented in Scheme 1.1.

Dopamine, serotonin, norepinephrine and epinephrine are important neurotransmitters that belong to the monoamine neurotransmitter group. These are a fundamental class of transmitters, and many of them are electroactive which means they can be electrochemically detected at an electrode directly implanted into the brain[17]. Hence, the chemical fluctuations can be quantitatively studied [12].

Table 1.1: Classification of neurotransmitters and associated diseases. Adapted from reference[10].

Category	Analytes	Associated diseases
Amino acid	Glutamic acid	Seizures, neural degeneration, lethargy, cognitive dysfunction
	Aspartic acid	Stroke, chronic fatigue syndrome, depression, Huntington's disease
	Tyrosine	Parkinson's disease, a behavioral deficit
Biogenic amines	Nor-epinephrine	Schizophrenia, depression, ADD (Attention deficit disorder)
	Epinephrine	Depression, Addison's disease, palpitation, high blood pressure
	Dopamine	Tourette's disease, schizophrenia, psychosis, depression, Parkinson's disease, ADD
	Serotonin	Depression, anxiety disorders, especially obsessive-compulsive disorder
	Histamine	Immune system disorder, schizophrenia, convulsion, seizure, and Parkinson's disease
Acetyl choline	Acetylcholine, choline	Depression, Alzheimer's disease, dementia
Soluble gases	Nitric oxide	Huntington's disease, Alzheimer's Parkinson's disease, vascular stroke.
	Hydrogen sulphide	Down syndrome, Chronic obstructive pulmonary disease

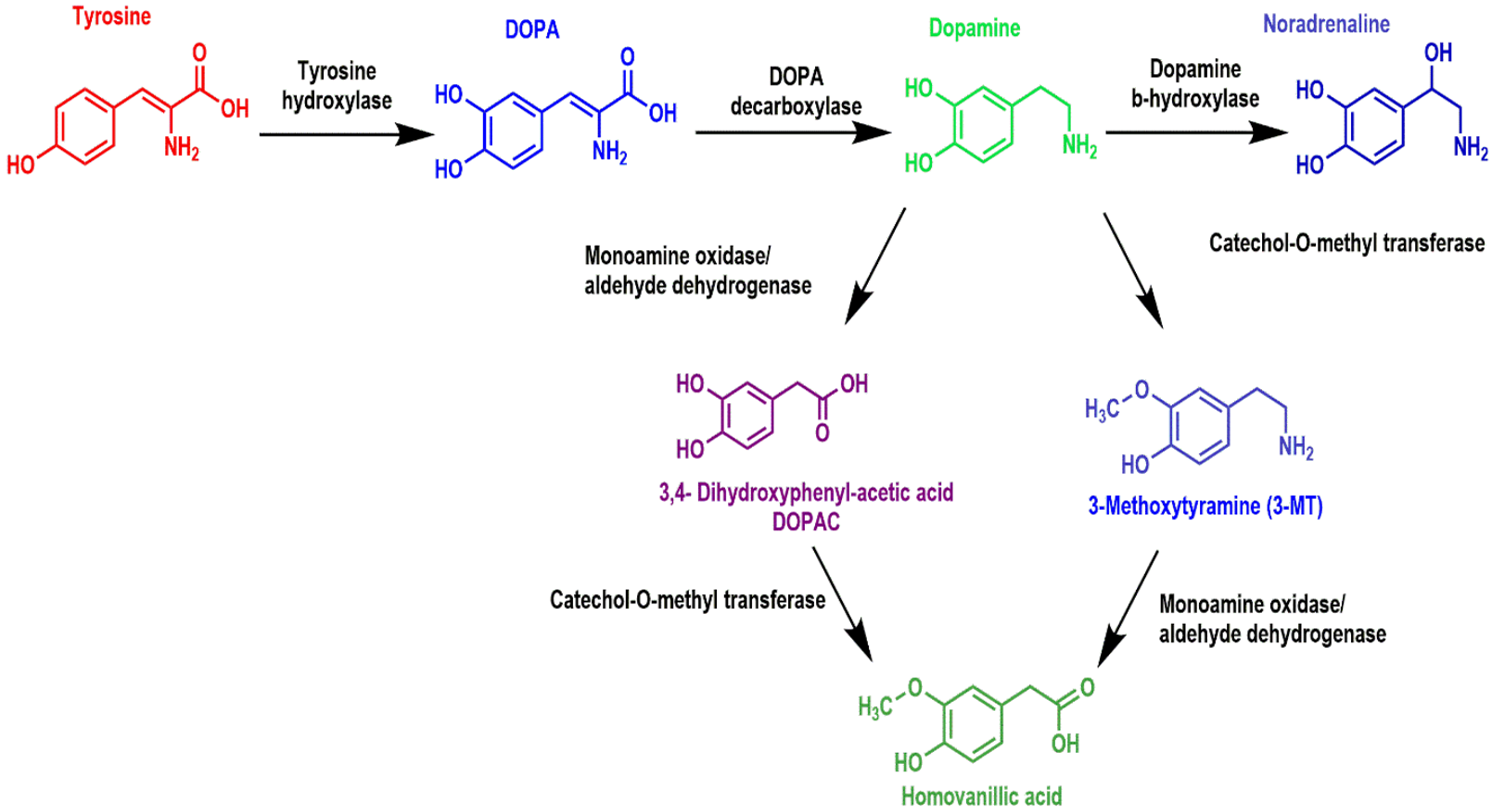

Scheme 1.1. Metabolism of neurotransmitters. Adapted from reference[16].

Several diseases of the brain are either due to or associated with the spatial and temporal kinetics of these neurotransmitters where any changes in the concentration of neurotransmitters usually lead to severe neurological disorders that require continuous healthcare support. For example, psychiatric and neurodegenerative diseases such as depression, Parkinson's, Huntington's, schizophrenia, glaucoma, and several types of drug and alcohol abuse are directly linked with abnormalities of neurotransmission in the brain[17-18]. Additionally, reports of mood disorders and substance abuse, perhaps due to modern societal and environmental stressors, are surging [12]. New advances in neuroscience are now presenting that many diseases affect multiple neurotransmitter systems. For instance, interactions of dopamine and serotonin systems are known to occur in schizophrenia[19]. In addition to this, pharmacological agents such as cocaine exert effects on both dopamine and serotonin transporters, which regulate neurotransmission by clearing the neurotransmitter from the extracellular space[20].

1.2.1.1 Dopamine

Dopamine is an inhibitory neurotransmitter (discovered in the 1950s by Arvid Carlsson[21]) that plays a significant role in the regulation of physiological events such as movement, behaviour and stress. It is synthesised in the neuron from L-DOPA using the enzyme DOPA decarboxylase and then packaged into membrane-bound vesicles (Scheme 1.1). The neurotransmission of dopamine occurs among the neurons crossing the striatum and other sites of basal ganglia in the brain[22].

Dopaminergic neurons contain two types of projections attached to the cell body namely dendrites and an axon, where dopamine is released at the terminal of an axon and received by the dendrites of the adjacent neurons. Most of the dopaminergic cell bodies are in the sabstantia nigra/ventral tegmental area, and their axons project to

various regions, including the caudate-putamen or the nucleus accumbens[23]. The average levels of dopamine in human blood and serum samples are estimated to be between 10^{-6} to 10^{-9} M range[24]. Alterations in the optimal concentration of dopamine (195.8 pmol L^{-1}) has been associated with various neurodegenerative and psychotic disorders including schizophrenia, addiction, epilepsy and Parkinson's diseases where the brain dopamine neurons experience degeneration[25-27]. For instance, during Parkinson's disease, the most serious loss of dopaminergic neurotransmission arises in the caudate-putamen, and consequently, this region has been associated with motor control[6]. Dopamine transients in rats were shown to range from 50 to 100 nM and they would reach higher than 200 nM with the use of drugs[28]. Specific monoamines such as dopamine, epinephrine, and norepinephrine are found in high levels ranging from 0.1 to 1.0 M in adrenal chromaffin cells and also the related rat adrenal pheochromocytoma cells (PC12 cells)[9].

1.2.1.2 Norepinephrine

Norepinephrine is one of the key monoamine neurotransmitters in the central nervous system and peripheral organs of vertebrate organisms, and plays a significant role in a plethora of physiological processes, permitting these organisms to cope with their ever changing internal and external environments[29]. It is released *via* exocytosis in the synaptic cleft and is transported by passive diffusion to the postsynaptic membrane where it activates R- and α-adrenergic receptors leading to the propagation of a nerve impulse[30]. Norepinephrine from presynaptic terminals binds to different subtypes of adrenergic receptors to elicit a variety of physiological and pharmacological responses. In the nervous system, norepinephrine plays critical roles such as regulating blood pressure[31] and heart functions[32]. It also has strong effects on attention and response

activities within the brain and is involved in the fight-or-flight responses, directly increasing heart rate, activating glucose release from energy stores, and increasing blood flow to skeletal muscles[30]. Enzymes such as catechol-*o*-methyltransferase or monoamine oxidases can enzymatically degrade extracellular norepinephrine and it can also be taken back into the presynaptic terminal by the norepinephrine transporter called a Na/K pump[33]. The enzymatic degradation and re-uptake to the presynaptic terminal control the levels of extracellular norepinephrine at the synapse. Collective evidence suggests the involvement of norepinephrine systems in Alzheimer's disease, with the progress of Alzheimer's disease showing a profound neuronal loss in the locus coeruleus where the majority of noradrenergic neurons are located[34]. Normal norepinephrine levels in plasma are 0 to 600 pg/mL, and although usual plasma concentrations are often 176 to 386 pg mL^{-1} it has been reported that during or after stress the levels increases by almost 20-fold[35].

1.2.1.3 Epinephrine

Epinephrine is also an important neurotransmitter and a hormone. It is often used in medications that allow the transmission of messages between two nerve cells[36]. It is the last in the biosynthesis line of catecholamines that is converted from norepinephrine by the enzyme phentolamine N-methyltransferase and is related to the fight-or-flight response of the autonomic nervous system. It is a hormone released from the adrenal medulla in response to stress and is meditated by sympathetic fibres[36]. As with dopamine and norepinephrine, the mission of epinephrine can be terminated by different mechanisms including oxidation, however, under physiological conditions (pH 7.4), the auto-oxidation of epinephrine proceeds gradually; although its rate can be improved by increasing the pH[37] and enzymatic degradation. Epinephrine does not

have its own receptors. Instead as its chemical structure resembles norepinephrine, epinephrine stimulates norepinephrine receptors both in the brain as well as peripherally[38].

1.2.1.4 Serotonin

Serotonin is a neurotransmitter involved in the regulation of numerous behavioural and biological functions in the body; playing a role in both psychological processes in the central nervous system as well as in peripheral tissues such as the bone and gut[39-40]. While serotonin is best known as a neurotransmitter in the brain, close to 95% of the serotonin in the body is actually synthesised, stored, and released by cells in the intestinal mucosa known as enterochromaffin cells[41-42]. Enterochromaffin cells are a subtype of intestinal enteroendocrine cells that generate serotonin from the dietary amino acid L-tryptophan using the rate-limiting enzyme tryptophan hydroxylase[43]. Serotonin is synthesised from its precursor the dietary acquired essential amino acid L-tryptophan, by the enzyme tryptophan hydroxylase 1 in the periphery and pineal gland, and by the enzyme tryptophan hydroxylase 2 in the central nervous system[44]. Although the enteric nervous system of the gut contains the majority (>95%) of the body's serotonin, it is within the central nervous system that this neurotransmitter mediates mood, appetite, and behaviours including aggression and sociability. Serotonin is implicated in sensory, motor, emotional, and cognitive processing and is thought to be involved to some extent in most psychiatric disorders[45]. The most well-identified functions of serotonin are its involvement in anxiety, depression, and impulsivity[46]. Low levels of serotonin (<101 to 283 ng mL^{-1}) in the brain may be an indicator of depression, while its presence in the blood, serum, plasma, and platelets may be considered as a peripheral biochemical marker for depression[47].

1.3 Significance of neurotransmitter detection

All neurotransmitters are medically important. Therefore, the detection and analysis of these molecules plays a vital role in the diagnosis and treatment of neurodegenerative and psychotic diseases. Real time measurement of neurotransmitters will help neuroscientists address questions related to the microscopic steps of release and uptake[7]. Some of the questions include:

1. the size units that contain the neurotransmitter molecules;
2. the kinetics that control vesicular opening;
3. if there is only a single type of neurotransmitter present in each vesicle;
4. the half-life of a neurotransmitter after release.

Neurotransmitters are recognised as vital regulators of cognition and behaviour. However, very little is known about their effects on human brain processing owing to the absence of a reliable method to study neurotransmission in a live human brain[48]. Monitoring neurotransmitter levels is a major research strategy for determining the functions of neuronal systems, specifically the ascending neuromodulator systems[49]. The accurate measurement of the neurotransmitters in the brain would provide a better understanding of the associated diseases as well as a tool to follow up on the possible treatments. Additionally, monitoring the chemical dynamics in the synaptic cleft, where the neurotransmitter molecules are released and with millisecond time resolution, would provide better understanding of neurotransmission processes. Moreover, several neurological disorders of the brain such as epilepsy, schizophrenia, Alzheimer's, Parkinson's disease and their exact pathological mechanisms are yet to be elucidated, impeding the development of new therapeutics. Monitoring neurotransmitter concentration changes will help address the mechanisms behind these

neurological disorders and allow for a better understanding of the brain functions. Monoamines are amenable to real-time electrochemical detection using fast-scan cyclic voltammetry, which allows resolution of the sub-second dynamics of release and re-uptake in response to a single action potential[46]. This approach has greatly improved the understanding of dopamine transmission and has facilitated an integrated view of how dopamine mediates behavioural control. For instance, the most well-identified functions of serotonin are its involvement in anxiety, depression, and impulsivity[45]. Although detailed knowledge on the pharmacological and cellular effects of antidepressants, anxiolytics and other psychotropic drugs that target the serotonin system has emerged, there is no detailed relationship of how these drugs translate into raised mood or decreased anxiety. Similarly, anxiolysis on reducing brain serotonin is well established, suggesting that serotonin increases anxiety[46]. However, anxiety is often related to depression which is naturally associated with low serotonin levels. This suggests that there is no collective relationship between serotonin levels and behaviour. However, it is also possible that studies to date have not provided a sufficiently detailed understanding of serotonin signalling on a time scale that is commensurate with neuronal transmission. An understanding of the detailed dynamics of serotonin might, therefore, clarify how serotonin governs behaviour[46].

1.4 Methods of neurotransmitter detection

The main detection strategies for neurotransmitters in the brain are *in vivo* and *in vitro* methods, each of which holds specific advantages and disadvantages. *In vitro* methods are usually simpler, though they often require a freshly deceased organism and a skilled dissector[50]. Although most *in vitro* studies provide varying information on the chemical environment of the tissue of interest, *in vivo* techniques compliment largely the

chemical and/or spatial evidence obtained *in vitro* by providing a sampling method that is perfect for time-dependent studies. Several examples of *in vivo* techniques commonly used for neurotransmitters detection are described below.

1.4.1 Microdialysis

Microdialysis is an *in vivo* technique that allows continuous sampling of the small molecular weight substances such as neurotransmitters from the extracellular space in the brain of a freely moving animal[51]. Although implantation of the probe has to be conducted under anaesthesia, this can also be achieved in awake and freely moving animals as it is not painful[52]. Small molecules can exchange across the membrane, and the internal fluid is removed for chemical analysis without further purification as the obtained dialysate is pure and does not contain protein. Schematic diagram of a microdialysis probe is shown in Figure 1.2.

A major element of microdialysis is the probe with a semi-permeable membrane. Molecules in extracellular fluid surrounding the probe pass through the dialysis membrane where they passively diffuse along their concentration gradient from an area of higher to an area of lower concentration as explained by Fick's first law of diffusion[51]. The permeability of the probe is determined by parameters such as material and pore size of the dialysis membrane, surface area, and perfusion rate. The diffusion of substances in or out of the probe is limited by their molecular weight, shape, and charge.

Monitoring neurotransmitters using microdialysis in the brain extracellular environment has several distinct advantages. Firstly, it can be used to study a diverse range of neurotransmitters. The chemical resolution is very good because the dialysate,

which is removed from the brain, can be analysed with a variety of techniques. Although efforts are underway to improve the time resolution of microdialysis, samples are typically collected at 1-10 min intervals, making this technique best suited for measuring changes on a minute timescale[6].

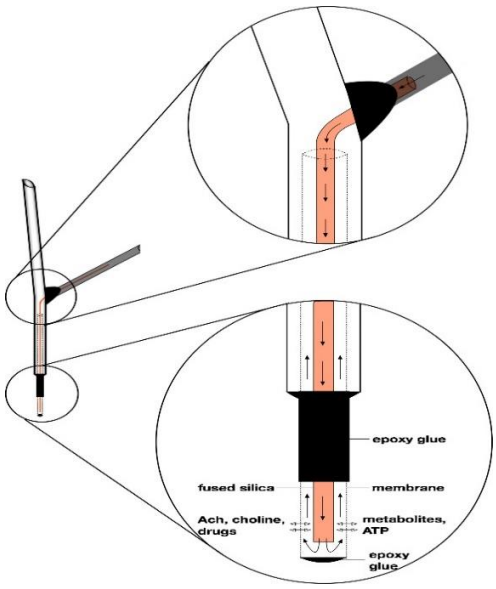

Figure 1.2. Schematic illustration of a microdialysis probe. Adapted from reference[53].

There are considerable problems associated with microdialysis. Firstly, microdialysis experiments include invasive techniques and brain damage has been frequently reported as the size of the microdialysis probe is typically >200 µm in diameter, which is large compared to the size (~ 1 µm) of the nerve terminal[28, 51]. Several groups have reported that there is an immune response after the probe implantation affecting the integrity of the blood-brain barrier with a decrease in the flow of blood in the area and abnormal release of neurotransmitters[54]. In addition to this, these experiments are based on the collection of dialysate through a concentration gradient, which in conjunction with the

invasive nature of the procedure, may cause significant tissue damage and potentially misleading results[50]. This technique was originally thought to measure absolute concentrations of the species of interest in the extracellular fluid when used with the "no-net-flux" technique or with ultra-low flow rate. "No-net-flux" is observed when the concentration of the analyte in the perfusate and the surrounding tissue is equal. This may potentially compromise the results as the "no-net-flux" equilibrium position also includes the balance between the rate of uptake and diffusion of neurochemicals through the damaged tissues near the probe and the technique is time-consuming[28]. An equilibrium between the dialysate and the tissue is not established when the commonly used flowrates are employed during the sample collection (0.5-2 μL min^{-1}) which affects the recovery. However, by using ultra-low flow rates (0.05-0.5 μL min^{-1}), the equilibrium can be established leading to 100% recovery[54]. Despite these drawbacks, observed concentration changes of neurotransmitters in a millisecond timescale with a variety of manipulations suggests that the information obtained using this technique does not provide insights into neuronal processes.

1.4.2 Chromatographic techniques

Liquid chromatography with mass spectrometry detection has been used to quantify neurotransmitters in various biological matrices and derivatisation or addition of iron pair reagents was used to achieve good chromatographic separation[55]. The quantification of catecholamines in biological samples using this technique typically involves elaborate and labor-intensive clean up processes not only due to their low physiological concentrations and chemical instability, but also due to the complexity of biological matrices and to the presence of potentially interfering compounds[56]. Using this technique, biological sample preparation including homogenisation and metabolic

extraction become a critical step in an accurate and reliable assay. Zhang *et al.*[57] derivatised a method to simultaneously detect serotonin, dopamine and norepinephrine using microdialysis coupled with liquid chromatography-mass spectrometry. The brain microdialysate concentration of serotonin, dopamine and epinephrine are usually in the sub pM range[58]. They were able to achieve a limit of detection between 60-100 pM range for serotonin, dopamine, and norepinephrine but were unable to acquire good linearity around the calibration range of sub pM due to background peak interference. Similarly, Olesti *et al.*[15] reported the development and validation of liquid chromatography-tandem mass spectrometry for simultaneous detection of 16 endogenous small polar compounds in rat plasma and brain homogenates. Although a lot of researchers were able to obtain a limit of detection of <100 pM, most chromatographic separation requires minutes to hours for simultaneous quantification of the neurotransmitters[55, 57]. Very often, chromatographic techniques require the dialysate to be pre-treated to obtain accurate and reliable results. The detection procedures using microdialysis coupled with chromatographic techniques are very slow and frequently require extensive sample preparation steps. Hence, these techniques are not appropriate for real-time detection of neurotransmitters *in vivo* as the concentrations of these analytes fluctuate within seconds.

1.4.3 Electrochemical methods

Electrochemical techniques have been identified as a simple, inexpensive, and less time-consuming process to detect the neurotransmitters in the brain as a majority of neurotransmitters present in the brain are electrochemically active[59]. For example, under physiological pH (p*Ka* 8.86)[60], dopamine exists mostly as a cation. As novel electrode materials are rapidly evolving to improve sensitivity and selectivity,

electrochemical techniques play a major part in the understanding of synaptic neural networks and thus the development of synapse-based neural interfaces[61]. A variety of electrochemical techniques including fast-scan cyclic voltammetry, high speed chronoamperometry and constant potential amperometry have been reported[17] for the detection of neurotransmitters both *in vivo* and *in vitro*.

The detection of neurotransmitters is generally through the oxidation or reduction of the targeted neurotransmitter at the electrode surface and the corresponding current generated provides a quantitative measure of the dynamic chemical changes[62]. Electrochemical methods have several advantages which include low fabrication costs, minimal power requirements, simple designs, facile user interfaces, ease of miniaturisation of electrodes, robust measurements, low detection limits, and small operating volumes[63].

Voltammetry is suited for the study of the dynamics of intracellular communications due to its high temporal and spatial resolution and excellent sensitivity. Voltammetric techniques are extensively applied to *in vivo* measurements in anaesthetised and awake animals, *ex vivo* measurements in brain slices and synaptosomes, *in vitro* measurements from peripheral cells, and for interrogating neurotransmitter release from single cells[64]. Moreover, voltammetric methods particularly amperometry have been used to investigate a variety of neurochemicals (*e.g*. dopamine, norepinephrine, serotonin, ascorbate, uric acid, adenosine, choline, and acetylcholine) with the aim of understanding chemical neurotransmission and its role in normal and altered brain functions. For example, Tertis *et al.*[65] applied a tailored platform consisting of electrochemically generated polypyrrole that was decorated with gold nanoparticles to detect serotonin. They reported improved surface properties attributable to a 73%

increased active surface arising from polypyrrole nanostructure and a catalytic effect from the gold nanoparticles. This sensor exhibited recoveries between 100.3% and 103.1% serotonin in human serum samples.

Li *et al.*[66] developed a carboxyl-functionalised mesoporous molecular sieve/colloidal gold modified nano-carbon ionic liquid paste electrode for electrochemical detection of serotonin. The modified electrode presented was demonstrated to show good electrocatalytic properties towards serotonin. For comparison, the authors used a conventional carbon paste electrode and nano-carbon paste electrode prepared using nano-graphite powder and paraffin oil. They reported a 2.4-fold higher serotonin oxidation current at the nano-carbon paste electrode whereas they obtained a 2.8-fold higher current at the gold modified nano-carbon ionic liquid paste electrode.

Haldorai *et al.*[67] used a TiN-reduced graphene oxide nanocomposite glassy carbon electrode to detect dopamine in urine samples. They obtained a detection sensitivity of 35.8 $\mu A\ \mu M^{-1}\ cm^{-2}$ and observed 97-101% recoveries of dopamine. The authors attributed this to the fast electron transfer kinetics and a good electrocatalytic response towards dopamine. Singh *et al.*[68] applied a N'-phenyl-p-phenylenediamine/multiwalled carbon nanotubes modified screen-printed electrode for the detection of the neurotransmitter dopamine. The authors reported enhanced dopamine oxidation signal attributable to the electrode active area of screen-printed electrode of 1.1×10^{-9} mol/cm^2 relative to 4.3×10^{-10} mol cm^{-2} of glassy carbon electrode. Based on a standard addition procedure, the authors obtained a 97.6% to 103.5% recovery of dopamine in a dopamine hydrochloride injection[68]. Although considerable success has been achieved in this area of research, most of the

modification procedures require very complex and demanding procedures or synthesis.

A widely used method for quantifying exocytosis with high temporal resolution is amperometry [4]. During amperometric detection, the electrode is held at a constant potential to oxidise the analyte of interest and the oxidation current is measured as a function of time. This technique offers excellent response time and sensitivity but poor selectivity because all electroactive species with a similar oxidation potential can contribute to the signal arising from dopamine release that occurs on a millisecond timescale. Amperometric detection methods relying on the electroactive properties of many biological amines such as dopamine, norepinephrine, epinephrine, histamine and serotonin have been used to analyse single cell exocytosis for almost 30 years[69]. During amperometric measurements, a microelectrode is typically placed close to the cell surface with a sufficiently oxidative applied potential to oxidise the analyte of interest. When exocytosis occurs, the released transmitters are oxidised at the electrode with a 'spike-like' feature of oxidative current and the analysis of size and shape of the spike provides the direct information of the dynamics of the releasing events[4].

Recently, Ewing's group developed two technical approaches to measure the vesicular content known as 'intracellular vesicle impact electrochemical cytometry', where a thin and sharp nanotip carbon-fibre electrode is placed inside the cell by carefully penetrating the plasma membrane. Secretary vesicles then adsorb and stochastically break on the active microsurface of the electrode. This method permits the detection of the contents in the native environment of the organelles[70]. The other technique is known as 'vesicle impact electrochemical cytometry' which works based on a similar mechanism, but instead of *in-situ* measurements, the vesicles are isolated and

maintained in suspension in an intracellular physiological buffer[4, 9]. This technique has the advantage of allowing the modification of the bathing media, thus treatment of secretary vesicles without potential interference from the rest of the cellular mechanisms[71].

1.5 *In vivo* detection of neurotransmitters using microelectrodes

Carbon-based microelectrodes are typically employed for the detection of neurotransmitters as they offer advantages including wide potential window, low background current and high electrical conductivity. The development and application of carbon microelectrodes over the past decades has gained a lot of attention mainly for electrochemical applications owing to the advantages bestowed by their micrometre dimension[72]. The use of a small electrode imparts several unique features during *in vivo* electrochemical measurement such as nonlinear diffusion, enhanced mass transport, and low capacitance facilitating fast response time[73]. Firstly, the small dimension of the electrode allows for rapid alteration of the applied potential, where rapid sweeping is necessary in fast scan cyclic voltammetry. Secondly, the small dimension of the electrode minimises tissue damage caused by electrode penetration. The implantation of a 7-µm diameter carbon fibre electrode has been reported to elicit a significantly less immune response than a 200-µm diameter microdialysis probe in a rat dorsal striatum[74]. In addition to this, the small dimension of the electrodes improves the quality of analysis and the following range of experiments then became possible. Notably, the small dimension of microelectrodes makes them most suitable for *in vivo* measurements, such as the detection of a neurotransmitter in a brain performed in a very small sample volume. The small size of the microelectrodes also permits careful selection of neuronal regions to be investigated[75]. Some of the commonly used

examples of carbon-based microelectrodes used for *in vivo* detection of neurotransmitters such as carbon fiber electrodes, carbon nanopipette electrode and boron-doped diamond electrodes are presented in Figure 1.3.

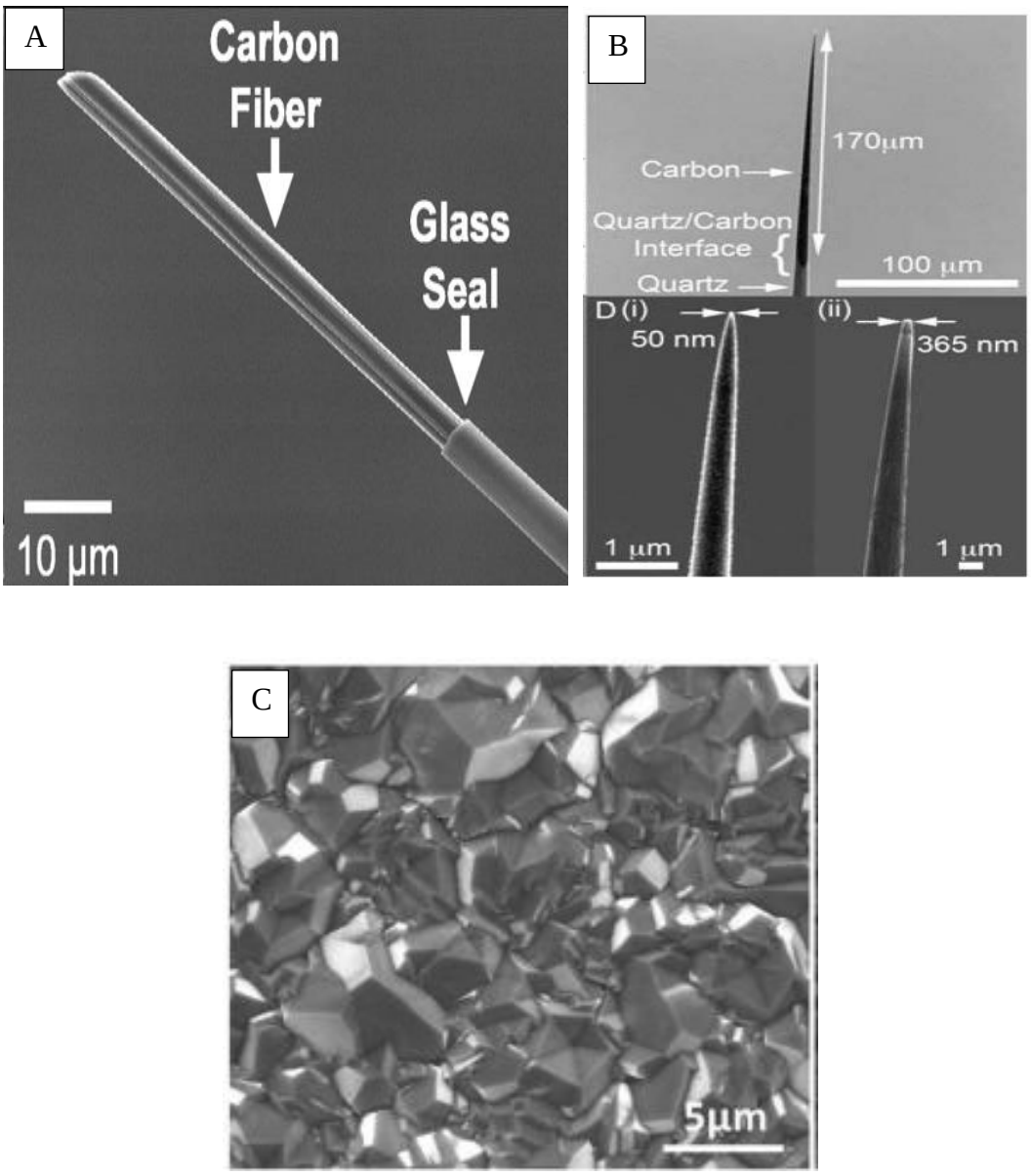

Figure 1.3. Scanning electron micrographs of a (A) carbon fibre electrode[76], (B) a carbon nanopipette electrode[77] and (C) boron-doped diamond electrode[26].

For example, Jaquins-Gerstl and Micheal[74] reported a substantially higher concentration of dopamine levels detected using voltammetry than microdialysis. The

idea is that as the result of the smaller penetration injury caused by microelectrodes, their closer position to dopamine terminals provides a simple explanation for the higher voltammetry-based concentration values. The importance of a smaller distance between the electrode and nearby dopamine terminals has a two-fold origin. Firstly, once dopamine is released into the extracellular space, the distance it can diffuse is controlled by an avid uptake mechanism. Second, if each dopamine terminal is regarded as a source of dopamine, then dopamine undergoes dilution as it diffuses from the terminal into an ever-expanding volume of extracellular space. These two effects combine to form a 'diffusion sphere' of dopamine around each dopamine terminal. Positioning the electrode closer to dopamine terminals enables the detection of dopamine within the diffusion sphere, *i.e.* before the dopamine concentration decreases due to the actions of dopamine uptake and dilution[78].

1.5.1 Carbon fibre microelectrodes

While an electrode with a sharp tip with good mechanical strength is desired during an *in vivo* measurement for easy membrane penetration with minimum tissue damage, it is also important that such an electrode is easily fabricated with high sensitivity to detect nanomolar concentrations. Among the microelectrodes fabricated for *in vivo* measurements, carbon fibre electrodes are among the most commonly used electrodes for electrochemical detection of neurotransmitters. Carbon fibre microelectrodes are often fabricated by sealing a carbon fibre in a pulled capillary such that a 100-500 μm length is left protruding outside the capillary[75, 79]. The larger cylindrical surface area compared to that of an ultra-small carbon ring electrode often used in intracellular voltammetry is readily accessible for diffusing species giving rise to a higher detection

signal at the carbon fibre electrodes[80]. This is an essential feature in measuring analytes of interest present in trace levels *in vivo*.

More recently, Venton's group has reported the fabrication of fibres made of carbon nanotubes with easy fabrication procedure[81-82]. For example, Ross and Venton employed a Nafion-carbon nanotube coated carbon fibre electrode for enhanced detection of andenosine and to minimise interference from adenosine triphosphate because the electroactive moiety, adenine, is the same for both molecules[81]. Nafion is a permselective polymer that enhances sensitivity to cations and decreases sensitivity to anions. At physiological pH adenosine triphosphate is negatively charged while adenosine is neutral. Thus, Nafion coated carbon fibre electrode discriminated against adenosine from adenosine triphosphates due to charge repulsion between Nafion and adenosine triphosphate. In separate work, Venton's group also reported the fabrication of polyethylene carbon nanotube fibre electrode, chlorosulfonic acid carbon nanotube fibre electrode and carbon nanotube yarn electrode for neurotransmitter detection[82]. Highest dopamine oxidation current density and fast electron transfer kinetics was obtained using carbon nanotube yarn electrode attributable to the purity of carbon nanotubes, the abundance of oxygen containing functionalities, and moderate surface roughness. Their work concluded that small crevices, high conductivity and abundant oxygen containing functional groups, led to high sensitivity for amine neurotransmitter detection such as dopamine and serotonin.

Oh *et al.*[83] used a poly(3,4-ethylenedioxythiophene) : Nafion modified carbon fibre microelectrode to measure tonic levels of dopamine *in vivo* by multiple cyclic square wave voltammetry. They reported a tonic concentration of 120 ± 18 nM with high selectivity against ascorbic acid and 3,4-dihydroxyphenylacteic acid. Pharmacological

treatments with different dopaminergic agents were also used to modulate the tonic dopamine levels and study selectivity towards dopamine *in vivo*. Their work demonstrated the measurement of changes in the tonic levels of dopamine in the central dopaminergic neuronal systems and advanced our understanding on the range of neurological and psychiatric disorders and the fundamental relationship between neurochemistry, neuropharmacology and behaviour.

Zu *et al.*[84] prepared a graphene-iron tetrasulfophthalocyanine modified carbon fibre microelectrode to measure dopamine and serotonin simultaneously in a mouse brain cortex using differential pulse voltammetry. They demonstrated the effects of a Chinese medicine, Gou-teng, towards the concentration of both dopamine and serotonin and concluded that it has similar pharmacological effects to that of antipsychotic medicine. Their work demonstrated the application of electrochemical methods in studying the effects of traditional medicine which could possibly be an effective tool for pharmacology, physiology, and pathology studies. Hashemi *et al.*[85] conducted simultaneous detection of serotonin and histamine in the rat *substantia nigra pars reticulata* by electrical stimulation in the mid forebrain bundle using a carbon fibre microelectrode. This mid forebrain stimulation led to the simultaneous release of serotonin and an additional species in the *substantia nigra pars reticulata*. Using fast scan cyclic voltammetry, this species was confirmed to be histamine. Their work highlighted the importance of *in vivo* voltammetric techniques in exploring the dynamics of neurotransmitters.

Notably, owing to the soft mechanical strength of carbon fibres, the frequent vibrations under a microscope often make it a challenging task to manipulate the electrode into the microenvironment within the specimen being investigated in an *in vivo* detection

experiment. In addition, it is a challenge to penetrate such an electrode through the cell membrane during the *in vivo* detection of neurotransmitters[75].

1.5.2 Structurally small conical-tip carbon electrodes

Several researchers have reported the use of nanopipette electrodes for monitoring the neurotransmitters in the brain. Rees *et al.*[86] reported the detection of dopamine in drosophila using carbon nanopipette electrode. Specifically, carbon was deposited using chemical vapor deposition at 900 °C inside a pulled quartz capillary. The capillary with carbon deposit was then chemically etched to expose the carbon tip with 50 - 400 nm diameters. More recently, Yang *et al.*[87] reported the detection of dopamine using cavity carbon-nanopipette fabricated by depositing carbon inside the pulled capillary using chemical vapor deposition using methane and argon at 945 °C. They reported cavity-carbon nanopipette electrodes with tip diameters within the range of few hundreds of nanometres for nanoscale electrochemistry. High currents were observed at the fabricated electrodes due to small cavity traps which increases the local dopamine concentration. The trapping resulted in fast-scan cyclic voltammetry frequency-independent responses. Additionally, exogenously applied dopamine was detected in the brain slices showing the they do not clog in tissue[87]. Ding *et al.*[88] developed a glass-sealed gold nanoelectrode for the *in vivo* monitoring of dopamine. They fabricated the electrodes by first pre-thinning the silica capillaries using a laser puller, before introducing a gold wire that was pulled down to a fine tip, and finally sealing using epoxy resin. To further enhance electron transfer kinetics, they electrodeposited gold nanostructures on the electrode surface. Using this gold nanostructure modified gold nanowire electrode, they were able to report 6.3-fold higher sensitivity during detection of dopamine *in vivo*.

Our laboratory has reported the use of conical-tip carbon electrodes fabricated in and on the shank of pulled quartz capillaries (< 2 μm tip diameter and ~ 8 μm axial length) for *in vivo* and *in vitro* monitoring of dopamine[89-90]. There are several advantages of conical-tip carbon electrodes over conventionally used carbon fibre electrodes. The quartz substrate provides mechanical strength, while a sharp tip aids in easy membrane penetration with minimal tissue damage during implantation. Additionally, the open-ended based edge of a conical-tip electrode is more accessible to the mass transport of the analyte, compared to an insulating plane at the finite capillary-fibre junction on carbon fibre electrodes. Therefore, conical-tip carbon electrodes of a similar dimension to carbon fibre electrode were found to show an improved signal-to-noise ratio in detecting dopamine[80].

1.6 Graphite and sp^2 hybridised carbon electrode materials for neurotransmitter detection

Electrochemical sensors based on carbon have been extensively used as electrode materials in the detection of neurotransmitters[91]. The slower oxygen kinetics and hydrogen evolution on carbon than most commonly used metal electrodes gives rise to a wide potential window of carbon materials for electrodes[92]. Examples of carbon based electrochemical sensors include glassy carbon electrodes[67], carbon fibre electrodes, diamond electrodes (boron or nitrogen doped)[93-94], and conical-tip carbon electrodes[95].

Glassy carbon is widely used in electrochemistry due to its properties of high temperature resistance, hardness, low density and low electrical resistance[96]. It is a type of non-graphitic carbon formed by pyrolysis of polymeric precursors such as

phenylcarbyne[97] and polymerised furfuryl alcohol[98] . The microstructure of glassy carbon is composed of discrete fragments of curved carbon planes, akin to imperfect fullerene-related nanoparticles. Several researchers have reported the detection of transmitters using bare/modified glassy carbon electrodes. For example, Shahbakhsh and Noroozifa[99] reported the application of a polydopamine-multiwalled carbon nanotube modified glassy carbon electrode for the simultaneous detection of dopamine, acetaminophen, and xanthin. The authors attributed this to the electrocatalytic oxidation of all three analytes by the dopamine/dopamine-quinone functional groups from polydopamine coated multiwalled carbon nanotubes[99]. Similarly, Selvarajan *et al.*[100] developed a Ag/polypyrrole/Cu_2O nanocomposite immobilised glassy carbon electrode for selective and sensitive detection of serotonin. Well separated differential pulse voltammetric serotonin oxidation peaks were obtained even in the presence of ascorbic acid and uric acid. They also reported that no shift in the oxidation peak of serotonin was observed in the presence of interfering species. This was because the polypyrrole used was a cation exchanger with negatively charged hydroxide groups and it thus resisted the negatively charged species (ascorbic acid and uric acid) and provided transport channels for the cationic serotonin under physiological pH. Using differential pulse voltammetry, the linear range was reported to be from 0.01-250 µM and detection limit of 0.0124 µM.

Carbon fibre microelectrodes have been used for *in vivo* neurochemical monitoring for decades due to their efficient electrical conductivity, adsorptive capabilities and small size[91, 101]. The dimension of carbon fibres generally ranges from 5-50 µm and are made from small hydrocarbons (*e.g.* methane[102]), polymers (*e.g* polyacrylonitrile[103]) or vapor-grown hydrocarbon gases[91, 104]. Their small size provides spatially resolved measurements in the brain. An important advantage of carbon fibre microelectrodes

includes their ability to make rapid measurements when used with fast electrochemical techniques such as amperometry, high-speed chronoamperometry, and fast-scan cyclic voltammetry. While a lot of work focused on improving the sensitivity and selectivity of the electrode, the detection of multiple analytes in complex mixtures or one analyte in the presence of interfering compounds is necessary[105].

1.7 Challenges during dopamine detection

Measuring neurotransmitter dopamine in the brain is challenging because of their vast number of detection signals on different time and length scales[62] as well as its low concentrations in the presence of interferences. Many other electrochemically active species coexist with catecholamines in an organism, such as catecholamine metabolite, other neurotransmitters (such as serotonin), uric acid, and ascorbic acid among other[1]. Therefore, selectivity against electrochemically active species that coexist with a targeted neurotransmitter is a crucial requirement in developing an electrochemical probe for use in biological samples[106]. In detecting dopamine, ascorbic acid and uric acid are among some of the major species that always coexist in the extracellular matrix of the central nervous system and serum in mammals. Signal overlap from multiple neurotransmitters that have relatively close oxidation potential (*e.g.* +0.2 V for dopamine, +0.2 V for ascorbic acid and +0.3 V for uric acid[107]) pose problems with the discrimination of signal. Thus, these species are likely to be indistinguishable based on a simple electrochemical measurement at unmodified/bare electrodes. This has stimulated a lot of developments involving modified electrodes to improve selective detection of a targeted catecholamine in the presence of interfering species. In particular, electrochemical detection methods offer important benefits such as rapid response, high sensitivity, easy operation, and low cost. However, the crucial problem

for *in vivo* monitoring dopamine (typically 10 nM) is the relatively high concentration of coexisted ascorbic acid (0.05 – 0.5 mM) and uric acid (155 – 357 μM in females and 208 – 428 μM in males)[108]. In this respect, pharmacological drugs were reportedly[109] used to either inhibit the release of interfering neurotransmitters or to enhance the dopamine signal by inhibiting the reuptake of dopamine. For example, during *in vivo* measurement of dopamine in a mice brain using an enzyme based carbon fibre electrode, a dopamine uptake inhibitor, nomifensine (5 mg kg^{-1}) was injected 30-40 min prior to dopamine measurement to ensure the response was from oxidation of dopamine[110].

Fouling is another major problem encountered during *in vivo* measurements. This involves a mechanical damage of the active surface as probe is being implanted in a tissue [89, 111]. These phenomena are often controlled by manipulating and tailoring the chemical nature of the sensing surface[112].

Carbon surfaces can be easily modified by chemical means to improve the analytical performance of electrodes. For example, modifying compounds can be covalently attached to oxide groups on the surface to tune the surface charge and active site density[104]. Enzymes can also be attached to carbon surfaces, thus allowing the detection of non-electroactive compounds. A major problem with the application of carbon fibre microelectrodes for the study of biogenic amines and other biological signalling molecules *in vitro* and *in vivo* is their response sensitivity and stability in physiological environments. This problem is associated with sp^2 hybridised carbon and the presence of surface hydroxyl groups on a carbon fibre surface, both of which promote strong adsorption of polar analytes *via* dipole-dipole, ion-dipole, and hydrogen bonding interactions[64, 113].

1.7.1 Electrode Fouling

Electrode fouling involves surface passivation by a fouling agent that forms an increasingly impermeable layer on an electrode. This layer then inhibits direct contact of the analyte with the electrode surface for electron transfer, resulting in reduced sensitivity of the electrochemical sensors[114-116]. Detection of neurotransmitters by electrochemical means offers advantages including the cost, *in vivo* compatibility, real time measurements and requiring simple instruments[117]. However, chemical fouling that occurs during the electrochemical detection of several neurotransmitters such as dopamine[118-119] and serotonin[120] remains a challenging problem. This type of fouling is commonly encountered during the detection of neurotransmitters *in vivo* using carbon electrodes[121]. It is well recognised in literature that the initial stages of dopamine fouling involves two-electron quasi-reversible oxidation of dopamine to dopamine-*o*-quinone on carbon-based electrodes. Next, this intermediate undergoes an intramolecular addition when the amine is protonated, resulting in a cyclization leading leucodopaminochrome which undergoes a two-electron oxidation to form dopaminochrome. Dopaminochrome may polymerize to melanin on the electrode by a free radical polymerisation[122-124]. Higher pH facilitates dopamine / dopamine-*o*-quinone cyclization at the electrode interface, where faster desorption rates result in higher dopamine sensitivity through increased availability of dopamine[125]. An example of electrochemical oxidation of dopamine and serotonin is shown in Scheme 1.4.

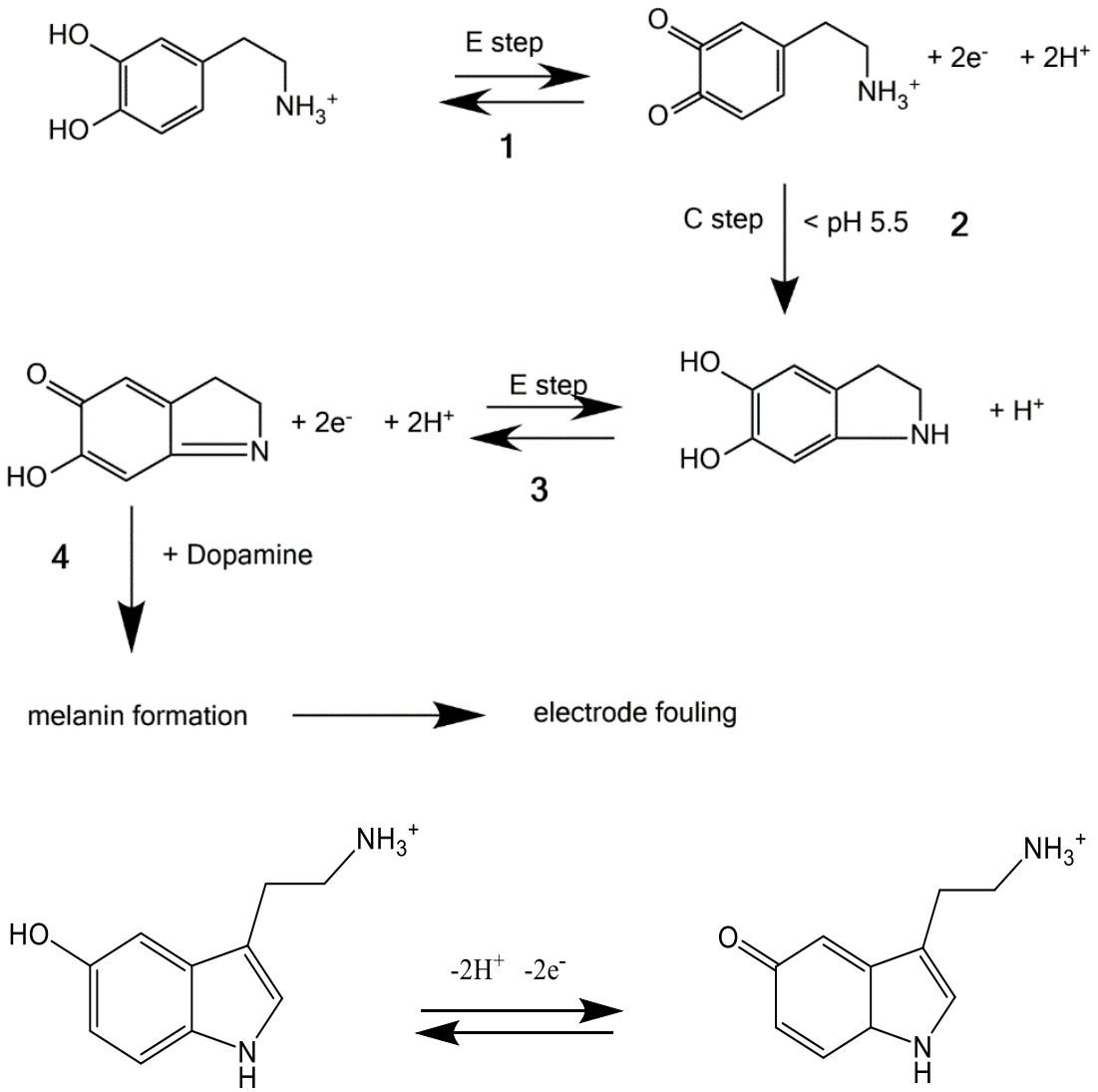

Scheme 1.4. The electropolymerisation of dopamine and serotonin during electrochemical oxidation in aqueous solution. Adapted from references[47, 126].

The oxidation products of dopamine and serotonin are very reactive and they form an insulating film on the electrode surface, which then inhibits the physical contact of the analyte of interest on an electrode surface for electron transfer[127]. Thus, the use of a bare carbon electrode for *in vivo* determination of dopamine or serotonin results in low sensitivity and selectivity.

For example, Harreither *et al.*[118] compared the rate of electrochemical fouling in using a carbon nanotube modified fibre electrode and a carbon fibre electrode. They reported a 50% loss in the amperometric current after a 2-h recording in 100 µM dopamine using carbon fibre electrode *in vitro*. In separate work, Harreither *et al.*[117] investigated the electrochemical fouling from dopamine, serotonin and octopamine to further establish the stability of carbon nanotube fibre surfaces as these molecules induce more severe surface fouling than dopamine. The rate of surface fouling was assessed by recording the slow decrease in the amperometric current as an insulating film forms and grows on the electrode. In all cases, after 1000 s recording, they reported a corresponding current decrease of 82%, 79% and 61% for dopamine, serotonin and octopamine using carbon fibre electrodes while a corresponding 43%, 38% and 14% current decline was estimated at carbon nanotube modified fibre electrodes. The less prominent fouling on carbon nanotube modified fibre electrode shows resistance towards fouling arises from a lower affinity of the fouling film on the carbon nanotube surface rather than a slower film growth induced by lower availability of the oxidised precursors.

Peltola *et al.*[27] investigated electrochemical fouling *via* oxidation of dopamine at different carbon electrode materials including amorphous carbon, tetrahedral carbon and pyrolytic carbon. In all cases, they reported a positive shift in the separation of the reduction peak potential and the oxidation peak potential (ΔEp) after 1st, 2nd and 10th cycle in 1.0 mM dopamine in phosphate buffered saline (pH 7.4) at all the carbon materials, indicating severe electrochemical fouling. To minimise fouling, they electrochemically cleaned the surface of the electrode materials in 0.15 M H_2SO_4. During the cleaning process, they reported that cycling in H_2SO_4 effectively removed the polydopamine layer from all surfaces except the pyrolytic carbon surface possibly due to stronger polydopamine adsorption. The differences in the degree of surface

fouling strongly depend on the surface characteristics of the electrode material used, as dopamine is known as an inner-sphere redox species that is likely to react at specific adsorption sites. The sites favour oxidation of dopamine, and consequently, they may be exposed to a higher level of dopamine quinone, which then takes part in the fouling cascade. Subsequently, these sites are the most probable to be subjected to electrochemical fouling.

On the other hand, biological fouling is caused by non-specific adsorption of high molecular proteins, peptides and lipids present in a biological sample due to a high affinity of the electrode surface adsorption properties. The adsorption of proteins, peptides and lipids on carbon electrodes are caused by an amphiphilic-hydrophilic interaction between the molecules and the electrode [116]. Biological fouling must be minimised for optimal sensor performance because adsorption affects mass transport and electron transfer kinetics [128]. Several methodologies exist in literature that focuses on minimising electrode fouling during *in vivo* detection of neurotransmitters. For example, Vreeland *et al.*[129] applied a thin, uniform coating of a polyethylenedioxythiophene and Nafion on an electrode to enhance the detection selectivity towards dopamine, 3,4 dihydroxyphenylacetic acid and ascorbic acid. The resistance towards fouling *in vitro* was estimated using pre-calibration and post-calibration dopamine sensitivity by implanting the electrode in 40 g L^{-1} bovine serum albumin in pH 7.4 artificial cerebrospinal fluid for 2 h. The authors reported a 40% loss in the sensitivity to a 1 µM bolus of dopamine using uncoated carbon fibre microelectrodes while the low-density polyethylenedioxythiophene : Nafion coated electrodes lost only 5% sensitivity. Fouling was also studied at an uncoated carbon fibre microelectrode separately implanted in the prefrontal cortex and nucleus accumbens of a male Sprague-Dawley for 30 min, while a low-density

polyethylenedioxythiophene : Nafion coated electrode was implanted for 6 h. Uncoated carbon fibre lost 60% and 33% of their sensitivity to dopamine over a course of 30 min implantation in the prefrontal cortex and nucleus accumbens, respectively. In contrast, the low density polyethylenedioxythiophene : Nafion coated carbon fibre microelectrodes lost only 9% of the pre-calibration sensitivity after being implanted for 6 h.

Venton's group reported carbon nanotube yarn microelectrode (CNTYME) treated by laser to improve the detection sensitivity to dopamine[130]. In their work, they measured dopamine *in vivo* using a non-laser treated CNTYME and a laser treated CNTYME. They reported a 3-fold increase in dopamine current using the laser treated CNTYME. The increase in the current at laser treated CNTYME was attributed to an increase in the surface area and the quantity of oxygen-containing functional groups that provided more adsorption sites for dopamine.

Our laboratory reported the use of a chemical vapor deposition method to hydrogenate conical-tip carbon electrodes for dopamine detection *in vivo* with over 30% loss in the oxidation current after the first 30 min and at least 50% current remained over the next half-period during a 60 min experiment[89].

Swami and Venton used 25 consecutive flow injection analysis experiments to test the extent to which a single-walled carbon nanotube treatment would reduce the fouling of carbon fibre electrodes by serotonin. The electrode was incubated in a 3 s injection of 1 mM serotonin every 15 s. The regular dopamine oxidation waveform was used, scanning from -0.4 to 1.0 V and back at 400 V s^{-1} every 100 ms. Oxidation currents were normalised to the first response for each electrode to account for varying sensitivities between the electrodes. Bare carbon fibre electrodes lost ~40% of their

sensitivity by the 25th injection, while the sensitivity of the single-walled carbon nanotube-coated electrodes decreased by less than 10%. Therefore, they concluded that carbon nanotubes do provide protection against fouling when using fast-scan cyclic voltammetry[19].

Algarra *et al.*[131] employed a carbon quantum dot modified glassy carbon electrode to enhance the electrochemical oxidation signal for dopamine in presence of uric acid. The quantum dots were prepared using the Hummers method in their research and were later deposited on a glassy carbon surface. They noted that, although the modified electrode enhanced (~10-fold) the signal for both dopamine and uric acid, there was a prominent positive shift (from +0.2 V at bare glassy carbon electrode to +0.6 V at carbon quantum dot modified glassy carbon electrode) in the anodic potential during dopamine detection, which was caused by electrochemical fouling. They attributed this to the presence of highly ordered sp^2 crystal structures of the modified surface.

1.8 Diamond electrodes

The sp^3 hybridised, tetrahedral bonding of diamond results in both its hardness and low electrical conductivity with the latter property making polycrystalline or single diamond uninteresting as an electrode material. However, intentional introduction of impurities such as boron or nitrogen into diamond during deposition can increase the conductivity of diamond sufficiently to make electrodes with distinct electrochemical properties [91]. Conductive diamond has proven extremely useful for electroanalysis owing to its wide working potential window, low background current, favourable electron transfer kinetics and high resistance to fouling [62]. The Swain group has first demonstrated that diamond microelectrodes (76 μm Pt wire with diamond film thickness of 3 - 5 μm) can be used for electrochemical detection of neurochemicals in

biological samples [132-133]. Diamond microelectrodes are attractive for electroanalytical measurements in biological environments because of its (i) hard and lubricious nature that allows easy penetration into tissue with negligible peripheral damage, (ii) low and stable background current over a wide potential range, (iii) good chemical and microstructural stability, (iv) low surface oxygen content (H-terminated), (v) chemical inertness and (iv) a non-polar, hydrophobic surface which renders it resistant to molecular adsorption [132].

Shin *et al.*[134] investigated the resistance of glassy carbon, carbon paste and as-grown diamond electrodes to surfactants and proteins. The resistance to surfactant and protein fouling was evaluated using square wave voltammetry in the presence of bovine serum albumin, gelatin and Triton X-100. Ten repetitive measurements were conducted in the presence of the proteins and surfactant using the three types of carbon electrodes including a glassy carbon electrode, a carbon paste electrode and a diamond electrode. They reported 4.3% and 6.2% decline in the initial current in the presence of 100 ppm Triton X-100 and gelatin on diamond electrodes respectively, compared to 45.2% and 34.4% at glassy carbon electrodes[134].

Chen and Swain[135] investigated the physical structure, electrochemical reactivity and response stability of glassy carbon electrodes hydrogenated using microwave assisted chemical vapour deposition. The resulting hydrogenated glassy carbon demonstrated a low-oxide and hydrophobic surface. The H atom chemisorption converts the planar sp^2 hybridised carbon rings to a combination of alicyclic sp^3 hybridised rings and sp^3 hybridised aliphatic hydrocarbon surface functionalities. From their findings, the hydrogenated glassy carbon electrode exhibits (i) lower background voltammetric current and double-layer capacitance, (ii) comparable electron transfer kinetics for

several aqueous based redox analytes, and electron transfer kinetics consistent with low-oxide surfaces, (iii) negligible adsorption of 2,6-anthraquinone disulfonic acid, (iv) long-term response stability, and (v) improved response reproducibility, compared with that of a polished glassy carbon[135].

Surface chemistry of a typical carbon electrode with possible oxygen and nitrogen containing functional groups is schematically shown in Figure 1.5. A bare carbon electrode surface with oxygen containing groups is characteristically hydrophilic in nature and is highly susceptible to fouling when used for analyte detection in a biological fluid due to electrostatic interaction between the amphiphilic non-targeted species and the hydrophilic electrode surface [116]. As stated on page 36, our group has previously reported a strategy to minimise fouling by hydrogenating conical tip carbon electrodes using chemical vapour deposition for *in vivo* measurement of dopamine [89-90]. The hydrogenation converted the sp^2 hybridised carbon to sp^3 hybridised carbon, giving rise to a hydrophobic surface that can minimise adsorption of amphiphilic lipids, proteins and peptides. During *in vivo* detection of dopamine at the hydrogenated carbon electrodes, ~70% of the dopamine oxidation current remained after the first 30 min of a 1 h experiment and at least 50% remained over next half of the experiment[121]. Although promising results were obtained after hydrogenating using chemical vapour deposition, the success rate was reported to be low as the carbon tips are very fragile and they easily broke in an environment with as high as 900 °C temperature.

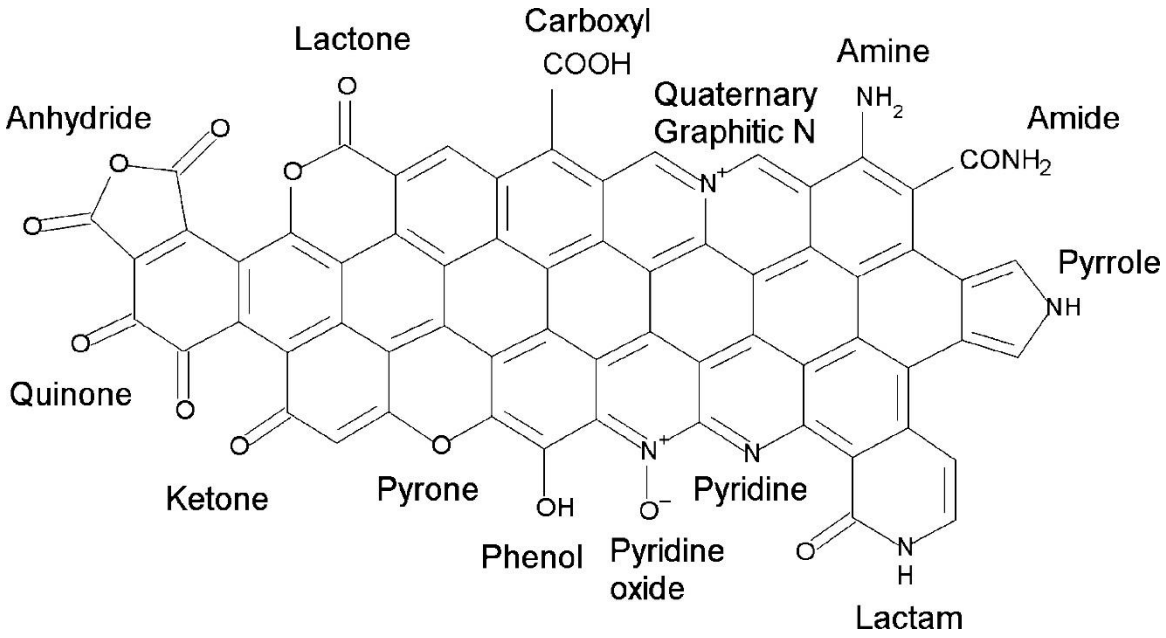

Figure 1.5. Surface chemistry of a graphitic carbon surface showing possible oxygen and nitrogen containing groups. Adapted from reference[136].

1.9 Scope of present study

Measuring dopamine in the brain is challenging due to the presence of numerous other electroactive endogenous compounds. Several easily oxidisable compounds have been identified in the extracellular fluid, including dopamine metabolites such as 3,4-dihydroxyphenylacetic acid and homovanillic acid, the antioxidant ascorbic acid and other neurotransmitters such as nitric oxide, norepinephrine, and serotonin. Many of these compounds are present in large concentrations, making selectivity an important requirement in discriminating the dopamine signal[6]. A common challenge during the dopamine measurement is that the oxidation of dopamine in the presence of ascorbic acid results in homogeneous catalytic oxidation of ascorbic acid.

As mentioned in Section 1.7.1 one of the major problems encountered during *in vivo* measurement of dopamine is electrode fouling. A common approach to minimise

electrode fouling during *in vivo* measurement of neurotransmitters is to apply hydrophobic, 'diamond-like' carbon electrodes. This is because most of the high molecular-weight species in the brain such as proteins, peptides, and lipids are hydrophilic. At a bare carbon electrode, the surface comprises of a mixture of sp^3 and sp^2 carbon atoms attached to hydroxyl and carbonyl molecules at the surface[137]. Due to these oxygen-containing functional groups, the bare carbon surface is a polar and hydrophilic surface,[138] on which other hydrophilic molecules adsorb readily. Hence, these oxygen-containing functional groups is reportedly promoting the non-specific adsorption of proteins, peptides, and lipids on a bare electrode surface[89, 116, 139]. Therefore, the aim of this work is to fabricate structurally small carbon electrodes with an antifouling surface with low oxygen-containing functional groups with higher percentage of sp^3 hybridised carbon that can be readily applied to *in vivo* measurement of dopamine.

Initially, the electrodes will be fabricated by following a procedure previously described by our group[75]. Briefly, in fabricating such an electrode, a pulled quartz capillary is housed in an NMR tube before acetylene is thermally pyrolysed to deposit carbon at the tip (~2 μm diameter) and on the shank (~7 μm length) of the pulled capillary. Graphite powder and a conducting wire are introduced through the larger end of the capillary to complete the construction of a small conical-tip carbon electrode. Our group previously reported the antifouling property of *n*-butylsilane hydrogenated conical-tip carbon electrodes. This method of hydrogenation reportedly reduces the alcohols, ketones and carboxylic acids to their corresponding alkyl groups[140-141]. In addition, the phenolic functional group is not reduced but is instead salinised to form siloxane dendrimers. The presence of butylsiloxane dendrimers hydrogenated carbon electrodes has been reported to be one of the antifouling characteristics which

suppresses non-specific adsorption of proteins, peptides and lipids. To improve the antifouling characteristic of the small carbon electrodes, in our work, the fabricated electrodes are hydrogenated using triethylsilane or phenylsilane in the presence of tris(pentaflourophenyl) borane and anhydrous dichloromethane to achieve a hydrogen-terminated surface with low oxygen containing functional groups with structurally bulkier siloxane dendrimers. Further justification for using the silane reduction method will be explicitly provided in Chapter 3. All experimental procedures and instrumentation used in this study to acquire data are described in Chapter 2.

Chapter 3 commences with the fabrication of structurally small carbon electrodes by pyrolysing acetylene in and on pulled quartz capillaries with tip diameters of ~2 µm and axial length of ~7 µm. Initially, all fabricated carbon electrodes were electrochemically characterised using $[Ru(NH_3)_6]^{3+}$ to identify functioning electrodes. These electrodes were then subjected to hydrogenation using either triethylsilane or phenylsilane in the presence of anhydrous dichloromethane and tris(pentafluorophenyl) borane under ambient conditions. Following hydrogenation, X-ray photoelectron spectroscopy and Raman spectroscopy were used to determine the elemental composition and the sp^3/sp^2 of the electrodes. Chapter 4 is further devoted to the electrochemical characterisation of hydrogenated electrodes using different redox markers including $Fe(CN)_6^{3-}$, dopamine, dihydroxyphenyl acetic acid, 4-methylcatechol and anthraquinone 2,4 disulfonate to carefully study their electron transfer kinetics. All the results were compared to those of non-hydrogenated carbon electrodes in evaluating the electrochemical behaviour of the hydrogenated carbon surface.

In Chapter 4, we initially describe the surface characteristics of hydrogenated carbon electrodes using two-dimensional atomic force microscopy. Next, electroanalytical detection performance of dopamine at the hydrogenated carbon electrodes was assessed. The sensitivity and limit of detection of the hydrogenated electrodes were then estimated from the calibration plot. The selectivity towards ascorbic acid and uric acid is also evaluated at the hydrogenated electrodes. Finally, the chapter concludes with the performance comparison between non-hydrogenated and the hydrogenated electrodes in a laboratory synthetic fouling solution containing 2.0% (w/v) bovine serum albumin, 0.01% (w/v) cytochrome *c*, 0.001% (w/v) human fibrinopeptide and 1.0% (v/v) caproic acid.

One significant challenge during both *in vivo* and *in vitro* dopamine detection is electrode fouling, often caused by adsorption of amphiphilic proteins, peptides and lipids present in the biological fluid on hydrophilic carbon electrode surfaces. Chapter 5 describes the performance of triethylsilane and phenylsilane hydrogenated carbon electrodes for detection of neurotransmitter dopamine in two *in vitro* models, the neuroblastoma cell line SH-SY5Y and brain slices to assess the practicality of the hydrogenated carbon electrodes for *in vivo* dopamine measurements. To evaluate fouling in dopaminergic SH-SY5Y cells, a hydrogenated carbon electrode was positioned close to the cells using an inverted microscope and a micromanipulator. Using amperometry, a constant potential of 0.5 V was applied to the carbon working electrode to promote the oxidation of dopamine released from cells that were continuously depolarised using 0.1 M KCl for 1 h. The transient changes in peak current were evaluated to determine the rate of electrode fouling. Rate of fouling in a brain slice was evaluated by first positioning a hydrogenated carbon electrode in the brain tissue while continuously cycling the potential between –0.4 V and +1.2 V (versus

a Ag|AgCl reference electrode) at 400 V s^{-1}, and a repetition rate of 10 Hz for 1-h. The rate of electrode fouling was evaluated by comparing the dopamine oxidation peak before and after the electrodes were exposed to the brain tissue.

Chapter 6 concludes with the outcomes of this study including a summary of the performance of the electrodes fabricated in this study. Some suggestions for future work are also presented in this chapter.

1.10 References

(1) Ribeiro, J. A.; Fernandes, P. M. V.; Pereira, C. M.; Silva, F. Electrochemical sensors and biosensors for determination of catecholamine neurotransmitters: A review. *Talanta* **2016,** *160*, 653-679, DOI: https://doi.org/10.1016/j.talanta.2016.06.066.

(2) Adams, R. N. Probing brain chemistry with electroanalytical techniques. *Analytical Chemistry* **1976,** *48* (14), 1126A-1138A, DOI: 10.1021/ac50008a001.

(3) Fletcher, A. Nerve cell function and synaptic mechanisms. *Anaesthesia & Intensive Care Medicine* **2019,** *20* (4), 238-242, DOI: https://doi.org/10.1016/j.mpaic.2019.01.015.

(4) Majdi, S.; Larsson, A.; Najafinobar, N.; Borges, R.; Ewing, A. G. Extracellular ATP Regulates the Vesicular Pore Opening in Chromaffin Cells and Increases the Fraction Released During Individual Exocytosis Events. *ACS Chemical Neuroscience* **2019**, DOI: 10.1021/acschemneuro.8b00722.

(5) Phan, N. T. N.; Li, X.; Ewing, A. G. Measuring synaptic vesicles using cellular electrochemistry and nanoscale molecular imaging. *Nature Reviews Chemistry* **2017,** *1*, 0048, DOI: 10.1038/s41570-017-0048.

(6) Venton, B. J.; Wightman, R. M. Psychoanalytical Electrochemistry: Dopamine and Behavior. *Analytical Chemistry* **2003,** *75* (19), 414 A-421 A, DOI: 10.1021/ac031421c.

(7) Michael, D. J.; Wightman, R. M. Electrochemical monitoring of biogenic amine neurotransmission in real time. *Journal of Pharmaceutical and Biomedical Analysis* **1999,** *19* (1–2), 33-46, DOI: http://dx.doi.org/10.1016/S0731-7085(98)00145-9.

(8) Fröhlich, F. Introduction. In *Network Neuroscience*; Fröhlich, F., Ed.; Academic Press: San Diego, 2016; p 1.

(9) Li, X.; Dunevall, J.; Ewing, A. G. Quantitative Chemical Measurements of Vesicular Transmitters with Electrochemical Cytometry. *Accounts of Chemical Research* **2016,** *49* (10), 2347-2354, DOI: 10.1021/acs.accounts.6b00331.

(10) Moon, J.-M.; Thapliyal, N.; Hussain, K. K.; Goyal, R. N.; Shim, Y.-B. Conducting polymer-based electrochemical biosensors for neurotransmitters: A review. *Biosensors and Bioelectronics* **2018,** *102*, 540-552, DOI: https://doi.org/10.1016/j.bios.2017.11.069.

(11) Bucher, E. S.; Wightman, R. M. Electrochemical Analysis of Neurotransmitters. *Annual Review of Analytical Chemistry* **2015,** *8* (1), 239-261, DOI: 10.1146/annurev-anchem-071114-040426.

(12) Lama, R. D.; Charlson, K.; Anantharam, A.; Hashemi, P. Ultrafast Detection and Quantification of Brain Signaling Molecules with Carbon Fiber Microelectrodes. *Analytical Chemistry* **2012,** *84* (19), 8096-8101, DOI: 10.1021/ac301670h.

(13) Center, G. S. L., Neurons Transmit Messages In The Brain 2015; p https://learn.genetics.utah.edu/content/neuroscience/neurons/.

(14) Ren, L.; Mellander, L. J.; Keighron, J.; Cans, A.-S.; Kurczy, M. E.; Svir, I.; Oleinick, A.; Amatore, C.; Ewing, A. G. The evidence for open and closed exocytosis as the primary release mechanism. *Quarterly Reviews of Biophysics* **2016,** *49*, e12, DOI: 10.1017/S0033583516000081.

(15) Olesti, E.; Rodríguez-Morató, J.; Gomez-Gomez, A.; Ramaekers, J. G.; de la Torre, R.; Pozo, O. J. Quantification of endogenous neurotransmitters and related compounds by liquid chromatography coupled to tandem mass spectrometry. *Talanta* **2019,** *192*, 93-102, DOI: https://doi.org/10.1016/j.talanta.2018.09.034.

(16) Grant, P. Neurotransmitters A2 - Wright, James D. In *International Encyclopedia of the Social & Behavioral Sciences (Second Edition)*; Elsevier: Oxford, 2015; pp 749-754.

(17) Hasanzadeh, M.; Shadjou, N.; Guardia, M. d. l. Current advancement in electrochemical analysis of neurotransmitters in biological fluids. *TrAC Trends in Analytical Chemistry* **2017,** *86*, 107-121, DOI: https://doi.org/10.1016/j.trac.2016.11.001.

(18) Ferapontova, E. E. Electrochemical Analysis of Dopamine: Perspectives of Specific In Vivo Detection. *Electrochimica Acta* **2017,** *245*, 664-671, DOI: https://doi.org/10.1016/j.electacta.2017.05.183.

(19) Swamy, B. E. K.; Venton, B. J. Carbon nanotube-modified microelectrodes for simultaneous detection of dopamine and serotoninin vivo. *Analyst* **2007,** *132* (9), 876-884, DOI: 10.1039/B705552H.

(20) Verma, V. Classic Studies on the Interaction of Cocaine and the Dopamine Transporter. *Clin Psychopharmacol Neurosci* **2015,** *13* (3), 227-238, DOI: 10.9758/cpn.2015.13.3.227.

(21) Carlsson, A.; Lindqvist, M.; Magnusson, T. O. R. 3,4-Dihydroxyphenylalanine and 5-Hydroxytryptophan as Reserpine Antagonists. *Nature* **1957,** *180*, 1200, DOI: 10.1038/1801200a0.

(22) Demuru, S.; Nela, L.; Marchack, N.; Holmes, S. J.; Farmer, D. B.; Tulevski, G. S.; Lin, Q.; Deligianni, H. Scalable Nanostructured Carbon Electrode Arrays for Enhanced Dopamine Detection. *ACS Sensors* **2018**, DOI: 10.1021/acssensors.8b00043.

(23) Wightman, R. M.; May, L. J.; Michael, A. C. Detection of Dopamine Dynamics in the Brain. *Analytical Chemistry* **1988,** *60* (13), 769A-793A, DOI: 10.1021/ac00164a718.

(24) Sajid, M.; Baig, N. Chemically modified electrodes for electrochemical detection of dopamine: Challenges and opportunities. *TrAC Trends in Analytical Chemistry* **2019**, DOI: https://doi.org/10.1016/j.trac.2019.05.042.

(25) Baranwal, A.; Chandra, P. Clinical implications and electrochemical biosensing of monoamine neurotransmitters in body fluids, in vitro, in vivo, and ex vivo models. *Biosensors and Bioelectronics* **2018,** *121*, 137-152, DOI: https://doi.org/10.1016/j.bios.2018.09.002.

(26) Mei, X.; Wei, Q.; Long, H.; Yu, Z.; Deng, Z.; Meng, L.; Wang, J.; Luo, J.; Lin, C.-T.; Ma, L.; Zheng, K.; Hu, N. Long-term stability of Au nanoparticle-anchored porous boron-doped diamond hybrid electrode for enhanced dopamine detection.

Electrochimica Acta **2018,** *271*, 84-91, DOI: https://doi.org/10.1016/j.electacta.2018.03.133.

(27) Peltola, E.; Sainio, S.; Holt, K. B.; Palomäki, T.; Koskinen, J.; Laurila, T. Electrochemical Fouling of Dopamine and Recovery of Carbon Electrodes. *Analytical Chemistry* **2018,** *90* (2), 1408-1416, DOI: 10.1021/acs.analchem.7b04793.

(28) Robinson, D. L.; Hermans, A.; Seipel, A. T.; Wightman, R. M. Monitoring Rapid Chemical Communication in the Brain. *Chemical Reviews* **2008,** *108* (7), 2554-2584, DOI: 10.1021/cr068081q.

(29) Feng, J.; Zhang, C.; Lischinsky, J. E.; Jing, M.; Zhou, J.; Wang, H.; Zhang, Y.; Dong, A.; Wu, Z.; Wu, H.; Chen, W.; Zhang, P.; Zou, J.; Hires, S. A.; Zhu, J. J.; Cui, G.; Lin, D.; Du, J.; Li, Y. A Genetically Encoded Fluorescent Sensor for Rapid and Specific In Vivo Detection of Norepinephrine. *Neuron* **2019**, DOI: https://doi.org/10.1016/j.neuron.2019.02.037.

(30) Yadav, T.; Mukherjee, V. Structural confirmation and spectroscopic study of a biomolecule: Norepinephrine. *Spectrochimica Acta Part A: Molecular and Biomolecular Spectroscopy* **2018,** *202*, 222-237, DOI: https://doi.org/10.1016/j.saa.2018.05.040.

(31) Zimmerman, B. G. Adrenergic Facilitation by Angiotensin: Does it Serve a Physiological Function? *Clinical Science* **1981,** *60* (4), 343, DOI: 10.1042/cs0600343.

(32) Brodde, O.-E.; Bruck, H.; Leineweber, K.; Seyfarth, T. Presence, distribution and physiological function of adrenergic and muscarinic receptor subtypes in the human

heart. *Basic Research in Cardiology* **2001,** *96* (6), 528-538, DOI: 10.1007/s003950170003.

(33) Gannon, M.; Wang, Q. Complex noradrenergic dysfunction in Alzheimer's disease: Low norepinephrine input is not always to blame. *Brain Research* **2019,** *1702*, 12-16, DOI: https://doi.org/10.1016/j.brainres.2018.01.001.

(34) Peterson, A. C.; Li, C.-S. R. Noradrenergic Dysfunction in Alzheimer's and Parkinson's Diseases-An Overview of Imaging Studies. *Front Aging Neurosci* **2018,** *10*, 127-127, DOI: 10.3389/fnagi.2018.00127.

(35) Boyanova, L. Stress hormone epinephrine (adrenaline) and norepinephrine (noradrenaline) effects on the anaerobic bacteria. *Anaerobe* **2017,** *44*, 13-19, DOI: https://doi.org/10.1016/j.anaerobe.2017.01.003.

(36) Feher, J. 4.2 - Cells, Synapses, and Neurotransmitters. In *Quantitative Human Physiology (Second Edition)*; Feher, J., Ed.; Academic Press: Boston, 2012; pp 375-388.

(37) Tao, Z.; Wang, G.; Goodisman, J.; Asefa, T. Accelerated Oxidation of Epinephrine by Silica Nanoparticles. *Langmuir* **2009,** *25* (17), 10183-10188, DOI: 10.1021/la900958f.

(38) Kapalka, G. M. Chapter 4 - Substances Involved in Neurotransmission. In *Nutritional and Herbal Therapies for Children and Adolescents*; Kapalka, G. M., Ed.; Academic Press: San Diego, 2010; pp 71-99.

(39) Gershon, M. D. Serotonin: Its Role and Receptors in Enteric Neurotransmission. In *Kynurenine and Serotonin Pathways: Progress in Tryptophan Research*; Schwarcz,

R.; Young, S. N.; Brown, R. R., Eds.; Springer New York: Boston, MA, 1991; pp 221-230.

(40) Wu, H.; Denna, T. H.; Storkersen, J. N.; Gerriets, V. A. Beyond a neurotransmitter: The role of serotonin in inflammation and immunity. *Pharmacological Research* **2018**, DOI: https://doi.org/10.1016/j.phrs.2018.06.015.

(41) Gershon, M. D.; Drakontides, A. B.; Ross, L. L. Serotonin: Synthesis and release from the myenteric plexus of the mouse intestine. *Science* **1965,** *149* (3680), 197-199, DOI: 10.1126/science.149.3680.197.

(42) Costedio, M. M.; Hyman, N.; Mawe, G. M. Serotonin and Its Role in Colonic Function and in Gastrointestinal Disorders. *Diseases of the Colon & Rectum* **2007,** *50* (3), 376-388, DOI: 10.1007/s10350-006-0763-3.

(43) Yu, P. L.; Fujimura, M.; Okumiya, K.; Kinoshita, M.; Hasegawa, H.; Fujimiya, M. Immunohistochemical localization of tryptophan hydroxylase in the human and rat gastrointestinal tracts. *J. Comp. Neurol.* **1999,** *411* (4), 654-665, DOI: 10.1002/(SICI)1096-9861(19990906)411:4<654::AID-CNE9>3.0.CO;2-H.

(44) Garbarino, V. R.; Gilman, T. L.; Daws, L. C.; Gould, G. G. Extreme enhancement or depletion of serotonin transporter function and serotonin availability in autism spectrum disorder. *Pharmacological Research* **2018**, DOI: https://doi.org/10.1016/j.phrs.2018.07.010.

(45) Lv, J.; Liu, F. The Role of Serotonin beyond the Central Nervous System during Embryogenesis. *Frontiers in cellular neuroscience* **2017,** *11*, 74-74, DOI: 10.3389/fncel.2017.00074.

(46) Jennings, K. A. A Comparison of the Subsecond Dynamics of Neurotransmission of Dopamine and Serotonin. *ACS Chemical Neuroscience* **2013,** *4* (5), 704-714, DOI: 10.1021/cn4000605.

(47) Sharma, S.; Singh, N.; Tomar, V.; Chandra, R. A review on electrochemical detection of serotonin based on surface modified electrodes. *Biosensors and Bioelectronics* **2018,** *107*, 76-93, DOI: https://doi.org/10.1016/j.bios.2018.02.013.

(48) Badgaiyan, R. D. Imaging dopamine neurotransmission in live human brain. *Progress in brain research* **2014,** *211*, 165-182, DOI: 10.1016/B978-0-444-63425-2.00007-6.

(49) Sarter, M.; Kim, Y. Interpreting Chemical Neurotransmission in Vivo: Techniques, Time Scales, and Theories. *ACS Chemical Neuroscience* **2015,** *6* (1), 8-10, DOI: 10.1021/cn500319m.

(50) Stuart, J. N.; Hummon, A. B.; Sweedler, J. V. Peer Reviewed: The Chemistry of Thought: Neurotransmitters in the Brain. *Analytical Chemistry* **2004,** *76* (7), 120 A-128 A, DOI: 10.1021/ac041534b.

(51) König, M.; Thinnes, A.; Klein, J. Microdialysis and its use in behavioural studies: Focus on acetylcholine. *Journal of Neuroscience Methods* **2018,** *300*, 206-215, DOI: https://doi.org/10.1016/j.jneumeth.2017.08.013.

(52) Lietsche, J.; Gorka, J.; Hardt, S.; Karas, M.; Klein, J. Self-built microdialysis probes with improved recoveries of ATP and neuropeptides. *Journal of Neuroscience Methods* **2014,** *237*, 1-8, DOI: https://doi.org/10.1016/j.jneumeth.2014.08.015.

(53) Porada, S.; Weinstein, L.; Dash, R.; van der Wal, A.; Bryjak, M.; Gogotsi, Y.; Biesheuvel, P. M. Water Desalination Using Capacitive Deionization with Microporous Carbon Electrodes. *ACS Applied Materials & Interfaces* **2012,** *4* (3), 1194-1199, DOI: 10.1021/am201683j.

(54) Saylor, R. A.; Thomas, S. R.; Lunte, S. M. SEPARATION-BASED METHODS COMBINED WITH MICRODIALYSIS SAMPLING FOR MONITORING NEUROTRANSMITTERS AND DRUG DELIVERY TO THE BRAIN. In *Compendium of In Vivo Monitoring in Real-Time Molecular Neuroscience*; pp 1-45.

(55) Forgacsova, A.; Galba, J.; Garruto, R. M.; Majerova, P.; Katina, S.; Kovac, A. A novel liquid chromatography/mass spectrometry method for determination of neurotransmitters in brain tissue: Application to human tauopathies. *Journal of Chromatography B* **2018,** *1073*, 154-162, DOI: https://doi.org/10.1016/j.jchromb.2017.12.015.

(56) Bicker, J.; Fortuna, A.; Alves, G.; Falcão, A. Liquid chromatographic methods for the quantification of catecholamines and their metabolites in several biological samples—A review. *Analytica Chimica Acta* **2013,** *768*, 12-34, DOI: https://doi.org/10.1016/j.aca.2012.12.030.

(57) Zhang, M.; Fang, C.; Smagin, G. Derivatization for the simultaneous LC/MS quantification of multiple neurotransmitters in extracellular fluid from rat brain microdialysis. *Journal of Pharmaceutical and Biomedical Analysis* **2014,** *100*, 357-364, DOI: https://doi.org/10.1016/j.jpba.2014.08.015.

(58) Yoshitake, T.; Kehr, J.; Todoroki, K.; Nohta, H.; Yamaguchi, M. Derivatization chemistries for determination of serotonin, norepinephrine and dopamine in brain

microdialysis samples by liquid chromatography with fluorescence detection. *Biomedical Chromatography* **2006,** *20* (3), 267-281, DOI: 10.1002/bmc.560.

(59) Durairaj, S.; Sidhureddy, B.; Cirone, J.; Chen, A. Nanomaterials-Based Electrochemical Sensors for In Vitro and In Vivo Analyses of Neurotransmitters. *Applied Sciences* **2018,** *8* (9), 1504.

(60) Berfield, J. L.; Wang, L. C.; Reith, M. E. A. Which form of dopamine is the substrate for the human dopamine transporter: the cationic or the uncharged species? *J. Biol. Chem.* **1999,** *274* (8), 4876-4882, DOI: 10.1074/jbc.274.8.4876.

(61) Jeon, J.; Hwang, I.; Chung, T. D. Electrochemical detection of neurotransmitters: Toward synapse-based neural interfaces. *Biomedical Engineering Letters* **2016,** *6* (3), 123-133, DOI: 10.1007/s13534-016-0230-6.

(62) Ganesana, M.; Lee, S. T.; Wang, Y.; Venton, B. J. Analytical Techniques in Neuroscience: Recent Advances in Imaging, Separation, and Electrochemical Methods. *Analytical Chemistry* **2017,** *89* (1), 314-341, DOI: 10.1021/acs.analchem.6b04278.

(63) Veloso, A. J.; Cheng, X. R.; Kerman, K. 1 - Electrochemical biosensors for medical applications A2 - Higson, Séamus. In *Biosensors for Medical Applications*; Woodhead Publishing: 2012; pp 3-40.

(64) Singh, Y. S.; Sawarynski, L. E.; Dabiri, P. D.; Choi, W. R.; Andrews, A. M. Head-to-Head Comparisons of Carbon Fiber Microelectrode Coatings for Sensitive and Selective Neurotransmitter Detection by Voltammetry. *Analytical Chemistry* **2011,** *83* (17), 6658-6666, DOI: 10.1021/ac2011729.

(65) Tertiș, M.; Cernat, A.; Lacatiș, D.; Florea, A.; Bogdan, D.; Suciu, M.; Săndulescu, R.; Cristea, C. Highly selective electrochemical detection of serotonin on polypyrrole and gold nanoparticles-based 3D architecture. *Electrochemistry Communications* **2017,** *75*, 43-47, DOI: https://doi.org/10.1016/j.elecom.2016.12.015.

(66) Li, Y.; Ji, Y.; Ren, B.; Jia, L.; Ma, G.; Liu, X. Carboxyl-functionalized mesoporous molecular sieve/colloidal gold modified nano-carbon ionic liquid paste electrode for electrochemical determination of serotonin. *Materials Research Bulletin* **2019,** *109*, 240-245, DOI: https://doi.org/10.1016/j.materresbull.2018.10.002.

(67) Haldorai, Y.; Vilian, A. T. E.; Rethinasabapathy, M.; Huh, Y. S.; Han, Y.-K. Electrochemical determination of dopamine using a glassy carbon electrode modified with TiN-reduced graphene oxide nanocomposite. *Sensors and Actuators B: Chemical* **2017,** *247*, 61-69, DOI: https://doi.org/10.1016/j.snb.2017.02.181.

(68) Singh, M.; Tiwari, I.; Foster, C. W.; Banks, C. E. Highly sensitive and selective determination of dopamine using screen-printed electrodes modified with nanocomposite of N′-phenyl-p-phenylenediamine/multiwalled carbon nanotubes/nafion. *Materials Research Bulletin* **2018,** *101*, 253-263, DOI: https://doi.org/10.1016/j.materresbull.2018.01.011.

(69) Leszczyszyn, D. J.; Jankowski, J. A.; Viveros, O. H.; Diliberto, E. J., Jr.; Near, J. A.; Wightman, R. M. Nicotinic receptor-mediated catecholamine secretion from individual chromaffin cells. Chemical evidence for exocytosis. *J. Biol. Chem.* **1990,** *265* (25), 14736-7.

(70) Ozel, R. E.; Bulbul, G.; Perez, J.; Pourmand, N. Functionalized Quartz Nanopipette for Intracellular Superoxide Sensing: A Tool for Monitoring Reactive Oxygen Species

Levels in Single Living Cell. *ACS Sensors* **2018,** *3* (7), 1316-1321, DOI: 10.1021/acssensors.8b00185.

(71) Dunevall, J.; Fathali, H.; Najafinobar, N.; Lovric, J.; Wigström, J.; Cans, A.-S.; Ewing, A. G. Characterizing the Catecholamine Content of Single Mammalian Vesicles by Collision–Adsorption Events at an Electrode. *Journal of the American Chemical Society* **2015,** *137* (13), 4344-4346, DOI: 10.1021/ja512972f.

(72) Suzuki, A.; Ivandini, T. A.; Yoshimi, K.; Fujishima, A.; Oyama, G.; Nakazato, T.; Hattori, N.; Kitazawa, S.; Einaga, Y. Fabrication, Characterization, and Application of Boron-Doped Diamond Microelectrodes for in Vivo Dopamine Detection. *Analytical Chemistry* **2007,** *79* (22), 8608-8615, DOI: 10.1021/ac071519h.

(73) Rodeberg, N. T.; Sandberg, S. G.; Johnson, J. A.; Phillips, P. E. M.; Wightman, R. M. Hitchhiker's Guide to Voltammetry: Acute and Chronic Electrodes for in Vivo Fast-Scan Cyclic Voltammetry. *ACS chemical neuroscience* **2017,** *8* (2), 221-234, DOI: 10.1021/acschemneuro.6b00393.

(74) Jaquins-Gerstl, A.; Michael, A. C. Comparison of the brain penetration injury associated with microdialysis and voltammetry. *Journal of Neuroscience Methods* **2009,** *183* (2), 127-135, DOI: https://doi.org/10.1016/j.jneumeth.2009.06.023.

(75) McNally, M.; Wong, D. K. An in vivo probe based on mechanically strong but structurally small carbon electrodes with an appreciable surface area. *Analytical chemistry* **2001,** *73* (20), 4793-4800.

(76) Robinson, D. L.; Venton, B. J.; Heien, M. L. A. V.; Wightman, R. M. Detecting Subsecond Dopamine Release with Fast-Scan Cyclic Voltammetry in Vivo. *Clinical Chemistry* **2003,** *49* (10), 1763, DOI: 10.1373/49.10.1763.

(77) Rees, H. R.; Anderson, S. E.; Privman, E.; Bau, H. H.; Venton, B. J. Carbon Nanopipette Electrodes for Dopamine Detection in Drosophila. *Analytical Chemistry* **2015,** *87* (7), 3849-3855, DOI: 10.1021/ac504596y.

(78) Cragg, S. J.; Rice, M. E.; Greenfield, S. A. Heterogeneity of Electrically Evoked Dopamine Release and Reuptake in Substantia Nigra, Ventral Tegmental Area, and Striatum. *Journal of Neurophysiology* **1997,** *77* (2), 863-873, DOI: 10.1152/jn.1997.77.2.863.

(79) Zhao, Y.; Yang, Z.; Fan, W.; Wang, Y.; Li, G.; Cong, H.; Yuan, H. Carbon nanotube/carbon fiber electrodes via chemical vapor deposition for simultaneous determination of ascorbic acid, dopamine and uric acid. *Arabian Journal of Chemistry* **2018**, DOI: https://doi.org/10.1016/j.arabjc.2018.11.002.

(80) Chandra, S.; Wong, D. Electrochemical Detection of Neurotransmitters at Structurally Small Electrodes. 2009; p 21.

(81) Ross, A. E.; Venton, B. J. Nafion–CNT coated carbon-fiber microelectrodes for enhanced detection of adenosine. *Analyst* **2012,** *137* (13), 3045-3051, DOI: 10.1039/C2AN35297D.

(82) Yang, C.; Trikantzopoulos, E.; Jacobs, C. B.; Venton, B. J. Evaluation of carbon nanotube fiber microelectrodes for neurotransmitter detection: Correlation of

electrochemical performance and surface properties. *Analytica Chimica Acta* **2017,** *965*, 1-8, DOI: https://doi.org/10.1016/j.aca.2017.01.039.

(83) Oh, Y.; Heien, M. L.; Park, C.; Kang, Y. M.; Kim, J.; Boschen, S. L.; Shin, H.; Cho, H. U.; Blaha, C. D.; Bennet, K. E.; Lee, H. K.; Jung, S. J.; Kim, I. Y.; Lee, K. H.; Jang, D. P. Tracking tonic dopamine levels in vivo using multiple cyclic square wave voltammetry. *Biosensors and Bioelectronics* **2018,** *121*, 174-182, DOI: https://doi.org/10.1016/j.bios.2018.08.034.

(84) Zhu, M.; Zeng, C.; Ye, J.; Sun, Y. Simultaneous in vivo voltammetric determination of dopamine and 5-Hydroxytryptamine in the mouse brain. *Applied Surface Science* **2018,** *455*, 646-652, DOI: https://doi.org/10.1016/j.apsusc.2018.05.190.

(85) Hashemi, P.; Dankoski, E. C.; Wood, K. M.; Ambrose, R. E.; Wightman, R. M. In vivo electrochemical evidence for simultaneous 5-HT and histamine release in the rat substantia nigra pars reticulata following medial forebrain bundle stimulation. *Journal of Neurochemistry* **2011,** *118* (5), 749-759, DOI: 10.1111/j.1471-4159.2011.07352.x.

(86) Rees, H. R.; Anderson, S. E.; Privman, E.; Bau, H. H.; Venton, B. J. Carbon Nanopipette Electrodes for Dopamine Detection in Drosophila. *Anal. Chem. (Washington, DC, U. S.)* **2015,** *87* (7), 3849-3855, DOI: 10.1021/ac504596y.

(87) Yang, C.; Hu, K.; Wang, D.; Zubi, Y.; Lee, S. T.; Puthongkham, P.; Mirkin, M. V.; Venton, B. J. Cavity Carbon-Nanopipette Electrodes for Dopamine Detection. *Analytical Chemistry* **2019,** *91* (7), 4618-4624, DOI: 10.1021/acs.analchem.8b05885.

(88) Ding, S.; Liu, Y.; Ma, C.; Zhang, J.; Zhu, A.; Shi, G. Development of Glass-sealed Gold Nanoelectrodes for in vivo Detection of Dopamine in Rat Brain. *Electroanalysis* **2018,** *30* (6), 1041-1046, DOI: 10.1002/elan.201700522.

(89) Chandra, S.; Miller, A. D.; Bendavid, A.; Martin, P. J.; Wong, D. K. Y. Minimizing Fouling at Hydrogenated Conical-Tip Carbon Electrodes during Dopamine Detection in Vivo. *Analytical Chemistry* **2014,** *86* (5), 2443-2450, DOI: 10.1021/ac403283t.

(90) Chandra, S.; Miller, A. D.; Wong, D. K. Y. Evaluation of physically small p-phenylacetate-modified carbon electrodes against fouling during dopamine detection in vivo. *Electrochimica Acta* **2013,** *101*, 225-231, DOI: https://doi.org/10.1016/j.electacta.2012.11.022.

(91) McCreery, R. L. Advanced Carbon Electrode Materials for Molecular Electrochemistry. *Chemical Reviews* **2008,** *108* (7), 2646-2687, DOI: 10.1021/cr068076m.

(92) Kaivosoja, E.; Sainio, S.; Lyytinen, J.; Palomäki, T.; Laurila, T.; Kim, S. I.; Han, J. G.; Koskinen, J. Carbon thin films as electrode material in neural sensing. *Surface and Coatings Technology* **2014,** *259*, 33-38, DOI: https://doi.org/10.1016/j.surfcoat.2014.07.056.

(93) Zanin, H.; May, P. W.; Fermin, D. J.; Plana, D.; Vieira, S. M. C.; Milne, W. I.; Corat, E. J. Porous Boron-Doped Diamond/Carbon Nanotube Electrodes. *ACS Applied Materials & Interfaces* **2014,** *6* (2), 990-995, DOI: 10.1021/am4044344.

(94) Qi, Y.; Long, H.; Ma, L.; Wei, Q.; Li, S.; Yu, Z.; Hu, J.; Liu, P.; Wang, Y.; Meng, L. Enhanced selectivity of boron doped diamond electrodes for the detection of

dopamine and ascorbic acid by increasing the film thickness. *Applied Surface Science* **2016,** *390*, 882-889, DOI: http://dx.doi.org/10.1016/j.apsusc.2016.08.158.

(95) Rowley-Neale, S. J.; Banks, C. E. Electrocatalytic Properties of Carbon Electrode Surfaces A2 - Wandelt, Klaus. In *Encyclopedia of Interfacial Chemistry*; Elsevier: Oxford, 2018; pp 531-538.

(96) Yi, Y.; Weinberg, G.; Prenzel, M.; Greiner, M.; Heumann, S.; Becker, S.; Schlögl, R. Electrochemical corrosion of a glassy carbon electrode. *Catalysis Today* **2017,** *295*, 32-40, DOI: https://doi.org/10.1016/j.cattod.2017.07.013.

(97) Sun, Z.; Shi, X.; Tay, B. K.; Flynn, D.; Wang, X.; Zheng, Z.; Sun, Y. Low pressure polymer precursor process for synthesis of hard glassy carbon and diamond films. *Diamond and Related Materials* **1997,** *6* (2), 230-234, DOI: https://doi.org/10.1016/S0925-9635(96)00620-6.

(98) Lentz, C. M.; Samuel, B. A.; Foley, H. C.; Haque, M. A. Synthesis and Characterization of Glassy Carbon Nanowires. *Journal of Nanomaterials* **2011,** *2011*, 8, DOI: 10.1155/2011/129298.

(99) Shahbakhsh, M.; Narouie, S.; Noroozifar, M. Modified glassy carbon electrode with Polydopamine-multiwalled carbon nanotubes for simultaneous electrochemical determination of biocompounds in biological fluids. *Journal of Pharmaceutical and Biomedical Analysis* **2018,** *161*, 66-72, DOI: https://doi.org/10.1016/j.jpba.2018.08.034.

(100) Selvarajan, S.; Suganthi, A.; Rajarajan, M. A novel highly selective and sensitive detection of serotonin based on Ag/polypyrrole/Cu2O nanocomposite modified glassy

carbon electrode. *Ultrasonics Sonochemistry* **2018,** *44*, 319-330, DOI: https://doi.org/10.1016/j.ultsonch.2018.02.038.

(101) Gonon, F.; Cespuglio, R.; Ponchon, J. L.; Buda, M.; Jouvet, M.; Adams, R. N.; Pujol, J. F. [In vivo continuous electrochemical determination of dopamine release in rat neostriatum]. *C R Acad Sci Hebd Seances Acad Sci D* **1978,** *286* (16), 1203-1206.

(102) Matsuhisa, Y.; Bunsell, A. R. 16 - Tensile failure of carbon fibers. In *Handbook of Tensile Properties of Textile and Technical Fibres*; Bunsell, A. R., Ed.; Woodhead Publishing: 2009; pp 574-602.

(103) Inagaki, M. CHAPTER 4 - Carbon Fibers. In *New Carbons - Control of Structure and Functions*; Inagaki, M., Ed.; Elsevier Science: Oxford, 2000; pp 82-123.

(104) Huffman, M. L.; Venton, B. J. Carbon-fiber microelectrodes for in vivo applications. *The Analyst* **2009,** *134* (1), 18-24, DOI: 10.1039/b807563h.

(105) Si, B.; Song, E. Recent advances in the detection of neurotransmitters. *Chemosensors* **2018,** *6* (1), 1/1-1/24, DOI: 10.3390/chemosensors6010001.

(106) Özel, R. E.; Hayat, A.; Andreescu, S. Recent Developments in Electrochemical Sensors for the Detection of Neurotransmitters for Applications in Biomedicine. *Analytical Letters* **2015,** *48* (7), 1044-1069, DOI: 10.1080/00032719.2014.976867.

(107) Lovinger, D. M. Neurotransmitter roles in synaptic modulation, plasticity and learning in the dorsal striatum. *Neuropharmacology* **2010,** *58* (7), 951-961, DOI: 10.1016/j.neuropharm.2010.01.008.

(108) Lin, X.; Zhang, Y.; Chen, W.; Wu, P. Electrocatalytic oxidation and determination of dopamine in the presence of ascorbic acid and uric acid at a poly (p-nitrobenzenazo resorcinol) modified glassy carbon electrode. *Sensors and Actuators B: Chemical* **2007,** *122* (1), 309-314, DOI: https://doi.org/10.1016/j.snb.2006.06.004.

(109) Borcherding, B.; Rendleman, R. L.; Walkup, J. T. 60 - Neuropsychopharmacology. In *Swaiman's Pediatric Neurology (Sixth Edition)*; Swaiman, K. F.; Ashwal, S.; Ferriero, D. M.; Schor, N. F.; Finkel, R. S.; Gropman, A. L.; Pearl, P. L.; Shevell, M. I., Eds.; Elsevier: 2017; pp 489-495.

(110) Njagi, J.; Chernov, M. M.; Leiter, J. C.; Andreescu, S. Amperometric Detection of Dopamine in Vivo with an Enzyme Based Carbon Fiber Microbiosensor. *Analytical Chemistry* **2010,** *82* (3), 989-996, DOI: 10.1021/ac9022605.

(111) McNally, M.; Wong, D. K. Y. An in Vivo Probe Based on Mechanically Strong but Structurally Small Carbon Electrodes with an Appreciable Surface Area. *Analytical Chemistry* **2001,** *73* (20), 4793-4800, DOI: 10.1021/ac0104532.

(112) Edwards, G. A.; Bergren, A. J.; Porter, M. D. 8 - Chemically Modified Electrodes. In *Handbook of Electrochemistry*; Zoski, C. G., Ed.; Elsevier: Amsterdam, 2007; pp 295-327.

(113) Singh, Y. S.; Sawarynski, L. E.; Michael, H. M.; Ferrell, R. E.; Murphey-Corb, M. A.; Swain, G. M.; Patel, B. A.; Andrews, A. M. Boron-Doped Diamond Microelectrodes Reveal Reduced Serotonin Uptake Rates in Lymphocytes from Adult Rhesus Monkeys Carrying the Short Allele of the 5-HTTLPR. *ACS Chemical Neuroscience* **2010,** *1* (1), 49-64, DOI: 10.1021/cn900012y.

(114) Kim, A. R.; Park, T. J.; Kim, M. S.; Kim, I.-H.; Kim, K.-S.; Chung, K. H.; Ko, S. Functional fusion proteins and prevention of electrode fouling for a sensitive electrochemical immunosensor. *Analytica Chimica Acta* **2017,** *967*, 70-77, DOI: https://doi.org/10.1016/j.aca.2017.02.026.

(115) Chandra, S.; Siraj, S.; Wong, D. K. Y. Recent Advances in Biosensing for Neurotransmitters and Disease Biomarkers using Microelectrodes. *ChemElectroChem* **2017,** *4* (4), 822-833, DOI: 10.1002/celc.201600810.

(116) Hanssen Benjamin, L.; Siraj, S.; Wong Danny, K. Y., Recent strategies to minimise fouling in electrochemical detection systems. In *Reviews in Analytical Chemistry*, 2016; Vol. 35, p 1.

(117) Harreither, W.; Trouillon, R.; Poulin, P.; Neri, W.; Ewing, A. G.; Safina, G. Cysteine residues reduce the severity of dopamine electrochemical fouling. *Electrochim. Acta* **2016,** *210*, 622-629, DOI: 10.1016/j.electacta.2016.05.124.

(118) Harreither, W.; Trouillon, R.; Poulin, P.; Neri, W.; Ewing, A. G.; Safina, G. Carbon Nanotube Fiber Microelectrodes Show a Higher Resistance to Dopamine Fouling. *Anal. Chem. (Washington, DC, U. S.)* **2013,** *85* (15), 7447-7453, DOI: 10.1021/ac401399s.

(119) Chang, A.-Y.; Dutta, G.; Siddiqui, S.; Arumugam, P. U. Surface Fouling of Ultrananocrystalline Diamond Microelectrodes during Dopamine Detection: Improving Lifetime via Electrochemical Cycling. *ACS Chemical Neuroscience* **2018**, DOI: 10.1021/acschemneuro.8b00257.

(120) Patel, A. N.; Unwin, P. R.; Macpherson, J. V. Investigation of film formation properties during electrochemical oxidation of serotonin (5-HT) at polycrystalline boron doped diamond. *Physical Chemistry Chemical Physics* **2013,** *15* (41), 18085-18092, DOI: 10.1039/C3CP53513D.

(121) Chandra, S.; Miller, A. D.; Bendavid, A.; Martin, P. J.; Wong, D. K. Y. Minimizing Fouling at Hydrogenated Conical-Tip Carbon Electrodes during Dopamine Detection in Vivo. *Anal. Chem. (Washington, DC, U. S.)* **2014,** *86* (5), 2443-2450, DOI: 10.1021/ac403283t.

(122) Gonon, F.; Buda, M.; Cespuglio, R.; Jouvet, M.; Pujol, J.-F. In vivo electrochemical detection of catechols in the neostriatum of anaesthetized rats: dopamine or DOPAC? *Nature* **1980,** *286* (5776), 902-904, DOI: 10.1038/286902a0.

(123) Hawley, M. D.; Tatawawadi, S. V.; Piekarski, S.; Adams, R. N. Electrochemical Studies of the Oxidation Pathways of Catecholamines. *Journal of the American Chemical Society* **1967,** *89* (2), 447-450, DOI: 10.1021/ja00978a051.

(124) Tse, D. C. S.; McCreery, R. L.; Adams, R. N. Potential oxidative pathways of brain catecholamines. *Journal of Medicinal Chemistry* **1976,** *19* (1), 37-40, DOI: 10.1021/jm00223a008.

(125) Chang, A.-Y.; Dutta, G.; Siddiqui, S.; Arumugam, P. U. Surface Fouling of Ultrananocrystalline Diamond Microelectrodes during Dopamine Detection: Improving Lifetime via Electrochemical Cycling. *ACS Chemical Neuroscience* **2019,** *10* (1), 313-322, DOI: 10.1021/acschemneuro.8b00257.

(126) Harreither, W.; Trouillon, R.; Poulin, P.; Neri, W.; Ewing, A. G.; Safina, G. Carbon Nanotube Fiber Microelectrodes Show a Higher Resistance to Dopamine Fouling. *Analytical Chemistry* **2013,** *85* (15), 7447-7453, DOI: 10.1021/ac401399s.

(127) Yang, C.; Jill Venton, B. In *Carbon Nanomaterials for Neuroanalytical Chemistry*, John Wiley & Sons, Inc.: 2017; pp 55-83.

(128) Patel, J.; Radhakrishnan, L.; Zhao, B.; Uppalapati, B.; Daniels, R. C.; Ward, K. R.; Collinson, M. M. Electrochemical Properties of Nanostructured Porous Gold Electrodes in Biofouling Solutions. *Analytical Chemistry* **2013,** *85* (23), 11610-11618, DOI: 10.1021/ac403013r.

(129) Vreeland, R. F.; Atcherley, C. W.; Russell, W. S.; Xie, J. Y.; Lu, D.; Laude, N. D.; Porreca, F.; Heien, M. L. Biocompatible PEDOT:Nafion Composite Electrode Coatings for Selective Detection of Neurotransmitters in Vivo. *Analytical Chemistry* **2015,** *87* (5), 2600-2607, DOI: 10.1021/ac502165f.

(130) Yang, C.; Trikantzopoulos, E.; Nguyen, M. D.; Jacobs, C. B.; Wang, Y.; Mahjouri-Samani, M.; Ivanov, I. N.; Venton, B. J. Laser Treated Carbon Nanotube Yarn Microelectrodes for Rapid and Sensitive Detection of Dopamine in Vivo. *ACS Sensors* **2016,** *1* (5), 508-515, DOI: 10.1021/acssensors.6b00021.

(131) Algarra, M.; González-Calabuig, A.; Radotić, K.; Mutavdzic, D.; Ania, C. O.; Lázaro-Martínez, J. M.; Jiménez-Jiménez, J.; Rodríguez-Castellón, E.; del Valle, M. Enhanced electrochemical response of carbon quantum dot modified electrodes. *Talanta* **2018,** *178*, 679-685, DOI: https://doi.org/10.1016/j.talanta.2017.09.082.

(132) Park, J.; Show, Y.; Quaiserova, V.; Galligan, J. J.; Fink, G. D.; Swain, G. M. Diamond microelectrodes for use in biological environments. *Journal of Electroanalytical Chemistry* **2005,** *583* (1), 56-68, DOI: https://doi.org/10.1016/j.jelechem.2005.04.032.

(133) Dong, H.; Wang, S.; Galligan, J. J.; Swain, G. M. Boron-doped diamond nano/microelectrodes for biosensing and in vitro measurements. *Frontiers in bioscience (Scholar edition)* **2011,** *3*, 518-540.

(134) Shin, D.; Tryk, D. A.; Fujishima, A.; Merkoçi, A.; Wang, J. Resistance to Surfactant and Protein Fouling Effects at Conducting Diamond Electrodes. *Electroanalysis* **2005,** *17* (4), 305-311, DOI: 10.1002/elan.200403104.

(135) Chen, Q.; Swain, G. M. Structural Characterization, Electrochemical Reactivity, and Response Stability of Hydrogenated Glassy Carbon Electrodes. *Langmuir* **1998,** *14* (24), 7017-7026, DOI: 10.1021/la980907z.

(136) Arrigo, R.; Hävecker, M.; Wrabetz, S.; Blume, R.; Lerch, M.; McGregor, J.; Parrott, E. P. J.; Zeitler, J. A.; Gladden, L. F.; Knop-Gericke, A.; Schlögl, R.; Su, D. S. Tuning the Acid/Base Properties of Nanocarbons by Functionalization via Amination. *Journal of the American Chemical Society* **2010,** *132* (28), 9616-9630, DOI: 10.1021/ja910169v.

(137) Roberts, J. G.; Moody, B. P.; McCarty, G. S.; Sombers, L. A. Specific Oxygen-Containing Functional Groups on the Carbon Surface Underlie an Enhanced Sensitivity to Dopamine at Electrochemically Pretreated Carbon Fiber Microelectrodes. *Langmuir* **2010,** *26* (11), 9116-9122, DOI: 10.1021/la9048924.

(138) Kaibara, Y.; Sugata, K.; Tachiki, M.; Umezawa, H.; Kawarada, H. Control wettability of the hydrogen-terminated diamond surface and the oxidized diamond surface using an atomic force microscope. *Diamond and Related Materials* **2003,** *12* (3-7), 560-564, DOI: Doi: 10.1016/s0925-9635(02)00373-4.

(139) Siraj, S.; McRae, C. R.; Wong, D. K. Y. Effective activation of physically small carbon electrodes by n-butylsilane reduction. *Electrochemistry Communications* **2016,** *64*, 35-41, DOI: http://dx.doi.org/10.1016/j.elecom.2016.01.007.

(140) Nimmagadda, R. D.; McRae, C. A novel reduction reaction for the conversion of aldehydes, ketones and primary, secondary and tertiary alcohols into their corresponding alkanes. *Tetrahedron Letters* **2006,** *47* (32), 5755-5758, DOI: http://dx.doi.org/10.1016/j.tetlet.2006.06.007.

(141) Nimmagadda, R. D.; McRae, C. Characterisation of the backbone structures of several fulvic acids using a novel selective chemical reduction method. *Organic Geochemistry* **2007,** *38* (7), 1061-1072, DOI: http://dx.doi.org/10.1016/j.orggeochem.2007.02.016.

CHAPTER 2: GENERAL METHODOLOGY

2.1 Introduction

A long-term goal of this work is to develop structurally small antifouling carbon electrodes that are implantable in a mammalian brain to obtain meaningful results during *in vivo* detection of neurotransmitter dopamine. However, one of the major challenges during *in vivo* monitoring of neurotransmitters is the adsorption of non-targeted species on the electrode surface, which subsequently impedes the analytical performance of the electrode. Therefore, in this work, we report the fabrication of small antifouling carbon electrodes for *in vivo* measurement of dopamine. Apart from the small physical dimension electrodes with antifouling characteristics required for *in vivo* measurement of neurotransmitters, the fabrication procedure must also be simple and convenient to perform with a relatively high success rate. As such, we routinely fabricate implantable carbon electrodes in our laboratory using a simple procedure developed by McNally and Wong[1]. To obtain an antifouling surface, the fabricated carbon electrodes are hydrogenated using a silane reduction method in presence of a catalyst and anhydrous CH_2Cl_2[2-3]. After hydrogenation, the carbon electrodes are initially characterised using X-ray photoelectron spectroscopy, Raman spectroscopy and atomic force microscopy to determine the surface characteristics. Electrochemical characterisation is then conducted using several redox markers to evaluate the effectiveness of the hydrogenation procedure. To determine the antifouling properties, the electrodes are incubated in a laboratory synthetic fouling solution mimicking the extracellular matrix for a defined period, in SH-SY5Y dopamine cells and brain slices. The percentage change in the current is used to estimate the degree of fouling. The present chapter is devoted to the detailed description of the general instrumentation and

experimental procedure adopted such that the most reliable results can be obtained. Description related to a specific aspect of work will be presented in the Experimental section of each of the following chapters in this thesis.

2.2 General chemicals and reagents

The list below shows the general chemicals and reagents used in this study.

Chemicals / Reagents (Purity %)	**Source**
4-Methylcatechol (95%)	Sigma Aldrich
Acetylene	BOC Australia
Anhydrous CH_2Cl_2 (99.8%)	Sigma Aldrich
Anthraquinone disulfonic acid	Sigma Aldrich
Ascorbic acid	Sigma Aldrich
Bovine serum albumin (98%)	Sigma Aldrich
Citric acid (99%)	Sigma Aldrich
Cytochrome *c*	Sigma Aldrich
Dihydroxyphenylacetic acid (98%)	Sigma Aldrich
Dopamine hydrochloride	Sigma Aldrich
Ethanol (70%)	Sigma Aldrich
Graphite powder	Sigma Aldrich
Hexaammineruthenium(II) chloride (99%)	Sigma Aldrich
Hexanoic acid (98%)	Sigma Aldrich
Human fibrino peptide B (98%)	Sigma Aldrich
Nitrogen	BOC Australia
Phenylsilane (97%)	Sigma Aldrich
Potassium chloride (>99%)	Sigma Aldrich
Potassium hexacyanoferrate (III)	Sigma Aldrich
Sodium phosphate dibasic heptahydrate (98%)	Sigma Aldrich
Sulfuric Acid	Sigma Aldrich
Triethylsilane (99%)	Sigma Aldrich
Trispentafluorophenyl borane (95%)	Sigma Aldrich
Uric acid (99%)	Sigma Aldrich

2.3 Fabrication of structurally small carbon electrodes

Structurally small conical-tip carbon electrodes are routinely fabricated in our lab. All working electrodes used in this work were fabricated as previously described[4]. Initially,

quartz capillaries (1.0 mm outside diameter, 0.5 mm inside diameter and 75 mm length; Sutter Instruments, Novato, CA, USA) were pulled down to small tip using a P-2000 Sutter Puller (Sutter Instruments Co.) as illustrated in Figure 2.1. Depending on the parameters used for pulling, different sizes and shapes of pulled capillaries were obtained. The pulled quartz capillaries were then visually examined under the microscope to ensure the tip was not broken or cracked before they were used further.

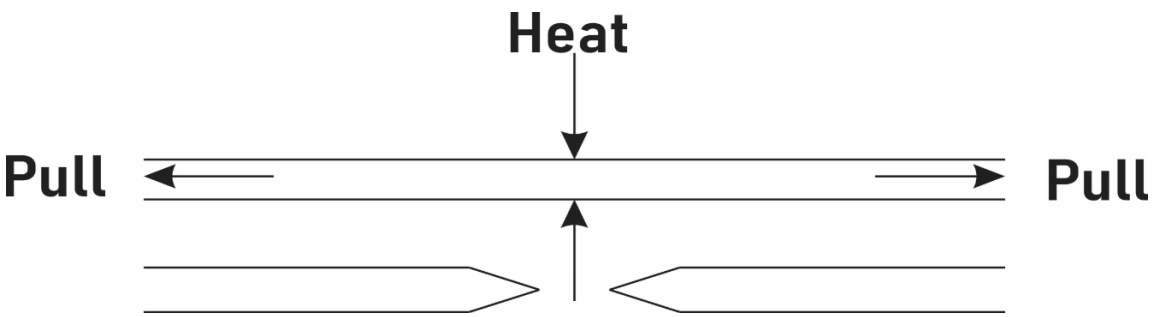

Figure 2.1. Schematic illustrating pulling of quartz capillaries by a Sutter Micropipette Puller.

Carbon was then deposited at the tip and on the shank of pulled capillaries. In this step, a pulled capillary was housed in a 10-cm long nuclear magnetic resonance tube using a stainless-steel T-piece ($^1/_{16}$"×$^1/_{16}$"×$^1/_{16}$") as illustrated in Figure 2.2. Through the T-piece, acetylene (50 kPa) was delivered *via* the larger end of the pulled capillary, while a stream of nitrogen (60 mL min^{-1}) was counter-flowing through the nuclear magnetic resonance tube. By thermally pyrolysing acetylene for 4 min, carbon was deposited at the tip and on the shank of the pulled capillary tube to obtain a conical-tip carbon electrode. To prevent thermal shock to the capillary which would lead to tip fracture, it was crucial to begin thermally heating the end of the nuclear magnetic resonance tube

away from the tip at the start, slowly moving the flame along the region of the nuclear magnetic resonance tube housing-the capillary.

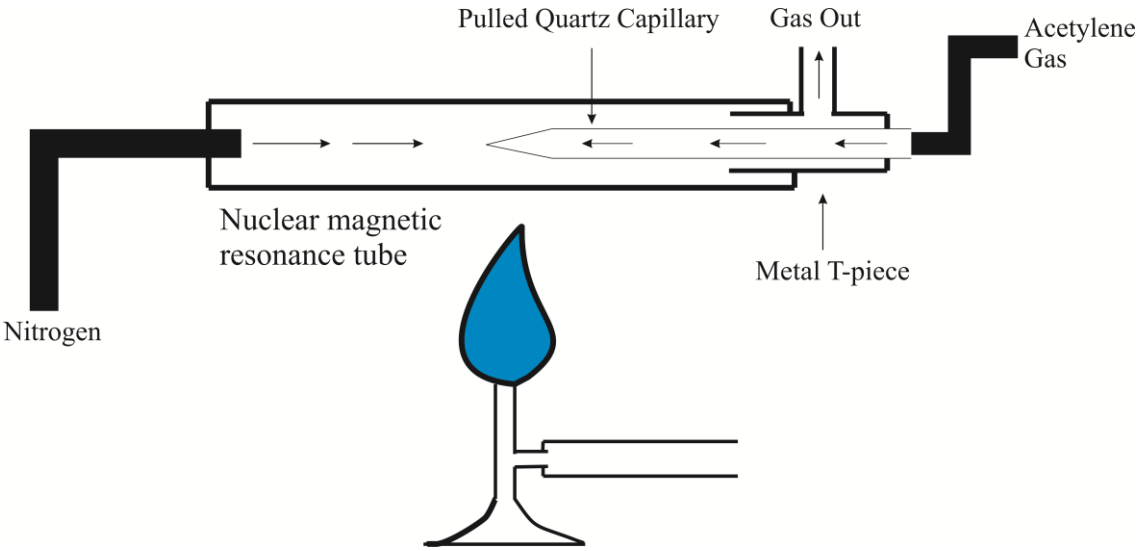

Figure 2.2. Schematic illustration of depositing carbon in and on a pulled quartz capillary.

After cooling for 30 s, the capillary was rinsed with MilliQ water to remove any impurities. To accomplish an electrical connection, graphite powder was introduced through the larger end of the capillary, before securing a copper wire with epoxy resin at the junction of the capillary. A schematic illustration of a small carbon electrode is shown in Figure 2.3

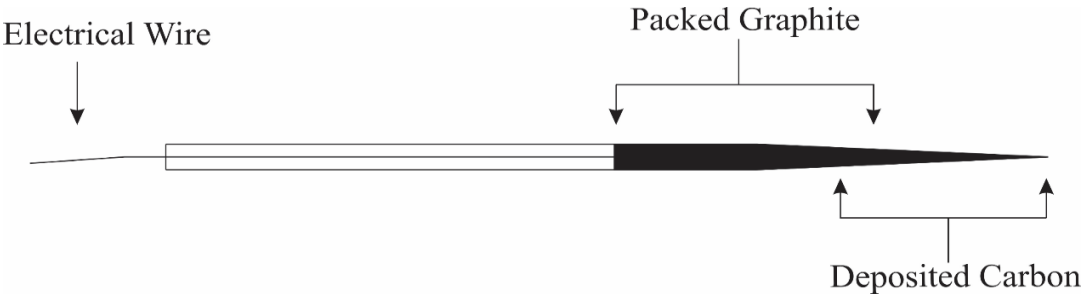

Figure 2.3. Schematic of a structurally small carbon electrode.

2.4 Silane Hydrogenation

Silane hydrogenation has been reported to be one of the simplest ways to reduce alcohols, aldehydes, ketones and carboxylic acids to their respective alkyl groups with the formation of siloxane dendrimers through the phenol functionality[2-3]. In this study, triethylsilane and phenylsilane were used to hydrogenate the small carbon electrodes to obtain an antifouling surface.

To hydrogenate, 5 mg of $B(C_3F_5)_3$ (reaction catalyst) was dissolved in 5 mL of anhydrous CH_2Cl_2 by stirring for approximately 10 min before introducing 25 µL of triethylsilane or phenylsilane. Next, a conical-tip carbon electrode was carefully placed in the solution containing $B(C_3F_5)_3$, anhydrous CH_2Cl_2 and either triethylsilane or phenylsilane continuously purged with nitrogen. The setup was then sealed properly to avoid any moisture contact and the treatment was persisted for 2 h at ambient temperature.

After hydrogenation, the electrodes were left in sealed containers for at least 1 h before further use.

2.5 Electrochemical Characterisation

Electrodes fabricated in this work were characterised using several redox markers to evaluate the surface chemistry before and after they were hydrogenated. Cyclic voltammetry was used to characterise the electrodes using a low-current picostat (eDAQ Pty Ltd., Sydney Australia) operated using EChem software version 2.1.2 on a PC with an E-corder interface. A single compartment three-electrode cell consisting of

an Ag|AgCl reference electrode, a Pt wire counter and a conical-tip carbon working electrode. All experiments were carried out in a Faraday cage at ambient temperature.

2.5.1 Cyclic Voltammetry

Cyclic voltammetry was used to electrochemically characterise all fabricated electrodes in this work. In this work, a voltage is scanned linearly from an initial value to a predetermined limit (also known as a switching potential) from where the direction of the scan is reversed[5]. Table 2.1 shows the list of redox markers, the supporting electrolyte and the oxidation/reduction potential range for each redox reaction used in this work to electrochemically characterise the fabricated electrodes. To minimise any effects of oxygen, all solutions degassed by nitrogen before they were kept under a stream of nitrogen gas with constant stirring for 10 min prior to each measurement. All electrochemical experiments were carried out in a Faraday cage.

Table 2.1. Redox markers used to characterise fabricated electrodes, the supporting electrolyte used and the reduction/ oxidation potential range.

Redox Marker	**Supporting Electrolyte**	**Redox Potential Range/ V**
1.0 mM $[Ru(NH_3)_6]^{3+}$	1.0 M KCl	+0.2 to -0.6
1.0 mM $[Fe(CN)_6]^{3-}$	1.0 M KCl	+0.2 to -0.4
1.0 mM Dopamine	pH 7.4 citrate/phosphate buffer	-0.2 to +0.6
1.0 mM Anthraquinone 2,6 disulfonic acid	pH 7.4 citrate/phosphate buffer	+0.6 to -0.8
1.0 mM 4-methylcatechol	pH 7.4 citrate/phosphate buffer	-0.2 to +0.8
1.0 mM Dihydroxyphenylacetic acid	pH 7.4 citrate/phosphate buffer	-0.2 to +0.8

2.5.2 Chronoamperometry

Chronoamperometry was employed to determine the tip dimension and electroactive area of the fabricated carbon electrodes. This technique involves application of a constant potential to the electrode and the resultant current was measured as a function of time[6]. The potential waveform used in chronoamperometry is depicted in Figure 2.4(a). As with cyclic voltammetry, this technique is conducted using a stationary electrode, initially at a potential where the target analyte does not undergo any electrochemical reaction. The potential is then stepped to a point beyond that required for the analyte to be electrochemically oxidised or reduced[7]. Here its surface concentration becomes effectively zero and the resulting current-time dependence is monitored, and a typical plot is shown in Figure 2.4(b). In this work, the $[Ru(NH_3)_6]^{3+}$ in 1.0 M KCl redox system was used with its reduction potential pre-determined using cyclic voltammetry. Accordingly, a constant potential was applied to a carbon electrode and the corresponding current decay was measured as a function of time. A plot of the decaying current at a specific potential in Figure 2.4(b) is then plotted against $(t)^{-1/2}$ based on Equation (2.1)[8] for the current (i) obtained at an electrode of a cylindrical geometry.

$$i = \frac{nFADC}{r}\left[0 \cdot 5 + \frac{r}{\sqrt{\pi D t}}\right] \qquad \text{Equation 2.1}$$

where n is the moles of electrons involves in the reaction, F is Faradays Constant (96485 C mol^{-1}, A is the electrochemical area (cm^2), D is diffusion coefficient (5.3×10^{-6} cm^2 s^{-1}), C is the concentration (mol cm^{-3}), and r is the radius of the electrode (cm). Previous work from our group has shown that all conical-tip carbon electrodes constructed in this work exhibit a cylindrical surface area on their shank ~130 times larger than that

of a disc at the tip[1]. Accordingly, the fractional contribution from the disc current is relatively small. Therefore, as an approximation, we will consider the total current at a conical-tip carbon electrode to be represented by *i* in Equation (2.1). Based on the slope of the straight-line plot of decaying current against $(t)^{-1/2}$, A can be calculated. The length of the electrode can be estimated after evaluating *r* from the ordinate intercept and the known *A* value.

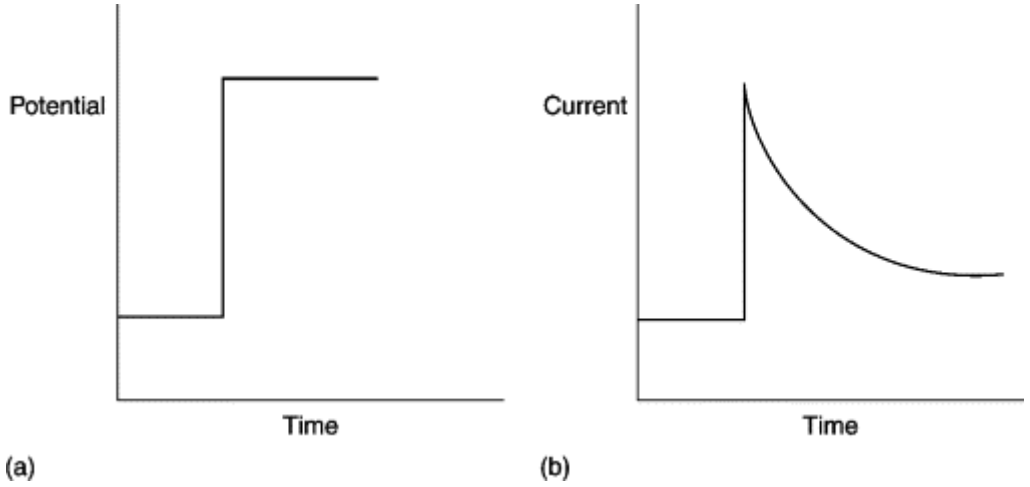

Figure 2.4. Typical potential waveform and the resulting current-versus time plot[7].

2.6 Laboratory synthetic fouling solution

To evaluate the antifouling characteristics of fabricated electrodes, a laboratory synthetic fouling solution containing 2.0 % (w/v) bovine serum albumin (a protein), 0.01 % (w/v) cytochrome *c* (a protein), 0.001% (w/v) human fibrinopeptide (a peptide) and 0.01% (w/v) caproic acid (a lipid) was prepared in pH 7.4 citrate/phosphate buffer to mimic the extracellular fluid. Next, the electrodes were incubated in the fouling solution for 1-week to assess their fouling resistance by comparing the voltammetric limiting current (I_{lim}) before incubation versus after incubation in the fouling solution.

2.7 Statistical Analysis

The statistical significance of all correlation coefficients at the 95% confidence interval was tested using Student's *t*-test. The linearity of all the calibration line used was determined using the Wald-Wolfowitz runs test and the uncertainties associated with the slope and the intercept of a calibration plot are expressed as 95% confidence limits[9].

2.8 References

(1) McNally, M.; Wong, D. K. Y. An in Vivo Probe Based on Mechanically Strong but Structurally Small Carbon Electrodes with an Appreciable Surface Area. *Analytical Chemistry* **2001,** *73* (20), 4793-4800, DOI: 10.1021/ac0104532.

(2) Nimmagadda, R. D.; McRae, C. A novel reduction reaction for the conversion of aldehydes, ketones and primary, secondary and tertiary alcohols into their corresponding alkanes. *Tetrahedron Letters* **2006,** *47* (32), 5755-5758, DOI: http://dx.doi.org/10.1016/j.tetlet.2006.06.007.

(3) Nimmagadda, R. D.; McRae, C. Characterisation of the backbone structures of several fulvic acids using a novel selective chemical reduction method. *Organic Geochemistry* **2007,** *38* (7), 1061-1072, DOI: http://dx.doi.org/10.1016/j.orggeochem.2007.02.016.

(4) McNally, M.; Wong, D. K. An in vivo probe based on mechanically strong but structurally small carbon electrodes with an appreciable surface area. *Analytical chemistry* **2001,** *73* (20), 4793-4800.

(5) Mabbott, G. A. An introduction to cyclic voltammetry. *Journal of Chemical Education* **1983,** *60* (9), 697, DOI: 10.1021/ed060p697.

(6) Britz, D.; Chandra, S.; Strutwolf, J.; Wong, D. K. Y. Diffusion-limited chronoamperometry at conical-tip microelectrodes. *Electrochimica Acta* **2010,** *55* (3), 1272-1277, DOI: https://doi.org/10.1016/j.electacta.2009.10.025.

(7) Honeychurch, K. C. 13 - Printed thick-film biosensors. In *Printed Films*; Prudenziati, M.; Hormadaly, J., Eds.; Woodhead Publishing: 2012; pp 366-409.

(8) Amatore, C.; Rubinstein, I. Physical electrochemistry: Principles, methods and applications. *I Rubenstein, Marcel Dekker, New York* **1995,** *131*.

(9) Miller, J. C.; Miller, J. N. *Statistics and Chemometrics for Analytical Chemistry, 4th Edition*, Prentice Hall: 2000; p 271 pp.

CHAPTER 3: SURFACE CHARACTERISTICS OF STRUCTURALLY SMALL TRIETHYLSILANE AND PHENYLSILANE HYDROGENATED CARBON ELECTRODES

3.1 Introduction

This Chapter begins with the fabrication of small carbon electrodes outlined by the procedure previously reported by our group[1]. Initially, the fabricated electrodes were characterised using $[Ru(NH_3)_6]^{3+}$ to assess the electrode functionality. During detection of neurotransmitters in biological tissues, one of the major problems encountered is the non-specific adsorption of non-targeted species on the electrode surface caused by the amphiphilic-hydrophilic attraction between non-targeted species such as proteins, peptides and lipids present in a biological tissue and a bare carbon surface. Such adsorbates affect the transients, electrode active area and detection sensitivity. Hydrogenation is one way to minimise adsorption of non-targeted species on the hydrophilic carbon surface. In this work, the small carbon electrodes were hydrogenated using triethylsilane and phenylsilane in the presence of the catalyst trispentafluorophenyl borane ($B(C_6F_5)_3$) and anhydrous dichloromethane (CH_2Cl_2) as outlined in Section 2.4. The hydrogenated electrodes were then characterised using scanning electron microscopy, X-ray photoelectron spectroscopy and Raman spectroscopy to evaluate the elemental composition of the fabricated electrodes, followed by electrochemical characterisation in several redox markers including $[Fe(CN)_6]^{3-}$, dopamine, dihydroxyphenylacetic acid (DOPAC), 4-methylcatechol and

anthraquinone 2,4 disulfonic acid (AQDS). All the data acquired were compared to those obtained at non-hydrogenated carbon electrodes.

3.2 Electrode Fouling

Electrode fouling is a common problem encountered during the electrochemical detection of neurotransmitters *in vivo*, which has often been recognised as a significant reason for failures in electrochemical biosensor development[2]. There are generally two main types of fouling arising from different mechanisms. The first type is biological fouling that occurs after an insulating film has been formed by non-specific adsorption of amphiphilic proteins, peptides and lipids, preventing analytes of interest from making physical contact with the electrode, resulting in diminishing transient detection signals. In many cases, this adsorption is promoted by the hydrophilic nature of a carbon electrode surface arising from oxygen-containing functional groups such as carboxyl, aldehyde, ketone, and phenols[3]. The second type is electrochemical fouling where an insulating film is formed on the sensing surface upon the redox reaction of the analyte itself during detection. This type of fouling is typical of the oxidation of several neurotransmitters such as dopamine and serotonin[2]. For example, the presence of hydroxy groups on a carbon fibre surface in combination with sp^2 hybridised carbon contribute to the adsorption of polar neurotransmitters and metabolites, their oxidation products and large biomolecules[4-5]. The above phenomena reduce both the electron transfer kinetics and the detection capability of electrodes upon subsequent measurements[3, 6-8]. Notably, minimising the nonspecific adsorption on the sensing interface is an essential step towards practical applications of biosensors. In this respect, microelectrodes void of surface carbon–oxygen functional groups that only facilitates weak molecular adsorption are preferred for these applications[9].

3.3 Development of antifouling surfaces

Several methodologies involving modification of sensing surfaces with materials have been developed to alleviate problems arising from electrode fouling. For example, Zhu *et al.*[10] implanted a graphene-iron-tetrasulfophthalocyanine modified carbon fibre microelectrode (~7 μm diameter and 200 μm length) in a mouse brain to simultaneously detect dopamine and serotonin using differential pulse voltammetry. The authors reported that the modified carbon fibre electrode demonstrated improved antifouling properties with only a 20% decline in the amperometric current that stabilised after 250 s following implantation.

Liu *et al.*[11] reported a pre-treated multi-walled carbon nanotube/carbon fibre microelectrode with an artificial bovine serum albumin containing cerebral fluid before they were calibrated for *in vivo* measurements. In this way, the authors estimated a post-calibration sensitivity to pre-calibration sensitivity ratio close to 94%. Primarily, the strategy is to pre-foul electrodes before implantation, and thus they will be less sensitive to bovine serum albumin over adsorption or changes in their surface hydrophobicity upon implantation *in vivo*.

In a separate work, Zestos *et al.*[12] applied a polyethyleneimine carbon nanotube fibre electrode to detect neurotransmitters in a brain slice. The authors did not observe any change in the neurotransmitter oxidation current after a 30 min implantation period *in vivo*. The authors' evaluation of electrode fouling by the serotonin oxidation product in the presence of 5-hydroxyindoleacetic acid (a serotonin metabolite that is the main cause of carbon fibre microelectrode fouling during detection of serotonin) revealed no significant change in the oxidation or reduction (repeated measures one-way ANOVA, $p = 0.4604$, N = 6). Swami and Venton[13] used 25 consecutive flow injection analysis

experiments to examine the extent to which single-walled carbon nanotube treated carbon fibre electrodes would reduce the fouling rate by serotonin. Oxidation currents were normalised to the first response for each electrode to account for varying sensitivities between electrodes. In their study, bare carbon fibre electrodes lost ~40% of their sensitivity by the 25th injection, while a corresponding <10% loss in sensitivity was observed at a single-walled carbon nanotube-modified carbon fibre electrode. Therefore, they concluded that carbon nanotubes provide protection against fouling in conjunction with fast-scan cyclic voltammetry.

Aptamer based electrodes for detection of neurotransmitters such as dopamine in biological fluids are also affected by non-specific adsorption of media, which predominantly takes place at positively charged spots on an electrode surface[14]. Alvares-Martos *et al*.[15] showed that an RNA aptamer tethered through the alkanethiol linkage to a cysteamine-modified electrode and electrostatically interacting with it through the sugar-phosphate backbone of RNA minimises electrode fouling to some extent. In a separate work, the same group further evaluated the fouling resistance of aptamer based gold electrodes in serum and blood[14]. Using electrochemical impedance spectroscopy, the authors reported the effects of serum and blood adsorption on aptamer/cysteamine, aptamer and cysteamine modified gold electrodes. Accordingly, they reported that aptamer/cysteamine electrodes were more resistant to serum protein adsorption with capacitance electric-double layer in serum more than that of blood. At the same electrode, the charge transfer resistance was reported to be 0.24 kΩ compared to 1.4 kΩ at an aptamer modified gold electrode in a pH 7.4 phosphate buffered saline[14].

Wu and colleagues[16] reported the antifouling characteristics of a 3-thienylphosphonic acid modified gold electrode. The authors compared the response of a bare gold

electrode to that of a 3-thienylphosphonic acid modified gold electrode by successive potential scans. They reported a continuous positive shift of the oxidation potential arising from the polymerisation of dopamine oxidation product at the bare gold electrode. On the other hand, the 3-thienylphosphonic acid modified gold electrode showed only 5% decrease in the peak potential and a 15-mV positive shift of the peak potential. They attributed the antifouling characteristics of 3-thienylphosphonic acid modified gold electrode to completely deprotonated -PO_3H_2 groups of the 3-thienylphosphonic acid self-assembled monolayers in a pH 7.4 buffer which would then bind strongly with positively charged dopamine through the electrostatic interaction or hydrogen bonding. The supramolecular complex between 3-thienylphosphonic acid and dopamine was energetically stable due to charge balance. Moreover, a higher density of negatively charged PO_3H_2 groups on the modified surface was likely to stabilise the chain of dopamine, preventing the ring closure reaction of dopamine-*o*-quinone that would otherwise further polymerises on the surface[16].

3.4 Boron-doped diamond electrodes

There have been substantial developments involving boron-doped diamond as an oxide free and a hydrogen-terminated electrode material that offers a wide Faradaic electrochemical potential window, low background currents, and excellent dimensional stability, and low concentrations of polar surface functional groups with less surface passivation and conductivity loss, making these electrodes hold great promise for neurochemical monitoring[6, 17-19]. This is because natural diamond is an electrically insulating material that cannot be used as an electrode, but the introduction of impurities within the sp^3-hybridised tetrahedral lattice of diamond makes it conductive. For example, Trouillon and O'Hare[20] compared the performance of three carbon-based

electrodes, glassy carbon, glassy carbon with low surface oxides, and boron-doped diamond electrode towards the voltammetric detection of $[Ru(NH_3)_6]^{3+}$, $[Fe(CN)_6]^{4-}$, and dopamine in the absence and presence of bovine serum albumin and homogenised chicken liver to mimic the extracellular matrix. Their results showed that the boron-doped diamond electrode exhibited better performance than the glassy carbon or glassy carbon with low surface oxides, respectively. The sp^3 carbon structure of the sample|sensor interface is expected to provide better resistance to fouling. In conjunction with low-capacitance and biocompatibility, these electrodes are ideal candidates as sensors for biological sample analysis[6, 20-22].

Swain's group demonstrated minimum fouling at boron-doped diamond electrodes that were exposed to laboratory atmosphere and in contact with biological tissues without deactivation[6, 22]. Their work demonstrated that non-deactivated and fouling resistant surface was due to the presence of the non-polar, H-terminated surface with no extended π electron system. This characteristic of a microelectrode is useful for sensitive, reproducible and stable electroanalytical detection of catecholamines in a complex biological environment.

Recently, Hebert *et al.*[23] reported the application of boron doped diamond electrodes to neural interfacing *in vivo* as this electrode material is highly stable and biocompatible. Most materials used for neural interfacing degrade and/or are encapsulated by the proximal tissue leading to loss of efficiency. They observed a reduced magnetic resonance imaging artifact when the fabricated device was implanted on a rat cortex, suggesting that boron-doped diamond is a very promising electrode material for functional imaging[23].

3.5 Scope of this work

There is an extensive need for the development of low cost, easy-to-use biosensors capable of sensitive and selective detection of neurotransmitters. They should also ideally offer the feasibility of being integrated into portable devices for point-of-care use. Electrochemical sensors are one of the most promising platforms with the potential to achieve these goals and they have been used to detect a number of analytes. The application of biosensors to complex samples are however limited by fouling due to non-specific adsorption of materials present in the biological matrix onto the sensing surface. Therefore, minimising this non-specific adsorption on the sensing surfaces is a great challenge in development of sensors for analyte detection in biological samples[24]. Notably, as non-specific adsorption is promoted by the hydrophilic nature of many carbon-based electrodes due to the presence of oxygenated functional groups such as phenols, alcohols, ketones and carboxylic acids, one way of minimising non-specific adsorption is to reduce the surface oxygen-containing functional groups.

Previously, McRae's group successfully applied reduction reactions involving *n*-butylsilane and diethylsilane to convert polycarboxylic acids, ketones, aldehydes, and alcohols to alkanes without losing the important backbone information and also without any effect on the double bonds and ether[25-26]. The reduction mechanism is shown in Scheme 3.1 (A). This hydrogenation is based on the intermediate products observed during the reaction, where silanes act as a hydride source in presence of tris(pentafluorophenyl)borane. In addition, a siloxane formed is further condensed to form cyclotrisiloxanes and higher polymers. Our research group previously adopted the use of *n*-butylsilane to hydrogenate a carbon surface to develop a hydrophobic sp^3 carbon surface by reducing the surface functional groups to their respective alkanes[8].

This method of hydrogenation has also been shown to activate non-functional carbon electrodes, attributable to the formation of *n*-butylsiloxane dendrimers in the microfractures on the carbon surface *via* the phenol functionality. Our group has also attributed the antifouling activity of *n*-butylsilane hydrogenated to the formation of a smooth and H-terminated surface that prevented the adsorption of biomolecules, while the siloxane dendrimers prevented large biomolecules from adsorbing on the surface. Notably, silane hydrogenated electrodes offer two important advantages during the electrochemical detection of dopamine *in vivo*. A fouling resistant H-terminated carbon surfaces, and the siloxane dendrimers formed (which are further condensed to form cyclotrisiloxanes and higher polymers), prevented the non-specific adsorption of polymeric oxidation products and high molecular weight compounds present in the extracellular matrix.

In a different study, several researchers have employed polyethylene glycol as an antifouling reagent for minimising non-specific adsorption. The antifouling behaviour of polyethylene glycol reportedly arises from repulsive elastic forces resulted from the compression of the polyethylene glycol chains when such large molecules as proteins approach a polyethylene glycol immobilised sensing surface. Their work concluded that the protein resistance of the surface should increase monotonically with the surface density of the grafted polyethylene glycol and its chain length[27]. The same group later modelled the proteins and concluded that, for a given surface density of a polymer, an increase in chain length would lead to greater protein resistance[28].

Owing to the abovementioned advantages of silane reduction method and inspired by the research carried out using polymers to obtain an antifouling surface, our group has since adopted this reduction method to hydrogenate carbon electrode surfaces to form

a hydrophobic carbon surface. In the present work, reduction reactions involving triethylsilane and phenylsilane, instead of *n*-butylsilane, were employed. An illustration of a triethylsilane and phenylsilane hydrogenated carbon surface is shown in Scheme 3.1 (B). We expect the bulky side chains of triethylsilane and phenylsilane to provide additional protection against large biomolecules compared to the *n*-butylsilane side chain. Also, the formation of phenylsiloxane dendrimers on the surface of phenylsilane hydrogenated carbon electrodes are likely to enhance the electrocatalytic properties of the hydrogenated electrodes *via* the phenyl ring. Therefore, this Chapter focusses on microscopic, spectroscopic and electrochemical characterisation of conical-tip carbon electrodes hydrogenated using triethylsilane and phenylsilane. The results obtained will be used to evaluate the effectiveness of the hydrogenation procedure involving triethylsilane and phenylsilane in producing antifouling surface.

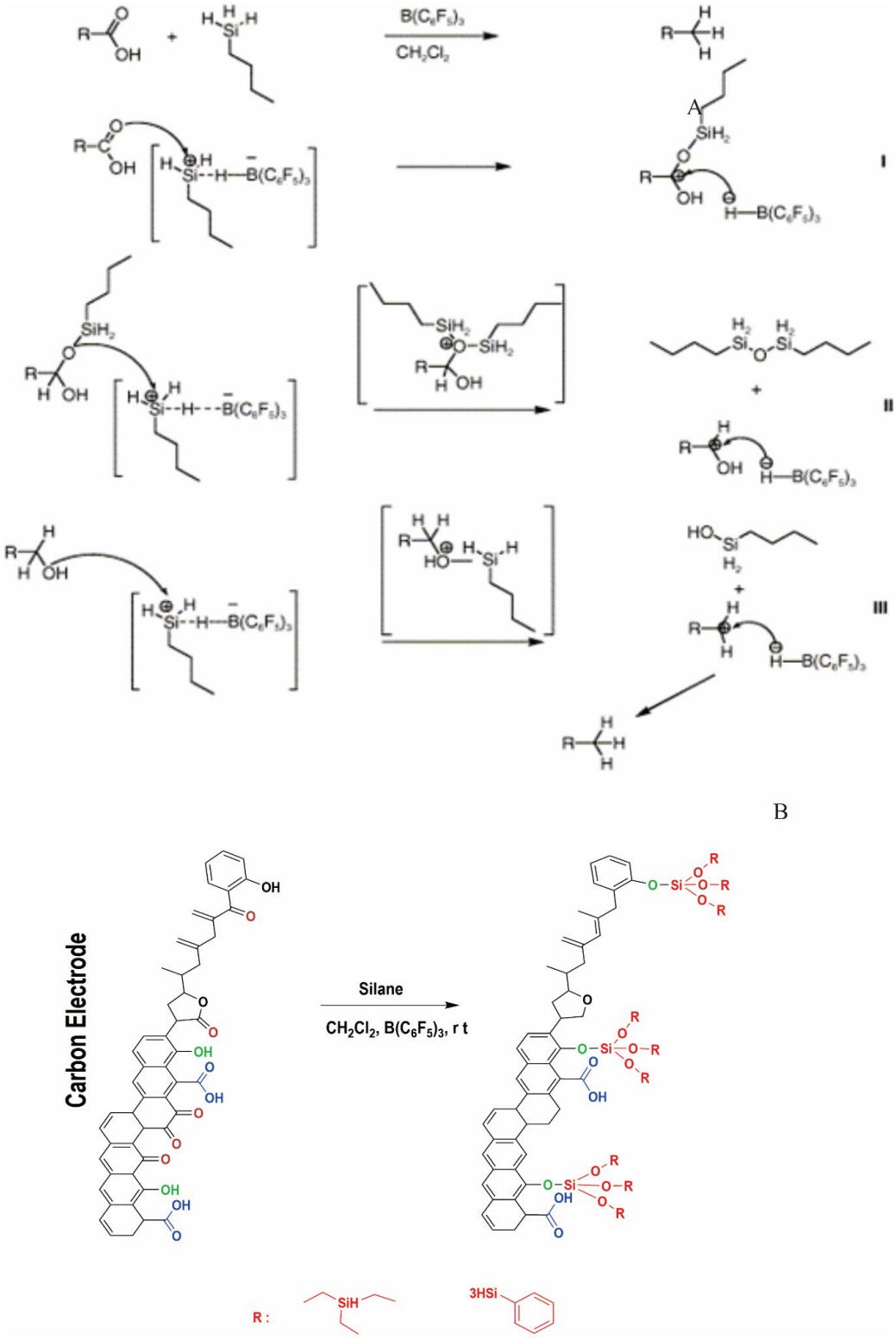

Scheme 3.1. (A) Silane reduction mechanism and (B) an illustration of silane hydrogenated carbon electrode. Adapted from [25].

3.6 Experimental

3.6.1 Chemicals and reagents

A list of all chemical and reagents used in this work was presented in Section 2.2.

3.6.2 Electrode fabrication and hydrogenation

Structurally small carbon electrodes were fabricated and hydrogenated using the procedure outlined in Sections 2.3 and 2.4.

3.6.3 Electrode characterisation

The instrumentation used to characterise the fabricated electrode was described in Section 2.5.

3.6.4 Scanning electron microscopy

Scanning electron micrographs were used to visually examine the electrode tip and the shank of the fabricated carbon electrode. In our work, scanning electron micrographs were obtained using a JEOL JSM 7100F Field Emission scanning microscope at the Microscopy Unit, Department of Biological Sciences, Macquarie University. Before the micrographs were acquired, all carbon electrodes were firstly coated with 20 nm chromium.

3.6.5 Chronoamperometry

Chronoamperometry of $[Ru(NH_3)_6]^{3+}$ in 1.0 M KCl supporting electrolyte was employed to determine the tip dimension and electroactive area of the fabricated carbon electrodes. In this technique, a potential initially identified from a cyclic voltammogram at which $[Ru(NH_3)_6]^{3+}$ does not undergo any electrochemical reaction is applied for a desired duration. The potential is then stepped to a point beyond that required for $[Ru(NH_3)_6]^{3+}$ to be electrochemically reduced[29]. Here its surface concentration becomes effectively zero and the resulting current-time dependence is monitored. This current-time relation can be expressed by Cottrell equation (see page 74) Cottrell equal was used to estimate the tip diameter and axial length of the electrodes as described in Section 2.5.2.

3.6.6 X-Ray photoelectron spectroscopy

X-Ray photoelectron spectroscopy spectra were obtained using an ESCALAB250Xi Spectrometer (Thermo Scientific, United Kingdom). The radiation was generated by a monochromated Al Kα (1486.68 eV) operating at 150 W (13 kV × 12 mA) power. The analysis was performed using the take-off angle of 90°, and the vacuum pressure in the analysis chamber was about 2×10^{-9} mbar. The analysed spot area was 500 μm^2 and the spectrometer energy scale was calibrated using the $Au4f^7$, $Ag3d^5$, and $Cu2p^3$ core level peaks set at corresponding binding energies of 89.96 eV, 368.21 eV and 932.62 eV with a reference energy scale for C1s at 284.8 eV for adventitious hydrocarbon.

3.6.7 Raman spectroscopy

Raman spectra were obtained using a Renishaw 1000 model Raman microscope with a Peltier cooled charge-coupled detector and a holographic notch filter operating at 532 nm (Renishaw model RL532C50).

3.7 Results and discussion

In this work, structurally small electrodes were fabricated using a procedure previously reported by our group[1]. Only electrodes that displayed a sigmoidal-shape cyclic voltammogram with a small charging current between forward and backward scan were used further in hydrogenation experiments. A sigmoidal-shaped voltammogram arising from both linear and non-linear diffusion around an electrode with a small surface area, indicating that the electrode is physically small[30]. In addition, the presence of a small gap between the forward and reverse scans suggests a well-sealed electrode with minimal holes, cracks and crevices. Our group has also previously reported the hydrogenation of carbon electrodes using an *n*-butylsilane reduction method to obtain an antifouling carbon electrode surface[8, 31]. The resultant hydrogenated carbon surface was reported to have a smooth, H-terminated surface with butylsiloxane dendrimers. The antifouling property of the *n*-butylsilane hydrogenated electrodes was evaluated after they were incubated in a laboratory synthetic fouling solution for a defined period. The siloxane dendrimers formed during the hydrogenation was one of the features of the hydrogenated electrode that minimised non-specific adsorption[31]. In this study, we explored the use of triethylsilane and phenylsilane, both with bulky side chains to hydrogenate the fabricated carbon electrodes, and the resultant hydrogenated electrodes are demonstrated to further restrict the biomolecules from adsorbing on the carbon

surface. Additionally, owing to effect of the reduction of surface oxides on the electron transfer kinetics, we also explored the use of silane with a phenyl ring to enhance the electrocatalytic activity of hydrogenated electrode *via* the formation of phenyl siloxane dendrimers.

3.7.1 Silane Hydrogenation Mechanism

The two main challenges in the fabrication of biosensors are (i) a simple modification/fabrication procedure that can be completed in a short time, and (ii) the fabricated surface should be ideally foul free when the biosensors are applied in a biological matrix. Silane hydrogenation is reportedly[25-26] one of the simplest ways to reduce alcohols, aldehydes, ketones, and carboxylic acids to their respective alkyl groups with the formation of siloxane dendrimers through the phenol functionality. This method of hydrogenation does not require sophisticated reaction procedures as this can be done in one-pot at ambient temperature. Specifically, we have explored in this work the use of triethylsilane and phenylsilane in hydrogenating carbon electrodes to produce a H-terminated surface. The silanes form a reactive intermediate with the $B(C_6F_5)_3$, which reduces the polycarboxylic acids, ketones, aldehydes, and alcohols to their corresponding alkanes, while siloxane dendrimers are formed *via* the phenol functional group, which is further condensed to form cyclotrisiloxanes and higher polymers[25-26]. Upon hydrogenation, the electrodes were initially characterised by scanning electron microscopy, X-ray photoelectron spectroscopy and Raman spectroscopy.

3.7.2 Scanning Electron Microscopy

Scanning electron microscopy was used to examine the carbon deposits near the tip of electrodes, as well as to determine their integrity and dimension. Figure 3.1 shows the scanning electron micrographs of a carbon electrode fabricated in this study. In Figure 3.1(a), using a 500× magnification, a broken carbon electrode was intentionally examined to gain a view of the carbon deposit inside the capillary, where a smooth layer of carbon film is readily observable. In Figure 3.1 (b), a uniform carbon deposit appearing in white is observed at the tip and on the shank of the electrode.

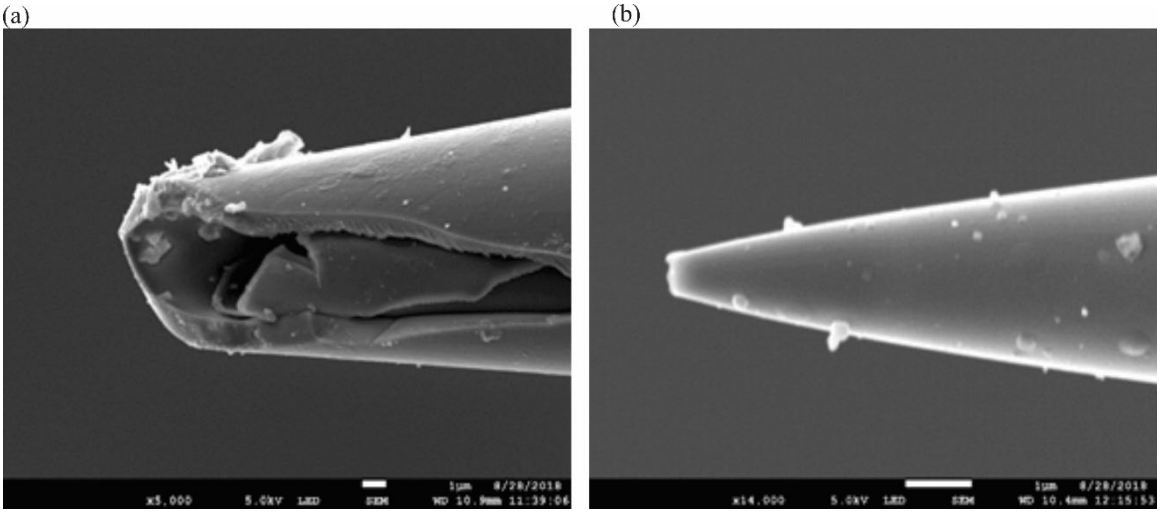

Figure 3.1. Scanning electron micrographs of a small carbon electrode. (a) At 500× magnification is used to view the carbon deposit inside a quartz capillary; (b) at 14000× magnification, carbon deposits can be observed on the tip and on the shank of the quartz capillary. The scale bar for both micrographs is 1 μm.

Using these micrographs, we can confirm that carbon was deposited on the tip and on the shank of the electrode. As expected, the pulled end is also observed to be of a conical shape. Based on scanning electron micrographs, the tip diameter of this electrode was estimated to be less than 1 μm, and its axial length was ~6 μm.

3.7.3 Chronoamperometry

As discussed in Section 2.5.2, chronoamperometry was used to estimate the dimension of small carbon electrodes fabricated in this study[32-33]. Accordingly, the decaying current between 4-5 s from the chronoamperogram shown in Figure 3.2 (A) was measured. Based on Equation 1, by constructing a current versus $(t)^{-1/2}$ plot as shown in Figure 3.2(B), the slope and the ordinate intercept of the plot were used to evaluate the tip diameter to be 1.9 µm (95% confidence interval (95% CI) 0.68 µm, N=10), and axial length of 8.6 µm (95% CI 0.35 µm, N=10). These results are in good agreement with the dimensions estimated using the micrographs as shown Figure 3.1.

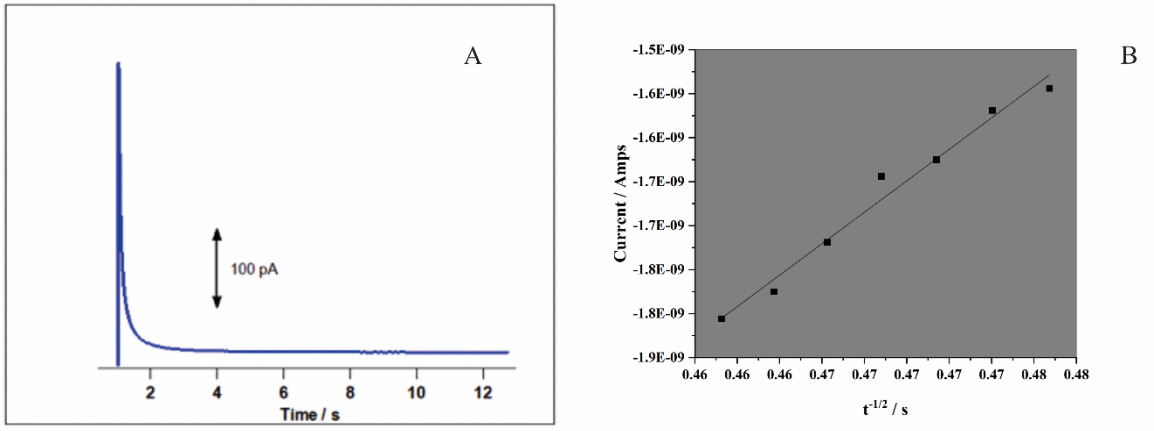

Figure 3.2. (A) Chronoamperogram obtained at a small conical-tip carbon electrode in 1.0 mM $[Ru(NH_3)_6]^{3+}$ in 1.0 M KCl supporting electrolyte and (B) a plot of current versus $t^{-½}$ to obtain tip diameter and axial length.

3.7.4 X-Ray Photoelectron spectroscopy

X-ray photoelectron spectroscopy is a widely used technique for characterising the chemical and electronic properties of highly ordered carbon nanostructures such as

carbon nanotubes and graphene[34]. In this work, X-ray photoelectron spectroscopy was conducted to probe the surface composition of carbon electrodes before and after hydrogenation. The survey spectra and the Gaussian-fitted results obtained at non-hydrogenated and hydrogenated electrodes are presented in Figures 3.3 - 3.5. Survey X-ray photoelectron spectra obtained at non-hydrogenated, triethylsilane hydrogenated and phenylsilane hydrogenated electrode is depicted in Figure 3.3 (a), (b) and (c), respectively, which shows three major peaks centred at ~532 eV (O 1s), ~284 eV (C 1s) and ~103 eV (Si 2p) peaks at non-hydrogenated, triethylsilane hydrogenated, and phenylsilane hydrogenated electrodes.

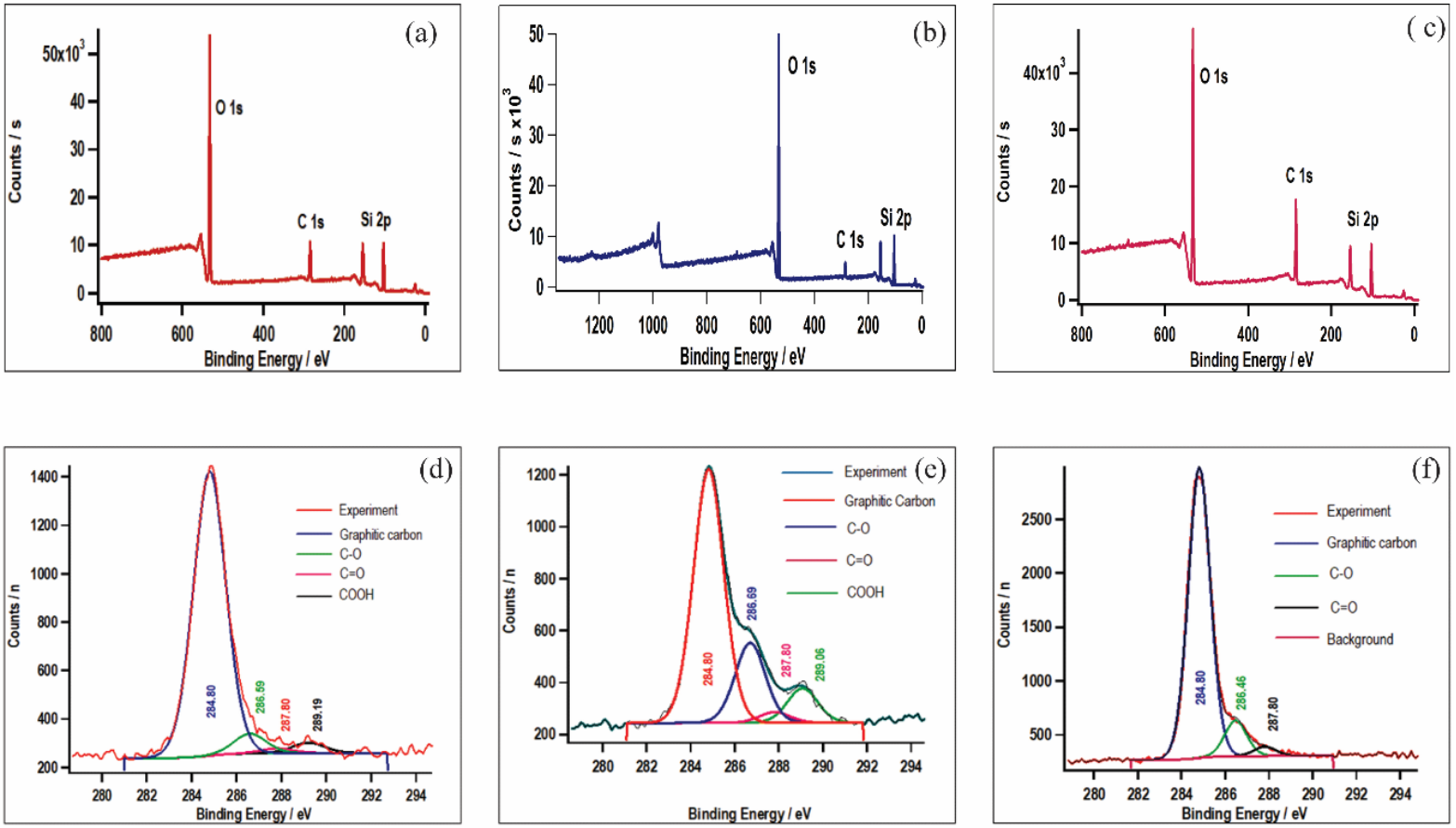

Figure 3.3. X-ray photoelectron survey and high-resolution C 1s spectra obtained at (a) and (d) non-hydrogenated, (b) and (e) at triethylsilane hydrogenated and (c) and (f) at phenylsilane hydrogenated conical-tip carbon electrodes.

The deconvoluted C1s core level X-ray photoelectron spectrum of the non-hydrogenated electrode is shown in Figure 3.3 (d) where four distinct peaks at 284.8 eV, 286.4 eV, 287.8 eV, and 289.12 eV are correspondingly identified as graphitic carbon/carbon atoms in hexatomic ring structure (C-C), C–O (alcohol, ether or epoxy groups), C=O (ketone and aldehyde) and O-C=O (carboxyl and ester) by comparing to the high resolution C1s spectra of an oxidised glassy carbon electrode and a carbon fibre electrode[35-37]. As shown in Figure 3.3(e) and (f), in the spectra obtained after hydrogenating the electrodes using either triethylsilane or phenylsilane, peaks corresponding to C–O, C=O and O-C=O functionalities on the surface, along with a graphitic carbon peak that is of ~72% higher peak intensity than non-hydrogenated carbon surface at 286.6 eV further support the formation of new oxygen containing groups on the surface. The absence of peak at ~289.1 eV on the phenylsilane hydrogenated electrode is used to infer here a low presence of carboxyl/ester species, suggesting phenylsilane was more effective in reducing O-C=O functional group than triethylsilane. The ability of various silanes to reduce carboxylic acids was found to be dependent upon steric hinderance where the less sterically hindered silanes were reported to be more effective[25]. For example, Nimmaganda and McRae reported that triethylsilane and dimethylethylsilane were able to reduce straight chain di-carboxylic acids and reported that the length of reaction with dimethylethylsilane was less than that for triethylsilane due to less bulky substituents on demethylethylsilane. They further studied the use of diethylsilane and *n*-butylsilane for reduction of di- and polycarboxylic acids. They reported that diethylsilane was able to reduce polycarboxylic acids albeit with a low yield. Notably, *n*-butylsilane was found to reduce di- and polycarboxylic acids with a high yield[25]. For example, the percentage

yield to reduce 1,2,3 polycarboxylic acid using diethylsilane was only 34% while the yield using n-butylislane was 71%.

As depicted in Figure 3.4, the deconvoluted O 1s spectrum of non-hydrogenated, triethylsilane hydrogenated and phenylsilane hydrogenated carbon electrodes is dominated by the peak at ~533 eV. Peak positioned between 531.5–532.6 eV are usually assigned as contributions from ketones, carboxylic acids and esters[38]. As mentioned in Section 2.3, all carbon electrodes used in this work were fabricated using quartz capillaries as they can withstand temperatures as high as 1670 °C. As a result, the use of quartz capillaries in fabricating carbon electrodes contributes to the peak at ~533 eV in Figure 3.4 (a) which is in good agreement with that obtained for quartz itself[39]. This is further supported by the presence of a peak at ~103.7 eV in the Si 2p spectra, which is assigned to the Si species in a quartz substrate[40]. However, no peak is observed in the proximity of 531.6 eV, indicating low presence of C=O moiety in the surface layer. This result may indicate that majority of the oxygen present was in the form of hydroxyls/ester[38].

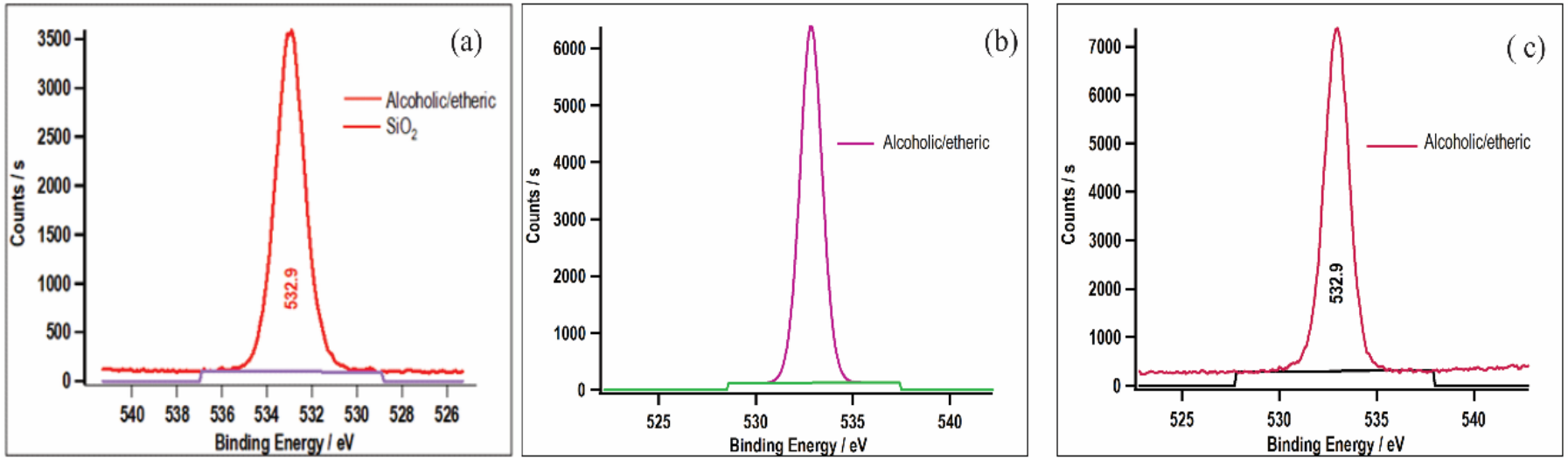

Figure 3.4. High-resolution O 1s spectra of a conical-tip carbon electrode (a) before hydrogenation (b) after triethylsilane hydrogenation and (c) phenylsilane hydrogenation.

The deconvoluted Si 2p spectrum in Figure 3.5 is dominated by a peak at ~103 eV, which corresponds to the Si species possibly originating from the quartz substrate[39] used in electrode fabrication. After hydrogenating the electrodes using triethylsilane and phenylsilane, two peaks at different binding energies at ~103.5 eV and ~102.2 eV indicate the presence of two chemical states of Si[41]. O'Hare *et al.*[42] developed a methodology for the X-ray photoelectron spectroscopic curve fitting of Si 2p core level of siloxane materials and reported a peak at 101.99 ± 0.1 eV from a high-molecular weight polydimethylsiloxane linear homopolymer to be representative of the siloxy unit. The additional peak obtained at the hydrogenated carbon electrodes confirms the formation of new –Si containing species on the surface, which was absent in the Si 2p spectrum of a non-hydrogenated carbon electrode. This peak is assigned to be originating from the siloxane dendrimers formed on a hydrogenated electrode surface during hydrogenation[42]. A noticeable difference between the siloxane dendrimers formed in Figure 3.4 (b), compared to Figure 3.4 (c), could possibly be due to the reduction of triethylsilane. For example, Nimmagadda and McRae reported that triethylsilane was found to reduce straight chain dicarboxylic acids readily into their corresponding alkanes. However, the alicyclic and aryl dicarboxylic acids were converted into their corresponding silyl ethers requiring six equivalents of triethylsilane for each carboxylic acid group[25]. Therefore, these results supported a successful hydrogenation method that has reduced the C=O and C–OH functional groups with the formation of new oxygen-containing species, *i.e.* the extended siloxane dendrimers.

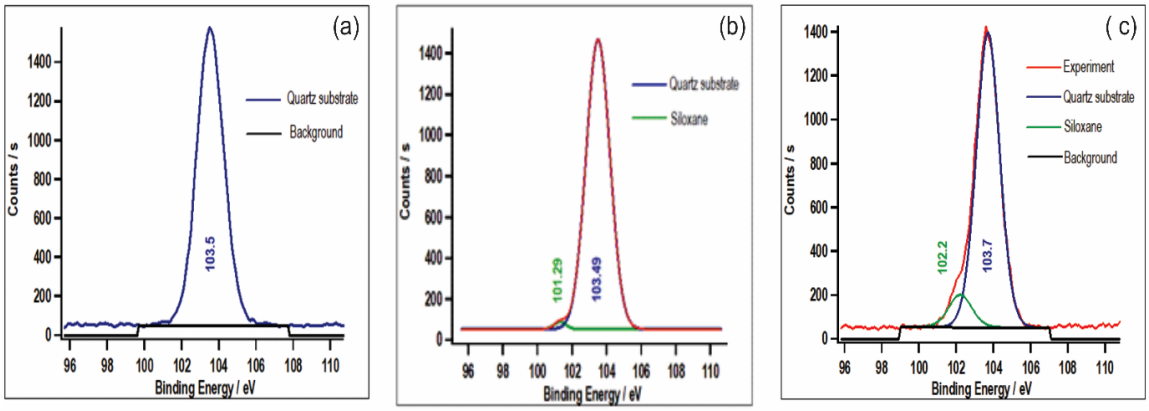

Figure 3.5. High resolution Si 2p spectra of (a) non-hydrogenated conical-tip carbon electrode, (b) triethylsilane hydrogenated and (c) phenylsilane hydrogenated carbon electrode.

3.7.5 Raman Spectroscopy

Owing to its non-destructive nature, Raman spectroscopy is extensively used to characterise the structural quality of carbon-based films and to obtain detailed bonding type and cluster sizes[43-45]. In this work, the surface chemistry of the non-hydrogenated and hydrogenated carbon electrodes was further investigated using Raman spectroscopy. The Raman spectra of hydrogenated carbon films are usually characterised by (i) a G-peak (E2g mode) at ~1550 cm^{-1} caused by the stretching vibration of any pairs of sp^2 sites in C=C or in aromatic rings, and (ii) a D-peak (A1g mode) at ~1360 cm^{-1} arising from the breathing mode of the sp^2 sites and is related to disorder and deviation from perfect graphitic structure[46-47]. The D/G peak intensity ratio is often used to reveal the sp^3-hybridised content of a carbon film[48]. Hence, the lower the D to G ratio (I_D/I_G), the higher the level of graphitisation within the carbon[49]. The typical Raman spectra obtained of a non-hydrogenated and a hydrogenated carbon electrode are presented in Figure 3.6. The gaussian-fitted peaks were used to determine the I_D/I_G intensity ratio. In both spectra, we obtained a characteristic D peak centred at

1340 cm^{-1}, which is forbidden in perfect graphite and it only becomes active in the presence of disorder, and a G peak at 1567 cm^{-1} [46]. The I_D/I_G intensity ratio at the non-hydrogenated carbon surface was estimated to be 1.78 and this was improved to 2.2 and 2.7 at triethylsilane and phenylsilane hydrogenated carbon electrodes, respectively, with a downshift of the D peak from 1569 cm^{-1} to 1565 cm^{-1}. Similarly, Bogdanowicz *et al.*[50] reported the I_D/I_G ratio of boron-doped diamond films deposited using plasma assisted chemical vapour deposition on silicon and glassy carbon to be 4.6 and 0.5, respectively. Their evaluation of lower I_D/I_G ratio was that the layer deposited on glassy carbon (I_D/I_G ratio of 0.5) contains much more amorphous carbon than that deposited on silicon. The higher I_D/I_G ratio of the triethylsilane and phenylsilane hydrogenated electrodes compared to the non-hydrogenated counterpart is possibly due to the hydrogenation mechanism resulting in more sp^3 carbon on the surface. Zhao *et al.*[51] obtained an I_D/I_G ratio of 1.882 at carbon nanotube modified carbon fibre electrode, compared to 1.138 obtained at a bare carbon fibre electrode. The increase in the ratio was attributed to more sp^3 defects / disorders and smaller average size of the in-plane graphitic crystallite sp^2 domains upon carbon nanotube formation on the carbon fibre. More interestingly, the higher ratio at phenylsilane hydrogenated electrodes relative to that at the triethylsilane hydrogenated electrodes could have arisen from the phenyl ring within the siloxane dendrimers. Similarly, Zhu and colleagues reported an increase in the (I_D/I_G) ratio of graphene-iron-tetrasulfophthalocyanine modified carbon fiber electrode modified from 2.01 to 2.56 arising from two active centers of graphene and iron-tetrasulfophthalocyanine[10]. In fabricating a nanostructured glassy carbon electrode from a lithographically defined phenol containing polymeric nanostructure by pyrolysis at 900°C for 10 h, Demuru *et al.*[52] reported an I_D/I_G of ~1.1. They attributed the smaller ratio than the typical values of ~1.2-1.5 reported for the glassy carbon

electrodes to a less disordered and more graphitic microstructure of the pyrolysed polymer film[53]. In a separate work, Yang *et al.*[54] reported an I_D/I_G ratio of 2.2 at carbon nanotube–modified niobium substrates, which was attributed to a defect-rich surface. At a hydrogenated carbon surface, the G peak usually shifts toward a lower wavenumber due to the local environment compared to a non-hydrogenated carbon surface[55].

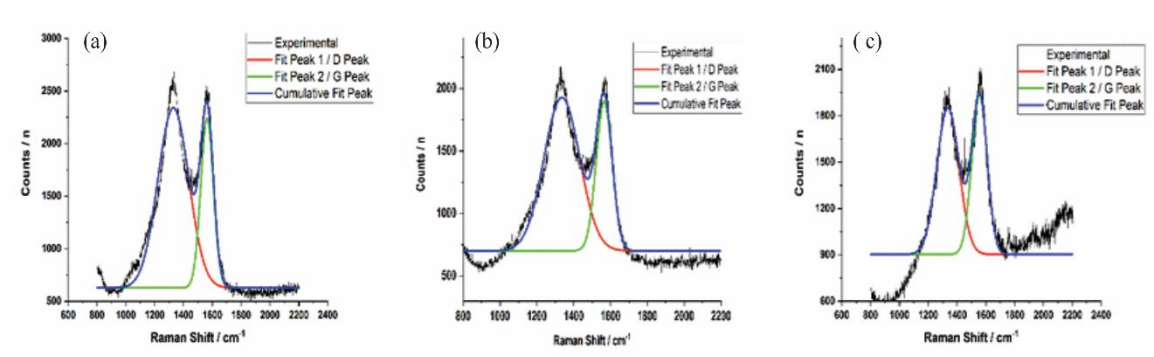

Figure 3.6. Raman spectra obtained at (a) non-hydrogenated, (b) triethylsilane silane hydrogenated and (c) phenylsilane hydrogenated conical-tip carbon electrode.

3.7.6 Electrochemical Characterisation

Following the spectroscopic characterisation, the charge transfer properties of non-hydrogenated and hydrogenated carbon electrodes were studied using cyclic voltammetry in (i) 1.0 mM $[Ru(NH_3)_6]^{3+}$ in 1.0 M KCl supporting electrolyte, (ii) 1.0 mM $[Fe(CN)_6]^{3-}$ in 1.0 M KCl supporting electrolyte, (iii) 1.0 mM dopamine in a pH 7.4 citrate/phosphate buffer or 0.1 M H_2SO_4 , (iv) 1.0 mM DOPAC in a pH 7.4 citrate/phosphate buffer or 0.1 M H_2SO_4, (v) 1.0 mM 4-methylcatechol in a pH 7.4 citrate/phosphate buffer or 0.1 M H_2SO_4, and (vi) 1.0 mM anthraquinone 2,4 disulfonic

acid in 0.1 M $HClO_4$. Excellent steady state responses were achieved with each redox system indicating that the diffusion layer thickness is larger than the radius of the electroactive area ($Dt^{1/2} > r_0$). Contrarily, when the diffusion layer is smaller than the electrode area ($Dt^{1/2} < r_0$), semi-infinite diffusion is observed and voltammetric peaks are obtained[56]. In assessing the electrochemical reversibility of the reactions at the carbon electrodes, the waveslope and half-wave potential ($E_{½}$), a potential at which the current is half of the limiting current, were estimated equation 3.1[56]:

$$E = E_{\frac{1}{2}} + \frac{0.0592}{n}\log_{10}\left[\frac{I_{\mathrm{lim}} - I}{I}\right] \qquad \text{Equation (3.1)}$$

where E is the potential, n number of electrons, I_{lim} the limiting current and I the current. Accordingly, a plot of E versus log (I_{lim} - I/I) is expected to yield a straight line with the slope being an estimate for the waveslope and the intercept an estimate for $E_{½}$. The waveslope and $E_{½}$ for all three redox markers are presented in Table 3.1.

Table 3.1. The estimated waveslope and $E_{½}$ of non-hydrogenated, triethylsilane and phenylsilane hydrogenated electrodes using different redox markers.

Redox Marker	Non-hydrogenated Electrodes		Triethylsilane Hydrogenated Electrodes		Phenylsilane Hydrogenated Electrodes	
	Waveslope / mV decade^{-1}	$E_{½}$ / mV	Waveslope / mV decade^{-1}	$E_{½}$ / mV	Waveslope / mV decade^{-1}	$E_{½}$ / mV
$[Ru(NH_3)_6]^{3+}$	68 (5)	-190 (7)	57 (5)	-192 (4)	58 (4)	-201 (3)
$Fe(CN)_6^{3-/4-}$	161 (16)	116 (19)	165 (13)	78 (21)	143 (17)	110 (28)
Dopamine	122 (17)	290 (30)	132 (7)	347 (17)	120 (20)	278 (19)

The values presented in the parentheses are the 95% confidence interval estimated from twelve electrodes.

3.7.6.1 Electrochemistry of $[Ru(NH_3)_6]^{3+}$

An ideal outer-sphere electron transfer reaction involves the tunnelling of one or more electrons without any significant chemical interactions developing between the solution | electrode interface[57]. $[Ru(NH_3)_6]^{3+}$ is an outer sphere redox marker and the redox process is insensitive to the surface characteristics[58]. Additionally, the electron transfer rate constant of this redox couple is insensitive to surface modification, which strongly implies that electron transfer does not depend on an interaction with a surface site or functional group[59]. In this case, the heterogeneous electron transfer kinetics depends mainly on the density of states, which is one of the most important parameters of an electrode and varies greatly with electrode materials[60]. These evidences suggest that the charge transfer kinetics of this redox system is not expected to change significantly upon modification. Cyclic voltammograms of 1.0 mM $[Ru(NH_3)_6]^{3+}$ in 1.0 M KCl supporting electrolyte at triethylsilane and phenylsilane hydrogenated carbon electrodes are shown in Figure 3.7(A) and (B). An estimated 27% and 33% decline in the I_{lim} of the reduction of $[Ru(NH_3)_6]^{3+}$ was obtained at triethylsilane and phenylsilane hydrogenated electrodes, respectively, compared to the non-hydrogenated counterparts. Similarly, a 20% decrease in the reduction I_{lim} is reported for *n*-butylsilane hydrogenated carbon electrodes[31]. The decline in the I_{lim} is possibly because of decline in mass transport arising from the siloxane dendrimers on the hydrogenated electrodes. Owing to the use of electrodes of dimensions ranging from a few micrometers to nanometers in the triethylsilane and phenylsilane hydrogenation experiments, a noticeable difference in the magnitude of current is observed in the cyclic voltammograms shown in Figure 3.7.

The corresponding estimated $E_{½}$ and waveslope values are presented in Table 3.1. The $E_{½}$ at non-hydrogenated electrodes was estimated to be -190 ± 7 mV (where errors are represented by 95% confidence interval; N=10). This shifted negatively by 2 mV and 11 mV after triethylsilane and phenylsilane hydrogenation, respectively. With regards to reaction reversibility, the outer-sphere reactions are often associated with fast electron transfer that is relatively independent of the nature of the substrate[57]. Accordingly, the corresponding waveslope of 62, 57 and 58 mV decade^{-1} was estimated for non-hydrogenated, triethylsilane and phenylsilane hydrogenated electrodes, which are consistent with a reversible one-electron transfer reaction of 58 mV decade^{-1}. As expected, no noticeable difference in the waveslope between the hydrogenated and non-hydrogenated electrodes was observed.

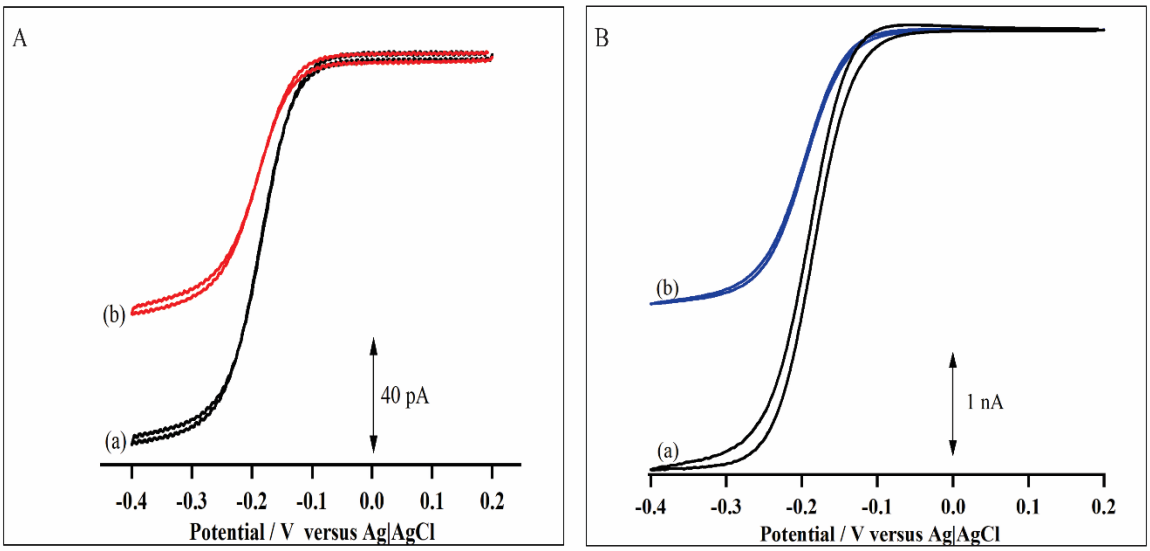

Figure 3.7. Cyclic voltammograms of 1.0 mM $[Ru(NH_3)_6]^{3+}$ in 1.0 M KCl (a) before and (b) after hydrogenation at (A) triethylsilane hydrogenated and (B) a phenylsilane hydrogenated conical-tip carbon electrode. Scan rate 100 mV s^{-1}.

3.7.6.2 Response of an inner-sphere redox system $[Fe(CN)_6]^{3-}$

In contrast to $[Ru(NH_3)_6]^{3+}$, $[Fe(CN)_6]^{3-}$ proceeds through a more inner-sphere electron transfer pathway as the electrode kinetics tend to be very sensitive to the surface termination[58, 61]. Several studies have reported that reduction in surface oxygen containing groups has minor effects on the electron transfer kinetics of this system and that the heterogeneous electron transfer rate for $[Fe(CN)_6]^{3-}$ is extremely sensitive to the microstructure of the conventional graphitic electrode[62]. In this work, cyclic voltammetry of 1.0 mM $[Fe(CN)_6]^{3-}$ in 1.0 M KCl supporting electrolyte was conducted at non-hydrogenated and hydrogenated carbon electrodes. Figure 3.8(A) displays the respective sigmoidal-shaped voltammogram obtained at a triethylsilane hydrogenated electrode compared to a non-hydrogenated electrode, while Figure 3.8(B) shows the representative voltammograms obtained after phenylsilane hydrogenation compared with a non-hydrogenated electrode. Accordingly, there was ~20% and ~15% decline in the I_{lim} after triethylsilane and phenylsilane hydrogenation, respectively. This could possibly be due to the reduction in mass transport arising from the presence of siloxane dendrimers on the surface.

The corresponding $E_{½}$ and waveslope values are presented in Table 3.1. After triethylsilane hydrogenation, a negative shift of $E_{½}$ from 116 ± 16 mV (N=12) to 78 ± 13 mV (N=12) is noticeable which indicates a reduction in the charge transfer kinetics. This could also be possibly due to a slow diffusion of $[Fe(CN)_6]^{3-}$ and mass transport through the siloxane dendrimers formed after hydrogenation. Our results are in good agreement with 81 ± 4 mV at a hydrogenated glassy carbon electrode[58]. More interestingly, a more positive $E_{½}$ of 110 ± 28 mV (N=12) was estimated for phenylsilane hydrogenated electrodes than 78 ± 21 mV (N=12) estimated at that of triethylsilane

hydrogenated electrodes, indicating faster electron transfer kinetics at the former. This difference is possibly associated with the formation of phenyl siloxane dendrimers where the phenyl ring facilitates the electron transfer kinetics due to availability of π electrons. An $E_{½}$ of 99.5 mV was reported after *n*-butylsilane hydrogenation[31]. The differences in the $E_{½}$ could be due to the tunnelling effect associated with the formation of siloxane dendrimers. For example, a triethylsilane hydrogenated electrode is expected to form bulkier siloxane dendrimers with effective surface coverage compared to that of an *n*-butylsilane hydrogenated electrode. Meanwhile, phenylsilane hydrogenated electrodes are expected to carry even bulkier siloxy units on the surface. The availability of π-electrons through the presence of phenyl ring will enhance the electron transfer kinetics.

From Table 3.1, the corresponding wavelsope of 161 mV decade^{-1}, 165 mV decade^{-1} and 143 mV decade^{-1} was estimated at non-hydrogenated, triethylsilane and phenylsilane hydrogenated carbon electrodes. There was no noticeable differences in the reversibility of $[Fe(CN)_6]^{3-}$ between non-hydrogenated and triethylsilane hydrogenated or non-hydrogenated and phenylsilane hydrogenated electrodes. However, a slightly slower reaction kinetics at triethylsilane hydrogenated electrodes is likely due to an increased tunnelling distance. After hydrogenation, the carbonyl, ketone, and alcohol functionalities were transformed to their corresponding alkyl groups (C–H extensions) with no extended π-electron transfer, resulting in a less reversible voltammogram. Similarly, waveslope of 210 mV decade^{-1} is reported after *n*-butylsilane hydrogenation of structurally small electrodes[31]. The $[Fe(CN)_6]^{3-}$ redox couple is generally accepted as a quasi-reversible redox couple[63]. The quasi-reversible reduction of $[Fe(CN)_6]^{3-}$ is likely due to the hydrogenation treatment, which transformed the highly porous edge-planes with appreciable surface defects to a more

uniform surface with fewer surface defects, leading to the formation of diamond-like, sp^3 carbon[64]. Some researchers have reported that the presence of oxygen containing functional groups does not necessarily interact with the $[Fe(CN)_6]^{3-}$ system. For example, Kuo and McCreery[65] reported that no significant difference in $[Fe(CN)_6]^{3-}$ voltammetry was observed at a freshly polished glassy carbon surface or a hydrogenated glassy carbon surface.

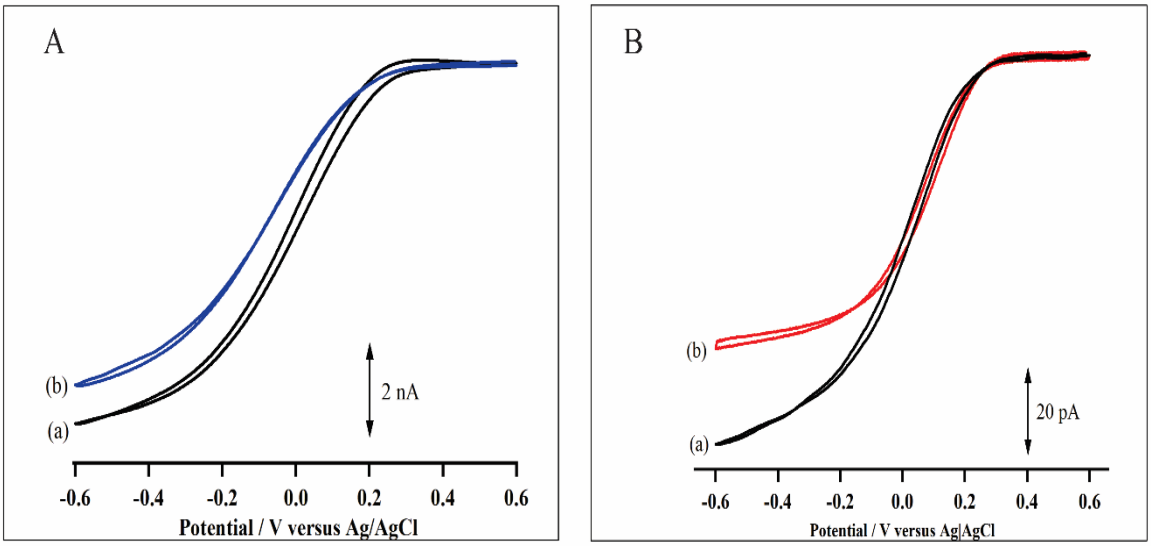

Figure 3.8. Reduction of 1.0 mM $[Fe(CN)_6]^{3-}$ in 1.0 M KCl supporting electrolyte (a) before hydrogenation and (b) after hydrogenation using (A) triethylsilane and (B) phenylsilane. Scan rate 100 mV s^{-1}.

3.7.6.3 Response of fabricated electrodes towards dopamine

Dopamine is a catecholamine neurotransmitter of interest in this work. The respective cyclic voltammograms of 1.0 mM dopamine in 0.1 M H_2SO_4 and pH 7.4 citrate/phosphate buffer are displayed in Figures 3.9 at (A and C) a triethylsilane and (B and D) a phenylsilane hydrogenated electrode.

After hydrogenating using triethylsilane and phenylsilane, there is a 24% and 27% decline in the oxidation I_{lim} in 0.1 M H_2SO_4, while a 22% decline for both hydrogenated electrodes in a pH 7.4 citrate/phosphate buffer. The observed decrease in I_{lim} is attributable to decline in mass transport as a result of reducing the functional groups including aldehyde, ketone, and carbonyl to their respective alkyl groups and the presence of siloxane dendrimers during silane reduction method [8, 25-26]. The corresponding $E_{½}$ estimated in two different supporting electrolytes is presented in Table 3.2.

Table 3.2: The $E_{½}$ estimated for oxidation of dopamine at non-hydrogenated and hydrogenated electrodes in two different supporting electrolytes.

Supporting Electrolyte	Non-Hydrogenated / mV	Triethylsilane hydrogenated / mV	Phenylsilane hydrogenated / mV
pH 7.4 citrate / phosphate	290 (30)	347 (17)	278 (19)
0.1 M H_2SO_4	608 (17)	616 (15)	603 (26)

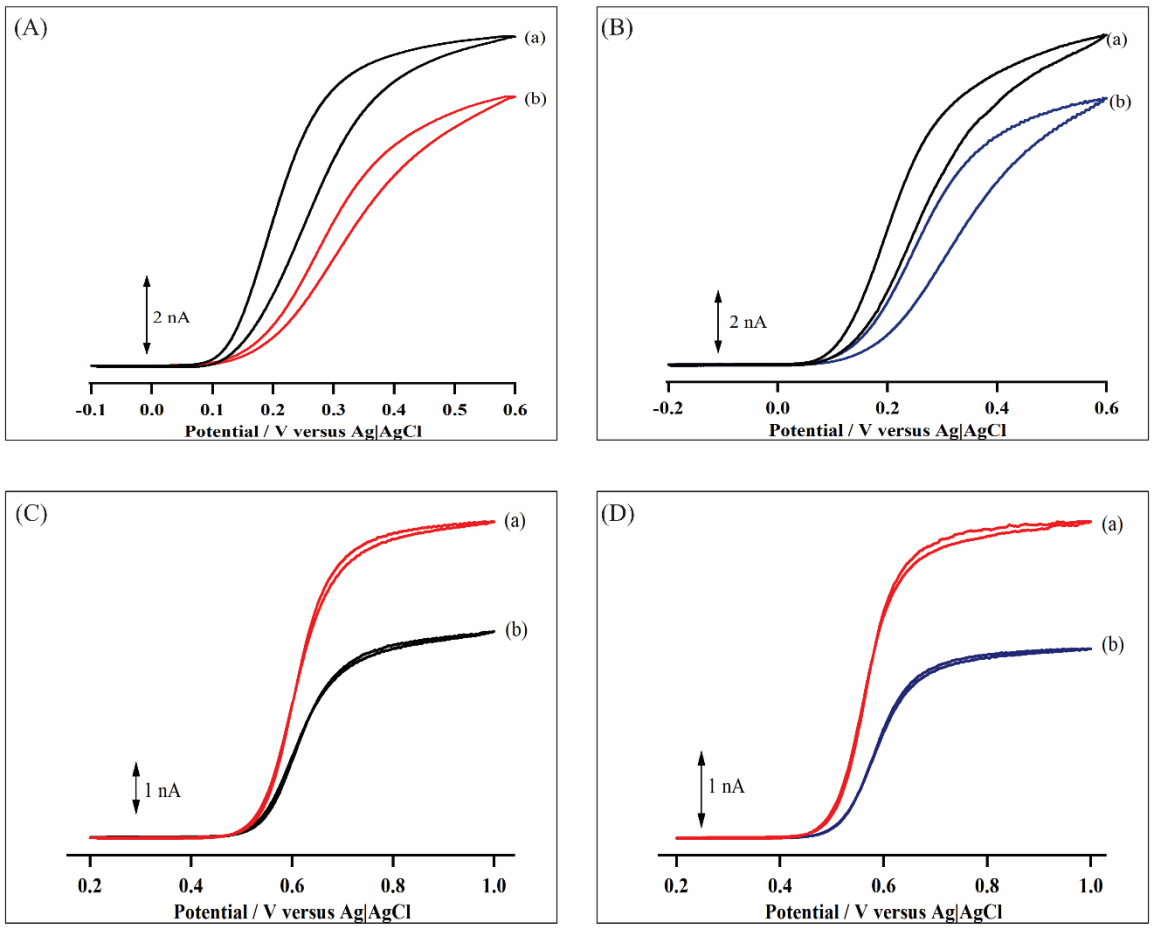

Figure 3.9: Oxidation of 1.0 mM dopamine in a pH 7.4 citrate/phosphate buffer (A and B) 0.1 M H_2SO_4 (C and D) before hydrogenation and (b) after hydrogenation using (A and C) triethylsilane and (B and D) phenylsilane. Scan rate 100 mV s^{-1}.

The $E_{½}$ of 290 mV is estimated at the non-hydrogenated electrodes in a pH 7.4 citrate/phosphate buffer as a supporting electrolyte. A more positive $E_{½}$ of 622 mV is estimated in the H_2SO_4 supporting electrolyte at non-hydrogenated electrodes. Similarly, ~0.9 V oxidation peak potential was obtained for dopamine in 0.1 H_2SO_4 using a glassy carbon electrode[66]. The shift in the $E_{½}$ is a clear indication that fundamentally different redox chemistries are occurring in these two different supporting electrolytes.

In the pH 7.4 citrate/phosphate buffer, a positive shift of $E_{½}$ from 291 mV to 347 mV is observed at triethylsilane hydrogenated electrodes, indicating slower mass transport at these electrodes. Similarly, oxidation of dopamine in M H_2SO_4 supporting electrolyte also resulted in the positive shift in the $E_{½}$ from 608 mV to 616 mV. This is likely due to the tunnelling effect arising from the formation of siloxane dendrimers. On the contrary, a faster mass transport was observed with a negative shift of the $E_{½}$ from 291 mV to 278 mV in a pH 7.4 citrate/phosphate buffer and a shift from 608 mV to 603 mV in H_2SO_4 at phenylsilane hydrogenated electrodes. The improved electron transfer kinetics after phenylsilane hydrogenation can be credited to the phenyl siloxane dendrimers that acts as 'electrical wires' facilitating the transport between dopamine and the hydrogenated electrode surface *via* π-π interaction.

In addition, the more negative half-wave potential in a pH 7.4 buffer than 608 mV indicates that the oxidation is easier, while the slope of 120 mV decade^{-1} indicates that the overall process much slower. It has been shown that in aqueous buffer of acidic, neutral and alkaline pH, anthracyclines, anthraquinones, and other para-quinones are reduced by two electrons generating one reversible wave in their cyclic voltammograms[67]. The reduction kinetics of quinone can be altered significantly in the presence of an acidic media[68]. At acidic pH, the reduction is a single step two-electron two-proton process and in alkaline pH, the reduction does not involve proton and only a case of two-electron reduction, while at neutral pH, the reduction is either by one proton two electrons or only two electrons with the participation of the proton. Furthermore, hydrogen bonding also plays an important role in determining the redox behaviour of hydroxy quinone system[69]. No noticeable differences in the waveslope was observed between non-hydrogenated and triethylsilane or phenylsilane hydrogenated carbon electrodes. This is in agreement with that reported for a

hydrogenated glassy carbon electrode that reduction in the surface oxygen containing functional groups should not affect the electron transfer kinetics of dopamine system[65].

In short, the decline in I_{lim} after hydrogenation is attributed to the decrease in the oxygen-containing functional groups on the electrode surface, which is consistent with previous reports[58]. Detection of positively charged neurotransmitters such as dopamine and serotonin are dependent on their adsorption to carbon-fibre microelectrodes[70]. Adsorption is known to promote fast kinetics of dopamine oxidation through self-catalysis at the electrode[71]. Thus, the decrease in I_{lim} could also be possibly due to decreased adsorption sites arising from a lower density of oxide groups on the hydrogenated carbon electrode[13].

Evidence shows dopamine oxidation proceeds through an inner sphere electron transfer with a quasi-reversible behaviour on carbon electrodes[72]. This is likely due to the tunnelling effect encountered due to the presence of triethylsiloxane dendrimers, which increases the distance dopamine must cross before it contacts the electrode surface. This shift in the $E_{½}$ of triethylsilane hydrogenated electrode could also be due to the slower reaction kinetics resulting from lower adsorption of dopamine. Similar shifts in the oxidation potential have been reported for serotonin and norepinephrine at boron-doped diamond microelectrodes compared to carbon fibre microelectrodes[6, 73]. A lack of hydrogen bonding sites on a given carbon based electrode surface was suggested to be a hinderance to the adsorption of dopamine and considerably slow down the oxidation reaction[74]. More interestingly, no noticeable difference in the $E_{½}$ was estimated between non-hydrogenated and phenylsilane hydrogenated electrodes. The presence of a phenyl ring facilitates the electron transfer kinetics between dopamine and the electrode with phenyl siloxane dendrimers *via* π-π interactions. This is likely

due to the ability of dopamine to establish attractive interaction *via* the π-system with the phenyl rings[75].

3.7.6.4 Response of hydrogenated electrodes towards DOPAC and 4-methylcatechol

DOPAC is a major metabolite of dopamine with similar electrochemical properties and is present at the highest concentration (>22 - 26 μM)[76] in the brain[77]. The oxidation of 4-methylcatechol and DOPAC in a pH 7.4 citrate/phosphate buffer at a non-hydrogenated is depicted in Figure 3.10, while the cyclic voltammograms obtained for the oxidation of DOPAC in a pH 7.4 citrate/phosphate and 0.1 M H_2SO_4 buffer after phenylsilane hydrogenation compared to that obtained at a non-hydrogenated counterpart is presented in Figure 3.11 (A) and (B), respectively.

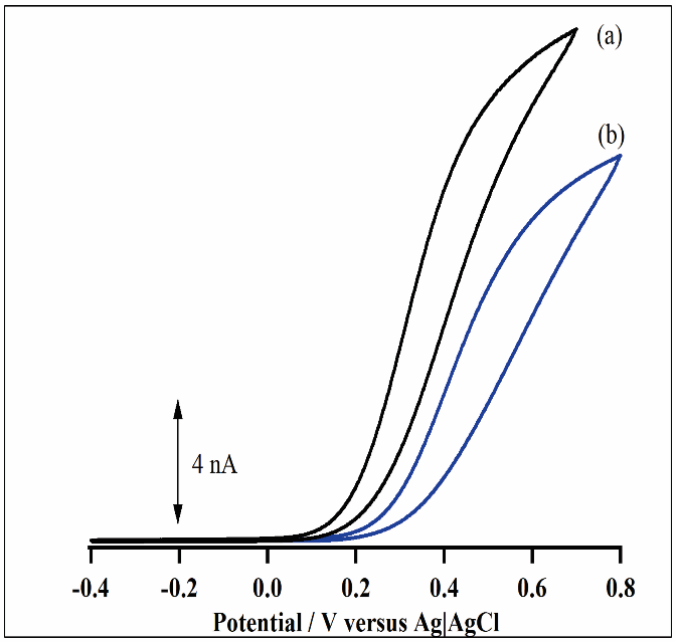

Figure 3.10. Cyclic voltammograms showing the oxidation of (a) 1.0 mM 4-methylcatechol and (b) 1.0 mM DOPAC in a pH 7.4 citrate/ phosphate buffer at a non-hydrogenated carbon electrode.

DOPAC is a catechol that follows the same oxidation mechanism pathway as other catechols. Thus, any acidic shift in the pH will shift the peak potential in a cyclic voltammogram for DOPAC to more positive potentials. As expected, the $E_{½}$ estimated for oxidation of DOPAC at a small carbon electrode in an acidic supporting electrolyte was more positive than that measured in a pH 7.4 citrate/phosphate buffer. Table 3.3 shows the $E_{½}$ values estimated at non-hydrogenated, triethylsilane hydrogenated and phenylsilane hydrogenated carbon electrodes in acidic and neutral supporting electrolyte. A waveslope of 166 ± 9 mV decade^{-1} (N=10) was estimated from the voltammogram obtained at a non-hydrogenated electrode in a pH 7.4 citrate/phosphate buffer, and 109 ± 16 mV decade^{-1} (N=10) from that obtained at a non-hydrogenated electrode in 0.1 M H_2SO_4. The experimental $E_{½}$ at the non-hydrogenated electrode in a pH 7.4 citrate/phosphate buffer and 0.1 M H_2SO_4 were 414 mV and 712 mV, respectively. The effects of pH on the voltammetric behaviour of DOPAC at a single-walled carbon nanotube modified glassy carbon electrode in 0.1 M acetate buffer (pH 4.4) was investigated by Wang *et al.*[78]. Their work also reported ~125 mV negative shift (from 420 mV at pH 3.2 to 295 mV at pH 4.4) of the peak potential when the pH was increased. Their experiment outcomes showed that the modified electrodes displayed high electrocatalytic activity towards oxidation of DOPAC, while the bare glassy carbon electrode exhibited an irreversible behaviour. However, in our work, unlike the bare glassy carbon electrodes, the redox behaviour towards DOPAC at non-hydrogenated electrode is more favourable as illustrated in Figure 3.14(b). Although it is possible to oxidise DOPAC and 4-methylcatechol at a non-hydrogenated electrode, the sensitivity of non-hydrogenated electrodes towards DOPAC is lesser compared to 4-methylcatechol and dopamine. This is consistent with that reported for the oxidation of catechols and hydroquinones at a bare glassy carbon electrode[79].

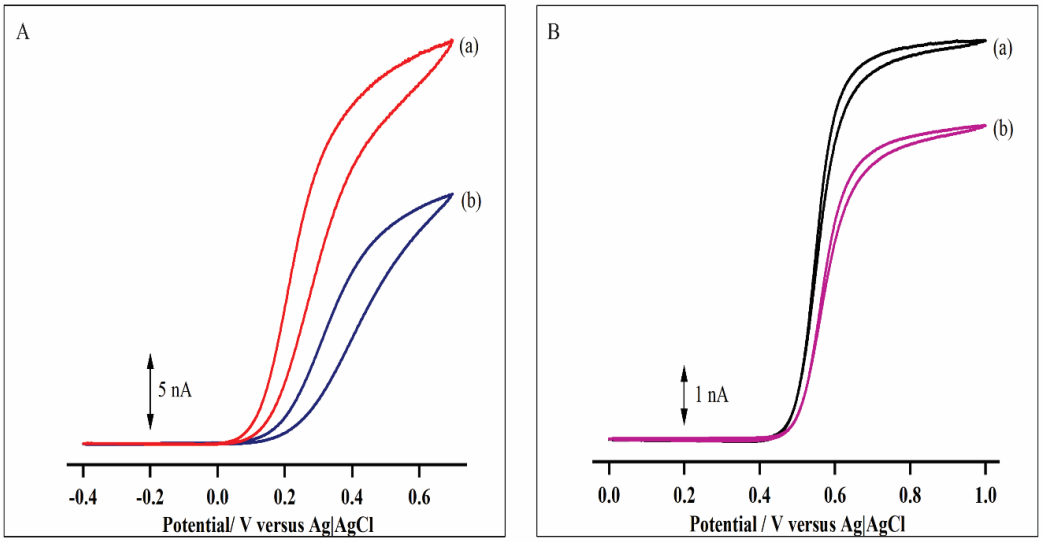

Figure 3.11. (A) Cyclic voltammograms showing the oxidation of 1.0 mM 4-methylcatechol in a pH 7.4 citrate/phosphate buffer (a) before hydrogenation and (b) after phenylsilane hydrogenation and (B) showing the cyclic voltammograms showing the oxidation of 1.0 mM DOPAC in 0.1 M H_2SO_4 at (a) non-hydrogenated and (b) at phenylsilane hydrogenated carbon electrode.

Table 3.3. The $E_{½}$ estimated for oxidation of DOPAC at non-hydrogenated, triethylsilane and phenylsilane hydrogenated carbon electrodes two different supporting electrolytes.

Supporting Electrolyte	Non-Hydrogenated / mV	Triethylsilane hydrogenated / mV	Phenylsilane hydrogenated / mV
pH 7.4	414 (30)	527 (42)	481 (26)
1.0 M H_2SO_4	712 (27)	735 (22)	677 (18)

The values presented in the parentheses are the 95% confidence interval estimated from ten electrodes.

The waveslope estimated after triethylsilane and phenylsilane hydrogenation in a pH 7.4 citrate/phosphate buffer are 216 ± 14 mVdecade^{-1} (N=10) and 191± 9 mVdecade^{-1} (N=10) respectively. Accordingly, it can be concluded that there was no significant difference in reversibility of DOPAC after hydrogenation. Similarly, waveslope values of 113 ± 14 mV decade^{-1} (N=10) and 102 ± 10 mV decade^{-1} (N=10) was estimated at triethylsilane and phenylsilane hydrogenated electrode respectively.

The $E_{½}$ values estimated after hydrogenated in two different supporting electrolytes is presented in Table 3.3. The respective $E_{½}$ of 735 mV and 677 mV observed in the voltammograms obtained at triethylsilane and phenylsilane hydrogenated carbon electrodes in 0.1 M H_2SO_4 suggest that phenylsilane hydrogenated electrodes showed improved electron transfer kinetics. However, there was a positive shift of $E_{½}$ after hydrogenating using both silanes likely resulted from the effect of tunnelling distance *via* the siloxane dendrimers. More interestingly, in comparison to oxidation of DOPAC in a pH 7.4 supporting electrolyte, the corresponding $E_{½}$ values at non-hydrogenated, triethylsilane and phenylsilane hydrogenated electrodes were 414 mV, 527 mV and 481 mV. Compared to triethylsilane and phenylsilane hydrogenation methods, phenylsilane hydrogenated electrodes showed improved electron transfer kinetics and that phenylsiloxane dendrimers play an important role in the oxidation of DOPAC. Similar trend was observed for oxidation of methylcatechol, however with much better electron transfer kinetics at both triethylsilane and phenylsilane hydrogenated electrodes as shown in Table 3.4.

Table 3.4. $E_{½}$ of 4-methylcatechol estimated at non-hydrogenated, triethylsilane and phenylsilane hydrogenated carbon electrodes in two different supporting electrolytes.

Supporting Electrolyte	Non-Hydrogenated / mV	Triethylsilane hydrogenated / mV	Phenylsilane hydrogenated / mV
pH 7.4 citrate/phosphate	229 (30)	297 (54)	342 (20)
1.0 M H_2SO_4	535 (40)	578 (17)	559 (26)

The values presented in the parentheses are the 95% confidence interval estimated from ten electrodes.

The oxidation of 4-methycatechol was compared with oxidation of DOPAC after triethylsilane and phenylsilane hydrogenation. A similar oxidation trend was observed at both triethylsilane and phenylsilane hydrogenated electrodes. However, a much slower kinectics is observed for oxidation of DOPAC at triethylsilane hydrogenated electrode, showing that DOPAC is not sensitive to triethylsilane hyrodrogenated electrode. This could be due to the tunnelling effect by the ethylsiloxane dendrimers preventing DOPAC from making contact with the electrode easily. On the other hand, improved oxidation was observed after phenylsilane hydrogenation. The explanation for this could be the presence of phenylsiloxane dendrimers facilitating electron trasnfer between electrode surface and analyte and that DOPAC does not need to cross the barrier created by siloxane layer.

3.7.6.5 Electrochemistry of AQDS

Hydrogen bonding and protonation are fundamental factors controlling potentials and mechanisms in the reduction of quinones[80]. AQDS undergoes a reversible two-

electron, two-proton redox reaction. The oxidised and reduced forms have been shown to adsorb strongly on Pt, Hg and glassy carbon, but weakly on the basal plane of highly ordered pyrolytic graphite. The reduction of 1.0 mM AQDS at (a) non-hydrogenated and those at (b) triethylsilane and phenylsilane hydrogenated carbon electrodes in 0.1 M $HClO_4$ supporting electrolyte are presented in Figure 3.12(A) and (B). A featureless voltammogram (*i.e.* non-sigmoidal) was obtained at the non-hydrogenated electrode. The reduction current observed in Figure 3.12 (A and B (trace a)) at the non-hydrogenated electrode is due to the adsorption of AQDS on oxygen containing functional groups on the carbon electrode. After hydrogenating with triethylsilane, a similar featureless voltammogram is obtained with ~30% smaller current, indicating removal of oxygen containing functionalities from the surface. Interestingly, a sigmoidal shaped voltammogram after hydrogenating using phenylsilane (Figure 3.12 (B) trace b). The phenyl rings formed during phenylsilane hydrogenation have likely facilitated the electron transfer kinetics by acting as a molecular wire due to π-conjugation. For example, Creager et al[81] attached ferrocene groups *via* oligo(phenylethylnyl) molecular wire bridges on gold electrodes, which was demonstrated to have promoted electron transfer[81]. Similarly, according to Kneten and McCreery, AQDS adsorption requires sufficient surface defect density such as those in graphitic edge regions[82]. Additionally, the ~30% decline in the current indicates a decrease in the presence of carbon oxygen functional groups on the surface, which in turn prohibited AQDS from adsorbing on the hydrogenated surface. The results of AQDS reduction at non-hydrogenated and hydrogenated carbon electrodes are consistent with those at a hydrogenated glassy carbon electrode and a diamond electrode. Similarly, Xu *et al.*[83] reported the little tendency of 2,4 AQDS to adsorb on

a hydrogenated glassy carbon electrode and a diamond electrode as these surfaces are nonpolar and hydrogen terminated.

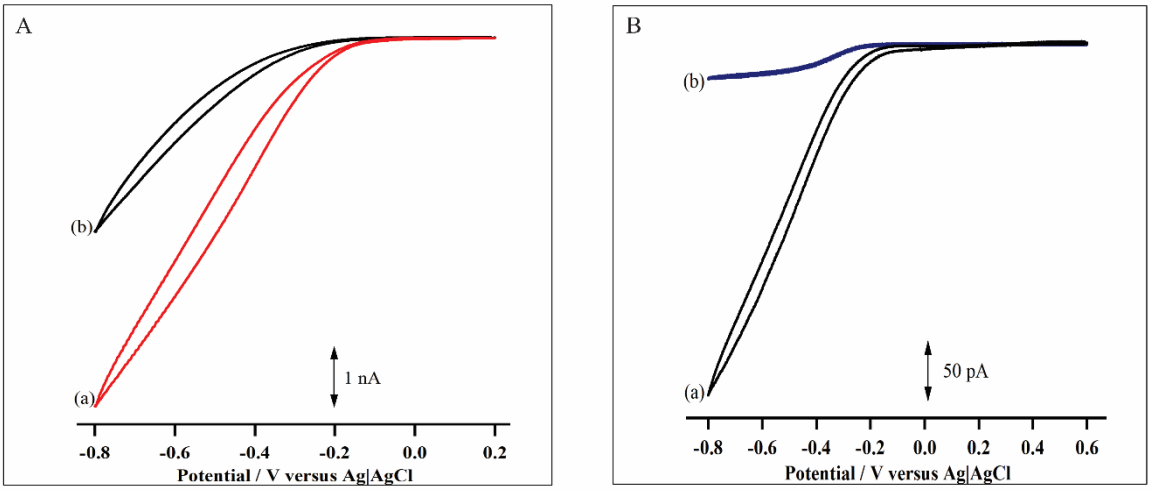

Figure 3.12. Cyclic voltammograms of 1.0 mM AQDS (a) before hydrogenation and (b) after hydrogenation using (A) triethylsilane and (B) phenylsilane. Scan rate 100 mV s^{-1}.

In summary, the characterisation of electrodes using two positively and one negatively charged redox markers namely $[Ru(NH_3)_6]^{3+}$, dopamine and $[Fe(CN)_6]^{3-}$ confirmed the presence of a hydrogenated surface, which further provided the insights into the surface characteristics after silane hydrogenation. The reversibility was unaffected by the hydrogenation procedures on all redox markers. The shifts in the $E_{½}$ indicate a slower electron transfer kinetics possibly due to slow diffusion and mass transport through the siloxane dendrimers compared to that at non-hydrogenated electrodes, as well as the formation of an oxide-free H-terminated surface that gives rise to a decline in the electrostatic attraction between the electrode and the analyte. Reduced electron transfer kinetics is also likely to be caused by a decrease in the surface roughness as well as

decreased oxide groups with low adsorption sites[70]. In addition, improved electron transfer kinetics was observed on phenylsilane hydrogenated electrodes. This is attributed to the presence of phenyl rings formed during the hydrogenation procedure. They facilitate the electron transfer rate *via* the π-π interaction with the phenyl ring of dopamine.

The results hitherto obtained indicate similar kinetics for all the catechols in the response to the surface modification and that some modifications have much greater effects on several catechols than others. For instance, McCreery's group studied the effects of glassy carbon surface modification on the catechol and hydroquinone adsorption[71, 79]. The experimental data concluded that pyridine treated glassy carbon removed the adventitious impurities, thus exposing a larger glassy carbon surface to catechol and methylene blue adsorption and that pyridine treated glassy carbon surface is reactive towards adsorption and electron transfer. In addition, they showed that the electron transfer kinetics for the catechol and hydroquinone on glassy carbon are largely independent of the coverage of oxygen containing functional groups.

Behan *et al.*[66] investigated the effects of oxidative pre-treatments on the activation of glassy carbon electrodes towards adsorption and oxidation of dopamine. In their work, well-defined surface chemistry achieved through pre-treatment protocols has resulted in surfaces with different properties and oxygen contents. Their results indicate that dopamine adsorption does not occur on highly oxidised glassy carbon surface, however dopamine readily adsorbs on a surface comprising low-oxygen content. Additionally, at a highly oxidised surface, the charge transfer tends to be quasi-reversible, while reversible charge transfer kinetics was observed at low oxide glassy carbon surface.

Their findings show the role of basal plane sites in facilitating electron transfer, as well as the effects of oxygen containing functional groups for catechol oxidation[66].

Adsorption is significantly enhanced by the presence of surface oxides, resulting in dipoles, electrostatic interaction and covalent bonding with the adsorbates. Kuo and McCreery[65] investigated the heterogenous electron transfer kinetics at a hydrogenated glassy carbon electrode with low surface oxides. Their work showed that electron transfer kinetics of $[Fe(CN)_6]^{3-}$, dopamine and ascorbic acid exhibited fast electron transfer on low-oxide surface, suggesting that oxygen containing functional groups are not necessarily involved in electron transfer mechanism. The redox behaviour of these redox systems was slower on surfaces with intentional monolayers such as methylene blue, bis(4-methylstyryl)benzene, anthraquinone 2,4 disulfonic acid and nitrophenyl[58], further implying that there may be some sort of interaction associated with electron transfer. Surface with low oxygen containing functional groups can still adsorb many analytes but at a reduced capacity[65].

3.8 Concluding Remarks

We reported the microscopic, spectroscopic and electrochemical characterisation of structurally small carbon electrodes that were hydrogenated using triethylsilane and phenylsilane. This hydrogenation mechanism reduces the surface functional groups such as aldehydes, ketones, alcohol and carboxylic acids, while forming siloxane dendrimers on the surface through the phenol functional group. In this study, we confirmed the presence of siloxane dendrimers using X-ray photoelectron spectroscopy. Raman spectroscopy was used to further investigate the effectiveness of the hydrogenation procedure on the sp^2 / sp^3 ratio on the hydrogenated carbon electrode. Cyclic voltammetry using the redox markers $[Ru(NH_3)_6]^{3+}$, $[Fe(CN)_6]^{3-}$, dopamine,

DOPAC, 4-methylcatechol and AQDS was used to electrochemically characterise the carbon electrodes. As expected, for the outer sphere redox system $[Ru(NH_3)_6]^{3+}$, there was no noticeable difference in the reversibility or $E_{½}$ after the hydrogenation using both silanes. In-case of the electrochemistry of $[Fe(CN)_6]^3$, catechols and quinones, different redox chemistries were observed as these are inner-sphere redox couples, which are very sensitive to the surface chemistry of the electrode.

3.9 References

(1) McNally, M.; Wong, D. K. Y. An in Vivo Probe Based on Mechanically Strong but Structurally Small Carbon Electrodes with an Appreciable Surface Area. *Analytical Chemistry* **2001,** *73* (20), 4793-4800, DOI: 10.1021/ac0104532.

(2) Peltola, E.; Sainio, S.; Holt, K. B.; Palomäki, T.; Koskinen, J.; Laurila, T. Electrochemical Fouling of Dopamine and Recovery of Carbon Electrodes. *Analytical Chemistry* **2018,** *90* (2), 1408-1416, DOI: 10.1021/acs.analchem.7b04793.

(3) Hanssen Benjamin, L.; Siraj, S.; Wong Danny, K. Y., Recent strategies to minimise fouling in electrochemical detection systems. In *Reviews in Analytical Chemistry*, 2016; Vol. 35, p 1.

(4) Frost, M.; Meyerhoff, M. E. In Vivo Chemical Sensors: Tackling Biocompatibility. *Analytical Chemistry* **2006,** *78* (21), 7370-7377, DOI: 10.1021/ac069475k.

(5) Wisniewski, N.; Moussy, F.; Reichert, W. M. Characterization of implantable biosensor membrane biofouling. *Fresenius' Journal of Analytical Chemistry* **2000,** *366* (6), 611-621, DOI: 10.1007/s002160051556.

(6) Park, J.; Show, Y.; Quaiserova, V.; Galligan, J. J.; Fink, G. D.; Swain, G. M. Diamond microelectrodes for use in biological environments. *Journal of Electroanalytical Chemistry* **2005,** *583* (1), 56-68, DOI: https://doi.org/10.1016/j.jelechem.2005.04.032.

(7) Chandra, S.; Siraj, S.; Wong, D. K. Y. Recent Advances in Biosensing for Neurotransmitters and Disease Biomarkers using Microelectrodes. *ChemElectroChem* **2017,** *4* (4), 822-833, DOI: 10.1002/celc.201600810.

(8) Siraj, S.; McRae, C. R.; Wong, D. K. Y. Effective activation of physically small carbon electrodes by n-butylsilane reduction. *Electrochemistry Communications* **2016,** *64*, 35-41, DOI: http://dx.doi.org/10.1016/j.elecom.2016.01.007.

(9) Park, J.; Quaiserová-Mocko, V.; Pecková, K.; Galligan, J. J.; Fink, G. D.; Swain, G. M. Fabrication, characterization, and application of a diamond microelectrode for electrochemical measurement of norepinephrine release from the sympathetic nervous system. *Diamond and Related Materials* **2006,** *15* (4), 761-772, DOI: https://doi.org/10.1016/j.diamond.2005.11.008.

(10) Zhu, M.; Zeng, C.; Ye, J.; Sun, Y. Simultaneous in vivo voltammetric determination of dopamine and 5-Hydroxytryptamine in the mouse brain. *Applied Surface Science* **2018,** *455*, 646-652, DOI: https://doi.org/10.1016/j.apsusc.2018.05.190.

(11) Liu, X.; Zhang, M.; Xiao, T.; Hao, J.; Li, R.; Mao, L. Protein Pretreatment of Microelectrodes Enables in Vivo Electrochemical Measurements with Easy Precalibration and Interference-Free from Proteins. *Analytical Chemistry* **2016,** *88* (14), 7238-7244, DOI: 10.1021/acs.analchem.6b01476.

(12) Zestos, A. G.; Jacobs, C. B.; Trikantzopoulos, E.; Ross, A. E.; Venton, B. J. Polyethylenimine Carbon Nanotube Fiber Electrodes for Enhanced Detection of Neurotransmitters. *Analytical Chemistry* **2014,** *86* (17), 8568-8575, DOI: 10.1021/ac5003273.

(13) Swamy, B. E. K.; Venton, B. J. Carbon nanotube-modified microelectrodes for simultaneous detection of dopamine and serotonin in vivo. *Analyst (Cambridge, U. K.)* **2007,** *132* (9), 876-884, DOI: 10.1039/b705552h.

(14) Álvarez-Martos, I.; Møller, A.; Ferapontova, E. E. Dopamine Binding and Analysis in Undiluted Human Serum and Blood by the RNA-Aptamer Electrode. *ACS Chemical Neuroscience* **2019,** *10* (3), 1706-1715, DOI: 10.1021/acschemneuro.8b00616.

(15) Álvarez-Martos, I.; Ferapontova, E. E. A DNA sequence obtained by replacement of the dopamine RNA aptamer bases is not an aptamer. *Biochemical and Biophysical Research Communications* **2017,** *489* (4), 381-385, DOI: https://doi.org/10.1016/j.bbrc.2017.05.134.

(16) Wu, X.; Li, P.; Zhang, Y.; Yao, D. Selective response of dopamine on 3-thienylphosphonic acid modified gold electrode with high antifouling capability and long-term stability. *Materials Science and Engineering: C* **2019,** *94*, 677-683, DOI: https://doi.org/10.1016/j.msec.2018.10.024.

(17) Garrett, D. J.; Tong, W.; Simpson, D. A.; Meffin, H. Diamond for neural interfacing: A review. *Carbon* **2016,** *102*, 437-454, DOI: https://doi.org/10.1016/j.carbon.2016.02.059.

(18) Panizza, M. Boron-Doped Diamond Electrodes A2 - Wandelt, Klaus. In *Encyclopedia of Interfacial Chemistry*; Elsevier: Oxford, 2018; pp 393-400.

(19) Stradolini, F.; Kilic, T.; Taurino, I.; De Micheli, G.; Carrara, S. Cleaning strategy for carbon-based electrodes: Long-term propofol monitoring in human serum. *Sensors and Actuators B: Chemical* **2018,** *269*, 304-313, DOI: https://doi.org/10.1016/j.snb.2018.04.082.

(20) Trouillon, R.; O'Hare, D. Comparison of glassy carbon and boron doped diamond electrodes: Resistance to biofouling. *Electrochimica Acta* **2010,** *55* (22), 6586-6595, DOI: http://dx.doi.org/10.1016/j.electacta.2010.06.016.

(21) Suzuki, A.; Ivandini, T. A.; Yoshimi, K.; Fujishima, A.; Oyama, G.; Nakazato, T.; Hattori, N.; Kitazawa, S.; Einaga, Y. Fabrication, Characterization, and Application of Boron-Doped Diamond Microelectrodes for in Vivo Dopamine Detection. *Analytical Chemistry* **2007,** *79* (22), 8608-8615, DOI: 10.1021/ac071519h.

(22) Dong, H.; Wang, S.; Galligan, J. J.; Swain, G. M. Boron-doped diamond nano/microelectrodes for biosensing and in vitro measurements. *Frontiers in bioscience (Scholar edition)* **2011,** *3*, 518-540.

(23) Hébert, C.; Warnking, J.; Depaulis, A.; Garçon, L. A.; Mermoux, M.; Eon, D.; Mailley, P.; Omnès, F. Microfabrication, characterization and in vivo MRI compatibility of diamond microelectrodes array for neural interfacing. *Materials Science and Engineering: C* **2015,** *46*, 25-31, DOI: https://doi.org/10.1016/j.msec.2014.10.018.

(24) Miodek, A.; Regan, E. M.; Bhalla, N.; Hopkins, N. A. E.; Goodchild, S. A.; Estrela, P. Optimisation and Characterisation of Anti-Fouling Ternary SAM Layers for Impedance-Based Aptasensors. *Sensors (Basel, Switzerland)* **2015,** *15* (10), 25015-25032, DOI: 10.3390/s151025015.

(25) Nimmagadda, R. D.; McRae, C. A novel reduction reaction for the conversion of aldehydes, ketones and primary, secondary and tertiary alcohols into their corresponding alkanes. *Tetrahedron Letters* **2006,** *47* (32), 5755-5758, DOI: http://dx.doi.org/10.1016/j.tetlet.2006.06.007.

(26) Nimmagadda, R. D.; McRae, C. Characterisation of the backbone structures of several fulvic acids using a novel selective chemical reduction method. *Organic Geochemistry* **2007,** *38* (7), 1061-1072, DOI: http://dx.doi.org/10.1016/j.orggeochem.2007.02.016.

(27) Jeon, S. I.; Andrade, J. D. Protein—surface interactions in the presence of polyethylene oxide: II. Effect of protein size. *Journal of Colloid and Interface Science* **1991,** *142* (1), 159-166, DOI: https://doi.org/10.1016/0021-9797(91)90044-9.

(28) Jeon, S. I.; Lee, J. H.; Andrade, J. D.; De Gennes, P. G. Protein—surface interactions in the presence of polyethylene oxide: I. Simplified theory. *Journal of Colloid and Interface Science* **1991,** *142* (1), 149-158, DOI: https://doi.org/10.1016/0021-9797(91)90043-8.

(29) Honeychurch, K. C. 13 - Printed thick-film biosensors. In *Printed Films*; Prudenziati, M.; Hormadaly, J., Eds.; Woodhead Publishing: 2012; pp 366-409.

(30) Bond, A. M.; Lay, P. A. Cyclic voltammetry at microelectrodes in the absence of added electrolyte using a platinum quasi-reference electrode. *Journal of Electroanalytical Chemistry and Interfacial Electrochemistry* **1986,** *199* (2), 285-295, DOI: https://doi.org/10.1016/0022-0728(86)80004-3.

(31) Siraj, S.; McRae, C. R.; Wong, D. K. Y. Antifouling Characteristics of a carbon electrode surface hydrogenated by n-butylsilane reduction. *Electrochimica Acta* **2019**, DOI: https://doi.org/10.1016/j.electacta.2019.01.188.

(32) Britz, D.; Chandra, S.; Strutwolf, J.; Wong, D. K. Y. Diffusion-limited chronoamperometry at conical-tip microelectrodes. *Electrochimica Acta* **2010,** *55* (3), 1272-1277, DOI: https://doi.org/10.1016/j.electacta.2009.10.025.

(33) Dickinson, E. J. F.; Streeter, I.; Compton, R. G. Theory of Chronoamperometry at Cylindrical Microelectrodes and Their Arrays. *The Journal of Physical Chemistry C* **2008,** *112* (31), 11637-11644, DOI: 10.1021/jp801867e.

(34) Carley, A. F.; Morgan, D. J. Surface Analysis: X-Ray Photoelectron Spectroscopy. In *Reference Module in Materials Science and Materials Engineering*; Elsevier: 2016.

(35) Brunetti, B.; De Giglio, E.; Cafagna, D.; Desimoni, E. XPS analysis of glassy carbon electrodes chemically modified with 8-hydroxyquinoline-5-sulphonic acid. *Surface and Interface Analysis* **2012,** *44* (4), 491-496, DOI: doi:10.1002/sia.3880.

(36) Tan, S.; Li, J.; Zhou, L.; Chen, P.; Xu, Z. Hydrophilic carbon fiber paper based electrode coated with graphene for high performance supercapacitors. *Materials Letters* **2018,** *233*, 278-281, DOI: https://doi.org/10.1016/j.matlet.2018.09.039.

(37) Yuan, J.-M.; Fan, Z.-F.; Yang, Q.-C.; Li, W.; Wu, Z.-J. Surface modification of carbon fibers by microwave etching for epoxy resin composite. *Composites Science and Technology* **2018,** *164*, 222-228, DOI: https://doi.org/10.1016/j.compscitech.2018.05.043.

(38) Bystron, T.; Sramkova, E.; Dvorak, F.; Bouzek, K. Glassy carbon electrode activation – A way towards highly active, reproducible and stable electrode surface. *Electrochimica Acta* **2019,** *299*, 963-970, DOI: https://doi.org/10.1016/j.electacta.2019.01.066.

(39) Görlich, E.; Haber, J.; Stoch, A.; Stoch, J. XPS study of α-quartz surface. *Journal of Solid State Chemistry* **1980,** *33* (1), 121-124, DOI: https://doi.org/10.1016/0022-4596(80)90555-1.

(40) Zakaznova-Herzog, V. P.; Nesbitt, H. W.; Bancroft, G. M.; Tse, J. S.; Gao, X.; Skinner, W. High-resolution valence-band XPS spectra of the nonconductors quartz and olivine. *Physical Review B* **2005,** *72* (20), 205113, DOI: 10.1103/PhysRevB.72.205113.

(41) Ma, P. C.; Kim, J.-K.; Tang, B. Z. Functionalization of carbon nanotubes using a silane coupling agent. *Carbon* **2006,** *44* (15), 3232-3238, DOI: https://doi.org/10.1016/j.carbon.2006.06.032.

(42) O'Hare, L.-A.; Parbhoo, B.; Leadley, S. R. Development of a methodology for XPS curve-fitting of the Si 2p core level of siloxane materials. *Surface and Interface Analysis* **2004,** *36* (10), 1427-1434, DOI: doi:10.1002/sia.1917.

(43) Lespade, P.; Marchand, A.; Couzi, M.; Cruege, F. Caracterisation de materiaux carbones par microspectrometrie Raman. *Carbon* **1984,** *22* (4), 375-385, DOI: https://doi.org/10.1016/0008-6223(84)90009-5.

(44) Tamor, M. A.; Vassell, W. C. Raman ''fingerprinting'' of amorphous carbon films. *Journal of Applied Physics* **1994,** *76* (6), 3823-3830, DOI: 10.1063/1.357385.

(45) Zeng, A.; Liu, E.; Tan, S. N.; Zhang, S.; Gao, J. Cyclic Voltammetry Studies of Sputtered Nitrogen Doped Diamond-Like Carbon Film Electrodes. *Electroanalysis* **2002,** *14* (15-16), 1110-1115, DOI: 10.1002/1521-4109(200208)14:15/16<1110::AID-ELAN1110>3.0.CO;2-E.

(46) Ferrari, A. C. Determination of bonding in diamond-like carbon by Raman spectroscopy. *Diamond and Related Materials* **2002,** *11* (3), 1053-1061, DOI: https://doi.org/10.1016/S0925-9635(01)00730-0.

(47) Ferrari, A. C. Raman spectroscopy of graphene and graphite: Disorder, electron–phonon coupling, doping and nonadiabatic effects. *Solid State Communications* **2007,** *143* (1), 47-57, DOI: https://doi.org/10.1016/j.ssc.2007.03.052.

(48) Filik, J.; May, P. W.; Pearce, S. R. J.; Wild, R. K.; Hallam, K. R. XPS and laser Raman analysis of hydrogenated amorphous carbon films. *Diamond and Related Materials* **2003,** *12* (3), 974-978, DOI: https://doi.org/10.1016/S0925-9635(02)00374-6.

(49) Holmberg, S.; Ghazinejad, M.; Cho, E.; George, D.; Pollack, B.; Perebikovsky, A.; Ragan, R.; Madou, M. Stress-activated pyrolytic carbon nanofibers for electrochemical

platforms. *Electrochimica Acta* **2018,** *290*, 639-648, DOI: https://doi.org/10.1016/j.electacta.2018.09.013.

(50) Bogdanowicz, R.; Czupryniak, J.; Gnyba, M.; Ryl, J.; Ossowski, T.; Sobaszek, M.; Siedlecka, E. M.; Darowicki, K. Amperometric sensing of chemical oxygen demand at glassy carbon and silicon electrodes modified with boron-doped diamond. *Sensors and Actuators B: Chemical* **2013,** *189*, 30-36, DOI: https://doi.org/10.1016/j.snb.2012.12.007.

(51) Zhao, Y.; Yang, Z.; Fan, W.; Wang, Y.; Li, G.; Cong, H.; Yuan, H. Carbon nanotube/carbon fiber electrodes via chemical vapor deposition for simultaneous determination of ascorbic acid, dopamine and uric acid. *Arabian Journal of Chemistry* **2018**, DOI: https://doi.org/10.1016/j.arabjc.2018.11.002.

(52) Demuru, S.; Nela, L.; Marchack, N.; Holmes, S. J.; Farmer, D. B.; Tulevski, G. S.; Lin, Q.; Deligianni, H. Scalable Nanostructured Carbon Electrode Arrays for Enhanced Dopamine Detection. *ACS Sensors* **2018**, DOI: 10.1021/acssensors.8b00043.

(53) Lim, Y.; Chu, J. H.; Lee, D. H.; Kwon, S.-Y.; Shin, H. Increase in graphitization and electrical conductivity of glassy carbon nanowires by rapid thermal annealing. *Journal of Alloys and Compounds* **2017,** *702*, 465-471, DOI: https://doi.org/10.1016/j.jallcom.2017.01.098.

(54) Yang, C.; Jacobs, C. B.; Nguyen, M. D.; Ganesana, M.; Zestos, A. G.; Ivanov, I. N.; Puretzky, A. A.; Rouleau, C. M.; Geohegan, D. B.; Venton, B. J. Carbon Nanotubes Grown on Metal Microelectrodes for the Detection of Dopamine. *Analytical Chemistry* **2016,** *88* (1), 645-652, DOI: 10.1021/acs.analchem.5b01257.

(55) Schwan, J.; Ulrich, S.; Batori, V.; Ehrhardt, H.; Silva, S. R. P. Raman spectroscopy on amorphous carbon films. *Journal of Applied Physics* **1996,** *80* (1), 440-447, DOI: 10.1063/1.362745.

(56) Wang, J. *Analytical electrochemistry / Joseph Wang*, 3rd ed. ed.; Hoboken, N.J. : J. Wiley: Hoboken, N.J., 2006.

(57) Mampallil, D.; Mathwig, K.; Kang, S.; Lemay, S. G. Reversible Adsorption of Outer-Sphere Redox Molecules at Pt Electrodes. *The Journal of Physical Chemistry Letters* **2014,** *5* (3), 636-640, DOI: 10.1021/jz402592n.

(58) Chen, P.; McCreery, R. L. Control of Electron Transfer Kinetics at Glassy Carbon Electrodes by Specific Surface Modification. *Analytical Chemistry* **1996,** *68* (22), 3958-3965, DOI: 10.1021/ac960492r.

(59) Vinokur, N.; Miller, B.; Avyigal, Y.; Kalish, R. Electrochemical behavior of boron-doped diamond electrodes. *J. Electrochem. Soc.* **1996,** *143* (10), L238-L240, DOI: 10.1149/1.1837157.

(60) McCreery, R. L. Advanced Carbon Electrode Materials for Molecular Electrochemistry. *Chemical Reviews* **2008,** *108* (7), 2646-2687, DOI: 10.1021/cr068076m.

(61) Swain, G. M. Chapter 4 Electroanalytical applications of diamond electrodes. In *Semiconductors and Semimetals*; Nebel, C. E.; Ristein, J., Eds.; Elsevier: 2004; pp 121-148.

(62) Xu, J.; Granger, M. C.; Chen, Q.; Strojek, J. W.; Lister, T. E.; Swain, G. M. Peer Reviewed: Boron-Doped Diamond Thin-Film Electrodes. *Analytical Chemistry* **1997,** *69* (19), 591A-597A, DOI: 10.1021/ac971791z.

(63) Lee, C.; Anson, F. C. Inhibition of the electroreduction of Fe(CN)63− at microelectrodes in the absence of supporting electrolyte: Mediation of the inhibited reduction by methyl viologen. *Journal of Electroanalytical Chemistry* **1992,** *323* (1), 381-389, DOI: https://doi.org/10.1016/0022-0728(92)80027-2.

(64) Alwarappan, S.; Butcher, K. S. A.; Wong, D. K. Evaluation of hydrogenated physically small carbon electrodes in resisting fouling during voltammetric detection of dopamine. *Sensors and Actuators B: Chemical* **2007,** *128* (1), 299-305.

(65) Kuo, T.-C.; McCreery, R. L. Surface Chemistry and Electron-Transfer Kinetics of Hydrogen-Modified Glassy Carbon Electrodes. *Analytical Chemistry* **1999,** *71* (8), 1553-1560, DOI: 10.1021/ac9807666.

(66) Behan, J. A.; Grajkowski, F.; Jayasundara, D. R.; Vilella-Arribas, L.; García-Melchor, M.; Colavita, P. E. Influence of carbon nanostructure and oxygen moieties on dopamine adsorption and charge transfer kinetics at glassy carbon surfaces. *Electrochimica Acta* **2019,** *304*, 221-230, DOI: https://doi.org/10.1016/j.electacta.2019.02.103.

(67) Guin, P. S.; Das, S.; Mandal, P. C. Electrochemical reduction of quinones in different media: a review. *Int. J. Electrochem.* **2011**, 816202, 22 pp., DOI: 10.4061/2011/816202.

(68) Marcus, M. F.; Hawley, M. D. Electrochemical studies of the redox behavior of α-tocopherylquinone and a related model quinone. *Biochimica et Biophysica Acta (BBA) - General Subjects* **1970,** *222* (1), 163-173, DOI: https://doi.org/10.1016/0304-4165(70)90361-2.

(69) Armendáriz-Vidales, G.; Martínez-González, E.; Cuevas-Fernández, H. J.; Fernández-Campos, D. O.; Burgos-Castillo, R. C.; Frontana, C. The stabilizing role of intramolecular hydrogen bonding in disubstituted hydroxy-quinones. *Electrochimica Acta* **2013,** *110*, 628-633, DOI: https://doi.org/10.1016/j.electacta.2013.05.123.

(70) Phillips, P. E. M.; Wightman, R. M. Critical guidelines for validation of the selectivity of in-vivo chemical microsensors. *TrAC Trends in Analytical Chemistry* **2003,** *22* (8), 509-514, DOI: https://doi.org/10.1016/S0165-9936(03)00907-5.

(71) DuVall, S. H.; McCreery, R. L. Self-catalysis by Catechols and Quinones during Heterogeneous Electron Transfer at Carbon Electrodes. *Journal of the American Chemical Society* **2000,** *122* (28), 6759-6764, DOI: 10.1021/ja000227u.

(72) Silva, T. A.; Zanin, H.; May, P. W.; Corat, E. J.; Fatibello-Filho, O. Electrochemical Performance of Porous Diamond-like Carbon Electrodes for Sensing Hormones, Neurotransmitters, and Endocrine Disruptors. *ACS Applied Materials & Interfaces* **2014,** *6* (23), 21086-21092, DOI: 10.1021/am505928j.

(73) Singh, Y. S.; Sawarynski, L. E.; Michael, H. M.; Ferrell, R. E.; Murphey-Corb, M. A.; Swain, G. M.; Patel, B. A.; Andrews, A. M. Boron-Doped Diamond Microelectrodes Reveal Reduced Serotonin Uptake Rates in Lymphocytes from Adult Rhesus Monkeys Carrying the Short Allele of the 5-HTTLPR. *ACS Chemical Neuroscience* **2010,** *1* (1), 49-64, DOI: 10.1021/cn900012y.

(74) Granger, M. C.; Witek, M.; Xu, J.; Wang, J.; Hupert, M.; Hanks, A.; Koppang, M. D.; Butler, J. E.; Lucazeau, G.; Mermoux, M.; Strojek, J. W.; Swain, G. M. Standard Electrochemical Behavior of High-Quality, Boron-Doped Polycrystalline Diamond Thin-Film Electrodes. *Analytical Chemistry* **2000,** *72* (16), 3793-3804, DOI: 10.1021/ac0000675.

(75) Behan, J. A.; Grajkowski, F.; Jayasundara, D. R.; Vilella-Arribas, L.; García-Melchor, M.; Colavita, P. E. Influence of carbon nanostructure and oxygen moieties on dopamine adsorption and charge transfer kinetics at glassy carbon surfaces. *Electrochimica Acta* **2019**, DOI: https://doi.org/10.1016/j.electacta.2019.02.103.

(76) Gonon, F.; Buda, M.; Cespuglio, R.; Jouvet, M.; Pujol, J.-F. In vivo electrochemical detection of catechols in the neostriatum of anaesthetized rats: dopamine or DOPAC? *Nature* **1980,** *286* (5776), 902-904, DOI: 10.1038/286902a0.

(77) Takmakov, P.; Zachek, M. K.; Keithley, R. B.; Bucher, E. S.; McCarty, G. S.; Wightman, R. M. Characterization of local pH changes in brain using fast-scan cyclic voltammetry with carbon microelectrodes. *Analytical chemistry* **2010,** *82* (23), 9892-9900, DOI: 10.1021/ac102399n.

(78) Wang, J.; Li, M.; Shi, Z.; Li, N.; Gu, Z. Electrocatalytic oxidation of 3,4-dihydroxyphenylacetic acid at a glassy carbon electrode modified with single-wall carbon nanotubes. *Electrochimica Acta* **2001,** *47* (4), 651-657, DOI: https://doi.org/10.1016/S0013-4686(01)00795-2.

(79) DuVall, S. H.; McCreery, R. L. Control of Catechol and Hydroquinone Electron-Transfer Kinetics on Native and Modified Glassy Carbon Electrodes. *Analytical Chemistry* **1999,** *71* (20), 4594-4602, DOI: 10.1021/ac990399d.

(80) Gupta, N.; Linschitz, H. Hydrogen-Bonding and Protonation Effects in Electrochemistry of Quinones in Aprotic Solvents. *Journal of the American Chemical Society* **1997,** *119* (27), 6384-6391, DOI: 10.1021/ja970028j.

(81) Creager, S.; Yu, C. J.; Bamdad, C.; O'Connor, S.; MacLean, T.; Lam, E.; Chong, Y.; Olsen, G. T.; Luo, J.; Gozin, M.; Kayyem, J. F. Electron Transfer at Electrodes through Conjugated "Molecular Wire" Bridges. *Journal of the American Chemical Society* **1999,** *121* (5), 1059-1064, DOI: 10.1021/ja983204c.

(82) Kneten, K. R.; McCreery, R. L. Effects of redox system structure on electron-transfer kinetics at ordered graphite and glassy carbon electrodes. *Analytical Chemistry* **1992,** *64* (21), 2518-2524, DOI: 10.1021/ac00045a011.

(83) Xu, J.; Chen, Q.; Swain, G. M. Anthraquinonedisulfonate Electrochemistry: A Comparison of Glassy Carbon, Hydrogenated Glassy Carbon, Highly Oriented Pyrolytic Graphite, and Diamond Electrodes. *Analytical Chemistry* **1998,** *70* (15), 3146-3154, DOI: 10.1021/ac9800661.

CHAPTER 4: ANALYTICAL CHARACTERISTICS AND ANTIFOULING PROPERTIES OF SILANE HYDROGENATED CARBON ELECTRODES

4.1 Introduction

A long-term goal of this research is to fabricate small antifouling carbon electrodes that can be used to obtain meaningful results during detection of neurotransmitter dopamine *in vivo*. As most neurotransmitters are present in trace quantities, our electrodes must demonstrate a targeted limit of detection and sensitivity for their practicality for *in vivo* measurements. In addition to this, the oxidation potentials of dopamine, ascorbic acid and uric acid are also known to be very similar to each other at conventional electrodes, resulting in severely overlapped voltammetric signals, making it difficult to monitor them simultaneously using conventional electrodes. In this Chapter, we will characterise the analytical perfomance and the selectivity towards dopamine in the presence of uric acid and ascorbic acid at structurally small hydrogenated carbon electrodes. Additionally, as discussed in Chapter 3 one of the major challenges during *in vivo* monitoring of dopamine is the adsorption of non-targeted species as well as the oxidation product, dopamine-*o*-quinone, on an electrode surface, which affects the sensitivity and repeatability of the measurement with time. Therefore, the present work will also study the antifouling property of hydrogenated carbon electrodes against dopamine-*o*-quinone by examining the effect of consecutive cycling in dopamine on the oxidation limiting current of dopamine. Biofouling arising from the adsorption of proteins, peptides and lipids is further assessed by incubating the hydrogenated carbon

electrodes in a laboratory synthetic fouling solution containing proteins, peptides and lipids, which mimics an extracellular fluid.

4.2 Challenges during dopamine detection

The neurotransmitter dopamine plays a significant role in the mammalian central nervous system[1]. Dopamine is known to be activated by natural rewards such as food, drink, and sex, as well as addictive drugs[2-3]. It is involved in a variety of brain disorders including schizophrenia, addiction, epilepsy and Parkinson's disease, where the brain dopamine neurons experience degeneration[3-4]. It is well established that these disorders account for a significant percentage of global healthcare costs, approximately AUD$1300 billion[5]. Therefore, monitoring neurotransmitters is a bottleneck in understanding the physiological indicators of chemical neurotransmission for early diagnosis of several neurodegenerative disorders[6]. Very often, the concentration of dopamine in the extracellular fluid is used as an important parameter for the diagnosis of neurodegenerative diseases. Coupled with anatomical, physiological and pharmacological evidence, electrochemical sensors are ideal candidates for the transient monitoring of neurotransmitters as these molecules can be easily oxidised at an electrode surface. Owing to their biocompatibility, easy fabrication procedures[7-8], wide potential window[9], inherent robustness[10], and excellent electrocatalytic activity[11-12] carbon-based electrochemical sensors are widely applied to the detection of electroactive neurotransmitters such as dopamine and serotonin. However, there are significant challenges during detection of dopamine due to the presence of other electroactive species that can oxidise at similar potentials (*e.g.* +0.235 V versus saturated calomel electrode) for dopamine, +0.2 V for ascorbic acid and +0.3 V for uric acid). There have been numerous studies reporting the use of different electrode

materials to address these challenges, for example, a gold nanoparticle and multiwalled carbon nanotube modified glassy carbon electrode[13-14], poly(2,4,6-triaminopyrmidine)/ gold nanoparticle[15] or poly(3,4-ethylenedioxythiophene)/graphene oxide coated carbon fibre electrodes[16], boron-doped diamond electrodes[4, 17-18], multiwalled carbon nanotubes/cellulose acetate composite[19-20] and poly(Rhodamine B) modified carbon paste electrodes[21-22] for the detection of dopamine in the presence of other electroactive interfering compounds. Such modifications usually enhance the electrocatalytic properties to selectively detect these species simultaneously.

4.3 Interference from electrochemically active species in the brain during dopamine detection

Electrochemical measurement of dopamine in a biological fluid using carbon electrodes faces several challenges. Neurotransmitters do not function on their own in a simple environment. Instead, they exist in a complicated biological matrix in the presence of other biological substances, some of which are electrochemically active. Multiple electroactive neurotransmitters are frequently released into the synaptic cleft from the same presynaptic neuron[23]. Electrochemically active biomolecules such as ascorbic acid, dopamine and uric acid coexist in the central nervous system and serum where they play an important role in the human metabolic processes[24-25]. Usually, dopamine and ascorbic acid coexist in the extracellular fluid while uric acid and ascorbic acid coexist in blood and urine[26]. Electrochemical methods have been extensively applied to simultaneously determine dopamine, uric acid and ascorbic acid. Accurate measurement of dopamine in the presence of ascorbic acid and dopamine is often challenging due to the presence of a large excess of ascorbic acid (>500 μM) coexisting with dopamine and uric acid in the central nervous system and human serum[27]. Owing

to their similar oxidation potentials, these electroactive species often show severely overlapped voltammetric responses obtained at conventional electrodes, making it difficult to discriminate the signals[28].

Ascorbic acid is one of the analytes present in the extracellular matrix that has been of greatest concern during the *in vivo* measurement of dopamine. It is a cyclic six-carbon backbone carbohydrate generally known as a reducing agent and is able to serve as an antioxidant in a free-radical mediated oxidation process[29]. It is involved in multiple functions in cell metabolism and survival such as participating as a cofactor in several enzyme reactions, including those involved in catecholamine synthesis, carnitine, cholesterol, amino acids and certain peptide hormones[30-31]. Uric acid is the end product of purine metabolism in humans and is an alternative physiological substrate for myeloperoxidase[32] and is excreted in urine[33]. In a healthy human, the normal level of uric acid in urine is in milli molar range whereas in serum it is in micro molar range[34]. Abnormal levels of uric acid in body fluids is a marker for several diseases. Excessive accumulation of uric acid can cause gout attacks, hyperuricemia and Lesch-Nyhan syndrome[33].

Despite significant development in electrochemical biosensors for single and/or multiplexed determination of biomarkers, direct determination in complex media and continuous operation in biological matrices remain an important challenge due to the occurrence of biofouling through non-specific adsorption of proteins and other biological materials such as cells, cell fragments, and DNA/RNA on the electrode surface[35]. Fouling of electrode surface during electrochemical detection can dramatically jeopardise the performance of the sensor[36]. Dopamine is a typical inner sphere redox marker involving surface adsorption, adsorbates will reduce the

electroactive surface area that prevents dopamine from making physical contact with the electrode surface for electron transfer kinetics resulting in diminishing transients[37]. In addition to this, as described in Section 1.7.1, electrochemical fouling arises from the oxidation of dopamine itself as its oxidation product, dopamine-*o*-quinone, is reactive to yield polydopamine that has a strong adhesion capability to practically all types of surfaces[3].

4.4 Addressing selectivity against interfering species

Several methodologies have been developed to simultaneously monitor dopamine in the presence of uric acid and ascorbic acid in a biological fluid using carbon-based electrodes[26, 38]. Chemically modified electrode is a conducting or semiconducting material that has been coated with a monomolecular, multi-molecular, ionic, or polymeric film that alters the electrochemical and other properties of the interface[39]. In addition to acting as an antifouling coating, and as a negatively charged polymer, Nafion is also often used to enhance the selectivity towards positively charged species. Several studies have reported the use of Nafion based electrochemical sensors for the detection of neurotransmitters *in vivo* or *in vitro*. For example, Vreeland *et al.*[40] immobilised a biocompatible Nafion and poly-3,4-ethylenedioxythiophene composite polymer on a carbon fibre microelectrode to achieve a mechanically stable, robust, and controllable electrode coating with selectivity and sensitivity for *in vivo* electrochemical measurements. In their work, by incorporating excess negatively charged Nafion in the positively charged, oxidised poly-3,4-ethylenedioxythiophene they have developed a more negatively charged polymer. They reported an improved dopamine sensitivity of 46 nA μM^{-1} (standard deviation 13 nA μM^{-1}) using the modified electrode compared to 13 nA μM^{-1} (standard deviation 2 nA μM^{-1}) using a

corresponding bare carbon fibre electrode[40]. In a separate study, Taylor *et al.*[16] also electro-polymerised 3,4-ethylenedioxythiophene on a carbon fibre electrode, followed by incorporation of negatively charged graphene oxide. By implanting the modified electrode in a mouse brain to detect dopamine, the authors reported a 5-fold increase in the sensitivity compared to that at a bare carbon fibre electrode. The improved performance of the fabricated electrode was attributed to the electrocatalytic activity and resistance to fouling of the 3,4-ethylenedioxythiophene / graphene oxide carbon fibre electrodes[16].

Graphene, an allotrope of carbon, has received immense interest amongst researchers for use in sensing surface modifications due to its excellent electronic conductivity[41], high mechanical strength, large specific surface area and stability[42-43]. Excellent electrocatalytic properties of graphene towards positively charged molecules is caused by an abundance of carboxyl functionalities with a strong electrostatic interaction. Several researchers have chemically modified electrode surfaces with graphene to enhance the selectivity of the analytes in biological samples. Targeted enhancements include improved selectivity, sensitivity, chemical and electrochemical stability, as well as a wide practical potential window and improved resistance to fouling[44]. For example, Kesavan *et al.*[45] modified a glassy carbon electrode using graphene by a two-step diazotisation protocol using melamine. Based on scanning electron microscopic results, the authors reported the presence of graphene layers on the modified electrode surface ascribed to π-π interaction between the graphene layers. This electrode was then used for simultaneous detection of theophylline and adenosine. Due to a better electrocatalytic activity of graphene, the authors reported 2.1 and 2.6-fold higher oxidation current for theophylline and adenosine, respectively. In another study, Wang *et al.*[46] reported the fabrication of three-dimensional porous

graphene modified glassy carbon electrode for the simultaneous detection of dopamine and uric acid in the presence of ascorbic acid. The electrode exhibited good linearity from 0.2 - 8.0 µM for dopamine and 1 - 60 µM for uric acid with 2.1 µA/µM and 0.29 µA/µM sensitivity for dopamine and uric acid, respectively. A limit of detection of 0.2 µM dopamine and 1 µM uric acid were achieved at this modified electrode.

The unique properties of carbon nanotubes such as high aspect ratio, high electrical conductivity, excellent chemical stability, high mechanical strength and large surface area have attracted a lot of attention in chemical biosensors[47-48]. Several researchers have applied carbon nanotubes to enhance selectivity, reduce undesired interferences, as well as for stable operation in complex media. Zhao and colleagues[33] grew carbon nanotubes on a carbon fibre electrode through chemical vapour deposition. The electrodes were applied to simultaneously detect ascorbic acid, dopamine and uric acid. They reported three well-defined peaks using differential pulse voltammetry at approximately -20 mV, 220 mV and 360 mV, corresponding to the oxidation of ascorbic acid, dopamine and uric acid. The authors suggested the selective detection of ascorbic acid, dopamine and uric acid might be due to the high density of oxygen containing groups on carbon nanotubes that provided a selective interface *via* hydrogen bonds with the proton donating of ascorbic acid, dopamine and uric acid, which aided in the catalysis of oxidation of the three analytes at the electrode surface. The π-π interaction between the carbon nanotubes and the analytes can also promote the charge transfer between the analytes and the electrode. According to the authors, the conducting loose structure on the carbon nanotube modified carbon fibre surface can alter the mass transport, such that the similar oxidation or reduction potentials of many species are resolved[33]. Similarly, Yang *et al.*[26] also modified a glassy carbon

electrodes using a single-walled carbon nanotube array to simultaneously detect dopamine, uric acid, and ascorbic acid. The authors reported well separated oxidation potentials of dopamine (~0.15 V) and uric acid (~0.3 V at acetone pre-treated electrodes. The authors explained that the acetone treated surface presented an increase in the surface roughness of the modified electrode availing more adsorption sites for oxidation[26]. The modified electrode exhibited a limit of detection of 0.19 µM for dopamine and 0.82 µM for uric acid.

Carbon nanofibres have shown similar mechanical strength and electric properties to carbon nanotubes and have been used for the simultaneous detection of dopamine, uric acid, and ascorbic acid. For example, Huang *et al.*[49] employed a palladium and carbon nanofibre modified carbon paste electrode for the simultaneous detection of dopamine, uric acid, and ascorbic acid at pH 4.5 with a corresponding peak-to-peak separation for ascorbic acid-dopamine, dopamine-uric acid, and uric acid-ascorbic acid of approximately 177 mV, 193 mV, and 370 mV. Yue and colleagues[50] also applied a tungsten disulfide nanosphere modified carbon nanofibre electrode for dopamine detection in the presence of uric acid. The authors reported that the modified electrode exhibited good selectivity towards dopamine with well separated oxidation peaks at ~0.16 V for dopamine and ~0.28 V for uric acid, as well as good reproducibility and stability. Improved sensitivity of 5.36 µA μM^{-1} cm^{-2} with limit of detection of 0.01 µM was observed for dopamine at the modified electrode compared to bare carbon nanofibre electrodes. The authors attributed the results to better electrocatalytic property arising from palladium nanoparticles and tungsten disulfide nanospheres that provided a large surface area for adsorption to facilitate oxidation of dopamine and uric acid[49-50].

In recent years, metal nanoparticles have also attracted a lot of attention in electroanalysis because of their unusual physical and chemical properties. Metal nanoparticle-modified electrodes usually display high electrocatalytic activities towards the compounds that have sluggish redox processes at bare electrodes. Savk *et al.*[51] selectively detected dopamine in the presence of ascorbic acid and uric acid using a multiwalled carbon nanotube/metal hybrid nanocomposite. The electrode surface characterisation results provided supporting evidence for excellent structural durability, pore channels and large surface area, which facilitated the mass transfer and electron conduction. In addition to this, the corresponding oxidation peak at +0.31 V, +0.50 V and +0.61 V for ascorbic acid, dopamine and uric acid was obtained using the fabricated sensor, indicating good peak-to-peak separation. The modified electrode displayed a limit of detection of 0.066 µM for dopamine and 0.088 µM for uric acid[51]. Murali *et al.*[52] reported the simultaneous detection of dopamine and ascorbic acid using a cerium oxide/reduced graphene oxide nanocomposite modified glassy carbon electrode and obtained a limit of detection of 2 µM dopamine and 10 µM ascorbic acid. The enhanced electrochemical property of the cerium oxide/reduced graphene oxide - glassy carbon electrode was attributed to introduction of oxygen vacancies *via* reduced graphene oxide, which resulted in the overall improvement of the conductivity, thereby leading to faster charge transfer[52]. Ma and colleagues[53] also immobilised a nanocomposite consisting of platinum-nickel bimetallic nanoparticle loaded molybdenum disulfide nanosheets on a glassy carbon electrode for the simultaneous detection of dopamine and uric acid. Improved electrocatalytic activity towards dopamine and uric acid at this electrode was attributable to the synergistic electrocatalytic effect of platinum-nickel nanoparticles and molybdenum disulfide sheets. The authors evaluated the selectivity of the electrode towards dopamine and uric acid using differential pulse voltammetry.

Accordingly, well separated dopamine peak at 0.15 V and uric acid peak at 0.30 V, with a limit of detection of 0.1 µM (*S/N* =3) for both dopamine and uric acid were obtained[53]. Recently, Immanuel *et al*.[38] developed a gold-silicon dioxide nanocomposite modified glassy carbon electrode to simultaneously monitor dopamine in the presence of uric acid. They estimated a limit of detection of 1.98 µM dopamine and 2.58 µM uric acid. In simultaneously determining dopamine and uric acid, the authors reported a peak-to-peak separation of 215 mV.

Graphene composites in combination with metals have also been reported due to their excellent catalytic performance. Xu *et al.*[54] employed a nanostructured platinum/reduced graphene oxide modified glassy carbon electrode to simultaneously monitor dopamine and uric acid and obtained a detection limit of 0.25 µM for dopamine and 0.45 µM for uric acid, while the oxidation of ascorbic acid was restrained. Similarly, Palanisamy *et al.*[55] fabricated spindle-like palladium nanostructures on a graphene oxide-cellulose microfibre composite. This sensor exhibited a 23 nM detection limit and a 0.3 - 196.3 µM linear dopamine response range. Enhanced selectivity towards dopamine in the presence of interfering hydroquinone, catechol, epinephrine, ascorbic acid and uric acid was attributed to the strong electrostatic interaction between dopamine and the metallic nanocomposite on the electrode surface. Metal nanocomposites are of great significance due to their catalytic, chemical magnetic and electrochemical properties which paves the way for a tailor-made synthesis towards specific application.

4.5 Minimising electrochemical and biofouling

As discussed in Chapter 3, an important challenge during detection of neurotransmitters is the occurrence of electrode fouling on conventional electrodes. Several

methodologies have been developed to minimise electrode fouling. For example, Harreiether *et al.*[56] evaluated the electrochemical properties and resistance to dopamine fouling of carbon nanotube fibre electrodes and carbon fibre electrodes using amperometry. The fouling resistance evaluated from the time required for the current to decrease by 50% at carbon nanotube fibre electrodes was found to be up to three times higher than that at conventional carbon fibre electrodes. Recently, the same group further investigated the electrochemical fouling of carbon nanotube fibre electrodes and carbon fibre electrodes by albumin[36]. The severity of fouling was assessed by tracking the slow decrease in the amperometric current as the insulating film formed and grew on the electrode surface. Their findings showed that albumin and other sulfur containing thiol moieties reduce the impact of dopamine fouling where sulfur competes with the amine moiety for the nucleophilic binding to the oxidised catechol, which is a critical step that initiates dopamine fouling[36].

Parviz *et al.*[57] assessed the ability of three phenyl phosphocholine based gold electrodes, (i) phenyl phosphocholine diazonium salt, (ii) dithiocarbonate phenyl phosphocholine self-assembled monolayers and (iii) lipoamide phenyl phosphocholine self-assembled monolayers, in limiting nonspecific adsorption of proteins to an electrode surface. Protein adsorption was evaluated using electrochemical impedance spectroscopy after being incubated in bovine serum albumin for 1 h. The authors reported charge transfer resistance of 734.7 Ω cm^2 at the lipoamide phenyl phosphocholine adsorbed, which was considered to be similar to 710.8 Ω cm^2 at a phenyl phosphocholine adsorbed electrode.

Song *et al.*[58] reported the antifouling properties of a poly(3,4-ethylenedioxythiophene) / insoluble ionic liquid modified glassy carbon electrode in the real-life serum samples. The antifouling characteristics were evaluated by various methods including

electrochemical impedance spectroscopy, scanning electron microscopy and confocal fluorescence. Accordingly, the charge transfer resistance at the unmodified glassy carbon electrode estimated by electrochemical impedance spectroscopy has substantially increased from 242 Ω before to 1407 Ω after incubation in human serum samples for 30 min, indicative of non-specific adsorption of proteins from the serum on the electrode. On the other hand, a corresponding charge transfer resistance of 108.3 Ω before and 107.9 Ω after incubation were estimated at a modified electrode, which shows that this coating prevents non-specific adsorption. Typically, it is hydrophilicity and uncharged surface of the modified electrode that have apparently contributed to non-specific adsorption of proteins. The modified electrode exhibited a limit of detection of 33 nM of dopamine in the presence of high concentration (20 mg mL^{-1}) of proteins.

4.6 Scope of this study

A substantial amount of research has focused on minimising fouling during the detection of dopamine. Researchers have used various strategies to improve the antifouling properties of electrochemical sensors, as well as the selectivity of the analyte of interest. For example, Peltola *et al.*[3] examined the electrochemical fouling from dopamine oxidation product on three different carbon materials, amorphous carb, tetrahedral amorphous carbon, and pyrolytic carbon. The authors reported that a dopamine fouled surface can be recovered by 10-20 cycles in 0.15 M H_2SO_4 except pyrolytic carbon. On the other hand, several studies reported the application of modified electrode surfaces to improve the selectivity of the analyte of interest. An electrochemically reduced graphene oxide-poly(eriochrome black T) / gold nanoparticle modified glassy carbon electrode was used in the simultaneous

measurement of ascorbic acid, dopamine, and uric acid[59]. There has been a significant progress in the development and characterisation of diamond electrodes and their application to analysis in biological samples[60-61]. Compared to many carbon-based electrodes (*e.g*. glassy carbon), diamond electrodes generally exhibit superior performance for many different reactions under most conditions, and are therefore preferred for measurements in biologically fouling environments[62-65]. This is mainly due to the presence of sp^3 hybridised carbon that makes the surface hydrophobic. This property of diamond electrodes prevents non-specific adsorption during *in vivo* studies. One way to convert the sp^2 carbon on a carbon electrode surface to sp^3 carbon is through hydrogenation. Interestingly, this can be achieved at room temperature in a one-pot reaction reported by McRae's group[66-67]. A schematic illustration (Scheme 4.1) shows the fouling on a bare carbon surface versus fouling of a hydrogenated carbon surface.

In Chapter 3, we reported the electrochemical and spectroscopic characterisation of triethylsilane hydrogenated and phenylsilane hydrogenated electrodes. In this Chapter, the antifouling properties of the fabricated electrodes will be evaluated by deliberately incubating them in a laboratory synthetic fouling solution for a defined period. Next, the analytical performance of the electrodes will be evaluated. We will also report the detection of dopamine at hydrogenated carbon electrodes in the presence of uric acid and ascorbic acid.

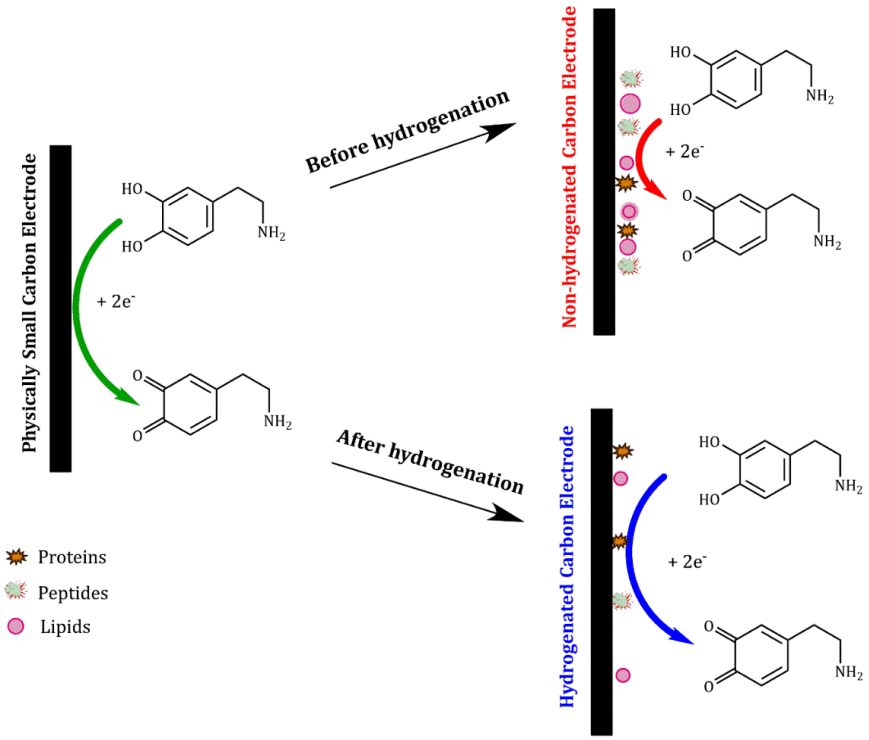

Scheme 4.1. Antifouling behaviour of the bare conical-tip carbon electrode and hydrogenated carbon electrodes.

4.7 Experimental

4.7.1 Chemicals and reagents

A list of all chemical and reagents used in this work was presented in Section 2.2.

4.7.2 Electrode fabrication and hydrogenation

Structurally small carbon electrodes were fabricated and hydrogenated using the procedure outlined in Section 2.3 and Section 2.4.

4.7.3 Instrumentation

The instrumentation used to characterise the fabricated electrode was as described in Section 2.5.

4.7.4 Atomic force microscopy

Surface morphology and roughness of hydrogenated carbon electrodes were determined using a Dimension ICON (Bruker Corp.) microscope, equipped with Quantitative nanomechanical mapping mode in Air, silicon Tip on Nitride Lever SCANASYST-Air spring constant 0.4 N m^{-1} and frequency 70 kHz was used. NanoScope Analysis software was applied for scan evaluation. The mean roughness value (R_a) represents the arithmetic average of the deviation from the centre plane of the sample.

4.7.5 *In vitro* fouling experiment

A laboratory synthetic fouling solution containing 2.0% (w/v) bovine serum albumin, 0.01% caproic acid (v/v), 0.05% (w/v) cytochrome *c* and 0.001% (w/v) human fibrinopeptide was prepared in a pH 7.4 citrate/phosphate buffer. The antifouling properties of the hydrogenated electrode were evaluated after incubating them in the laboratory synthetic fouling for a defined time.

4.8 Results and discussion

4.8.1 Surface characterisation using atomic force microscopy

Surface characteristics including (i) surface roughness and (ii) hydrophobicity have been demonstrated[68] to exhibit a direct impact on the adsorption of biomolecules on a sensor. In general, a smooth surface was reportedly unfavourable to biomolecules adsorption[69-70]. Well-faceted microcrystallites on diamond films are H-terminated and they give rise to a hydrophobic surface that is nonpolar and inert for adsorption of amphiphilic compounds present in biological samples. For example, in comparing the fouling resistance towards bovine serum albumin at three different carbon materials namely glassy carbon, diamond-like carbon and nano-carbon, Xue *et al.*[71] demonstrated that a smooth, hydrophobic nano-carbon exhibited 71.7% improved resistance towards bovine serum albumin fouling compared to diamond-like carbon (68.6%) and glassy carbon (55%). In this work, the surface morphology of hydrogenated carbon electrode was initially examined by the atomic force microscopy and the micrographs obtained are depicted in Figure 4.1. Notably, hydrogenation using silane resulted in a smooth carbon surface covered with structures of approximately 50 nm in size. Surface roughness also influences electrochemical properties. Previously, our group reported that there was a decrease in the surface roughness after *n*-butylsilane hydrogenation[72]. Nano-diamond films have been reported to be an intermediate between microcrystalline diamond and amorphous diamond-like carbon[73]. In addition to this, according to Yang *et al*.[68]dopamine-*o*-quinone desorbed from a smoother electrode surface can easily diffuse away, while that desorbed from a rough surface would remain close to the surface, allowing it to re-adsorb to generate a similar response to that in a thin layer cell. Dopamine and dopamine-*o*-quinone are more like to get trapped in a rough surface

leading to a reduction current of similar magnitude to oxidation current. Additionally, the response would be similar to that in a thin layer cell, where the dopamine-*o*-quinone would remain close to the surface even if it desorbs and thus could easily adsorb again.

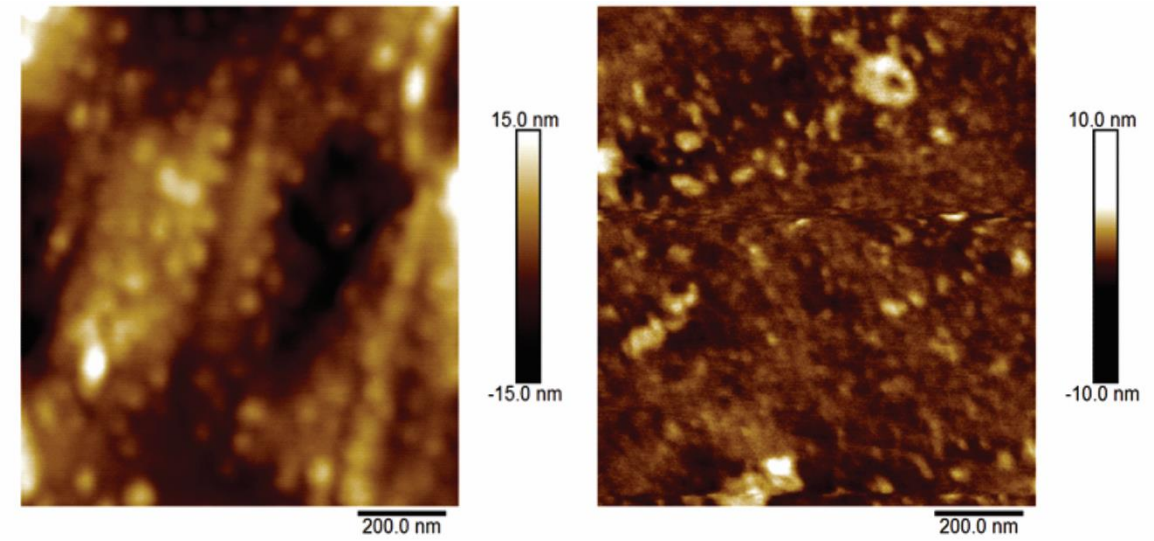

Figure 4.1. Atomic force micrograph of a triethylsilane hydrogenated carbon electrodes.

4.8.2 Cyclic voltammetry of dopamine

To investigate the electroanalytical performance, the cyclic voltammetric response of 1.0 mM dopamine was initially conducted from -0.2 V to +0.6 V at 100 mV s^{-1} and a representative cyclic voltammogram obtained at a non-hydrogenated carbon electrode is presented in Figure 4.2. Similarly, the response of hydrogenated electrodes to dopamine was also assessed and only electrodes that exhibited sigmoidal shaped voltammograms such as that shown in Figure 4.2 were used to further determine the electroanalytical characteristics.

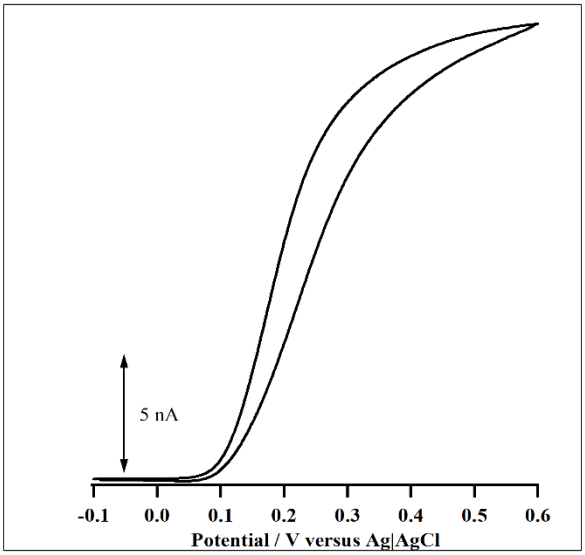

Figure 4.2. Representative cyclic voltammograms of 1.0 mM dopamine in pH 7.4 citrate/phosphate at a non-hydrogenated small carbon electrode. Scan rate 100 mV s^{-1}.

4.8.3 Electroanalytical performance of the small carbon electrodes

The electroanalytical performance of the non-hydrogenated and hydrogenated carbon electrodes was then evaluated by differential pulse voltammetry of dopamine in pH 7.4 citrate/phosphate buffer. In this experiment, voltammograms were obtained in dopamine solutions of increasing concentration from 0 to 10 µM and they are depicted in Figure 4.3 (A), (C) and (E). The oxidation peak current in these voltammograms was then used to construct a calibration plot shown in Figure 4.3 (B), (D) and (F). Using a two-sided *t*-test, the correlation coefficient was found to be statistically significant at the 95% confidence interval. In addition to this, based on the Wald-Wolfowitz runs test, the ordinate residuals of the calibration data were randomly distributed, supporting a satisfactory straight-line fit to the data.

Accordingly, based on a signal-to-noise ratio of 3, the respective limit of detection estimated at hydrogenated carbon electrodes by both the triethylsilane reduction and

phenylsilane reduction are presented in Table 4.1, together with those of other electrodes to facilitate comparison. The indicated errors represent the 95% confidence intervals. Both the hydrogenated carbon electrodes showed an improved limit of detection and sensitivity compared to 2.23 ± 0.99 μM and 3.24 ± 1.16 pA μM^{-1} at non-hydrogenated counterparts. This is highly relevant as we are approaching the physiological concentration of dopamine at ~0.01–1 μM in extracellular fluid[74]. There was a significant difference in the limit of detection and sensitivity between the two hydrogenated electrodes, however, higher sensitivity was obtained at phenylsilane hydrogenated carbon electrodes. We attribute the lower sensitivity at the triethylsilane hydrogenated carbon electrodes to the possible alteration in electrostatic interactions between dopamine and the hydrogenated or non-hydrogenated carbon electrode surface. Notably, there is enhanced attraction of dopamine towards the non-hydrogenated carbon electrode with carbonyl and quinone groups at the surface. Upon hydrogenation, these oxygen-containing functional groups were converted to C—H bonds, leading to a reduction of anionic sites on the hydrogenated electrode surface. Therefore, reduced electrostatic attraction existed between dopamine and the hydrogenated carbon surfaces, leading to reduced sensitivity for dopamine at these electrodes. The oxidation of dopamine at the carbon microelectrode is shown to involve the adsorption of both the reactant and product of the electrode reaction[75]. DuVall and McCreery's[76] work demonstrated that the electron transfer kinetics of catechols and hydroquinones strongly correlate with adsorption on glassy carbon electrode[76]. Thus, higher sensitivity at phenylsilane hydrogenated electrode is attributed to the presence of phenyl rings which provided more adsorption sites for dopamine oxidation.

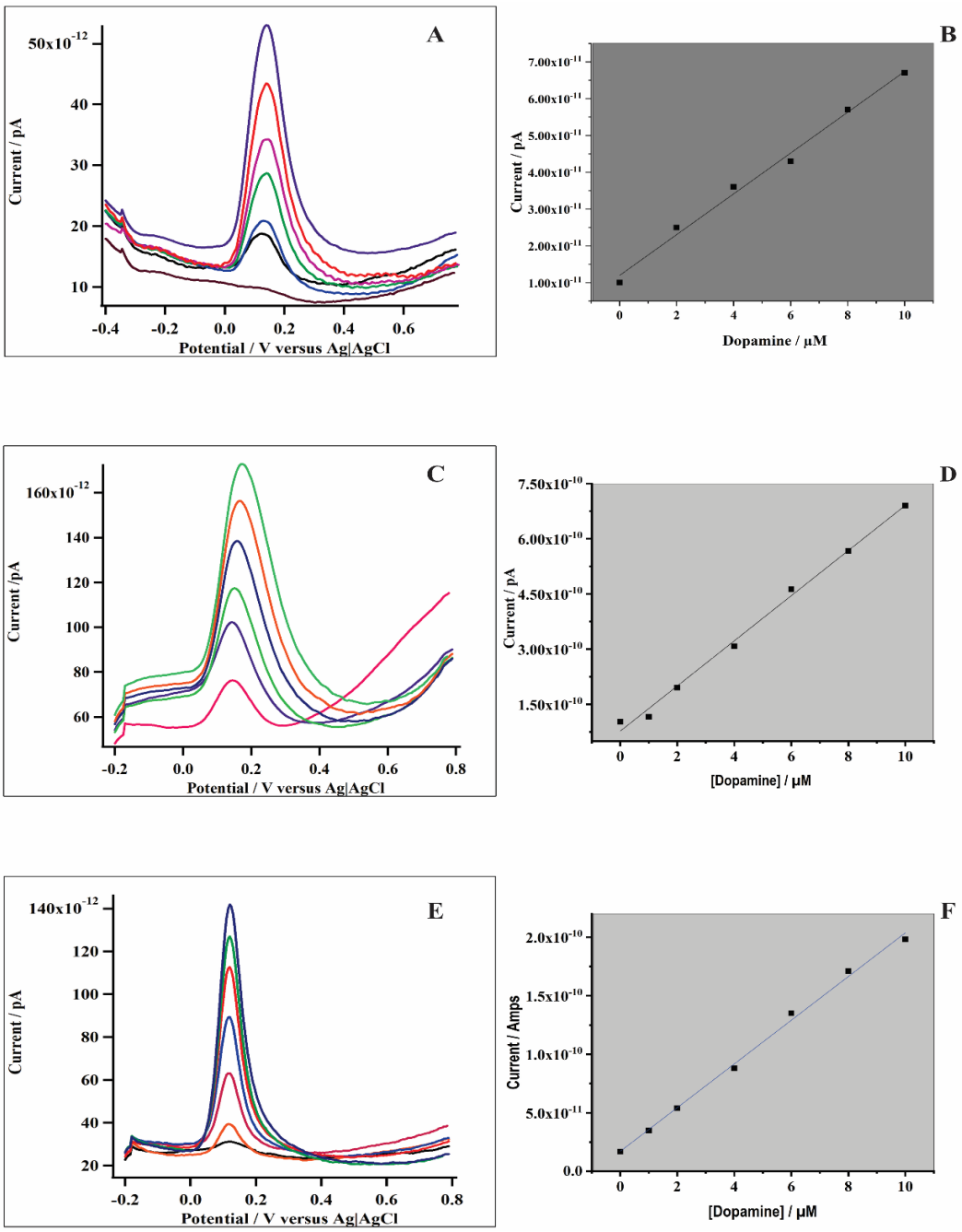

Figure 4.3. Differential pulse voltammetric response to dopamine with (A, C, E) different concentration of dopamine in pH 7.4 citrate/phosphate buffer and (B,D,F) a dopamine calibration plot obtained for (A) a non-hydrogenated, (B) triethylsilane and (C) phenylsilane hydrogenated carbon electrode, respectively. Scan rate 20 mV s^{-1} .

Table 4.1. Limit of detection and sensitivity of dopamine using different electrode types.

Electrode	Limit of detection / µM	Sensitivity / pA µM^{-1}	Reference
Triethylsilane hydrogenated carbon electrodes	0.84	23.15 ± 12.88	This work
Phenylsilane hydrogenated carbon electrodes	0.83	42.89 ± 22.69	This work
Tetrahedral-amorphous carbon-carboxyl functionalised zeta-	0.5	1.95×10^{13}	[77]
Tetrahedral-amorphous carbon-zeta positive hydrogenated	0.05	2.48×10^{13}	[77]
CeO_2/reduced graphene oxide – glassy carbon electrode	2.0		[52]

4.8.4 Evaluating dopamine selectivity of the hydrogenated carbon electrodes

Selectivity is an important requirement in developing an electrochemical sensor for use in detecting analytes present in the extracellular matrix, particularly with analytes that have very similar oxidation/reduction potentials. Measuring the levels of chemicals in a brain using a highly selective sensor will enable the analyst to appropriately discriminate the signal, which is otherwise difficult at a non-selective sensor. In this study, the selectivity of the fabricated electrodes was evaluated by detecting dopamine in the presence of ascorbic acid, uric acid, and serotonin.

4.8.4.1 Selectivity towards dopamine in the presence of ascorbic acid

A major problem encountered during simultaneous detection of dopamine and ascorbic acid is that both can be oxidised at very similar potential (~0.2 V versus Ag|AgCl) at most solid electrodes, causing an overlapping of voltammetric responses. To investigate the effects of interfering ascorbic acid at a triethylsilane hydrogenated carbon electrodes, cyclic voltammetry in 1.0 mM dopamine and 1.0 mM ascorbic acid was initially separately conducted and the results are presented in Figure 4.4. For brevity, only representative results obtained at triethylsilane hydrogenated electrodes are displayed. Here, the ascorbic acid oxidation response appears to be suppressed, compared to the dopamine oxidation response at the triethylsilane hydrogenated carbon electrode. This suppression in the ascorbic acid oxidation signal could possibly be due to the presence of low surface oxides and the hydrophobic nature of the hydrogenated carbon surface. Qui *et al.*[78] reported that improving the hydrophilicity allows the ascorbic acid molecules to easily diffuse and contact the carbon electrocatalyst. The effect of ascorbic acid on oxidation of dopamine at both triethylsilane and phenylsilane hydrogenated electrodes was also studied. Twenty consecutive cyclic voltammetric scans of 100 µM dopamine and 100 µM ascorbic acid are shown in Figure 4.5. No noticeable change was observed in the I_{lim} of dopamine indicating limited effect from ascorbic acid. An H-terminated surface would therefore repel ascorbic acid and only allow dopamine adsorption *via* π-π interaction. On the other hand, ascorbic acid oxidation is also an inner-sphere reaction and the electron transfer kinetics is sensitive to the electrode surface properties[79-80]. Jeong and Jeon[81] used a Nafion and single-walled carbon nanotube modified carbon fibre microelectrode to simultaneously detect dopamine and ascorbic acid. The authors reported that ascorbic acid exerted no effect on the determination of dopamine when the ascorbic acid concentration is 100 times higher than that of dopamine and the modified

electrode exhibited a limit of detection of 17 nM dopamine. The authors concluded that the negatively charged Nafion electrostatically attracted positively charged dopamine but repelled negatively charged ascorbic acid. On the other hand, the oxidation of ascorbic acid on a boron-doped diamond electrode occurs at +0.48 V (versus Ag|AgCl|KCl_{sat}) with sluggish electron transfer kinetics[82]. Indeed, compared to the oxidation of dopamine (Figure 4.4 trace (a)) at the same electrode, the oxidation of ascorbic acid (Figure 4.4 trace (b)) shows sluggish kinetic at the triethylsilane hydrogenated carbon electrode in our work. Similar results were also obtained at phenylsilane hydrogenated carbon electrodes. The results are consistent with that obtained using boron-doped diamond electrode. Based on oxidation of dopamine and ascorbic acid, Jiang and co-workers also reported that unmodified boron-doped diamond electrodes have higher selectivity towards dopamine oxidation than ascorbic acid oxidation[83].

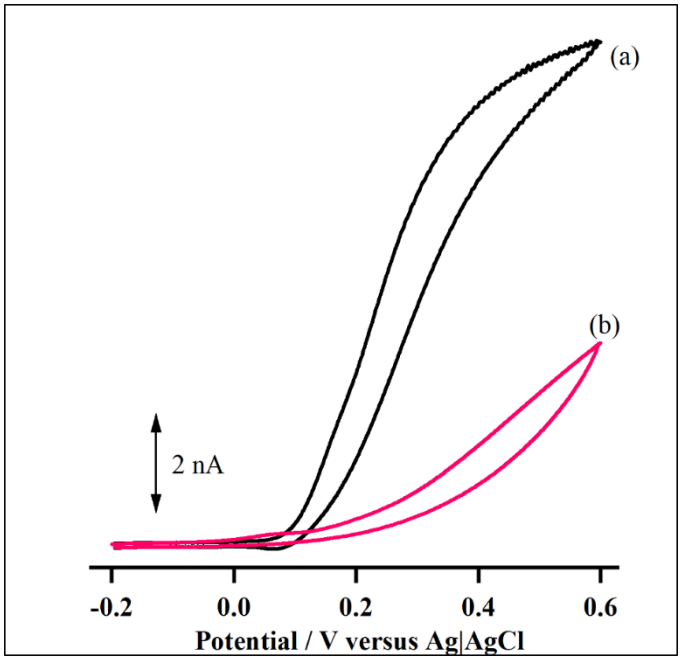

Figure 4.4. Response of a triethylsilane hydrogenated electrode in (a) 1.0 mM dopamine and (b) 1.0 mM ascorbic acid in pH 7.4 citrate/phosphate buffer. Scan rate 100 mV s^{-1}.

Another effect of ascorbic acid during dopamine detection is interference based on regeneration of dopamine from its oxidation product by a solution phase reaction with ascorbic acid. Next, the effects of ascorbic acid on dopamine response was investigated in 100 µM ascorbic acid. Figure 4.5 shows twenty repetitive cyclic voltammograms obtained at a triethylsilane hydrogenated carbon electrode in 100 µM dopamine in the presence of 100 µM ascorbic acid (pH 7.4 citrate/phosphate supporting electrolyte). No obvious change in the limiting current was observed, indicating that ascorbic acid has little to no effect on oxidation of dopamine, most likely due to repulsion of ascorbic acid by the H-terminated electrode while promoting dopamine oxidation.

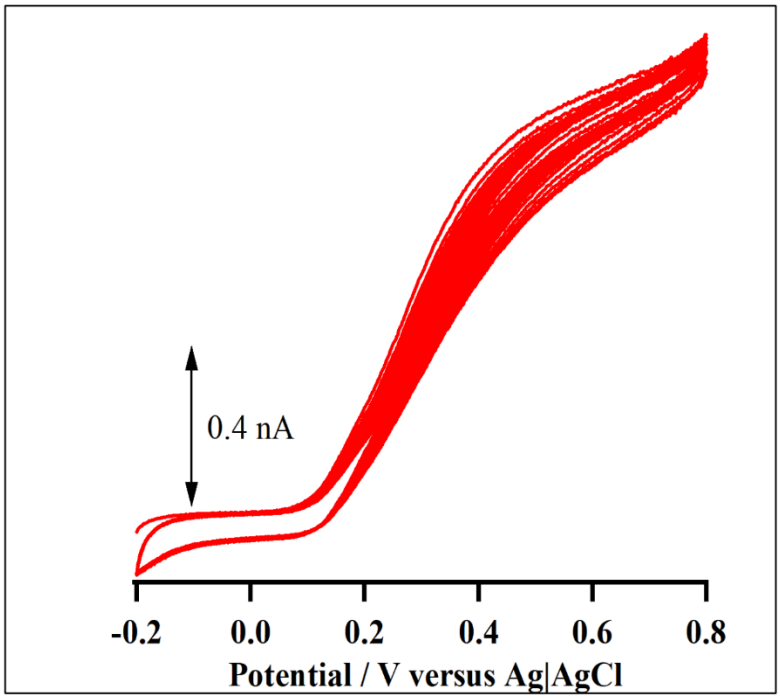

Figure 4.5. Twenty repetitive cyclic voltammograms in 100 µM ascorbic acid and 100 µM dopamine in pH 7.4 citrate/phosphate buffer. Scan rate 100 mV s^{-1}.

4.8.4.2 Selectivity of dopamine in the presence of uric acid

Uric acid is another interfering compound during dopamine detection as it can also be easily oxidised at a potential close to that of dopamine[49]. Uric acid generally shows sluggish electron transfers at conventional carbon electrodes[84]. Selectivity towards dopamine oxidation at hydrogenated carbon electrodes was next investigated in the presence of uric acid. Figure 4.6 (A) shows the differential pulse voltammograms obtained in dopamine alone with a peak potential at ~0.20 V and uric acid alone (Figure 4.6 (B)) at peak potential at ~0.48 V. These oxidation peak potentials are similar to ~0.28 V and ~0.39 V observed at a gold-silica dioxide modified glassy carbon electrode[38]. As shown in Figure 4.6 (C), the dopamine oxidation peak current increased with increasing concentrations of uric acid, but the dopamine oxidation potential essentially remained unchanged. By keeping the uric acid concentration constant at 50 μM, the peak current of dopamine was plotted against dopamine concentration (shown in the inset of Figure 4.3 (C and D)), a linear calibration plot (supported by the statistical significance of the correlation coefficient at the 95% confidence level and also the result of a Wald-Wolfowitz runs test), which can be expressed by $I_{peak}=(6.13 \pm 0.52) \times 10^{-11} C_{dopamine} + (7.73 \pm 2.95) \times 10^{-11}$, R=0.993; N=9 is obtained. Similarly, Figure 4.6 (D) shows a series of differential pulse voltammograms of uric acid in increasing concentration of dopamine. An oxidation peak at +0.48 V corresponding to the oxidation of uric acid is observed in these voltammograms. As depicted by the insert in Figure 4.6 (D), by keeping the dopamine concentration constant, the uric acid peak current increased linearly with increasing concentration ($I_{peak}=(0.022 \pm 0.006) \times 10^{-9} C_{uric\ acid} + (0.36 \pm 0.03) \times 10^{-9}$, R=0.989; N=8). From these results, the presence of uric acid did not appear to have significantly affected the oxidation of dopamine on the hydrogenated carbon electrodes. Albeit good selectivity towards uric acid, compensated sensitivity is noticeable in these

results too. The lower sensitivity towards uric acid than dopamine is also noticeable. With a pKa of 5.50, uric acid is expected to be a charge neutral within the pH ca. 7 solutions, while with a pKa of 8.9 dopamine exists as a cation at pH 7. This results in weak interaction between uric acid and the electrode interface.

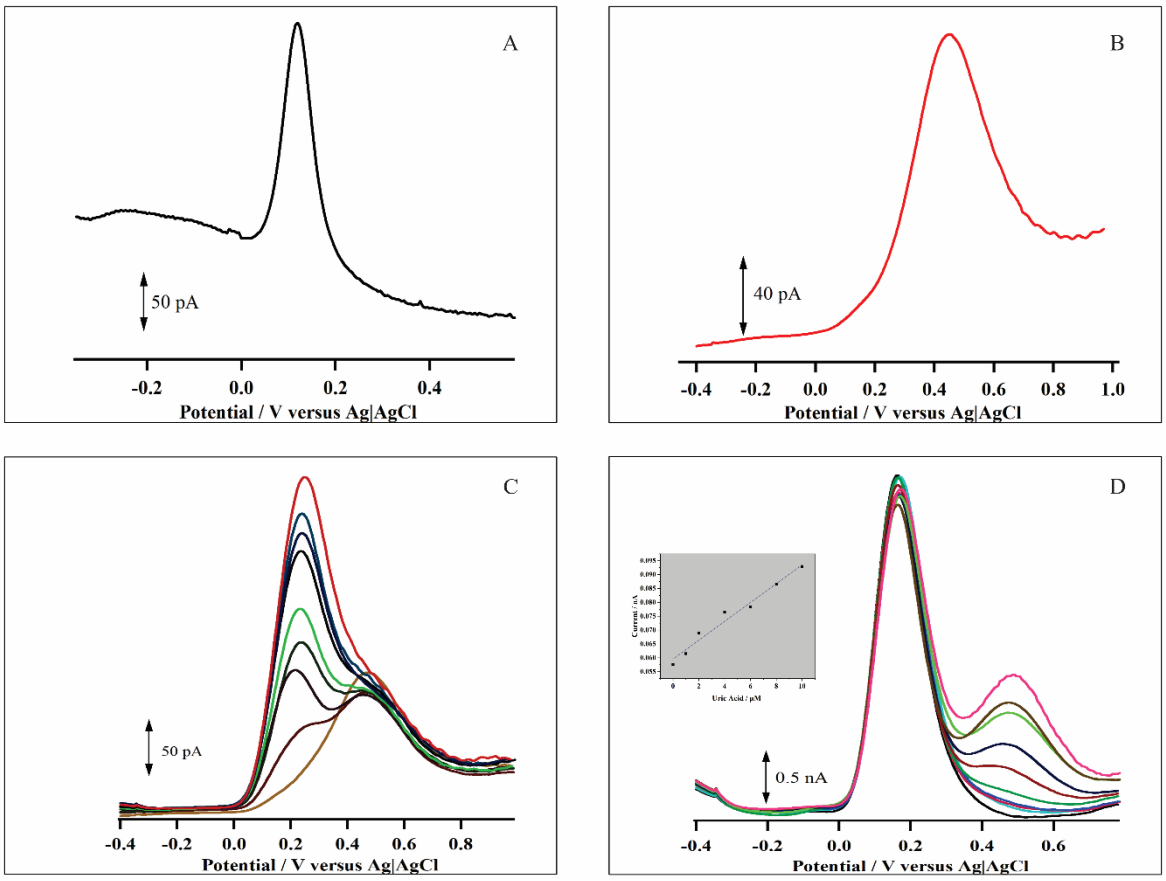

Figure 4.6. Differential pulse voltammograms obtained in (A) 1 µM dopamine, (B) 10 µM uric acid, (C) increasing concentration of dopamine in 50 µM uric acid and (D) increasing concentration of uric acid in 100 µM dopamine at a triethylsilane hydrogenated carbon electrode. Scan rate 20 mV s^{-1}.

.

4.8.5 Assessment of biofouling and electrochemical fouling at hydrogenated electrodes

The applications of biosensors to the analysis of complex samples are limited by their fouling properties due to no-specific adsorption of materials present in the biological matrix on the sensing surfaces. Therefore, eliminating or minimising this non-specific adsorption on a sensing surfaces is a great challenge in sensor development for analyte detection in biological samples[85].

4.8.5.1 Biofouling

Biofouling arises from non-specific adsorption and adhesion of biomolecules such as high molecular weight proteins, peptides, and lipids. This phenomenon hampers the selectivity of electrochemical sensors and deteriorates signal-to-noise (S/N) ratios over time[71]. In our work, the adsorption of high molecular weight compounds on carbon electrodes was evaluated after incubating them in a laboratory synthetic fouling solution containing 2.0% (w/v) bovine serum albumin (a protein), 0.01% (w/v) cytochrome *c* (a protein), 0.001% (w/v) human fibrinopeptide (a peptide) and 1.0% (v/v) caproic acid (a lipid) for a defined period. Voltammetric current of 1.0 mM dopamine was then measured at the electrodes prior to and after incubating them in the fouling solution in order to estimate the degree of fouling. Cyclic voltammetric responses of 1.0 mM dopamine at a non-hydrogenated carbon electrode before and after incubating in the fouling solution for 30 min are illustrated in Figure 4.8.

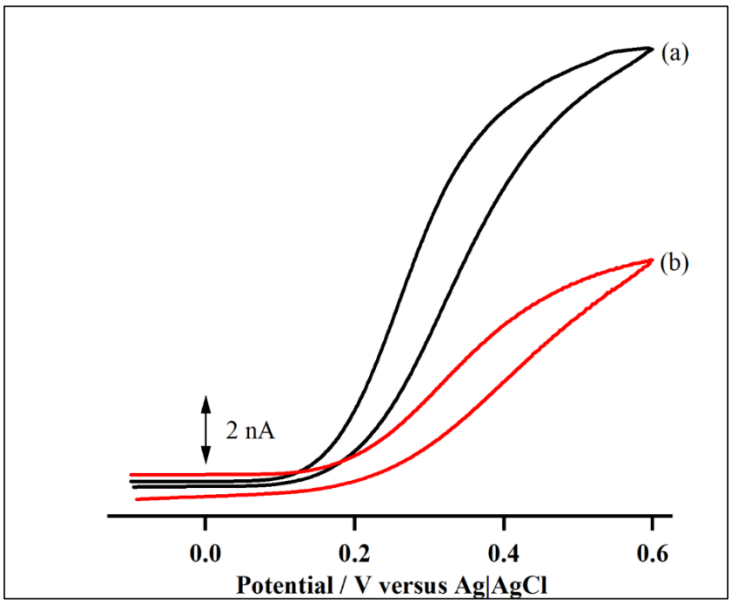

Figure 4.7. Cyclic voltammogram of 1.0 mM dopamine at a non-hydrogenated electrode in pH 7.4 citrate/phosphate buffer (a) before incubation in the laboratory synthetic fouling solution and (b) after the electrode was incubated in the fouling solution for 30 min. Scan rate 100 mV s^{-1}.

These electrodes (Figure 4.7 trace (b)) show a 53% $\pm$ 5.7% (95% confidence interval; N=10) decline in the limiting current. This is in good agreement with 58% obtained at a bare glassy carbon electrode with adsorbed protein[86]. Similarly, Singh *et al.*[87] reported a 25% - 40% reduction in current response after incubating bare carbon fibre microelectrodes in bovine serum albumin for 2 h or overnight. They also reported an even larger 60% - 70% reduction in the electrode sensitivity after incubating them in brain tissues. Nonetheless, the electrodes showed no further noticeable difference in the percentage of current drop after incubating them in brain tissues for 12 h, suggesting that most of the biofouling occurs early in the time course of electrode incubation in tissues. Therefore, it may be challenging in applying such electrodes for long term neurotransmitter monitoring in a biological environment.

It is important to determine the response of dopamine at the hydrogenated carbon electrodes after being incubated in the fouling solution. Similar to the non-hydrogenated carbon electrodes, hydrogenated carbon electrodes were also incubated in the fouling solution and the degree of fouling was determined by comparing the I_{lim} before and after incubation in 1.0 mM dopamine (in pH 7.4 citrate/phosphate buffer). Cyclic voltammograms of 1.0 mM dopamine at hydrogenated carbon electrodes before and after incubation in the fouling solution are depicted in Figure 4.8. From Figure 4.8 (A), after triethylsilane hydrogenated electrodes were incubated in the laboratory synthetic fouling solution for 30 min, there was a 23% $\pm$ 4.4% (95% confidence interval N=15) reduction in I_{lim} of dopamine oxidation. Compared to phenylsilane hydrogenated electrodes as shown in Figure 4.8 (B), only 18% (95% confidence interval; N=10) reduction in I_{lim} of dopamine oxidation is observed. After a 1-week incubation in the fouling solution, no noticeable difference in I_{lim} was observed in either of the hydrogenated carbon electrodes compared to a 30% decline in I_{lim} at a physically small carbon electrode hydrogenated by a radio frequency plasma-enhanced chemical vapour method, after being treated in a similar fouling solution for 30 min[88]. A graphical summary of percentage change in I_{lim} after incubating hydrogenated carbon electrodes for 30 min and 1-week in the laboratory synthetic fouling solution is shown in Figure 4.9. In this Figure, there was no significant difference in the change in I_{lim} between triethylsilane and phenylsilane hydrogenated carbon electrodes, although phenylsilane hydrogenated carbon electrodes showed more improved resistance towards fouling than the triethylsilane hydrogenated carbon electrodes. Our results are in good agreement with those obtained at boron-doped diamond electrodes. For example, after the 10th scan during oxidation of ascorbic acid in the presence of bovine serum albumin, Shin *et al.*[89] reported 18.3% and 47.8% decline in the ascorbic acid

peak current at boron doped diamond electrode and a glassy carbon electrode, respectively.

Fouling of electrodes caused by adsorption of biological materials on sensing surfaces, in addition to decreasing sensitivity, can lead to slower diffusion of analytes to a sensor surface-and/or slower electron transfer kinetics, an effect that is reflected in increased $E_{½}$. This is supported by a positive shift in $E_{½}$ from 346 mV (trace (a) in Figure 4.8 (A)) at triethylsilane hydrogenated carbon electrodes to 378 mV (trace (b) in Figure 4.8 (b and c)) after a 30-min incubation in the fouling solution, indicating more sluggish kinetics. In contrast, in Figure 4.8 (B) (trace (b and c)) at phenylsilane hydrogenated carbon electrodes, there was no noticeable shifts in the $E_{½}$ after a 30-min or a 1-week incubation in the fouling solution.

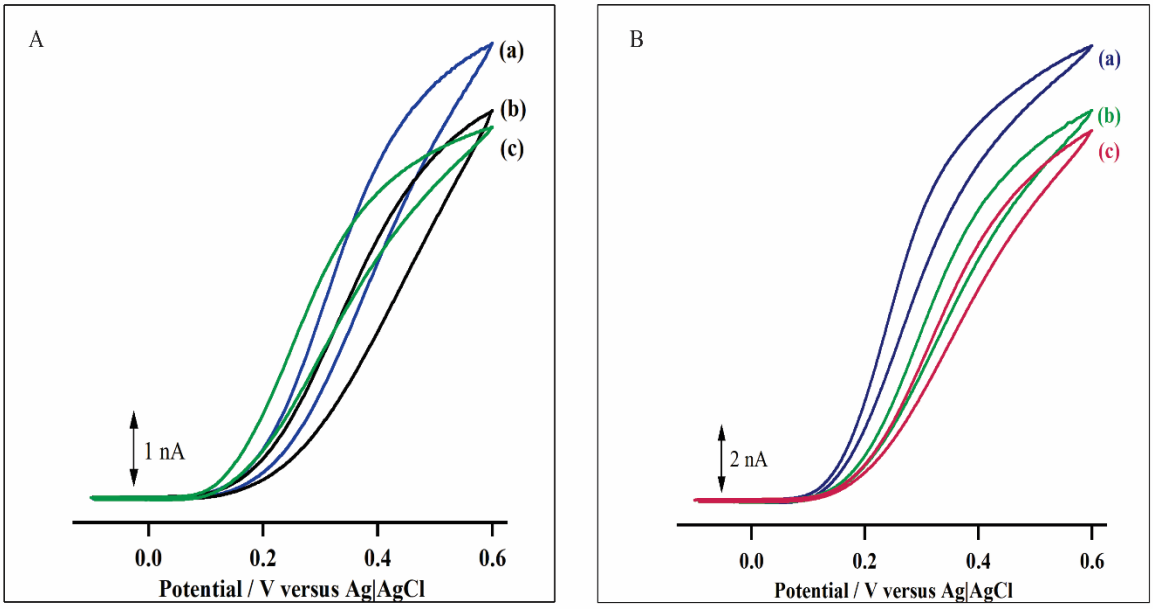

Figure 4.8. Cyclic voltammetry of 1.0 mM dopamine at (A) a triethylsilane hydrogenated carbon electrode and (B) a phenylsilane hydrogenated carbon electrode; trace (a) before trace (b) after incubation in the fouling solution for 30 min; trace (c) after incubation in the fouling solution for 1 week. Scan rate 100 mV s^{-1}.

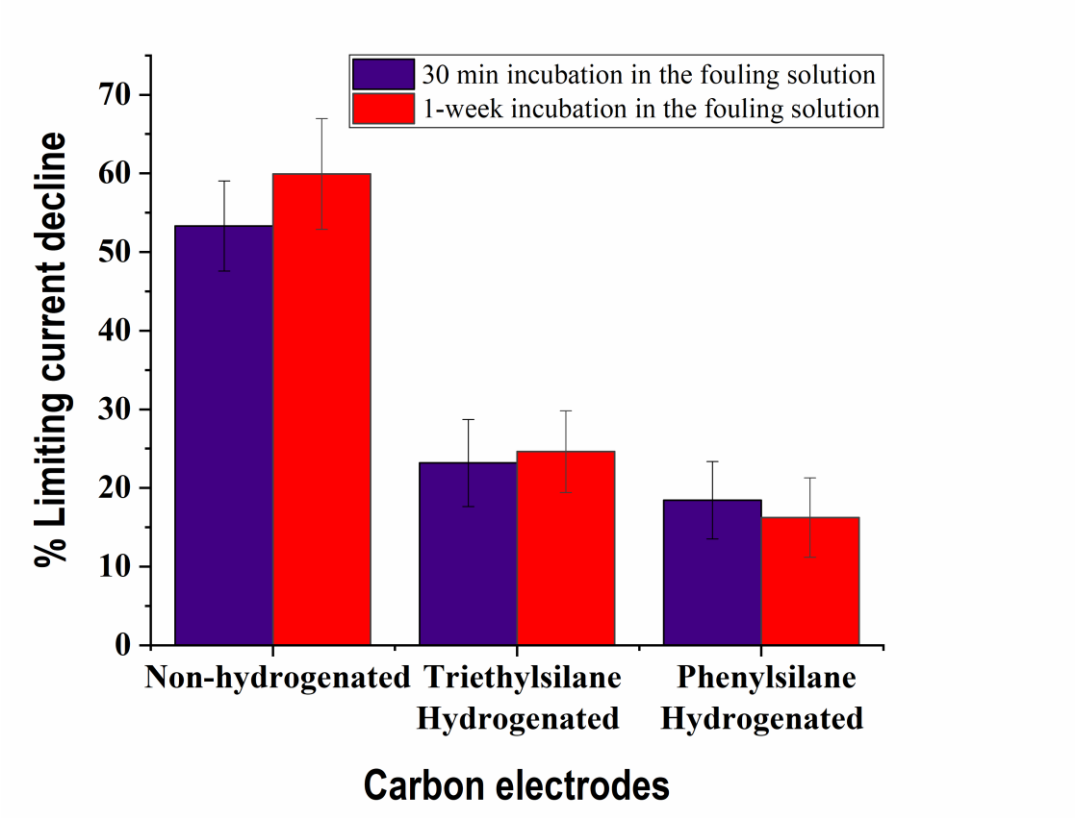

Figure 4.9. Percentage change in dopamine I_{lim} at carbon following a 30-min and 1-week incubation in a laboratory synthetic solution. The uncertainty represents 95% confidence interval.

4.8.5.1 Electrochemical fouling

Adsorption is particularly important in the electrochemical reactions of organic compounds especially on carbon-based electrodes. The degree of dopamine adsorption on carbon electrodes seems to affect both the sensitivity and the response time. In general, for carbon electrodes, the initial stages of dopamine fouling were reported to involve a two-electron quasi-reversible oxidation of dopamine to dopamine-*o*-quinone[90], which adsorbs on the electrode surface and forms a film that hinders further electron transfer of dopamine. This then leads to the degrading and diminishing dopamine oxidation signals[91].

We have duly investigated in this work the electrochemical fouling from dopamine-*o*-quinone at hydrogenated carbon electrodes. Ten cyclic voltammetric scans of 100 μM dopamine were then sequentially conducted at the triethylsilane hydrogenated and phenylsilane hydrogenated carbon electrodes. As usual, triethylsilane hydrogenated and phenylsilane hydrogenated carbon electrodes were initially characterised by a sigmoidal shape of the cyclic voltammogram of 1.0 mM $[Ru(NH_3)_6]^{3+}$ in 1.0 M KCl. Representative voltammograms are presented in Figure 4.10. Notably, a slightly peak-shaped voltammogram was obtained in the experiment, most likely because the low dopamine concentration (100 μM) used has caused a small depletion effect in the diffusion of dopamine towards the electrodes. Nonetheless, Figure 4.10 shows no noticeable change in the dopamine I_{lim} or the $E_{½}$ at either of the hydrogenated carbon electrodes. This indicates that triethylsilane and phenylsilane hydrogenated carbon electrodes are not susceptible to electrochemical fouling. A possible explanation for this is the presence of an sp^3 nonpolar carbon surface that has suppressed the adsorption of the dopamine-*o*-quinone. Additionally, dopamine polymerisation is known[92] to depend on dopamine concentration and ionic strength. In this respect, Li *et al.*[92] showed that at a very low dopamine concentration (< 20 μM), the concentration of dopamine-*o*-quinone as the monomer was too small to appear as a polymer deposit on a gold electrode surface and the polymer formation becomes less significant.

Several methodologies have been used to evaluate the extent of fouling through electrochemical oxidation of dopamine on electrode surfaces. For example, in addressing dopamine fouling arising from dopamine-*o*-quinone on a graphene-diamond hybrid electrode, Yuan *et al.*[10] initially calibrated the electrodes using different dopamine concentrations, and then incubated them in 1.0 mM dopamine for 10 min. In this way, the oxidation current of dopamine was used to assess fouling arising from

dopamine-*o*-quinone. The authors reported an approximately 50% loss in the signal after the first round of experiments highlighting performance degradation. Although the performance of their electrodes was regenerated by ultrasonication in a water bath, application of such a sensor for long-term monitoring of dopamine is not feasible.

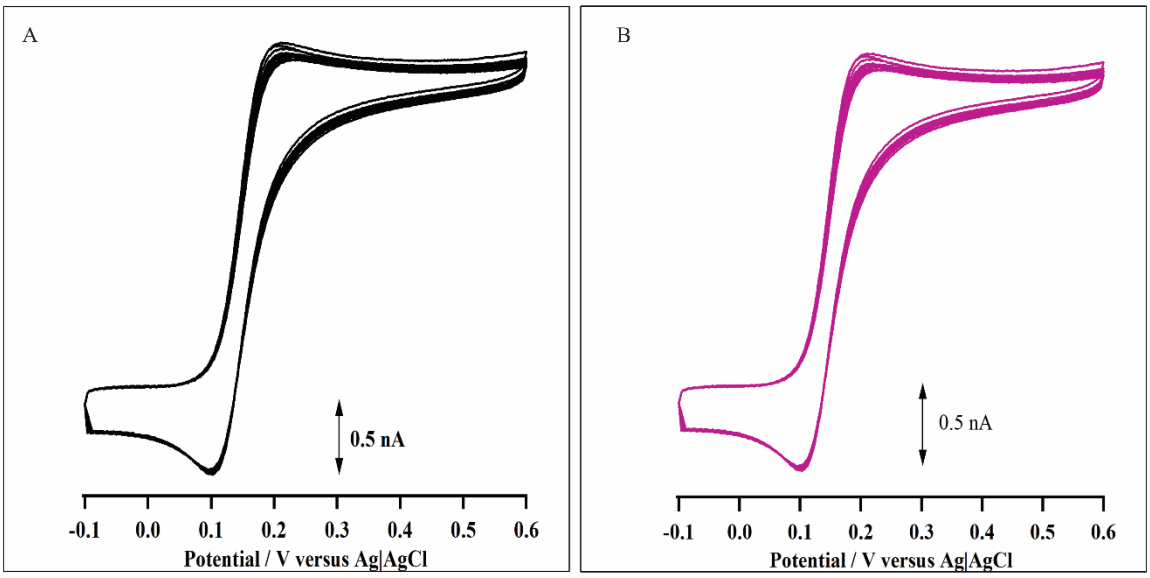

Figure 4.10. A representative cyclic voltammograms of 100 µM dopamine at a triethylsilane hydrogenated carbon electrode. Scan rate 100 mV s^{-1}.

Such divergent behaviour of the non-hydrogenated and silane hydrogenated carbon electrodes reflects the distinct surface properties and their interactions with the proteins, peptides, and lipids. Carbon electrodes fabricated in this work were characterised with scanning electron microscopy, Raman spectroscopy, X-ray photoelectron spectroscopy, and using electrochemistry. All results obtained were discussed in Chapter 3. The heterogeneous surface of a non-hydrogenated carbon electrode also contains considerable amounts of adsorption sites that will contribute to relatively high surface energy. Such surfaces are vulnerable to fast irreversible adsorption by fouling agents[89].

Non-hydrogenated electrodes were subjected to fouling arising from proteins, peptides and lipids and a 53% decline in the I_{lim} was obtained after only a 30-min incubation in the fouling solution. Severe fouling can also occur as a result of applied potential due to enhanced electrostatic interaction between the surface and fouling agents. However, the applied potential used in this work was not high enough to cause an electrostatic interaction between the electrode and the fouling reagents. Meanwhile, the hydrogenated carbon electrodes showed improved resistance to electrochemical fouling with no noticeable change in the I_{lim} after 10 repetitive cycling in 100 µM dopamine as well as fouling from proteins, peptides and lipids with a respective 23% and 18% decline in I_{lim} after a 30-min incubation in the fouling solution using triethylsilane and phenylsilane hydrogenated electrodes, respectively.

Roeser *et al.*[93] suggested that boron-doped diamond electrodes are a promising alternative to glassy carbon electrodes in terms of reducing adsorption and fouling during electrochemical oxidation and cleavage of peptides. Similarly, the antifouling behaviour of our hydrogenated carbon electrodes is attributed to an increase in sp^3/sp^2 ratio with a non-polar surface compared to that on non-hydrogenated carbon electrodes.

In addition to this, nonspecific adsorption of our hydrogenated carbon electrodes can be attributed to the bulkier siloxane dendrimers that effectively covered the sensing surface. The antifouling behaviour relies on the strategy that when the proteins approach the sensing surface, it results in compression of the bulky siloxy units leading to repulsive elastic forces. Although no noticeable difference in the antifouling characteristics was observed between triethylsilane and phenylsilane hydrogenated carbon electrodes, the latter showed slightly better performance in dopamine detection after being incubated in the laboratory synthetic solution for 30 min compared to the

former electrodes. The presence of phenyl rings enhances the electronic properties of hydrogenated carbon electrodes *via* a π-electron system that possibly induces lower electrical resistance between the carbon surface and the siloxane dendrimers in a similar manner to that reported for a self-assembled monolayer of 3-methylthiophene on a planar gold surface[94].

The resistance to fouling from the dopamine oxidation product, dopamine-*o*-quinone, is attributed to the low surface oxides present on the hydrogenated carbon surface. This is consistent with results obtained at cathodically treated boron-doped diamond electrodes, which were demonstrated to show low surface oxide because of H-terminations, compared to the corresponding anodically treated electrodes[95].

4.9 Concluding Remarks

In this work, triethylsilane and phenylsilane hydrogenated carbon electrodes were initially characterised using atomic force microscopy. The microscopic results confirmed the conversion of sp^2 carbon to sp^3 carbon and the formation of a smooth layer consisting of structures of approximately 50 nm in size. The electrodes were then characterised in different dopamine concentrations to evaluate their electroanalytical performance. Both, triethylsilane and phenylsilane hydrogenated carbon electrodes displayed good linearity in the range of 1.0 - 10 µM with a <1 µM detection limit. These electrodes displayed different selectivity towards dopamine, ascorbic acid, and uric acid. Suppressed response towards ascorbic acid was observed at hydrogenated carbon electrodes, while dopamine and uric acid were selectively detected at these electrodes. Finally, the hydrogenated carbon electrodes were incubated in a laboratory synthetic fouling solution containing bovine serum albumin, cytochrome *c*, human fibrinopeptide, and caproic acid to mimic extracellular fluid. The triethylsilane and

phenylsilane hydrogenated electrodes showed improved antifouling property with only 23% and 18% decline in the dopamine oxidation limiting current, respectively, compared to 53% estimated at the non-hydrogenated counterparts only after incubating for 30 min. This shows reduced adsorption of the fouling agents compared to the non-hydrogenated carbon electrodes. The hydrogenated electrodes were also assessed for electrochemical fouling from the dopamine oxidation product, dopamine-*o*-quinone. No noticeable change in the limiting current or the $E_{½}$ was observed after 10 sequential cyclic voltammograms in 100 µM dopamine. The antifouling behaviour is attributed to the formation of H-terminated surface during hydrogenation with formation of bulky siloxane dendrimers, which further provided a barrier against fouling.

4.10 References

(1) Heien, M. L. A. V.; Khan, A. S.; Ariansen, J. L.; Cheer, J. F.; Phillips, P. E. M.; Wassum, K. M.; Wightman, R. M. Real-time measurement of dopamine fluctuations after cocaine in the brain of behaving rats. *Proceedings of the National Academy of Sciences of the United States of America* **2005,** *102* (29), 10023, DOI: 10.1073/pnas.0504657102.

(2) Venton, B. J.; Wightman, R. M. Psychoanalytical Electrochemistry: Dopamine and Behavior. *Analytical Chemistry* **2003,** *75* (19), 414 A-421 A, DOI: 10.1021/ac031421c.

(3) Peltola, E.; Sainio, S.; Holt, K. B.; Palomäki, T.; Koskinen, J.; Laurila, T. Electrochemical Fouling of Dopamine and Recovery of Carbon Electrodes. *Analytical Chemistry* **2018,** *90* (2), 1408-1416, DOI: 10.1021/acs.analchem.7b04793.

(4) Mei, X.; Wei, Q.; Long, H.; Yu, Z.; Deng, Z.; Meng, L.; Wang, J.; Luo, J.; Lin, C.-T.; Ma, L.; Zheng, K.; Hu, N. Long-term stability of Au nanoparticle-anchored porous

boron-doped diamond hybrid electrode for enhanced dopamine detection. *Electrochimica Acta* **2018,** *271*, 84-91, DOI: https://doi.org/10.1016/j.electacta.2018.03.133.

(5) Ajetunmobi, A.; Prina-Mello, A.; Volkov, Y.; Corvin, A.; Tropea, D. Nanotechnologies for the study of the central nervous system. *Prog. Neurobiol. (Oxford, U. K.)* **2014,** *123*, 18-36, DOI: 10.1016/j.pneurobio.2014.09.004.

(6) Robinson, D. L.; Hermans, A.; Seipel, A. T.; Wightman, R. M. Monitoring Rapid Chemical Communication in the Brain. *Chemical Reviews* **2008,** *108* (7), 2554-2584, DOI: 10.1021/cr068081q.

(7) Lee, C.-S.; Baker, S. E.; Marcus, M. S.; Yang, W.; Eriksson, M. A.; Hamers, R. J. Electrically Addressable Biomolecular Functionalization of Carbon Nanotube and Carbon Nanofiber Electrodes. *Nano Letters* **2004,** *4* (9), 1713-1716, DOI: 10.1021/nl048995x.

(8) Dhanjai; Sinha, A.; Lu, X.; Wu, L.; Tan, D.; Li, Y.; Chen, J.; Jain, R. Voltammetric sensing of biomolecules at carbon based electrode interfaces: A review. *TrAC Trends in Analytical Chemistry* **2018,** *98*, 174-189, DOI: https://doi.org/10.1016/j.trac.2017.11.010.

(9) Rowley-Neale, S. J.; Banks, C. E. Electrocatalytic Properties of Carbon Electrode Surfaces A2 - Wandelt, Klaus. In *Encyclopedia of Interfacial Chemistry*; Elsevier: Oxford, 2018; pp 531-538.

(10) Yuan, Q.; Liu, Y.; Ye, C.; Sun, H.; Dai, D.; Wei, Q.; Lai, G.; Wu, T.; Yu, A.; Fu, L.; Chee, K. W. A.; Lin, C.-T. Highly stable and regenerative graphene–diamond hybrid

electrochemical biosensor for fouling target dopamine detection. *Biosensors and Bioelectronics* **2018,** *111*, 117-123, DOI: https://doi.org/10.1016/j.bios.2018.04.006.

(11) DeClements, R.; Swain, G. M.; Dallas, T.; Holtz, M. W.; Herrick, R. D.; Stickney, J. L. Electrochemical and Surface Structural Characterization of Hydrogen Plasma Treated Glassy Carbon Electrodes. *Langmuir* **1996,** *12* (26), 6578-6586, DOI: 10.1021/la960380v.

(12) Sun, K. C.; Memon, A. A.; Arbab, A. A.; Sahito, I. A.; Kim, M. S.; Yeo, S. Y.; Choi, Y. O.; Kim, Y. S.; Jeong, S. H. Electrocatalytic porous nanocomposite of graphite nanoplatelets anchored with exfoliated activated carbon filler as counter electrode for dye sensitized solar cells. *Solar Energy* **2018,** *167*, 95-101, DOI: https://doi.org/10.1016/j.solener.2018.04.002.

(13) Wang, Z.; Guo, H.; Gui, R.; Jin, H.; Xia, J.; Zhang, F. Simultaneous and selective measurement of dopamine and uric acid using glassy carbon electrodes modified with a complex of gold nanoparticles and multiwall carbon nanotubes. *Sensors and Actuators B: Chemical* **2018,** *255*, 2069-2077, DOI: https://doi.org/10.1016/j.snb.2017.09.010.

(14) Caetano, F. R.; Felippe, L. B.; Zarbin, A. J. G.; Bergamini, M. F.; Marcolino-Junior, L. H. Gold nanoparticles supported on multi-walled carbon nanotubes produced by biphasic modified method and dopamine sensing application. *Sensors and Actuators B: Chemical* **2017,** *243*, 43-50, DOI: https://doi.org/10.1016/j.snb.2016.11.096.

(15) Khudaish, E. A.; Al-Nofli, F.; Rather, J. A.; Al-Hinaai, M.; Laxman, K.; Kyaw, H. H.; Al-Harthy, S. Sensitive and selective dopamine sensor based on novel conjugated

polymer decorated with gold nanoparticles. *Journal of Electroanalytical Chemistry* **2016,** *761*, 80-88, DOI: https://doi.org/10.1016/j.jelechem.2015.12.011.

(16) Taylor, I. M.; Robbins, E. M.; Catt, K. A.; Cody, P. A.; Happe, C. L.; Cui, X. T. Enhanced dopamine detection sensitivity by PEDOT/graphene oxide coating on in vivo carbon fiber electrodes. *Biosensors and Bioelectronics* **2017,** *89*, 400-410, DOI: https://doi.org/10.1016/j.bios.2016.05.084.

(17) Li, Y.; Li, H.; Li, M.; Li, C.; Sun, D.; Yang, B. Porous boron-doped diamond electrode for detection of dopamine and pyridoxine in human serum. *Electrochimica Acta* **2017,** *258*, 744-753, DOI: https://doi.org/10.1016/j.electacta.2017.11.121.

(18) Qi, Y.; Long, H.; Ma, L.; Wei, Q.; Li, S.; Yu, Z.; Hu, J.; Liu, P.; Wang, Y.; Meng, L. Enhanced selectivity of boron doped diamond electrodes for the detection of dopamine and ascorbic acid by increasing the film thickness. *Applied Surface Science* **2016,** *390*, 882-889, DOI: http://dx.doi.org/10.1016/j.apsusc.2016.08.158.

(19) Vidya, H.; Kumara Swamy, B. E. Selective detection of dopamine and ascorbic acid at purified carbon nanotubes/Tween-20 modified carbon paste electrode. *Materials Today: Proceedings* **2017,** *4* (11, Part 3), 11991-11998, DOI: https://doi.org/10.1016/j.matpr.2017.09.121.

(20) Casella, I. G.; Gioia, D.; Rutilo, M. A multi-walled carbon nanotubes/cellulose acetate composite electrode (MWCNT/CA) as sensing probe for the amperometric determination of some catecholamines. *Sensors and Actuators B: Chemical* **2018,** *255*, 3533-3540, DOI: https://doi.org/10.1016/j.snb.2017.09.188.

(21) Jayaprakash, G. K.; Swamy, B. E. K.; Chandrashekar, B. N.; Flores-Moreno, R. Theoretical and cyclic voltammetric studies on electrocatalysis of benzethonium chloride at carbon paste electrode for detection of dopamine in presence of ascorbic acid. *Journal of Molecular Liquids* **2017,** *240*, 395-401, DOI: https://doi.org/10.1016/j.molliq.2017.05.093.

(22) Thomas, T.; Mascarenhas, R. J.; Kumara Swamy, B. E. Poly(Rhodamine B) modified carbon paste electrode for the selective detection of dopamine. *Journal of Molecular Liquids* **2012,** *174*, 70-75, DOI: https://doi.org/10.1016/j.molliq.2012.07.022.

(23) Boersma, A. J.; Brain, K. L.; Bayley, H. Real-Time Stochastic Detection of Multiple Neurotransmitters with a Protein Nanopore. *ACS Nano* **2012,** *6* (6), 5304-5308, DOI: 10.1021/nn301125y.

(24) Arrigoni, O.; De Tullio, M. C. Ascorbic acid: Much more than just an antioxidant. *Biochimica et Biophysica Acta - General Subjects* **2002,** *1569* (1-3), 1-9, DOI: 10.1016/S0304-4165(01)00235-5.

(25) Li, Y.; Chen, S.; Shao, X.; Guo, J.; Liu, X.; Liu, A.; Zhang, Y.; Wang, H.; Li, B.; Deng, K.; Liu, Q.; Holthöfer, H.; Zou, H. Association of uric acid with metabolic syndrome in men, premenopausal women and postmenopausal women. *International Journal of Environmental Research and Public Health* **2014,** *11* (3), 2899-2910, DOI: 10.3390/ijerph110302899.

(26) Yang, Y.; Li, M.; Zhu, Z. A novel electrochemical sensor based on carbon nanotubes array for selective detection of dopamine or uric acid. *Talanta* **2019,** *201*, 295-300, DOI: https://doi.org/10.1016/j.talanta.2019.03.096.

(27) Veera Manohara Reddy, Y.; Sravani, B.; Agarwal, S.; Gupta, V. K.; Madhavi, G. Electrochemical sensor for detection of uric acid in the presence of ascorbic acid and dopamine using the poly(DPA)/SiO2@Fe3O4 modified carbon paste electrode. *Journal of Electroanalytical Chemistry* **2018,** *820*, 168-175, DOI: https://doi.org/10.1016/j.jelechem.2018.04.059.

(28) Ensafi, A. A.; Taei, M.; Khayamian, T. A differential pulse voltammetric method for simultaneous determination of ascorbic acid, dopamine, and uric acid using poly (3-(5-chloro-2-hydroxyphenylazo)-4,5-dihydroxynaphthalene-2,7-disulfonic acid) film modified glassy carbon electrode. *Journal of Electroanalytical Chemistry* **2009,** *633* (1), 212-220, DOI: 10.1016/j.jelechem.2009.06.001.

(29) Mandl, J.; Szarka, A.; Bánhegyi, G. Vitamin C: Update on physiology and pharmacology. *British Journal of Pharmacology* **2009,** *157* (7), 1097-1110, DOI: 10.1111/j.1476-5381.2009.00282.x.

(30) Harrison, F. E.; May, J. M. Vitamin C function in the brain: vital role of the ascorbate transporter SVCT2. *Free Radical Biology and Medicine* **2009,** *46* (6), 719-730, DOI: 10.1016/j.freeradbiomed.2008.12.018.

(31) Chatterjee, I. B.; Majumder, A. K.; Nandi, B. K.; Subramanian, N. SYNTHESIS AND SOME MAJOR FUNCTIONS OF VITAMIN C IN ANIMALS*. *Annals of the New York Academy of Sciences* **1975,** *258* (1), 24-47, DOI: doi:10.1111/j.1749-6632.1975.tb29266.x.

(32) Carvalho, L. A. C.; Lopes, J. P. P. B.; Kaihami, G. H.; Silva, R. P.; Bruni-Cardoso, A.; Baldini, R. L.; Meotti, F. C. Uric acid disrupts hypochlorous acid production and

the bactericidal activity of HL-60 cells. *Redox Biology* **2018,** *16*, 179-188, DOI: https://doi.org/10.1016/j.redox.2018.02.020.

(33) Zhao, Y.; Yang, Z.; Fan, W.; Wang, Y.; Li, G.; Cong, H.; Yuan, H. Carbon nanotube/carbon fiber electrodes via chemical vapor deposition for simultaneous determination of ascorbic acid, dopamine and uric acid. *Arabian Journal of Chemistry* **2018**, DOI: https://doi.org/10.1016/j.arabjc.2018.11.002.

(34) Manjunatha, H.; Nagaraju, D. H.; Suresh, G. S.; Venkatesha, T. V. Detection of Uric Acid in the Presence of Dopamine and High Concentration of Ascorbic Acid Using PDDA Modified Graphite Electrode. *Electroanalysis* **2009,** *21* (20), 2198-2206, DOI: 10.1002/elan.200904662.

(35) Yáñez-Sedeño, P.; Campuzano, S.; Pingarrón, J. M. Pushing the limits of electrochemistry toward challenging applications in clinical diagnosis, prognosis, and therapeutic action. *Chemical Communications* **2019**, DOI: 10.1039/C8CC08815B.

(36) Harreither, W.; Trouillon, R.; Poulin, P.; Neri, W.; Ewing, A. G.; Safina, G. Cysteine residues reduce the severity of dopamine electrochemical fouling. *Electrochimica Acta* **2016,** *210*, 622-629, DOI: https://doi.org/10.1016/j.electacta.2016.05.124.

(37) DuVall, S. H.; McCreery, R. L. Self-catalysis by Catechols and Quinones during Heterogeneous Electron Transfer at Carbon Electrodes. *Journal of the American Chemical Society* **2000,** *122* (28), 6759-6764, DOI: 10.1021/ja000227u.

(38) Immanuel, S.; Aparna, T. K.; Sivasubramanian, R. A facile preparation of Au—SiO2 nanocomposite for simultaneous electrochemical detection of dopamine and uric

acid. *Surfaces and Interfaces* **2019,** *14*, 82-91, DOI: https://doi.org/10.1016/j.surfin.2018.11.010.

(39) Durst, R. A.; Bäumner, A. J.; Murray, R. W.; Buck, R. P.; Andrieux, C. P. Chemically modified electrodes: Recommended terminology and definitions. *Pure and Applied Chemistry* **1997,** *69* (6), 1317-1323.

(40) Vreeland, R. F.; Atcherley, C. W.; Russell, W. S.; Xie, J. Y.; Lu, D.; Laude, N. D.; Porreca, F.; Heien, M. L. Biocompatible PEDOT:Nafion Composite Electrode Coatings for Selective Detection of Neurotransmitters in Vivo. *Analytical Chemistry* **2015,** *87* (5), 2600-2607, DOI: 10.1021/ac502165f.

(41) Mani, V.; Dinesh, B.; Chen, S. M.; Saraswathi, R. Direct electrochemistry of myoglobin at reduced graphene oxide-multiwalled carbon nanotubes-platinum nanoparticles nanocomposite and biosensing towards hydrogen peroxide and nitrite. *Biosensors and Bioelectronics* **2014,** *53*, 420-427, DOI: 10.1016/j.bios.2013.09.075.

(42) Soldano, C.; Mahmood, A.; Dujardin, E. Production, properties and potential of graphene. *Carbon* **2010,** *48* (8), 2127-2150, DOI: https://doi.org/10.1016/j.carbon.2010.01.058.

(43) Diab, N.; Morales, D. M.; Andronescu, C.; Masoud, M.; Schuhmann, W. A sensitive and selective graphene/cobalt tetrasulfonated phthalocyanine sensor for detection of dopamine. *Sensors and Actuators B: Chemical* **2019,** *285*, 17-23, DOI: https://doi.org/10.1016/j.snb.2019.01.022.

(44) Edwards, G. A.; Bergren, A. J.; Porter, M. D. 8 - Chemically Modified Electrodes. In *Handbook of Electrochemistry*; Zoski, C. G., Ed.; Elsevier: Amsterdam, 2007; pp 295-327.

(45) Kesavan, S.; Gowthaman, N. S. K.; Alwarappan, S.; John, S. A. Real time detection of adenosine and theophylline in urine and blood samples using graphene modified electrode. *Sensors and Actuators B: Chemical* **2019,** *278*, 46-54, DOI: https://doi.org/10.1016/j.snb.2018.09.069.

(46) Wang, Y.; Huang, Y.; Wang, B.; Fang, T.; Chen, J.; Liang, C. Three-dimensional porous graphene for simultaneous detection of dopamine and uric acid in the presence of ascorbic acid. *Journal of Electroanalytical Chemistry* **2016,** *782*, 76-83, DOI: http://dx.doi.org/10.1016/j.jelechem.2016.09.050.

(47) Baughman, R. H.; Zakhidov, A. A.; de Heer, W. A. Carbon Nanotubes--the Route Toward Applications. *Science* **2002,** *297* (5582), 787, DOI: 10.1126/science.1060928.

(48) Azamian, B. R.; Davis, J. J.; Coleman, K. S.; Bagshaw, C. B.; Green, M. L. H. Bioelectrochemical Single-Walled Carbon Nanotubes. *Journal of the American Chemical Society* **2002,** *124* (43), 12664-12665, DOI: 10.1021/ja0272989.

(49) Huang, J.; Liu, Y.; Hou, H.; You, T. Simultaneous electrochemical determination of dopamine, uric acid and ascorbic acid using palladium nanoparticle-loaded carbon nanofibers modified electrode. *Biosensors and Bioelectronics* **2008,** *24* (4), 632-637, DOI: https://doi.org/10.1016/j.bios.2008.06.011.

(50) Yue, H. Y.; Wu, P. F.; Huang, S.; Gao, X.; Song, S. S.; Wang, W. Q.; Zhang, H. J.; Guo, X. R. Electrochemical determination of dopamine in the presence of uric acid

using WS2 nanospheres-carbon nanofibers. *Journal of Electroanalytical Chemistry* **2019,** *833*, 427-432, DOI: https://doi.org/10.1016/j.jelechem.2018.12.016.

(51) Savk, A.; Özdil, B.; Demirkan, B.; Nas, M. S.; Calimli, M. H.; Alma, M. H.; Inamuddin; Asiri, A. M.; Şen, F. Multiwalled carbon nanotube-based nanosensor for ultrasensitive detection of uric acid, dopamine, and ascorbic acid. *Materials Science and Engineering: C* **2019,** *99*, 248-254, DOI: https://doi.org/10.1016/j.msec.2019.01.113.

(52) Murali, A.; Lan, Y. P.; Sarswat, P. K.; Free, M. L. Synthesis of CeO2/reduced graphene oxide nanocomposite for electrochemical determination of ascorbic acid and dopamine and for photocatalytic applications. *Materials Today Chemistry* **2019,** *12*, 222-232, DOI: https://doi.org/10.1016/j.mtchem.2019.02.001.

(53) Ma, L.; Zhang, Q.; Wu, C.; Zhang, Y.; Zeng, L. PtNi bimetallic nanoparticles loaded MoS2 nanosheets: Preparation and electrochemical sensing application for the detection of dopamine and uric acid. *Analytica Chimica Acta* **2019,** *1055*, 17-25, DOI: https://doi.org/10.1016/j.aca.2018.12.025.

(54) Xu, T.-Q.; Zhang, Q.-L.; Zheng, J.-N.; Lv, Z.-Y.; Wei, J.; Wang, A.-J.; Feng, J.-J. Simultaneous determination of dopamine and uric acid in the presence of ascorbic acid using Pt nanoparticles supported on reduced graphene oxide. *Electrochimica Acta* **2014,** *115*, 109-115, DOI: https://doi.org/10.1016/j.electacta.2013.10.147.

(55) Palanisamy, S.; Velusamy, V.; Ramaraj, S.; Chen, S.-W.; Yang, T. C. K.; Balu, S.; Banks, C. E. Facile synthesis of cellulose microfibers supported palladium nanospindles on graphene oxide for selective detection of dopamine in pharmaceutical

and biological samples. *Materials Science and Engineering: C* **2019,** *98*, 256-265, DOI: https://doi.org/10.1016/j.msec.2018.12.112.

(56) Harreither, W.; Trouillon, R.; Poulin, P.; Neri, W.; Ewing, A. G.; Safina, G. Carbon Nanotube Fiber Microelectrodes Show a Higher Resistance to Dopamine Fouling. *Analytical Chemistry* **2013,** *85* (15), 7447-7453, DOI: 10.1021/ac401399s.

(57) Parviz, M.; Darwish, N.; Alam, M. T.; Parker, S. G.; Ciampi, S.; Gooding, J. J. Investigation of the Antifouling Properties of Phenyl Phosphorylcholine-Based Modified Gold Surfaces. *Electroanalysis* **2014,** *26* (7), 1471-1480, DOI: 10.1002/elan.201400102.

(58) Song, Z.; Sheng, G.; Cui, Y.; Li, M.; Song, Z.; Ding, C.; Luo, X. Low fouling electrochemical sensing in complex biological media by using the ionic liquid-doped conducting polymer PEDOT: application to voltammetric determination of dopamine. *Microchimica Acta* **2019,** *186* (4), 220, DOI: 10.1007/s00604-019-3340-x.

(59) Mohammed Modawe Alshik Edris, N.; Abdullah, J.; Kamaruzaman, S.; Saiman, M. I.; Sulaiman, Y. Electrochemical reduced graphene oxide-poly(eriochrome black T)/gold nanoparticles modified glassy carbon electrode for simultaneous determination of ascorbic acid, dopamine and uric acid. *Arabian Journal of Chemistry* **2018,** *11* (8), 1301-1312, DOI: https://doi.org/10.1016/j.arabjc.2018.09.002.

(60) Suzuki, A.; Ivandini, T. A.; Yoshimi, K.; Fujishima, A.; Oyama, G.; Nakazato, T.; Hattori, N.; Kitazawa, S.; Einaga, Y. Fabrication, Characterization, and Application of Boron-Doped Diamond Microelectrodes for in Vivo Dopamine Detection. *Analytical Chemistry* **2007,** *79* (22), 8608-8615, DOI: 10.1021/ac071519h.

(61) Dincer, C.; Ktaich, R.; Laubender, E.; Hees, J. J.; Kieninger, J.; Nebel, C. E.; Heinze, J.; Urban, G. A. Nanocrystalline boron-doped diamond nanoelectrode arrays for ultrasensitive dopamine detection. *Electrochimica Acta* **2015,** *185*, 101-106, DOI: http://dx.doi.org/10.1016/j.electacta.2015.10.113.

(62) Trouillon, R.; O'Hare, D. Comparison of glassy carbon and boron doped diamond electrodes: Resistance to biofouling. *Electrochimica Acta* **2010,** *55* (22), 6586-6595, DOI: http://dx.doi.org/10.1016/j.electacta.2010.06.016.

(63) Trouillon, R.; O'Hare, D.; Einaga, Y. Effect of the doping level on the biological stability of hydrogenated boron doped diamond electrodes. *Physical Chemistry Chemical Physics* **2011,** *13* (12), 5422-5429, DOI: 10.1039/C0CP02420A.

(64) Zhao, H.; Bian, X.; Galligan, J. J.; Swain, G. M. Electrochemical measurements of serotonin (5-HT) release from the guinea pig mucosa using continuous amperometry with a boron-doped diamond microelectrode. *Diamond and Related Materials* **2010,** *19* (2), 182-185, DOI: https://doi.org/10.1016/j.diamond.2009.10.004.

(65) Patel, A. N.; Unwin, P. R.; Macpherson, J. V. Investigation of film formation properties during electrochemical oxidation of serotonin (5-HT) at polycrystalline boron doped diamond. *Physical Chemistry Chemical Physics* **2013,** *15* (41), 18085-18092, DOI: 10.1039/C3CP53513D.

(66) Nimmagadda, R. D.; McRae, C. A novel reduction reaction for the conversion of aldehydes, ketones and primary, secondary and tertiary alcohols into their corresponding alkanes. *Tetrahedron Letters* **2006,** *47* (32), 5755-5758, DOI: http://dx.doi.org/10.1016/j.tetlet.2006.06.007.

(67) Nimmagadda, R. D.; McRae, C. Characterisation of the backbone structures of several fulvic acids using a novel selective chemical reduction method. *Organic Geochemistry* **2007,** *38* (7), 1061-1072, DOI: http://dx.doi.org/10.1016/j.orggeochem.2007.02.016.

(68) Yang, C.; Trikantzopoulos, E.; Jacobs, C. B.; Venton, B. J. Evaluation of carbon nanotube fiber microelectrodes for neurotransmitter detection: Correlation of electrochemical performance and surface properties. *Analytica Chimica Acta* **2017,** *965*, 1-8, DOI: https://doi.org/10.1016/j.aca.2017.01.039.

(69) Liu, N.; Xu, Z.; Morrin, A.; Luo, X. Low fouling strategies for electrochemical biosensors targeting disease biomarkers. *Analytical Methods* **2019,** *11* (6), 702-711, DOI: 10.1039/C8AY02674B.

(70) Ishige, H.; Akaike, S.; Hayakawa, T.; Hiratsuka, M.; Nakamura, Y. Evaluation of protein adsorption to diamond-like carbon (DLC) and fluorinedoped DLC films using the quartz crystal microbalance method. *Dental Materials Journal* **2019,** *advpub*, DOI: 10.4012/dmj.2018-060.

(71) Xue, Q.; Kato, D.; Kamata, T.; Umemura, S.; Hirono, S.; Niwa, O. Electron Cyclotron Resonance-Sputtered Nanocarbon Film Electrode Compared with Diamond-Like Carbon and Glassy Carbon Electrodes as Regards Electrochemical Properties and Biomolecule Adsorption. *Japanese Journal of Applied Physics* **2012,** *51*, 090124, DOI: 10.1143/jjap.51.090124.

(72) Siraj, S.; McRae, C. R.; Wong, D. K. Y. Effective activation of physically small carbon electrodes by n-butylsilane reduction. *Electrochemistry Communications* **2016,** *64*, 35-41, DOI: http://dx.doi.org/10.1016/j.elecom.2016.01.007.

(73) Pleskov, Y. V. Synthetic diamond electrodes for electroanalysis and electrolysis. In *Electroanalytical Chemistry Research Developments*; Jiang, P. N., Ed.; Nova Science Publishers Inc: Hauppauge, 2007; Chapter 4, pp 183-227.

(74) Wightman, R. M.; May, L. J.; Michael, A. C. Detection of dopamine dynamics in the brain. *Analytical Chemistry* **1988,** *60* (13), 769A-779A, DOI: 10.1021/ac00164a001.

(75) Michael, A. C.; Justice, J. B. Oxidation of dopamine and 4-methylcatechol at carbon fiber disk electrodes. *Analytical Chemistry* **1987,** *59* (3), 405-410, DOI: 10.1021/ac00130a006.

(76) DuVall, S. H.; McCreery, R. L. Control of Catechol and Hydroquinone Electron-Transfer Kinetics on Native and Modified Glassy Carbon Electrodes. *Analytical Chemistry* **1999,** *71* (20), 4594-4602, DOI: 10.1021/ac990399d.

(77) Peltola, E.; Wester, N.; Holt, K. B.; Johansson, L.-S.; Koskinen, J.; Myllymäki, V.; Laurila, T. Nanodiamonds on tetrahedral amorphous carbon significantly enhance dopamine detection and cell viability. *Biosensors and Bioelectronics* **2017,** *88*, 273-282, DOI: https://doi.org/10.1016/j.bios.2016.08.055.

(78) Qiu, C.; Chen, H.; Liu, H.; Zhai, Z.; Qin, J.; Lv, Y.; Gao, Z.; Song, Y. The hydrophilicity of carbon for the performance enhancement of direct ascorbic acid fuel cells. *International Journal of Hydrogen Energy* **2018,** *43* (48), 21908-21917, DOI: https://doi.org/10.1016/j.ijhydene.2018.09.213.

(79) Maleki, N.; Safavi, A.; Tajabadi, F. High-Performance Carbon Composite Electrode Based on an Ionic Liquid as a Binder. *Analytical Chemistry* **2006,** *78* (11), 3820-3826, DOI: 10.1021/ac060070+.

(80) Kneten, K. R.; McCreery, R. L. Effects of redox system structure on electron-transfer kinetics at ordered graphite and glassy carbon electrodes. *Analytical Chemistry* **1992,** *64* (21), 2518-2524, DOI: 10.1021/ac00045a011.

(81) Jeong, H.; Jeon, S. Determination of Dopamine in the Presence of Ascorbic Acid by Nafion and Single-Walled Carbon Nanotube Film Modified on Carbon Fiber Microelectrode. *Sensors (Basel, Switzerland)* **2008,** *8* (11), 6924-6935, DOI: 10.3390/s8116924.

(82) Roy, P. R.; Saha, M. S.; Okajima, T.; Park, S. G.; Fujishima, A.; Ohsaka, T. Selective Detection of Dopamine and Its Metabolite, DOPAC, in the Presence of Ascorbic Acid Using Diamond Electrode Modified by the Polymer Film. *Electroanalysis* **2004,** *16* (21), 1777-1784, DOI: 10.1002/elan.200303026.

(83) Jiang, L.; Nelson, G. W.; Abda, J.; Foord, J. S. Novel Modifications to Carbon-Based Electrodes to Improve the Electrochemical Detection of Dopamine. *ACS Applied Materials & Interfaces* **2016**, DOI: 10.1021/acsami.6b03879.

(84) Hassanvand, Z.; Jalali, F. Simultaneous determination of l-DOPA, l-tyrosine and uric acid by cysteic acid - modified glassy carbon electrode. *Materials Science and Engineering: C* **2019**, DOI: https://doi.org/10.1016/j.msec.2018.12.131.

(85) Miodek, A.; Regan, E. M.; Bhalla, N.; Hopkins, N. A. E.; Goodchild, S. A.; Estrela, P. Optimisation and Characterisation of Anti-Fouling Ternary SAM Layers for

Impedance-Based Aptasensors. *Sensors (Basel, Switzerland)* **2015,** *15* (10), 25015-25032, DOI: 10.3390/s151025015.

(86) Maeda, H.; Okada, T.; Matsumoto, Y.; Katayama, K.; Yamauchi, Y.; Ohmori, H. Electrochemical Coating with Poly(phenylene oxide) Films Bearing Oligoether Groups as a Tool for Elimination of Protein Adsorption to Electrode Surfaces. *Analytical Sciences* **1999,** *15* (7), 633-639, DOI: 10.2116/analsci.15.633.

(87) Singh, Y. S.; Sawarynski, L. E.; Dabiri, P. D.; Choi, W. R.; Andrews, A. M. Head-to-Head Comparisons of Carbon Fiber Microelectrode Coatings for Sensitive and Selective Neurotransmitter Detection by Voltammetry. *Analytical Chemistry* **2011,** *83* (17), 6658-6666, DOI: 10.1021/ac2011729.

(88) Chandra, S.; Miller, A. D.; Bendavid, A.; Martin, P. J.; Wong, D. K. Y. Minimizing Fouling at Hydrogenated Conical-Tip Carbon Electrodes during Dopamine Detection in Vivo. *Analytical Chemistry* **2014,** *86* (5), 2443-2450, DOI: 10.1021/ac403283t.

(89) Shin, D.; Tryk, D. A.; Fujishima, A.; Merkoçi, A.; Wang, J. Resistance to Surfactant and Protein Fouling Effects at Conducting Diamond Electrodes. *Electroanalysis* **2005,** *17* (4), 305-311, DOI: 10.1002/elan.200403104.

(90) Chang, A.-Y.; Dutta, G.; Siddiqui, S.; Arumugam, P. U. Surface Fouling of Ultrananocrystalline Diamond Microelectrodes during Dopamine Detection: Improving Lifetime via Electrochemical Cycling. *ACS Chemical Neuroscience* **2018**, DOI: 10.1021/acschemneuro.8b00257.

(91) Vulcu, A.; Biris, A. R.; Borodi, G.; Berghian-Grosan, C. Interference of ascorbic and uric acids on dopamine behavior at graphene composite surface: An

electrochemical, spectroscopic and theoretical approach. *Electrochimica Acta* **2018,** *282*, 822-834, DOI: https://doi.org/10.1016/j.electacta.2018.06.122.

(92) Li, Y.; Liu, M.; Xiang, C.; Xie, Q.; Yao, S. Electrochemical quartz crystal microbalance study on growth and property of the polymer deposit at gold electrodes during oxidation of dopamine in aqueous solutions. *Thin Solid Films* **2006,** *497* (1), 270-278, DOI: https://doi.org/10.1016/j.tsf.2005.10.048.

(93) Roeser, J.; Alting, N. F. A.; Permentier, H. P.; Bruins, A. P.; Bischoff, R. Boron-Doped Diamond Electrodes for the Electrochemical Oxidation and Cleavage of Peptides. *Analytical Chemistry* **2013,** *85* (14), 6626-6632, DOI: 10.1021/ac303795c.

(94) Terzi, F.; Seeber, R.; Pigani, L.; Zanardi, C.; Pasquali, L.; Nannarone, S.; Fabrizio, M.; Daolio, S. 3-Methylthiophene Self-Assembled Monolayers on Planar and Nanoparticle Au Surfaces. *The Journal of Physical Chemistry B* **2005,** *109* (41), 19397-19402, DOI: 10.1021/jp0530956.

(95) Trouillon, R.; Einaga, Y.; Gijs, M. A. M. Cathodic pretreatment improves the resistance of boron-doped diamond electrodes to dopamine fouling. *Electrochemistry Communications* **2014,** *47*, 92-95, DOI: https://doi.org/10.1016/j.elecom.2014.07.028.

CHAPTER 5: EVALUATING THE ANTIFOULING PROPERTY OF HYDROGENATED CARBON ELECTRODES IN REAL-LIFE BIOLOGICAL SAMPLES

5.1 Introduction

This Chapter describes the application of hydrogenated conical-tip carbon electrodes to the detection of neurotransmitter dopamine in two real-life biological samples, (i) neuroblastoma SH-SY5Y cell line and (ii) brain slices. Additionally, as previously discussed in Chapter 3 and Chapter 4, one significant challenge during dopamine detection both *in vivo* and *in vitro* is electrode fouling, often caused by adsorption of amphiphilic proteins, peptides and lipids present in extracellular fluid on hydrophilic carbon electrodes. The stability and robustness of hydrogenated carbon electrodes in laboratory synthetic fouling solution was reported in Chapter 4. In this Chapter, the antifouling characteristics of the silane hydrogenated small carbon electrodes is further evaluated in real-life biological samples to determine their applicability for monitoring neurotransmitter dopamine in extracellular fluid.

5.2 Monoamine Neurotransmitters

Monoamine neurotransmitters such as dopamine, norepinephrine and epinephrine play a significant role in the endocrine and central nervous systems[1]. Dopamine has also been associated with the reward system, the circuitry in the brain responsible for the motivation to seek out stimuli as well as the emotions of feeling satisfied and satiated in one's environment[2]. Dopamine is one of the most researched neurotransmitters due

to its important functions in the human central nervous system. Owing to its important role in neurotransmission in the brain, changes in the dopamine levels can lead to several neurological and immunological diseases such as Parkinson's disease and schizophrenia[3]. Therefore, chronic monitoring of the extracellular neurotransmitter is essential to the understanding of several brain disorders[4]. Techniques including chromatography, mass spectroscopy, and fluorescence approaches have been used to monitor neurotransmitters in real-life biological samples. However, these detection techniques frequently require sophisticated instrumentation and highly trained personnel, demanding and time consuming procedures, and they often induce excessive costs[1]. In contrast, electrochemical techniques are widely used for measuring neurotransmitters as they do not require pretreatment of samples, exhibit fast response time and allow real-time measurements[5-6].

5.3 Monitoring dopamine using electrochemical techniques in real-life biological samples

Voltammetry at carbon fibre microelectrodes is a powerful analytical tool for *in vivo* measurements of electroactive neurotransmitters. Electrochemical techniques such as fast scan cyclic voltammetry is routinely used to directly measure the changes in neurotransmitter levels[7-9]. This technique utilises rapid scan rates to achieve high measurement sensitivity with sub-second time resolution, while providing selectivity for neurotransmitter of interest, such as dopamine, often found at low concentrations relative to other electroactive species[10]. Therefore, electrochemical monitoring can help in understanding the dynamics of neurotransmitters *in vivo*. However, due to the ethical limitation of conducting research on humans, biological systems are often used to gather important information about human disorders. Although it is clear that

humans and rats differ significantly, it is vital to determine the translational capability of neurobiological studies in rodents by defining how well functional parameters in the rat and mouse brain are similar to non-human primates and humans[11]. Several real-life biological samples have been used to study the dopamine systems including adrenal pheochromocytoma cells (PC12 cells), neuroblastoma SH-SY5Y and brain slices. These samples have their own distinct advantages and disadvantages.

The PC12 cell line (ATCC® CRL-1721™) was derived from a tumor in the rat adrenal pheochromocytoma in 1976 and is widely used to study Parkinson's disease[12]. This line has a chromaffin-like character and shares its embryonic origin with dopaminergic neurons[13]. These cells synthesise and store dopamine and norepinephrine after being released upon depolarisation in a Ca^{2+} dependent pathway. but the release can be inhibited by an excess of Mg^{2+}. Therefore, the PC12 cell lines are good cellular models for examining dopamine regulation[12, 14-15]. Shinohara and Wang[16] used an enzyme-catalysed luminescence method to monitor dopamine released from PC12 cells as a nerve model upon stimulation with acetylcholine and an acetylcholine receptor agonist. Greene and Rein reported over 90% depletion of intracellular dopamine and norepinephrine from PC12 cells upon exposure to 10^{-5} M of the inhibitor reserpine, which has been shown to cause depletion of stored catecholamine in sympathetic neuron and adrenal chromaffin cells. These PC12 cells also showed the ability to take up norepinephrine from the external medium by means of saturable transport mechanism which follows Michaelis-Menten kinetics[15].

Several researchers have reported the electrochemical determination of neurotransmitters in PC12 cells. For example, Imran *et al.*[1] used differential pulse voltammetry and chronoamperometry to record dopamine secreted from PC12 cells

under K^+ stimulation using a NiO modified conducting indium tin oxide surface. In a similar work, Yang *et al.*[17] monitored nicotine induced dopamine release from PC12 cells with 97.6% recovery using a poly-celestine blue modified glassy carbon electrode. The fabricated sensor showed good linearity with a limit of detection of 1.2 nM and sensitivity of 17 $\mu A\ cm^2\ \mu M^{-1}$. Using internal calibration method, the authors estimated the concentration of 0.12 μM dopamine released from the PC12 cells. They reported that the method holds great potential for the detection of dopamine in biological samples and it would contribute to the diagnosis of diseases associated with dopamine deficiency[17].

Adams *et al.*[18] also reported amperometric detection of exocytotic release of dopamine from PC12 cells using a sol-gel silicate functionalised gold-nanoparticle network on a microelectrode. Their results showed significant difference in the kinetic peak parameters including shorter rise time, decay and half-width at the modified electrode compared to a bare carbon fibre electrode. The authors attributed the performance of the modified electrode to excellent sensing activity, prolonged shelf life stability and resistance to cellular debris fouling and dopamine polymerisation[18]. Similarly, Chiu *et al.*[14] employed amperometry to monitor dopamine release from dopaminergic PC12 cells using optogenetic stimulation at a self-assembled monolayer modified electrode. The optogenetic stimulation approach involves the use of channelrhodopsin-2, which depolarises the cells after exposure to ~473 nm blue light in a very short duration. Their work demonstrated that optogenetic stimulation can evoke voltage gates Ca^{2+} channel dependent dopamine exocytosis from PC12 cells and demonstrated PC12 as a good cell model for dopamine regulation[14].

Neuroblastoma SH-SY5Y cell line is also a real-life biological model widely used in Parkinson's disease research. This line is a subline of SK-N-SH cell line established in culture in 1970 from a bone marrow biopsy of a metastatic neuroblastoma of a 4-year old female and has undergone three rounds of clonal selection[19]. Initially, the cultured human neuroblastoma cell lines SK-N-SH, SK-N-BE(1), SK-N-BE(2) and SK-N-MC were assessed for their neurotransmitter features using cholinergic and adrenergic enzyme activities as well as detection from neurotransmitters synthesised from radioactive precursors. SK-N-SH, SK-N-BE(1) and SK-N-BE(2) cells showed moderately high levels of dopamine-β-hydroxylase activity[19]. The SH-SY5Y express properties for tyrosine hydroxylase and produce dopamine and norepinephrine, but only appear to store dopamine[19]. They are good real-life biological models for studying the neurotoxic and neuroprotective effects of dopamine related compounds as they also express dopamine transporter, the vesicular monoamine transporter 2, D_2 and D_3 dopamine receptors[20].

Brain slice is an *ex vivo* system that provides unique advantages of replicating many aspects of the *in vivo* biology such as preserving the tissue architecture, synaptic connectivity and regulatory machinery, and offer certain benefits over *in vivo* studies such as easier control of the extracellular matrix composition[21]. Normally, brains of freshly dispatched rodents are harvested and desired regions of the brain is sliced in 350-500 μm sections that may consist of cell bodies, projection axons and terminal regions[22]. The use of brain slices to study neurotransmitters do not require lengthy animal surgery and laborious monitoring of multiple physiological parameters following *in vivo* manipulation[22]. An additional feature of using brain slices is the ability to take measurements from multiple regions of the same slice as well as multiple

slices from the same animal. Brain slice tissue can also be minced or processed into synaptosomes for biochemical analysis[23].

Burrell *et al*.[24] used fast-scan controlled-adsorption voltammetry to investigate pharmacologically induced slow changes in tonic extracellular dopamine as well as stimulated release in brain slice. The adsorption dynamics and changes in the concentration of dopamine evoked by drugs was monitored using fast-scan controlled-adsorption voltammetry. They demonstrated that this technique can be efficiently used in brain slices to measure extended changes in the extracellular level of endogenous dopamine, complementing *in vivo* microdialysis studies.

Yang *et al*.[25] fabricated a cavity carbon nanopipette electrode by depositing carbon inside the pulled capillary using chemical vapour deposition with methane and argon at 945°C. The fabricated electrode cavity carbon-nanopipette electrode was used to detect dopamine in a mouse brain slices to test the stability and robustness of the fabricated electrode for tissue measurement. In their work, by measuring exogenously applied dopamine their work showed that the cavity carbon nanopipette electrodes were not clogged with tissues after being inserted into tissue[25].

5.4 Scope of this study

The use of real-life biological samples for monitoring of neurotransmitter dopamine hold great potential for the study of dopamine dynamics and could potentially bring great convenience to the diagnosis of diseases associated with dopamine deficiency. In Chapter 4, the antifouling characteristics of fabricated hydrogenated carbon electrodes was assessed in a laboratory synthetic fouling solution containing bovine serum albumin, cytochrome *c*, human fibrinopeptide and caproic acid. On the other hand,

having an appropriate *in vivo* system provides translational models for human diseases in an integral aspect of research in neurobiology and neurosciences[26]. Although several researchers have reported the use of *in vivo* experimental models to study neurotransmission, the existence of difficulties related to the increasing cost and time required for the studies as well as the animal ethical concerns, have limited their use[27]. Alternatively, real-life biological samples such as SH-SY5Y cell line and brain slices provide an understanding of the mechanistic basis at the cellular and molecular level to study dopamine dynamics. In this Chapter, the antifouling characteristics of the hydrogenated carbon electrodes are evaluated in two real-life biological samples, SH-SY5Y cell line and brain slices. The robustness of the fabricated electrodes after being in contact with tissues and detection of dopamine is evaluated. The results acquired are compared to those obtained at the non-hydrogenated counterparts.

5.5 Experimental

5.5.1 Reagents and chemicals

A list of all chemical and reagents used in this work was presented in Section 2.2.

5.5.2 Electrode fabrication and hydrogenation

Structurally small carbon electrodes were fabricated and hydrogenated using the procedure outlined in Sections 2.3 and 2.4.

5.5.3 Electrode characterisation

The instrumentation used to characterise the fabricated electrode was described in Section 2.5.

5.5.4 Amperometric data acquisition

Amperometric data were recorded with a low current potentiostat (eDAQ Pty LtD., Sydney, Australia),-was operated using the Chart software on a PC *via* an E-corder interface (eDAQ Pty Ltd.). The output was filtered at 10 Hz using an internal low pass filter.

5.5.5 Fast scan cyclic voltammetry instrumentation

Fast scan cyclic voltammetric experiments were carried out using a ChemClamp potentiostat and 10 MΩ headstage (Dagan, Minneapolis, MN). The buffer and test solutions were injected through the flow cell by a syringe pump (Harvard Apparatus, Holliston, MA) with a flow rate of 2 mL min^{-1} and a six-port sample loop with an air actuator (VIVI Valco Instruments, Houston, TX). The fast scan cyclic voltammetric waveform with a holding potential of –0.4 V, a switching potential of +1.2 V, a scan rate of 400 V s^{-1}, and a repetition rate of 10 Hz was applied to a working electrode versus a Ag|AgCl reference electrode. The data were collected and analysed by HDCV software (Department of Chemistry, University of North Carolina at Chapel Hill).

5.5.6 The SH-SY5Y Cell Culture

SY-SY5Y cells were obtained from Dr Mark Connors laboratory (Department of Biomedical Sciences, Macquarie University, Sydney). The SH-SY5Y cells were cultured in Dulbecco's Modified Eagle's Medium - high glucose (DMEM) in 25 mL flasks for 1 week. The cells were passaged weekly into petri dishes by initially washing with a pH 7.4-phosphate buffered saline. The phosphate buffered saline was left no more than 2 mins in the flask before it was aspirated and discarded. Next, to detach

cells from the surface of the flask, trypsin was added and was left for ~2 min, followed by addition of DMEM to inhibit trypsin. The cell solution was then spun down by centrifuging for 3-5 mins. The cells were then resuspended in DMEM before a drop was added to petri dish containing DMEM for attachment to the substrate. The cells were incubated at 37 °C overnight. At the start of all electrochemical experiments, the cells were washed with phosphate buffered saline to remove the DMEM media prior to adding the Hank's balanced salt solution (HBSS) media. HBSS media containing Ca^{2+} was used throughout the electrochemical experiment to avoid detachment of cells from the substrate at room temperature. All solutions used in cell culture were prewarmed at 37 °C in a water bath.

Next, using an inverted microscope (Olympus IX71/IX51) and a micromanipulator, a carbon electrode was positioned close to the cells but without the electrode touching the surface of the cell. A counter electrode and a reference electrode were also used. A low current potentiostat and an e-corder (edaq Pty Ltd, Sydney Australia) were used to acquire all the data. A constant potential of +0.5 V was applied to the working electrode for oxidation of dopamine. KCl solution was injected every 15 min for a duration of 1 h to stimulate dopamine release.

5.5.7 Brain slice experiments

All animal experiments were approved by the Animal Care and Use Committee of the University of Virginia. In our work, 400-µm slices of the caudate-putamen were prepared from an anesthetised mouse, from which the brain was removed within 2 min and placed in an artificial cerebral spinal fluid for 2 min. In biofouling experiments, fast scan cyclic voltammetry of 5 µM dopamine was performed at the tested electrode before and after it was being placed in a brain slice tissue for 1 h. To examine the ability

of the electrode to detect exogenously applied dopamine in the brain slice tissue, 1 mM dopamine was ejected into the tissue with a picospritzer (Parker Hannifin Corp.) with a pressure of 20 psi.

5.5.8 Data Analysis

The statistical significance of all correlation coefficients at the 95% confidence level was tested using Student's *t*-test.

5.6 Results and discussion

As one of the most important neurotransmitters, dopamine is widely recognised to be involved in many physiological processes in a mammalian central nervous system as an analytical biomarker for several neurological diseases including Parkinson's disease, schizophrenia, Alzheimer's disease[28]. Studies are largely undertaken real-life biological systems such as synaptosomes and brain slices, primary neuronal cultures and cell expression systems[23]. In this Chapter, hydrogenated carbon electrodes are assessed in neuroblastoma cell line SH-SY5Y and brain slices to further evaluate the stability and resistance towards biofouling at the electrodes.

5.6.1 SH-SY5Y Cell Line Model

SH-SY5Y cell line is reportedly known as a good biological model for measuring dopamine secretions of the dopaminergic neurons[29]. These cells were cultured for two weeks for them to reach maximum expression levels before they were utilised in electrochemical measurements. Initially, the cells were cultured in petri dishes overnight in DMEM medium to allow the cells to attach to the plates. Next, the cells

were washed with phosphate buffered saline before HBSS media was added. A carbon electrode was positioned close to the cell as schematically shown in Figure 5.1.

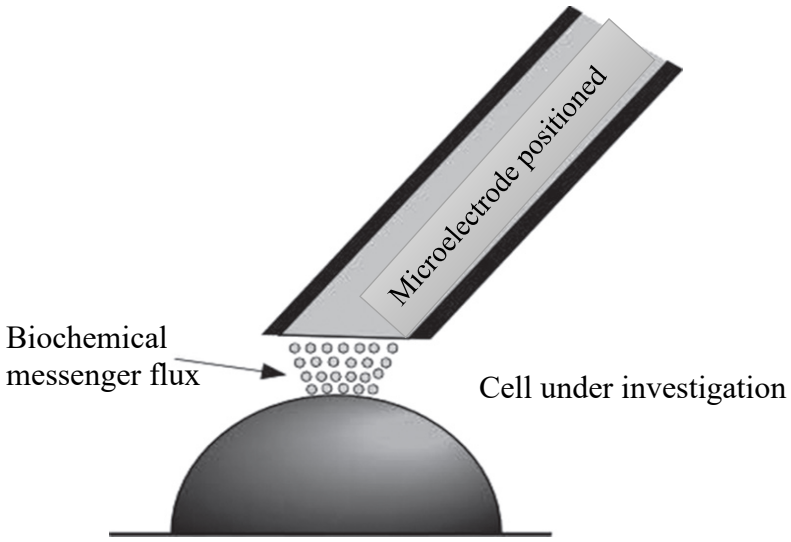

Figure 5.1. Scheme of the artificial synapse configuration for which a microelectrode is positioned near an emitting cell. Adapted from reference[30].

Several researchers have studied the electrochemical monitoring of exocytotic release within a cell configuration mimicking an artificial synapse[31]. Accordingly, a microelectrode substitutes a receptor cell to allow the real-time monitoring of neurotransmitters released as catecholamine neurotransmitters can be easily oxidised. The release of neurotransmitters *via* exocytosis relies on the distance between the electrode surface and the cells. Also, the short timescale of the release event necessitates the electrochemical setup to allow an accurate and very fast acquisition of the current. Generally, a carbon microelectrode is utilised during such experiments due to low capacitive current. The microelectrode was bevelled to a 45° angle and then positioned a few micrometres from the cell to be analysed[32]. Positioning of the microelectrode (adjacent to the single cell) was accomplished using micromanipulator. It is essential to understand why the electrode was placed close to the cell surface. Since

a large concentration does not mean a large quantity, a small number of molecules may correspond to a large concentration by limiting the volume in which these molecules are released[30].

In this work, the response of a phenylsilane hydrogenated carbon electrode was recorded using differential pulse voltammetry following stimulation using 0.1 M KCl. The peak position of dopamine released from the SH-SY5Y cells was observed at +0.15 V as shown in Figure 5.2 (A). To confirm the identity of the peak, the response of exogenously applied 10, 20 and 30 μM dopamine was recorded as illustrated in Figure 5.2 (B). The peak position slightly shifts from +0.15 V to +0.14 V after dopamine was applied exogenously. The oxidation peak potential of dopamine at most carbon-based electrodes has been reported to occur at ~0.15 V[33]. A single peak obtained between -0.1 V and +0.6 V further showed that no other interfering species were oxidised within this potential range. These cells express properties for tyrosine hydroxylase, and produce dopamine and norepinephrine but only appear to store dopamine[19]. During simultaneous detection of dopamine and serotonin using a graphene-iron-tetrasulfophthalocyanine coated carbon fibre microelectrode, Zu *et al.*[34] observed similar peaks for dopamine and serotonin at +0.158 V and +0.325 V, respectively.

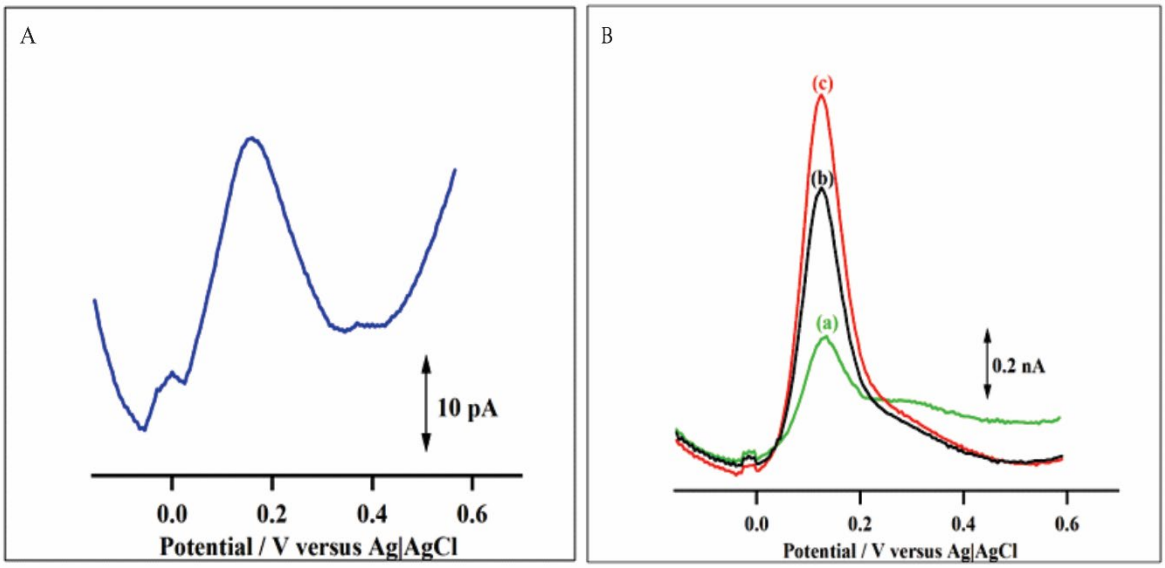

Figure 5.2. Differential pulse voltammogram of (A) K^+ triggered dopamine release and (B) exogenously applied (a) 10 µM, (b) 20 µM and (c) 30 µM dopamine in the SH-SY5Y cells at a triethylsilane hydrogenated carbon electrode. Scan rate 20 mV s^{-1}.

5.6.2 Amperometric detection of K^+ stimulated dopamine release from SH-SY5Y cells

A real-life biological sample widely used in Parkinson's disease research is the neuroblastoma SH-SY5Y cell line and it is a good model for studying the neurotoxic and neuroprotective effects of dopamine related compounds as they also express dopamine transporter, the vesicular monoamine transporter 2, D_2 and D_3 dopamine receptors[20]. The electrochemical monitoring of exocytosis events is generally carried out using either fast scan cyclic voltammetry or constant potential amperometry. During amperometric measurements, working electrode is held at a potential that is sufficient to oxidise or reduce the analyte of interest and the current, quantitatively related to the analyte by Faraday's law, is recorded as a function of time[35-36]. Amperometric detection has several advantages in understanding the chemical

communication in the brain such as fast temporal resolution and low limits of detection[37].

The concentration changes of K^+ in the brain have been reportedly linked to several neurological disorders including the abnormal release of neurotransmitters[38], suggesting that real time monitoring of K^+ stimulated dopamine release from neural cells is important for the understanding of dopaminergic dysfunctions[39]. In this work, amperometry was used to record the stimulated release of dopamine as a function of time, where the potential of the working carbon electrode was held at +0.5 V (versus a Ag|AgCl reference electrode). This oxidation potential of +0.5 V was estimated from the cyclic voltammogram of dopamine in pH 7.4 citrate/phosphate buffer. Spike-like electrical signals were observed after addition of K^+ indicating the release of dopamine. An elevated concentration of extracellular K^+ causes the depolarisation of dopaminergic cells and consequently triggers exocytosis by opening voltage-sensitive Na^+ channels, which causes the subsequent opening of voltage-sensitive Ca^{2+} channels[40]. K^+-induced cell membrane depolarisation is known to cause the fusion of dopamine containing vesicles with cell membrane and release dopamine into the extracellular region[41]. Dopamine release is measured by recording amperometric current signal to the oxidation of dopamine release after being triggered. Figure 5.3 (A) and (B) shows the amperometric responses of SH-SY5Y cells upon K^+ stimulation at a triethylsilane and phenylsilane hydrogenated electrode respectively. After each K^+ injection, strong dopamine peaks are observed indicating release. The current is produced by the transfer of electrons during the oxidation of the secreted, oxidisable neurotransmitter on the surface of the electrode and therefore the size of the current is proportional to the quantity of oxidisable neurotransmitter[42]. The rising phase of the peaks could possibly be from dopamine exocytosis events and the decay phase may be triggered by dopamine

re-uptake through dopamine transporter. The neuroblastoma SH-SY5Y cells is also known to show dopamine transporter characteristics as well as dopamine receptors[43]. For example, Mir *et al*.[41] studied the K^+ induced dopamine release from dopaminergic cells (PC12) using an ethylenediaminetetraacetic acid immobilised-poly 1,5-diaminonaphthalne layer comprising graphene oxide and gold nanoparticles on a glassy carbon electrode. They reported that K^+-stimulated dopamine release can be inhibited by a calcium channel inhibitor called Nifidipine. In addition, the changes in the amperometric rise and decline phases could potentially be due to diffusion towards the electrode (rising phase) and away from the electrode (decay phase). This technique has been successfully used for studies of neurotransmitter levels in the brain and brain slices[44], exocytosis of small synaptic vesicles[45], neuroblastoma and other cells[46-47].

Using KCl solution, the release of the neurotransmitters from vesicles docked at the cell membrane is triggered. A constant potential between the working carbon electrode and the reference electrode leads to oxidation of electroactive neurotransmitters where the release events are observed in the form of current transients, which appear as spikes in a current versus time plot. The observed spikes appear to be the consequence of fusion of the storage vesicles, discharge of the contents and subsequent oxidation of catecholamines to the electrode surface and are consistent with the hypothesis of exocytosis as mode a mode for cellular secretion[35]. A representative spike like signal is illustrated in Figure 5.3 (C).

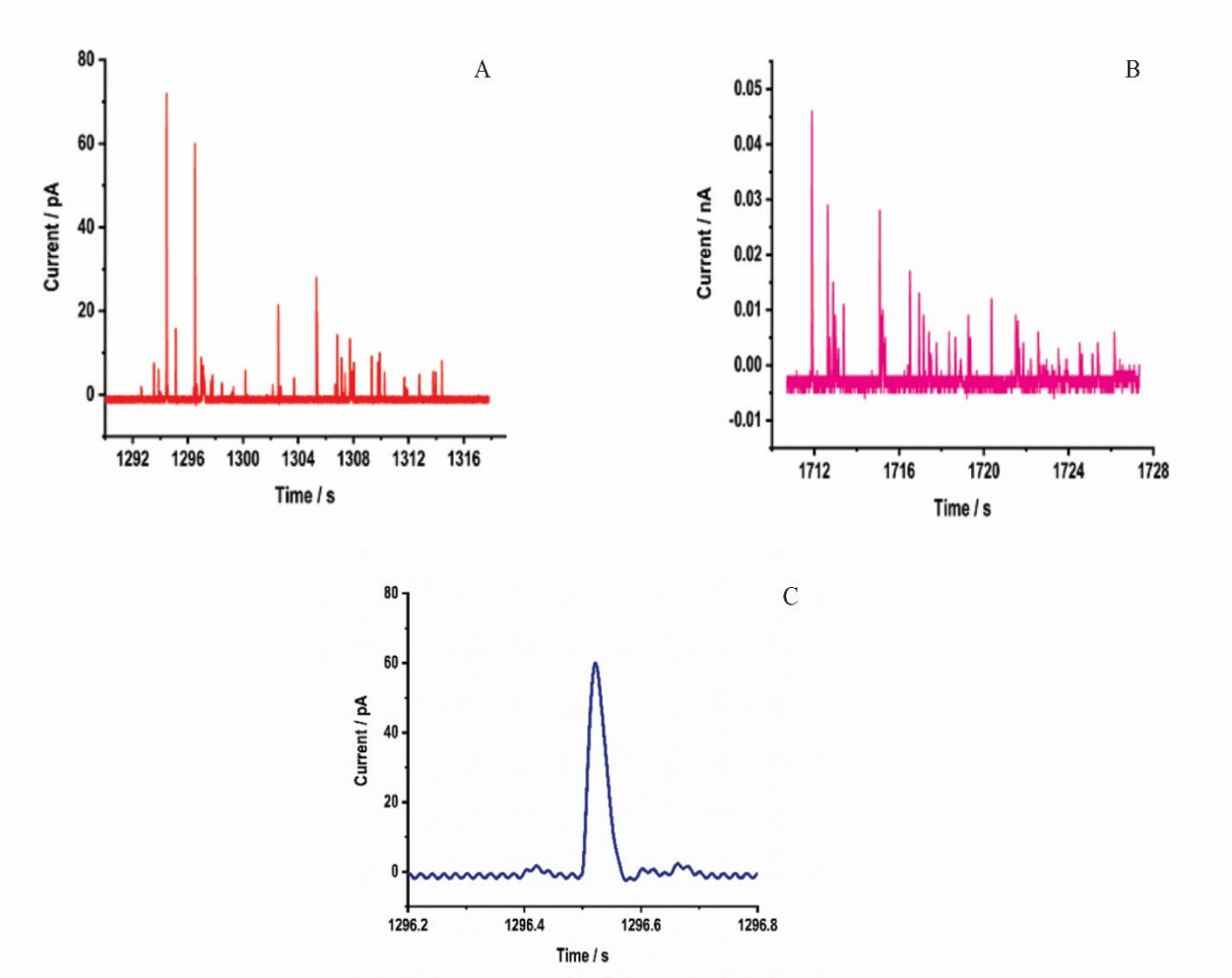

Figure 5.3. K^+ triggered amperometric dopamine spikes recorded from SHSY-5Y dopamine cells at (A) triethylsilane hydrogenated electrode and (B) a phenylsilane hydrogenated electrodes and (C) single amperometric dopamine spike initiated by K^+ stimulation.

As an example, using amperometry, Wang *et al*.[44] recorded random bursts of hundreds to thousands of rapid spontaneous glutamate exocytotic release evens at approximately 30 Hz frequency in the nucleus accumbens of a rodent brain slices. The characterisation of the single sub millisecond exocytosis release revealed the heterogeneity in spike shape characteristics and size quantal release further suggesting variability in fusion pore dynamics controlling glutamate release in brain cells[44].

5.6.3 Dopamine detection in a brain slice using hydrogenated carbon electrodes

To assess the stability and robustness of hydrogenated conical-tip carbon electrodes for dopamine detection real-life biological samples, oxidation of dopamine was monitored upon exogenously injecting different concentrations of dopamine in a brain slice. A representative time versus current graph is shown in Figure 5.4(A) and the representative fast scan cyclic voltammograms obtained are shown in Figure 5.4(B). Figure 5.4 A and B show the increase in the oxidation peak current with increase in the concentration of exogenously applied dopamine, while the electrode was implanted in the brain slice to detect dopamine in a tissue sample without the occurrence of fouling arising from dopamine oxidation product as well as the biomolecules. This further shows the stability of the hydrogenated carbon electrodes in the extracellular matrix.

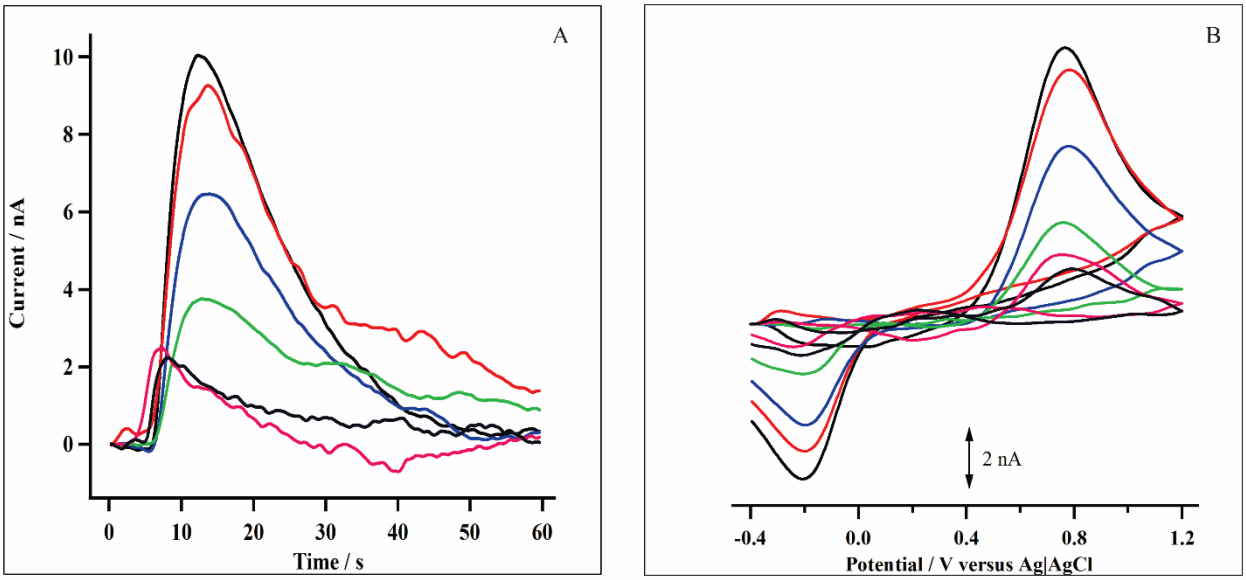

Figure 5.4. Current versus time response (A) and cyclic voltammograms of dopamine oxidation (B) at a phenylsilane hydrogenated carbon electrode after 0.84, 5.7, 12.5, 27.7, 48.8, and 73.1 fmol of dopamine was exogenously injected in a brain slice.

5.6.4 Evaluating Fouling in SH-SY5Y cells and Brain Slices

5.6.4.1 Electrochemical cycling SH-SY5Y cells

The adsorption of neurotransmitter dopamine oxidation product on sensing surfaces can dramatically jeopardise the practicality of the sensor [48]. *In vivo* electrochemical measurements are characteristically carried out in a complex matrix, composed of a wide diversity of biomolecules that are potentially able to affect detection by adsorbing on the sensing surfaces[48]. In Chapter 4, the passivation of the hydrogenated carbon electrode surface by dopamine oxidation product was evaluated. In this study, fouling by dopamine oxidation product was assessed in SH-SY5Y cells where ten consecutive cyclic voltammograms of exogenously applied dopamine were recorded. Figure 5.5 shows a series of successive cyclic voltammograms at a (A) triethylsilane and (B)

phenylsilane hydrogenated carbon electrodes containing 10 µM exogenously injected dopamine to the SH-SY5Y cells.

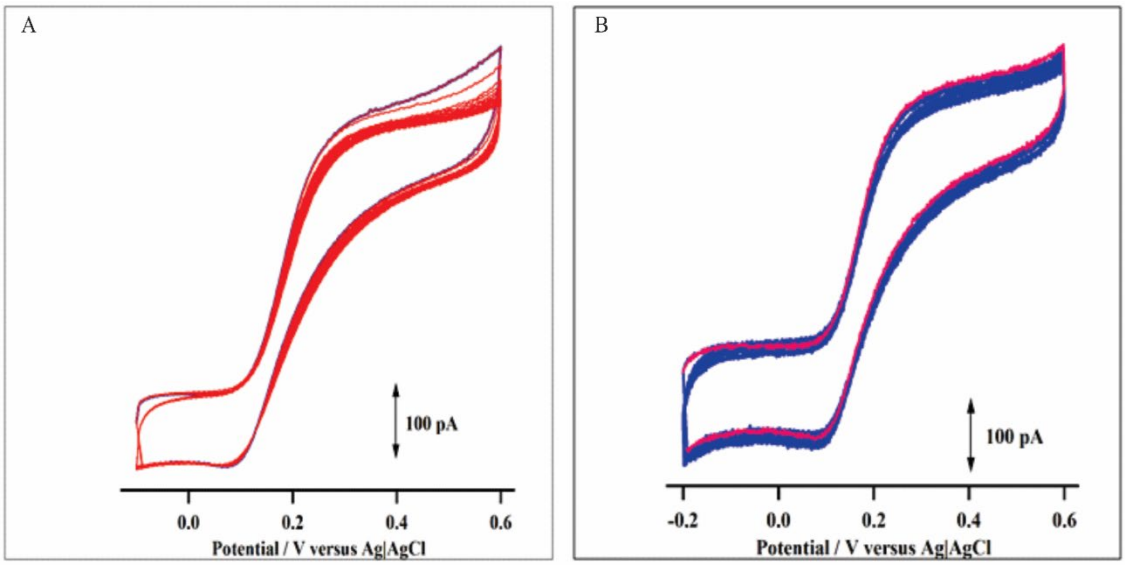

Figure 5.5. Ten consecutive cyclic voltammograms of exogenously applied 10 µM dopamine in SH-SY5Y cell line at (A) triethylsilane hydrogenated carbon electrodes and (B) phenylsilane hydrogenated carbon electrodes. Both the blue (in A) and pink trace (in B) are the first cyclic voltammograms. Scan rate 100 mV s^{-1}.

A 6% and 1.6% decline in the I_{lim} was estimated after the first three cycles at triethylsilane and phenylsilane hydrogenated electrodes, respectively, after which the current remained stable up to the tenth cycle. The initial 6% decline in the I_{lim} possibly arose from the dopamine oxidation product formed or the adsorption of cell membrane after exocytosis on to the exposed sites on sensing surface after the first three cycles. A smaller decline in the I_{lim} at phenylsilane hydrogenated carbon electrodes could possibly explain the effective surface coverage by the phenylsiloxane dendrimers that further protects the sensing surface from non-targeted species. The stable current obtained thereafter possibly explains resistance to surface fouling from cell debris or the dopamine-*o*-quinone and that dopamine fouling occurred within the first 2-3 cycles.

5.6.4.2 Biofouling

Surface fouling of hydrogenated carbon electrodes was next evaluated in SH-SY5Y cell line and in brain slices. The peak current after first K^+ stimulation versus the peak current after 1 h was used to estimate degree of fouling at the hydrogenated electrodes. Figure 5.6 illustrates the degree of electrode fouling evaluated by height of peak current after 1 h of amperometric recording.

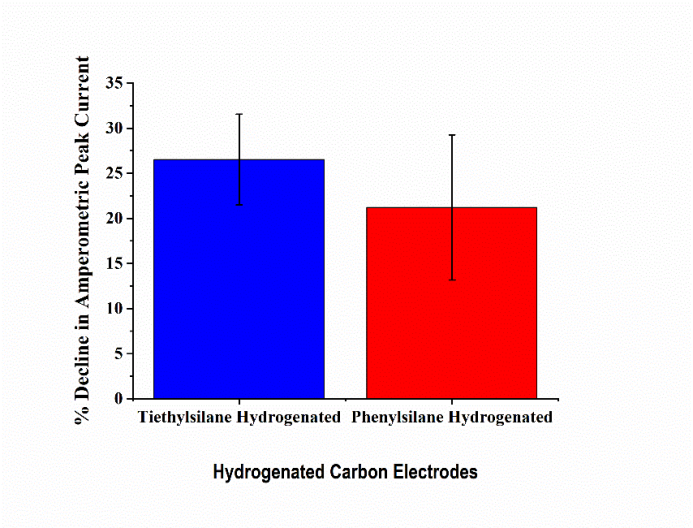

Figure 5.6. Percentage decline in the height of peak current at triethylsilane and phenylsilane hydrogenated carbon electrodes during amperometric recording of K^+ stimulated dopamine in SH-SY5Y cells for 1 h.

Accordingly, a respective 26% decline and 21% decline in the peak current was estimated at triethylsilane and phenylsilane hydrogenated carbon electrodes after 1 h of amperometric measurement. No noticeable difference in the percentage change in the peak current was observed between triethylsilane and phenylsilane hydrogenated electrodes after being incubated in the SH-SY5Y cells. Both the types of hydrogenation

produced a surface with low surface oxygen containing functional groups and a non-polar surface that limited the adsorption of non-targeted species present in the matrix.

The robustness of the hydrogenated carbon electrodes was also evaluated in brain slices to determine their practicality to detect dopamine in a biological tissue, which would otherwise foul the electrode surface. To evaluate this, the electrodes were implanted in a brain slice for 1 h while repeatedly cycling the potential from -0.4 V to +1.2 V versus Ag|AgCl at 400 V s^{-1}. Subsequent incubation in the brain slices, a comparison between the peak currents before incubation versus after incubation was used to study the degree of surface fouling. Figure 5.7 (A) shows the peak current remaining after incubation of small carbon electrodes in brain slices for 1 h, (B) shows the fast scan cyclic voltammograms obtained at a non-hydrogenated electrode, (C) cyclic voltammograms obtained at triethylsilane hydrogenated carbon electrode and (D) cyclic voltammograms obtained at a phenylsilane hydrogenated carbon electrodes (a) before and (b) after incubation in brain tissue. As shown in Figure 5.7 (A), only 23% oxidation peak current persisted after a non-hydrogenated electrode was exposed to the brain tissue. This is good agreement with other studies involving carbon-based electrodes for detection of neurotransmitters in a biological tissue. For example, Singh *et al*.[49] reported 25-40% decrease in sensitivity of bare carbon fibre microelectrode upon incubation in bovine serum albumin. Higher magnitude decreases in sensitivity (60-70%) was observed after incubation in brain tissue[49].

In evaluating the effectiveness of the hydrogenation procedure for developing an electrode surface with antifouling characteristics, triethylsilane and phenylsilane hydrogenated carbon electrodes were further incubated in brain tissues for 1 h. The magnitude of current decline was estimated by comparing the response to dopamine

before and after incubation in brain tissues. Figure 5.8 shows the cyclic voltammograms obtained at (A) triethylsilane and (B) phenylsilane hydrogenated electrode (a) before and (b) after incubation in brain tissue for 1 h. As illustrated in Figure 5.7 (A), 62% and 64% current remained following incubation and repeated cycling at high potential range at triethylsilane and phenylsilane hydrogenated electrodes, respectively. Compared to results obtained incubating electrodes in laboratory synthetic fouling solution (Chapter 4.9.1) and dopamine cells (Section 5.6.4.2), the hydrogenated carbon electrodes showed slightly lower resistance to biofouling. This is likely to be a chemically different matrix used in evaluating antifouling property when incubated in brain slices. For example, 5-hydroxyindoelacetic acid present in the extracellular fluid, which is a metabolite of serotonin with a physiological concentration ~10 times greater than that of serotonin[50], is reportedly a very strong fouling agent that adsorbs on surfaces even without application of an oxidation potential during detection of serotonin[51]. Addtionally, there is a possibility of incomplete hydrogenation on the small carbon electrodes, leaving some polar functional groups still available on the electrode surface. Meanwhile, only 22% current remained at non-hydrogenated carbon electrodes after being incubated in brain tissues for 1 h. This comparison confirms the severe electrode fouling during dopamine oxidation in brain tissues at non-hydrogenated carbon electrodes.

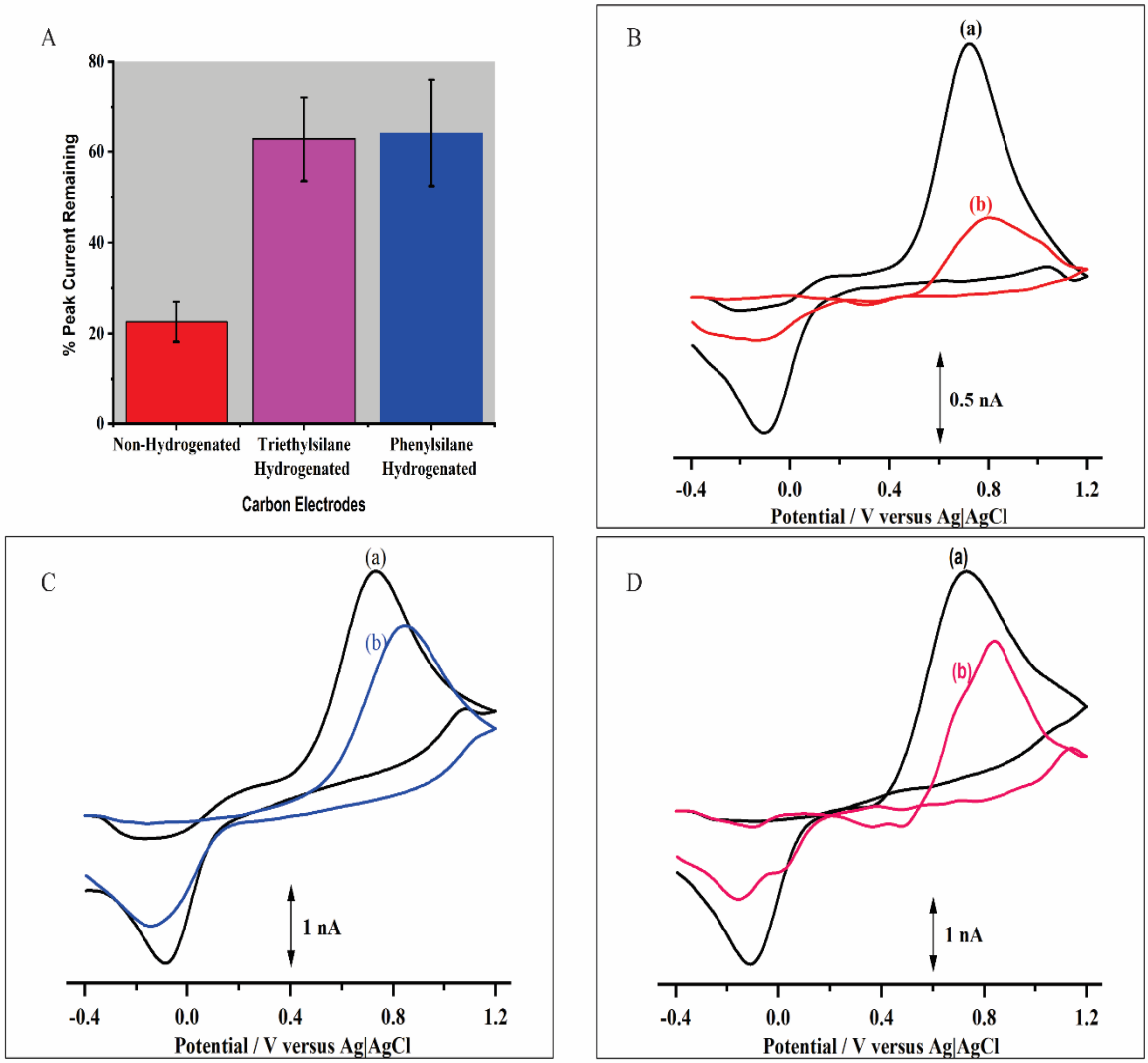

Figure 5.7. (A) A plot showing the % oxidation peak current remaining after the fabricated electrodes were incubated in a brain slice; the error bars represent 95% confidence limits and (B) the cyclic voltammograms obtained at a non-hydrogenated carbon electrode, (B) triethylsilane hydrogenated carbon electrode and (C) phenylsilane hydrogenated carbon electrode in 5 µM dopamine (a) before and (b) after exposure to brain tissue for 1 h while the potential was cycled from -0.4 V to +1.2 V versus Ag|AgCl at 400 Vs^{-1}.

In this study, electrochemical and biological fouling of hydrogenated carbon electrodes was assessed in two real-life biological samples, SH-SY5Y cells and brain slices. The results show that these electrodes are resistant to chemical fouling and are only affected

by biological fouling to a degree. More specifically, a 77% loss in the dopamine oxidation peak current shows the degree of a non-hydrogenated carbon electrode fouling in a biological matrix. The decrease is likely due to a combination of both chemical and biological fouling. A typical carbon surface encompasses oxygen containing functional groups which makes the surface hydrophilic[52]. The hydrophilic surface interacts with the hydrophilic proteins present in a biological matrix, as well as electrostatic interactions with electrodes possessing ionisable functional groups such as carboxylic acid[53-54]. During amperometric measurement of serotonin, an 85% loss of oxidation current was estimated at a carbon fibre electrode after 10 injections of serotonin[55].

There are specific sites on the carbon surface known to modulate the resistance to both chemical and biological fouling[56]. For example, Weese *et al*.[57] recently reported that defect sites modulate fouling resistance on carbon nanotubes fibre electrodes. Their work–investigated the chemical fouling from serotonin oxidation product, while biological fouling was assessed by implanting the electrodes in a brain slice for 2 h. The authors concluded that defects sites are detrimental to chemical fouling but are useful for biofouling[57].

The performance of the hydrogenated carbon electrodes in the two real-life biological samples show that they are robust and resistant biological fouling with 38% and 36% loss after being implanted in brain slices. The antifouling properties are attributed to the formation of a H-terminated and low oxygen containing species with the formation of siloxane dendrimers *via* the phenolic functional group on the electrode surface after silane hydrogenation. As discussed in Chapter 3, the electrochemical and spectroscopic characterisation revealed reduction of oxygen containing species after hydrogenation.

The reduction in the I_{lim} could be due to reduction in the mass transport due to the presence of siloxane film on a hydrogenated surface. X-ray photoelectron spectroscopic results in Section 3.7.4 confirmed the removal of surface functional groups, as well as formation of siloxane dendrimers on the hydrogenated carbon surface. In addition, Raman spectroscopic characterisation revealed higher ratio of sp^3 to sp^2 hybridised carbon on the hydrogenated surfaces forming an sp^3 rich film. The fouling resistance of silane hydrogenated carbon electrodes is likely due to the presence of inert sp^3 carbon structure that reduces adsorption. These results, in combination with those obtained using laboratory synthetic fouling solution, as well as in the two real-life biological samples, confirmed the antifouling properties of triethylsilane and phenylsilane hydrogenated carbon electrodes. In addition to all other surface properties of the hydrogenated carbon electrodes, the siloxane dendrimers formed on the electrode surface played a vital role in protecting the surface from the fouling agents. The superior performance of the phenylsilane hydrogenated electrodes is ascribed to the presence of bulkier siloxane dendrimers with phenyl rings that suppressed the adsorption of non-targeted species, while facilitating the oxidation of dopamine *via* π-electrons. Our group reported the antifouling properties of *n*-butylsilane hydrogenated carbon electrodes where the charge transfer resistance (R_{ct}) was estimated to be 2.2 kΩ, which essentially remained unchanged after 1-week incubation in the fouling solution. The R_{ct} of non-hydrogenated carbon electrodes increased by 15 and 45 times after a 30-min and 1-week incubation in a laboratory synthetic fouling solution[58].

Boron doped diamond electrodes have been reported to provide more stable, sensitive, reproducible measurements in the constant potential mode, selective oxidation of dopamine in the presence of ascorbic acid, an increase in the mass transport and the ability for use in high resistance media[53, 59-60]. For example, a slower degree of fouling

was observed at a boron doped diamond electrode (50% versus 85% at carbon fibre electrodes) after 10 injections of serotonin during amperometric measurement[55]. Meijs *et al*.[61] studied the biofouling resistance of boron-doped diamond electrodes and compared them to titanium nitride (TiN) electrodes. Initially, the measurement was conducted in an albumin solution and their results showed decreased capacitive current at the TiN electrode, but not at the boron-doped diamond electrodes. This indicated that the boron-doped diamond surface did not promote bovine serum albumin adsorption. The authors reported a decrease in the ΔEp from 496 ± 28 mV to 452 ± 20 mV at boron-doped diamond electrodes after adding albumin, which supported fouling resistant characteristics at boron doped diamond electrodes compared to ΔEp from 106 ± 10 mV to 136 ± 18 mV at TiN electrodes. The protein adsorption on the two surfaces was also evaluated where both electrodes were incubated in a fluorescein isothiocyanate-conjugated bovine serum albumin solution so that surface fouling could be assessed by fluorescence microscopy. Their observation showed that protein adsorption on boron doped diamond surfaces was ~52% lower than that of TiN surface as no fluorescence was detectable at the boron doped diamond surface[61]. The results herein suggest that hydrogenation is a successful method of resisting fouling by non-targeted species in a biological fluid.

5.7 Concluding Remarks

The major aim of this work was to evaluate the antifouling characteristic of the triethylsilane and phenylsilane hydrogenated carbon electrodes in an *in vitro* biological environment. In this regard, the electrodes were used to detect dopamine and their antifouling property was assessed in dopaminergic neuronal cell line SH-SY5Y and brain slices.

Using amperometry, a constant potential of +0.5 V (versus a Ag|AgCl reference electrode) was applied to a hydrogenated carbon electrode to oxidise K^+ stimulated dopamine release on the electrode surface. Spike-like signals as a function of time were obtained after K^+ was injected, suggesting the K^+ played a vital role in the opening of the vesicles. The amperometric measurement was carried out for 1 h. The peak height changes was measured as a function of time. Accordingly, triethylsilane hydrogenated electrodes lost 26% amperometric current while the phenylsilane hydrogenated electrodes lost 21% peak current. In addition, the electrochemical fouling arising from dopamine oxidation product was assessed following consecutive cycling in the presence of exogenously applied dopamine. We observed 6% decline in the I_{lim} after first three cycles at triethylsilane hydrogenated, while only 1.6% was estimated at that at phenylsilane hydrogenated electrodes.

Fouling was also assessed by incubating hydrogenated carbon electrodes in brain slices. Accordingly, 62% and 64% current remained after 1 h incubation in brain slices. Compared to the 77% fouling at non-hydrogenated carbon electrodes, the degree of fouling was improved at hydrogenated carbon electrodes, indicating their antifouling capability. However, a 38% and 36% degree of fouling was estimated from results obtained in brain slices, which is higher than that (23% and 18%) in a laboratory synthetic fouling solution and (26% and 21%) in cells using triethylsilane and phenylsilane hydrogenated electrodes, respectively. There is a possibility that electrodes used in this study were not completely hydrogenated. Unfortunately, there was a limited opportunity in conducting the experiments involving brain slices in the present study.

5.8 References

(1) Emran, M. Y.; Shenashen, M. A.; Mekawy, M.; Azzam, A. M.; Akhtar, N.; Gomaa, H.; Selim, M. M.; Faheem, A.; El-Safty, S. A. Ultrasensitive in-vitro monitoring of monoamine neurotransmitters from dopaminergic cells. *Sensors and Actuators B: Chemical* **2018,** *259*, 114-124, DOI: https://doi.org/10.1016/j.snb.2017.11.156.

(2) Venton, B. J.; Wightman, R. M. Psychoanalytical Electrochemistry: Dopamine and Behavior. *Analytical Chemistry* **2003,** *75* (19), 414 A-421 A, DOI: 10.1021/ac031421c.

(3) Buddhala, C.; Loftin, S. K.; Kuley, B. M.; Cairns, N. J.; Campbell, M. C.; Perlmutter, J. S.; Kotzbauer, P. T. Dopaminergic, serotonergic, and noradrenergic deficits in Parkinson disease. *Annals of Clinical and Translational Neurology* **2015,** *2* (10), 949-959, DOI: 10.1002/acn3.246.

(4) Alesch, F.; Pinter, M. M.; Helscher, R. J.; Fertl, L.; Benabid, A. L.; Koos, W. T. Stimulation of the ventral intermediate thalamic nucleus in tremor dominated Parkinson's disease and essential tremor. *Acta Neurochir (Wien)* **1995,** *136* (1-2), 75-81.

(5) Sangubotla, R.; Kim, J. Recent trends in analytical approaches for detecting neurotransmitters in Alzheimer's disease. *TrAC Trends in Analytical Chemistry* **2018,** *105*, 240-250, DOI: https://doi.org/10.1016/j.trac.2018.05.014.

(6) Moon, J.-M.; Thapliyal, N.; Hussain, K. K.; Goyal, R. N.; Shim, Y.-B. Conducting polymer-based electrochemical biosensors for neurotransmitters: A review. *Biosensors and Bioelectronics* **2018,** *102*, 540-552, DOI: https://doi.org/10.1016/j.bios.2017.11.069.

(7) Adams, R. N. Probing brain chemistry with electroanalytical techniques. *Analytical Chemistry* **1976,** *48* (14), 1126A-1138A, DOI: 10.1021/ac50008a001.

(8) Bledsoe, J. M.; Kimble, C. J.; Covey, D. P.; Blaha, C. D.; Agnesi, F.; Mohseni, P.; Whitlock, S.; Johnson, D. M.; Horne, A.; Bennet, K. E.; Lee, K. H.; Garris, P. A. Development of the wireless instantaneous neurotransmitter concentration system for intraoperative neurochemical monitoring using fast-scan cyclic voltammetry. *J. Neurosurg.* **2009,** *111* (4), 712-723, DOI: 10.3171/2009.3.JNS081348.

(9) Lowry, J. P.; Miele, M.; O'Neill, R. D.; Boutelle, M. G.; Fillenz, M. An amperometric glucose-oxidase/poly(o-phenylenediamine) biosensor for monitoring brain extracellular glucose: in vivo characterisation in the striatum of freely-moving rats. *Journal of Neuroscience Methods* **1998,** *79* (1), 65-74, DOI: https://doi.org/10.1016/S0165-0270(97)00171-4.

(10) Johnson, J. A.; Rodeberg, N. T.; Wightman, R. M. Measurement of Basal Neurotransmitter Levels Using Convolution-Based Nonfaradaic Current Removal. *Analytical Chemistry* **2018,** *90* (12), 7181-7189, DOI: 10.1021/acs.analchem.7b04682.

(11) Calipari, E. S.; Huggins, K. N.; Mathews, T. A.; Jones, S. R. Conserved dorsal–ventral gradient of dopamine release and uptake rate in mice, rats and rhesus macaques. *Neurochemistry International* **2012,** *61* (7), 986-991, DOI: https://doi.org/10.1016/j.neuint.2012.07.008.

(12) Greene, L. A.; Tischler, A. S. Establishment of a noradrenergic clonal line of rat adrenal pheochromocytoma cells which respond to nerve growth factor. *Proceedings of the National Academy of Sciences of the United States of America* **1976,** *73* (7), 2424-2428.

(13) Xicoy, H.; Wieringa, B.; Martens, G. J. M. The SH-SY5Y cell line in Parkinson's disease research: a systematic review. *Molecular neurodegeneration* **2017,** *12* (1), 10-10, DOI: 10.1186/s13024-017-0149-0.

(14) Chiu, W.-T.; Lin, C.-M.; Tsai, T.-C.; Wu, C.-W.; Tsai, C.-L.; Lin, S.-H.; Chen, J.-J. J. Real-Time Electrochemical Recording of Dopamine Release under Optogenetic Stimulation. *PLOS ONE* **2014,** *9* (2), e89293, DOI: 10.1371/journal.pone.0089293.

(15) Greene, L. A.; Rein, G. Release, storage and uptake of catecholamines by a clonal cell line of nerve growth factor (NGF) responsive pheochromocytoma cells. *Brain Research* **1977,** *129* (2), 247-263, DOI: https://doi.org/10.1016/0006-8993(77)90005-1.

(16) Shinohara, H.; Wang, F. Real-Time Detection of Dopamine Released from a Nerve Model Cell by an Enzyme-Catalyzed Luminescence Method and Its Application to Drug Assessment. *Analytical Sciences* **2007,** *23* (1), 81-84, DOI: 10.2116/analsci.23.81.

(17) Yang, C.; Liu, M.-M.; Bai, F.-Q.; Guo, Z.-Z.; Liu, H.; Zhong, G.-X.; Peng, H.-P.; Chen, W.; Lin, X.-H.; Lei, Y.; Liu, A.-L. An electrochemical biosensor for sensitive detection of nicotine-induced dopamine secreted by PC12 cells. *Journal of Electroanalytical Chemistry* **2019,** *832*, 217-224, DOI: https://doi.org/10.1016/j.jelechem.2018.10.018.

(18) Adams, K. L.; Jena, B. K.; Percival, S. J.; Zhang, B. Highly Sensitive Detection of Exocytotic Dopamine Release Using a Gold-Nanoparticle-Network Microelectrode. *Analytical Chemistry* **2011,** *83* (3), 920-927, DOI: 10.1021/ac102599s.

(19) Biedler, J. L.; Roffler-Tarlov, S.; Schachner, M.; Freedman, L. S. Multiple Neurotransmitter Synthesis by Human Neuroblastoma Cell Lines and Clones. *Cancer Research* **1978,** *38* (11 Part 1), 3751.

(20) Xicoy, H.; Wieringa, B.; Martens, G. J. M. The SH-SY5Y cell line in Parkinson's disease research: a systematic review. *Molecular Neurodegeneration* **2017,** *12* (1), 10, DOI: 10.1186/s13024-017-0149-0.

(21) Dingledine, R. Hippocampus. In *Brain Slices*; Dingledine, R., Ed.; Springer US: Boston, MA, 1984; pp 87-112.

(22) Cho, S.; Wood, A.; Bowlby, M. R. Brain slices as models for neurodegenerative disease and screening platforms to identify novel therapeutics. *Curr. Neuropharmacol.* **2007,** *5* (1), 19-33, DOI: 10.2174/157015907780077105.

(23) Hovde, M. J.; Larson, G. H.; Vaughan, R. A.; Foster, J. D. Model systems for analysis of dopamine transporter function and regulation. *Neurochemistry International* **2019,** *123*, 13-21, DOI: https://doi.org/10.1016/j.neuint.2018.08.015.

(24) Burrell, M. H.; Atcherley, C. W.; Heien, M. L.; Lipski, J. A Novel Electrochemical Approach for Prolonged Measurement of Absolute Levels of Extracellular Dopamine in Brain Slices. *ACS Chemical Neuroscience* **2015,** *6* (11), 1802-1812, DOI: 10.1021/acschemneuro.5b00120.

(25) Yang, C.; Hu, K.; Wang, D.; Zubi, Y.; Lee, S. T.; Puthongkham, P.; Mirkin, M. V.; Venton, B. J. Cavity Carbon-Nanopipette Electrodes for Dopamine Detection. *Analytical Chemistry* **2019,** *91* (7), 4618-4624, DOI: 10.1021/acs.analchem.8b05885.

(26) Shipley, M. M.; Mangold, C. A.; Szpara, M. L. Differentiation of the SH-SY5Y Human Neuroblastoma Cell Line. *Journal of visualized experiments : JoVE* **2016,** (108), 53193-53193, DOI: 10.3791/53193.

(27) Barbosa, D. J.; Capela, J. P.; de Lourdes Bastos, M.; Carvalho, F. In vitro models for neurotoxicology research. *Toxicology Research* **2015,** *4* (4), 801-842, DOI: 10.1039/C4TX00043A.

(28) Zhang, M.; Yu, P.; Mao, L. Rational Design of Surface/Interface Chemistry for Quantitative in Vivo Monitoring of Brain Chemistry. *Accounts of Chemical Research* **2012,** *45* (4), 533-543, DOI: 10.1021/ar200196h.

(29) Kim, D.-S.; Kang, E.-S.; Baek, S.; Choo, S.-S.; Chung, Y.-H.; Lee, D.; Min, J.; Kim, T.-H. Electrochemical detection of dopamine using periodic cylindrical gold nanoelectrode arrays. *Scientific Reports* **2018,** *8* (1), 14049, DOI: 10.1038/s41598-018-32477-0.

(30) Amatore, C.; Guille-Collignon, M.; Lemaitre, F. In *Recent investigations of single living cells with ultramicroelectrodes*, CRC Press: 2015; pp 439-468.

(31) Cans, A.-S.; Wittenberg, N.; Eves, D.; Karlsson, R.; Karlsson, A.; Orwar, O.; Ewing, A. Amperometric Detection of Exocytosis in an Artificial Synapse. *Analytical Chemistry* **2003,** *75* (16), 4168-4175, DOI: 10.1021/ac0343578.

(32) Lemaître, F.; Guille Collignon, M.; Amatore, C. Recent advances in Electrochemical Detection of Exocytosis. *Electrochimica Acta* **2014,** *140*, 457-466, DOI: https://doi.org/10.1016/j.electacta.2014.02.059.

(33) Britto, P. J.; Santhanam, K. S. V.; Ajayan, P. M. Carbon nanotube electrode for oxidation of dopamine. *Bioelectrochemistry and Bioenergetics* **1996,** *41* (1), 121-125, DOI: https://doi.org/10.1016/0302-4598(96)05078-7.

(34) Zhu, M.; Zeng, C.; Ye, J.; Sun, Y. Simultaneous in vivo voltammetric determination of dopamine and 5-Hydroxytryptamine in the mouse brain. *Applied Surface Science* **2018,** *455*, 646-652, DOI: https://doi.org/10.1016/j.apsusc.2018.05.190.

(35) Wightman, R. M.; Jankowski, J. A.; Kennedy, R. T.; Kawagoe, K. T.; Schroeder, T. J.; Leszczyszyn, D. J.; Near, J. A.; Diliberto, E. J.; Viveros, O. H. Temporally resolved catecholamine spikes correspond to single vesicle release from individual chromaffin cells. *Proceedings of the National Academy of Sciences* **1991,** *88* (23), 10754, DOI: 10.1073/pnas.88.23.10754.

(36) Jackowska, K.; Krysinski, P. New trends in the electrochemical sensing of dopamine. *Analytical and bioanalytical chemistry* **2013,** *405* (11), 3753-3771, DOI: 10.1007/s00216-012-6578-2.

(37) Barlow, S. T.; Louie, M.; Hao, R.; Defnet, P. A.; Zhang, B. Electrodeposited Gold on Carbon-Fiber Microelectrodes for Enhancing Amperometric Detection of Dopamine Release from Pheochromocytoma Cells. *Analytical Chemistry* **2018,** *90* (16), 10049-10055, DOI: 10.1021/acs.analchem.8b02750.

(38) Kofuji, P.; Newman, E. A. Potassium buffering in the central nervous system. *Neuroscience* **2004,** *129* (4), 1043-1054, DOI: https://doi.org/10.1016/j.neuroscience.2004.06.008.

(39) Pham Ba, V. A.; Cho, D.-g.; Hong, S. Nafion-Radical Hybrid Films on Carbon Nanotube Transistors for Monitoring Antipsychotic Drug Effects on Stimulated Dopamine Release. *ACS Applied Materials & Interfaces* **2019,** *11* (10), 9716-9723, DOI: 10.1021/acsami.8b18752.

(40) Zerby, S. E.; Ewing, A. G. The Latency of Exocytosis Varies with the Mechanism of Stimulated Release in PC12 Cells. *Journal of Neurochemistry* **1996,** *66* (2), 651-657, DOI: 10.1046/j.1471-4159.1996.66020651.x.

(41) Mir, T. A.; Akhtar, M. H.; Gurudatt, N. G.; Kim, J.-I.; Choi, C. S.; Shim, Y.-B. An amperometric nanobiosensor for the selective detection of K+-induced dopamine released from living cells. *Biosensors and Bioelectronics* **2015,** *68*, 421-428, DOI: https://doi.org/10.1016/j.bios.2015.01.024.

(42) Westerink, R. H. S. Exocytosis: Using Amperometry to Study Presynaptic Mechanisms of Neurotoxicity. *NeuroToxicology* **2004,** *25* (3), 461-470, DOI: https://doi.org/10.1016/j.neuro.2003.10.006.

(43) Arun, P.; Madhavarao, C. N.; Moffett, J. R.; Namboodiri, A. M. A. Antipsychotic drugs increase N-acetylaspartate and N-acetylaspartylglutamate in SH-SY5Y human neuroblastoma cells. *Journal of Neurochemistry* **2008,** *106* (4), 1669-1680, DOI: 10.1111/j.1471-4159.2008.05524.x.

(44) Wang, Y.; Mishra, D.; Bergman, J.; Keighron, J. D.; Skibicka, K. P.; Cans, A.-S. Ultrafast Glutamate Biosensor Recordings in Brain Slices Reveal Complex Single Exocytosis Transients. *ACS Chemical Neuroscience* **2019,** *10* (3), 1744-1752, DOI: 10.1021/acschemneuro.8b00624.

(45) Chen, P.; Xu, B.; Tokranova, N.; Feng, X.; Castracane, J.; Gillis, K. D. Amperometric Detection of Quantal Catecholamine Secretion from Individual Cells on Micromachined Silicon Chips. *Analytical Chemistry* **2003,** *75* (3), 518-524, DOI: 10.1021/ac025802m.

(46) Lama, R. D.; Charlson, K.; Anantharam, A.; Hashemi, P. Ultrafast Detection and Quantification of Brain Signaling Molecules with Carbon Fiber Microelectrodes. *Analytical Chemistry* **2012,** *84* (19), 8096-8101, DOI: 10.1021/ac301670h.

(47) Picollo, F.; Battiato, A.; Bernardi, E.; Marcantoni, A.; Pasquarelli, A.; Carbone, E.; Olivero, P.; Carabelli, V. Microelectrode Arrays of Diamond-Insulated Graphitic Channels for Real-Time Detection of Exocytotic Events from Cultured Chromaffin Cells and Slices of Adrenal Glands. *Analytical Chemistry* **2016,** *88* (15), 7493-7499, DOI: 10.1021/acs.analchem.5b04449.

(48) Harreither, W.; Trouillon, R.; Poulin, P.; Neri, W.; Ewing, A. G.; Safina, G. Cysteine residues reduce the severity of dopamine electrochemical fouling. *Electrochimica Acta* **2016,** *210*, 622-629, DOI: https://doi.org/10.1016/j.electacta.2016.05.124.

(49) Singh, Y. S.; Sawarynski, L. E.; Dabiri, P. D.; Choi, W. R.; Andrews, A. M. Head-to-Head Comparisons of Carbon Fiber Microelectrode Coatings for Sensitive and Selective Neurotransmitter Detection by Voltammetry. *Analytical Chemistry* **2011,** *83* (17), 6658-6666, DOI: 10.1021/ac2011729.

(50) Jackson, B. P.; Dietz, S. M.; Wightman, R. M. Fast-scan cyclic voltammetry of 5-hydroxytryptamine. *Anal. Chem.* **1995,** *67* (6), 1115-20, DOI: 10.1021/ac00102a015.

(51) Zestos, A. G.; Jacobs, C. B.; Trikantzopoulos, E.; Ross, A. E.; Venton, B. J. Polyethylenimine Carbon Nanotube Fiber Electrodes for Enhanced Detection of Neurotransmitters. *Analytical Chemistry* **2014,** *86* (17), 8568-8575, DOI: 10.1021/ac5003273.

(52) Hanssen Benjamin, L.; Siraj, S.; Wong Danny, K. Y., Recent strategies to minimise fouling in electrochemical detection systems. In *Reviews in Analytical Chemistry*, 2016; Vol. 35, p 1.

(53) Shin, D.; Tryk, D. A.; Fujishima, A.; Merkoçi, A.; Wang, J. Resistance to Surfactant and Protein Fouling Effects at Conducting Diamond Electrodes. *Electroanalysis* **2005,** *17* (4), 305-311, DOI: 10.1002/elan.200403104.

(54) McCreery, R. L. Advanced Carbon Electrode Materials for Molecular Electrochemistry. *Chemical Reviews* **2008,** *108* (7), 2646-2687, DOI: 10.1021/cr068076m.

(55) Patel, B. A.; Bian, X.; Quaiserová-Mocko, V.; Galligan, J. J.; Swain, G. M. In vitro continuous amperometric monitoring of 5-hydroxytryptamine release from enterochromaffin cells of the guinea pig ileum. *Analyst* **2007,** *132* (1), 41-47, DOI: 10.1039/B611920D.

(56) Güell, A. G.; Meadows, K. E.; Unwin, P. R.; Macpherson, J. V. Trace voltammetric detection of serotonin at carbon electrodes: comparison of glassy carbon, boron doped diamond and carbon nanotube network electrodes. *Physical Chemistry Chemical Physics* **2010,** *12* (34), 10108-10114, DOI: 10.1039/C0CP00675K.

(57) Weese, M. E.; Krevh, R. A.; Li, Y.; Alvarez, N. T.; Ross, A. E. Defect Sites Modulate Fouling Resistance on Carbon-Nanotube Fiber Electrodes. *ACS Sensors* **2019,** *4* (4), 1001-1007, DOI: 10.1021/acssensors.9b00161.

(58) Siraj, S.; McRae, C. R.; Wong, D. K. Y. Antifouling Characteristics of a carbon electrode surface hydrogenated by n-butylsilane reduction. *Electrochimica Acta* **2019**, DOI: https://doi.org/10.1016/j.electacta.2019.01.188.

(59) Cvačka, J.; Quaiserová, V.; Park, J.; Show, Y.; Muck, A.; Swain, G. M. Boron-Doped Diamond Microelectrodes for Use in Capillary Electrophoresis with Electrochemical Detection. *Analytical Chemistry* **2003,** *75* (11), 2678-2687, DOI: 10.1021/ac030024z.

(60) Suzuki, A.; Ivandini, T. A.; Yoshimi, K.; Fujishima, A.; Oyama, G.; Nakazato, T.; Hattori, N.; Kitazawa, S.; Einaga, Y. Fabrication, Characterization, and Application of Boron-Doped Diamond Microelectrodes for in Vivo Dopamine Detection. *Analytical Chemistry* **2007,** *79* (22), 8608-8615, DOI: 10.1021/ac071519h.

(61) Meijs, S.; Alcaide, M.; Sorensen, C.; McDonald, M.; Sorensen, S.; Rechendorff, K.; Gerhardt, A.; Nesladek, M.; Rijkhoff, N. J. M.; Pennisi, C. P. Biofouling resistance of boron-doped diamond neural stimulation electrodes is superior to titanium nitride electrodes in vivo. *J Neural Eng* **2016,** *13* (5), 056011.

CHAPTER 6: CONCLUSIONS AND RECOMMENDATIONS

6.1 Project Conclusions

Direct detection of targeted analytes in a complex biological matrix using conventional carbon electrodes is an enormous challenge due to the non-specific adsorption and severe biofouling of the electrode surface. Dopamine is among the important neurotransmitters involved in a variety of central nervous system functions. Abnormal levels of dopamine has been implicated with several neurological disorders[1]. For example, high levels of dopamine (>195.8 pmol L^{-1}) is known to be cardiotoxic leading to rapid heart rate, high blood pressure, and possible death of heart muscles; while a loss of dopamine containing neurons may result in Parkinson's disease[2]. Due to its crucial role in neurochemistry, detecting the levels of dopamine has attracted considerable research interest in the fields of electrochemistry as it can easily be oxidised at an electrode. However, one of the major challenges encountered during the electrochemical detection of dopamine *in vivo* using carbon-based electrodes is fouling, a phenomenon defined as the non-specific adsorption of high molecular weight amphiphilic proteins, peptides and lipids on a hydrophilic carbon surface. Such adsorbates impede sensor capability by reducing the electroactive area of the electrode resulting in diminishing signal transients. Notably, one of the ways of minimising electrode fouling is to use a hydrophobic carbon electrode. In this work, hydrophobic carbon electrodes were obtained by hydrogenating physically small conical-tip carbon electrodes using triethylsilane or phenylsilane in the presence of anhydrous dichloromethane and the catalyst, trispentaflourophenyl borane.

In this work, small carbon electrodes were initially fabricated using a procedure previously reported by our group[3]. Briefly, a quartz capillary was pulled down to a fine tip using a micropipette puller. Next, carbon was deposited at the tip and on the shank of the pulled capillary by thermally pyrolysing acetylene with the aid of a stream of counter-flowing nitrogen. To accomplish an electrical connection, graphite powder was packed through the larger end of the pulled capillary, followed by an electrical wire that was subsequently sealed with epoxy. In this way, physically small conical-tip carbon electrodes with an average tip diameter of ~2 μm and an axial length of carbon deposit of ~6 μm were routinely constructed.

To assess the functionality of the electrodes, all electrodes fabricated in this work were initially characterised using $[Ru(NH_3)_6]^{3+}$, an outer-sphere redox marker. Only functioning electrodes exhibiting a steady state response with a small capacitive current were used further in this study. Next, the functioning electrodes were hydrogenated using two silanes, triethylsilane and phenylsilane, in the presence of $B(F_5C_6)_3$ and anhydrous CH_2Cl_2. Following hydrogenation, the carbon electrodes were initially characterised using several spectroscopic techniques. The surface elemental composition of the hydrogenated carbon electrodes and non-hydrogenated carbon electrodes was assessed using x-ray photoelectron spectroscopy. The results showed a reduction in oxygen containing functional groups with formation of siloxane dendrimers via the phenol functionality on the surface (see Scheme 3.1 on page 87). Raman spectroscopy was then used to probe the sp^3/sp^2 ratio after hydrogenation. Our results show that after hydrogenation, the sp^2 hybridised carbon was successfully converted to sp^3 hybridised carbon, as indicated by an increase of the sp^3 carbon / sp^2 carbon ratio from 1.78 at non-hydrogenated electrodes to 2.2 and 2.7 after triethylsilane and phenylsilane hydrogenation, respectively. Clearly, such an increase in the sp^3

carbon / sp^2 carbon ratio indicates more sp^3 defects/disorders and smaller quantity of graphitic crystallite sp^2 hybridised carbon. The electrodes were next assessed using the corresponding cyclic voltammetry of $[Ru(NH_3)_6]^{3+}$, $[Fe(CN)_6]^{3-}$, dopamine, dihydroxyphenylacetic acid, 4-methylcatechol and anthraquinone 2,4 disulfonic acid. The I_{lim}, $E_{½}$ and waveslope of the hydrogenated electrodes were compared to those of non-hydrogenated carbon electrodes. After triethylsilane and phenylsilane hydrogenation, a ~20% and ~15% decline in the $[Fe(CN)_6]^{3-}$ I_{lim} was attributed to the loss of carbon-oxygen functional groups present on a typical carbon surface. A 22 mV positive shift in the $E_{½}$ was also observed after triethylsilane hydrogenation, which could potentially be due to the tunnelling effect caused by the formation of siloxane dendrimers. Additionally, we showed that the electron transfer kinetics of phenylsilane hydrogenated electrodes was 27% faster than that of triethylsilane hydrogenated electrodes. This is ascribed to the formation of phenylsiloxane dendrimers on the hydrogenated surface that facilitated the electron transfer kinetics via the phenyl ring.

The electroanalytical performance of the hydrogenated carbon electrodes was also evaluated. Accordingly, based on a signal/noise ratio of 3, the limit of detection was estimated to be 0.84 ± 0.35 μM (where the errors are represented by a 95% confidence interval; N=10) and 0.83 ± 0.14 μM (N=12) at triethylsilane and phenylsilane hydrogenated carbon electrodes, respectively, compared to 2.2 ± 0.99 μM (N=12) at non-hydrogenated carbon electrodes. The sensitivity at triethylsilane and phenylsilane hydrogenated electrode was estimated to be 23.2 ± 12.9 pA μM^{-1} (N=12) and 42.9 ± 22.7 pA μM^{-1} (N=12). One of the major interferents during dopamine detection *in vivo* is ascorbic acid. The selectivity of triethylsilane and phenylsilane hydrogenated carbon electrodes towards dopamine and ascorbic acid was next evaluated. The cyclic voltammograms obtained show that these hydrogenated carbon electrodes were more

sensitive to dopamine than ascorbic acid. The effects of ascorbic acid on dopamine oxidation was studied by consecutive cycling in a solution containing dopamine and ascorbic acid. The selectivity of triethylsilane hydrogenated carbon electrodes towards uric acid was also investigated using differential pulse voltammetry. The hydrogenated carbon electrodes showed good selectivity towards dopamine and uric acid with a dopamine oxidation peak at +0.2 V and a uric acid oxidation peak at +0.48 V.

The antifouling property of both triethylsilane and phenylsilane hydrogenated carbon electrodes was investigated in a laboratory synthetic fouling solution containing 2.0% (w/v) bovine serum albumin, 0.01% (w/v) cytochrome C, 0.001% (w/v) human fibrinopeptide and 1.0% (v/v) caproic acid in a pH 7.4 citrate/phosphate buffer mimicking the extracellular fluid. The non-hydrogenated and hydrogenated carbon electrodes were incubated in the fouling solution for the same duration and the degree of fouling was determined by comparing the I_{lim} before incubation and after incubation. Accordingly, the non-hydrogenated electrodes showed a 53% decline of the I_{lim} after 30 min incubation in the fouling solution. Similarly, the robustness and stability of the hydrogenated carbon electrodes in the fouling was also assessed. Only a respective 23% and 18% decline in the I_{lim} was observed at triethylsilane and phenylsilane hydrogenated electrodes. The improved antifouling property of the hydrogenated carbon electrodes is attributed to the low oxygen-containing functional groups and a hydrophobic surface as a result of hydrogenation, which reduced the interaction between proteins, peptides, and lipids and the hydrogenated carbon surface compared to a non-hydrogenated carbon surface. Additionally, the formation of bulky siloxane dendrimers on the surface during silane reduction also contributes to the antifouling property as the bulky siloxane dendrimers act as a physical barrier for non-specific adsorption.

Finally, the antifouling property of hydrogenated carbon electrodes was assessed by detecting dopamine in two real-life biological samples, namely (i) a neuroblastoma cell line SH-SY5Y and (ii) brain slices. In our work involving dopamine detection in the SH-SY5Y cell line, the cells were initially depolarised using a K^+ solution. Dopamine released was then monitored at a hydrogenated carbon electrode using amperometry by recording the oxidation current generated at the applied potential of +0.5 V as a function of time. Spike-like signals were obtained when K^+ was injected into the cells. Fouling was also assessed in these two real-life biological samples. The degree of fouling in cells was determined by the change in amperometric dopamine peak height response after 1 h. Accordingly, a respective 26% decline and 21% decline in the peak current was estimated at triethylsilane and phenylsilane hydrogenated carbon electrodes after 1 h of amperometric measurement. Similarly, the degree of fouling in brain slices was assessed based on the change in amperometric dopamine peak height response after implanting hydrogenated carbon electrodes in a freshly sliced mouse brain for 1 h. The response towards dopamine was compared to that before implantation to determine degree of fouling. A 62% and 64% current remained following incubation and repeated cycling at high potential range at triethylsilane and phenylsilane hydrogenated electrodes, respectively.

6.2 Future directions

This work has been focused on the development of structurally small carbon electrodes with antifouling property for the detection of dopamine. These antifouling carbon electrodes were prepared by hydrogenating the small carbon electrodes using a triethylsilane and a phenylsilane method, respectively, to reduce the carbon-oxygen functional groups on a carbon surface to their respective alkyl groups. We have

demonstrated that both the triethylsilane and phenylsilane hydrogenated electrodes showed improved performance in a laboratory synthetic fouling solution as well as in two real-life biological samples, compared to results obtained at their non-hydrogenated counterparts. Further study is required to determine the extent of hydrogenation using these two silanes. Although the two organosilanes studied were found to produce an antifouling surface, the percentage hydrogenation/conversion is still not known for the silanes used.

Several researchers have reported the use of polymers to minimise non-specific adsorption, which was influenced by the degree of polymerisation of the backbone and the length of polymer side chains[4]. Similarly, our group previously reported that the antifouling characteristic of *n*-butylsilane hydrogenated electrode was also influenced by the presence of bulky siloxane dendrimers. Future work may include other organosilanes with even bulkier side chains such as diphenylsilane. To enhance the electrocatalytic properties, further modification of the hydrogenated carbon electrodes that can be considered may include immobilising a negatively charged ion (*e.g.* chlorodiphenylsilane) to attract the positively charged dopamine. In this way, not only would the analytical performance of the small electrodes be improved, but the antifouling property of the hydrogenated carbon electrodes would also be enhanced.

In our work, the selectivity of the hydrogenated carbon electrodes was directed towards dopamine, ascorbic acid and uric acid. The aim of this work was to develop physically small, antifouling carbon electrodes for *in vivo* monitoring of dopamine. Future studies may expand to the detection of other electroactive neurotransmitters including serotonin, epinephrine and norepinephrine at the hydrogenated carbon electrodes.

Studies may also include other positively charges species to assess the response of hydrogenated electrodes on the charge of the species.

In addition to this, there is a growing research interest in the use of zwitterionic species in biological tissues due to their improved antifouling properties. Gooding's group previously reported anti-biofouling layers with zwitterionic properties prepared using aryl diazonium salts bearing charged functionalities[5]. Materials with biomimetic zwitterionic groups have received growing attention owing to their superior antifouling property that includes carboxybetaine, sulfobetaine and phosphocholine[6-7]. Electrodeposition of zwitterionic polymers such as poly(3,4-ethylenedioxythiophene) has also been reported[8]. The thickness of the deposited layer on the surface can also be controlled. This can be considered as a potential antifouling layer that can be electrodeposited on physically small carbon electrodes, which then enables a comparison of the antifouling characteristic of the hydrogenated carbon electrodes by silane reduction method.

In the past two decades, carbon nanomaterials have attracted much attention due to their unique mechanical, chemical and electrical properties. Among these, diamond has attracted significant attention in the electrochemical field due to its advantages such as a wide potential window, low and stable background currents, morphological and microstructural stabilities, high chemical and electrochemical stabilities and excellent resistance to fouling[9-11]. Several researchers have utilised nano-diamonds to modify the carbon electrode surfaces to obtain desirable characteristics. Baccarin *et al.*[12] electrochemically wired nano-diamonds on screen-printed electrodes to detect dopamine in the presence of uric acid. Future studies may therefore include

modification of small carbon electrodes using nanodiamonds to obtain hydrophobic surfaces.

Zhou *et al*.[13] recently reported the application of an electro-grafted silica-nanoporous membrane on a carbon fibre electrode for *in vivo* monitoring of oxygen. By implanting the electrode *in vivo* for 2 h, the authors estimated a post-calibration to pre-calibration sensitivity ratio of 0.85 (standard deviation 0.04) at the modified carbon fibre electordes, compared to 0.38 (standard deviation 0.06) at unmodified carbon fibre electrodes. The authors then claimed to have achieved improved resistance to biofouling at the former electrodes. Future work may include the modification of small carbon electrodes using silica-nanoporous membrane for *in vivo* detection of dopamine.

The antifouling characteristic of triethylsilane and phenylsilane hydrogenated electrodes were assessed *in vitro* using a laboratory synthetic fouling solution as well as in two real-life biological samples, SH-SY5Y cells and brain slices. Due to the heterogeneity of the extracellular matrix[14], it is also essential to evaluate the stability and robustness of the hydrogenated carbon electrodes in more complex biological environments.

The degree of fouling was also evaluated directly using cyclic voltammetry after incubating in the fouling solution, brain slices and dopamine cells for a defined period. The $I_{lim,}$ which is a measure of the rate of mass transport, was compared before and after incubation in the laboratory synthetic fouling solution and real0life biological samples to estimate degree of fouling. Other indirect techniques could also be used to assess fouling such as XPS and FTIR.

6.3 References

(1) Wu, X.; Li, P.; Zhang, Y.; Yao, D. Selective response of dopamine on 3-thienylphosphonic acid modified gold electrode with high antifouling capability and long-term stability. *Materials Science and Engineering: C* **2019,** *94*, 677-683, DOI: https://doi.org/10.1016/j.msec.2018.10.024.

(2) Kurzatkowska, K.; Dolusic, E.; Dehaen, W.; Sieroń-Stołtny, K.; Sieroń, A.; Radecka, H. Gold Electrode Incorporating Corrole as an Ion-Channel Mimetic Sensor for Determination of Dopamine. *Analytical Chemistry* **2009,** *81* (17), 7397-7405, DOI: 10.1021/ac901213h.

(3) McNally, M.; Wong, D. K. Y. An in Vivo Probe Based on Mechanically Strong but Structurally Small Carbon Electrodes with an Appreciable Surface Area. *Analytical Chemistry* **2001,** *73* (20), 4793-4800, DOI: 10.1021/ac0104532.

(4) Xu, B.; Liu, Y.; Sun, X.; Hu, J.; Shi, P.; Huang, X. Semifluorinated Synergistic Nonfouling/Fouling-Release Surface. *ACS Applied Materials & Interfaces* **2017,** *9* (19), 16517-16523, DOI: 10.1021/acsami.7b03258.

(5) Gui, A. L.; Luais, E.; Peterson, J. R.; Gooding, J. J. Zwitterionic Phenyl Layers: Finally, Stable, Anti-Biofouling Coatings that Do Not Passivate Electrodes. *ACS Applied Materials & Interfaces* **2013,** *5* (11), 4827-4835, DOI: 10.1021/am400519m.

(6) Gao, C.; Li, G.; Xue, H.; Yang, W.; Zhang, F.; Jiang, S. Functionalizable and ultra-low fouling zwitterionic surfaces via adhesive mussel mimetic linkages. *Biomaterials* **2010,** *31* (7), 1486-1492, DOI: 10.1016/j.biomaterials.2009.11.025.

(7) Zhang, Z.; Zhang, M.; Chen, S.; Horbett, T. A.; Ratner, B. D.; Jiang, S. Blood compatibility of surfaces with superlow protein adsorption. *Biomaterials* **2008,** *29* (32), 4285-4291, DOI: 10.1016/j.biomaterials.2008.07.039.

(8) Goda, T.; Miyahara, Y. Electrodeposition of Zwitterionic PEDOT Films for Conducting and Antifouling Surfaces. *Langmuir* **2019,** *35* (5), 1126-1133, DOI: 10.1021/acs.langmuir.8b01492.

(9) Pecková, K.; Musilová, J.; Barek, J. Boron-Doped Diamond Film Electrodes—New Tool for Voltammetric Determination of Organic Substances. *Critical Reviews in Analytical Chemistry* **2009,** *39* (3), 148-172, DOI: 10.1080/10408340903011812.

(10) Shahrokhian, S.; Ghalkhani, M. Glassy carbon electrodes modified with a film of nanodiamond–graphite/chitosan: Application to the highly sensitive electrochemical determination of Azathioprine. *Electrochimica Acta* **2010,** *55* (11), 3621-3627, DOI: https://doi.org/10.1016/j.electacta.2010.01.099.

(11) Granger, M. C.; Xu, J.; Strojek, J. W.; Swain, G. M. Polycrystalline diamond electrodes: Basic properties and applications as amperometric detectors in flow injection analysis and liquid chromatography. *Analytica Chimica Acta* **1999,** *397* (1-3), 145-161, DOI: 10.1016/S0003-2670(99)00400-6.

(12) Baccarin, M.; Rowley-Neale, S. J.; Cavalheiro, E. T. G.; Smith, G. C.; Banks, C. E. Nanodiamond based surface modified screen-printed electrodes for the simultaneous voltammetric determination of dopamine and uric acid. *Microchim. Acta* **2019,** *186* (3), 1-9, DOI: 10.1007/s00604-019-3315-y.

(13) Zhou, L.; Hou, H.; Wei, H.; Yao, L.; Sun, L.; Yu, P.; Su, B.; Mao, L. In Vivo Monitoring of Oxygen in Rat Brain by Carbon Fiber Microelectrode Modified with Antifouling Nanoporous Membrane. *Analytical Chemistry* **2019,** *91* (5), 3645-3651, DOI: 10.1021/acs.analchem.8b05658.

(14) Frantz, C.; Stewart, K. M.; Weaver, V. M. The extracellular matrix at a glance. *Journal of Cell Science* **2010,** *123* (24), 4195, DOI: 10.1242/jcs.023820.

Appendix 1. Conference Presentations

1. Rita Roshni, Christopher McRae, Danny K.Y Wong; Surface characteristics of small conical-tip carbon electrodes hydrogenated using a phenylsilane reduction method, 21st Australia and New Zealand Electrochemistry Symposium, 29-30 April 2019 Brisbane Australia. (*Oral Presentation*).
2. Rita Roshni, Christopher McRae, Danny K.Y Wong; Surface characteristics of physically small carbon electrodes hydrogenated using a phenylsilane reduction method, Pittsburgh Conference on Analytical Chemistry and Applied Spectroscopy, 17-21 March 2019, Philadelphia, USA. *(Oral Presentation)*
3. Rita Roshni, Christopher McRae, Danny K.Y Wong; Surface characteristics of structurally small electrodes using triethylsilane and phenylsilane. 26th Annual RACI Research and Development Topics Conference in Analytical and Environmental Chemistry, 2-5 December 2018, University of Canberra, Canberra. *(Poster Presentation)*
4. Rita Roshni, Christopher McRae, Danny K.Y Wong; Development of antifouling carbon electrodes for detecting dopamine. Royal Australian Chemical Institute Centenary Congress, 23-28 July 2017, Melbourne Australia. *(Oral Presentation)*
5. Rita Roshni, Shajahan Siraj, Christopher R.McRae, Danny K.Y.Wong; Fouling resistant conical-tip carbon electrodes for selective detection of the neurotransmitter dopamine. 24th Annual RACI Research and Development Topics Conference in Analytical and Environmental Chemistry, 4-7 December 2016 *(Oral Presentation)*